Serial Magnetic Resonance Spectroscopy Imaging in the Acute Stroke and the Relationship With Diffusion and Perfusion Parameters

Vera Cvoro

Doctor of Medicine
University of Edinburgh
2011

Abstract

The aim of this thesis is to investigate the changes in brain metabolite concentration in the acute stroke across the whole of the diffusion lesion and their relationship with the parameters that measure diffusion and perfusion. 51 patients with cortical strokes of mean (±SD) age 75 ±15 years, and mean NIHSS 11 ±8 were imaged within 24 hours of onset, mean of 11 ± 7 hours for the first, and 5 ±1, 12 ±2, 31 ±2, and 95 ±6 days for each of the subsequent scans. Follow-up scanning was not possible in all cases. From the 51 initial patients, 26 (51%) were scanned up to 1 month and 23 (45%) at 3 months. All patients had structural T2 imaging, diffusion weighted (DWI) imaging, perfusion weighted (PWI) imaging and spectroscopy (MRS) as well as full initial clinical assessment and functional outcome at 3 months (Rankin score, Barthel index and extended Nothingam ADL scale).

(1) Distribution of the metabolites within 24 h of stroke onset (region of interest (ROI) and MRS grid analysis). The metabolites were measured in the diffusion lesion classified according to its appearance on visual inspection (grid analysis). NAA differentiated 'definitely' from 'possibly abnormal', and 'possibly abnormal' from 'mismatch' (both comparisons $p<0.01$) voxels, but not 'mismatch' from 'normal' voxels. Lactate was highest in 'definitely abnormal', and progressively lower in 'possibly abnormal', 'mismatch', then 'normal' voxels (all differences $p<0.01$). There was no correlation between NAA and ADC or PWI values, but high lactate correlated with low ADC (Spearman $\varrho=-0.41$, $p=0.02$) and prolonged MTT (Spearman $\varrho=0.42$, $p=0.02$). The ROI analysis showed similar correlations.
Conclusion: ADC and MTT indicate the presence of ischemia (lactate) but not cumulative total neuronal damage (NAA) in acute ischemic stroke, suggesting that caution is required if using ADC and PWI parameters to differentiate salvageable from non-salvageable tissue.

(2) Choline and creatine are not reliable denominators for calculating metabolite ratios in acute ischemic stroke. Choline and creatine concentrations were measured by MR S in 51 patients at 5 times up to 3 months after stroke. Choline and creatine levels changed significantly in the ischemic region. Choline was significantly reduced during the first 2 weeks after stroke onset ($P=0.034$). Creatine was

significantly reduced during the whole period of the study (P=0.011). Choline and creatine concentrations are not reliable denominators for metabolite ratios in acute stroke because their levels vary significantly in ischemic brain regions.

(3) Changes in NAA and lactate over 3 months in the ischaemic lesion. NAA was significantly reduced from admission in definitely and possibly abnormal (p=0.01) compared to contralateral normal voxels, reaching a nadir by 2 weeks and remaining reduced at 3 months. Lactate was significantly increased in definitely and possibly abnormal voxels (p=0.01) during the first 5 days, falling to normal at 2 weeks, rising again later in these voxels.

(4) Correlation with functional outcome. In the ROI analysis there was no association between any of the metabolites and the NIHSS score. There was no correlation between the metabolites, ADC, MTT or CBF and three month Rankin score. However, the clinical parameter of NIHSS (measured at baseline) was associated with the three month Rankin score (Spearman's ϱ= 0.665, p=0.0001), in keeping with the known strong association between stroke severity and functional outcome.

Declaration

I composed this thesis and made substantial contribution to the work presented.

I performed the literature review which formed the basis of chapter 1. I saw around 300 patients of which I recruited 60 in to the study. I was present during all of the MRI scans and decided on the position of the spectroscopy slice. I also performed all the transcranial Doppler examinations. There were over 100 follow up scans and I organised all the follow up visits and took patients myself in the taxi between the rehabilitation hospitals and the MRI scanner. I collected all the data and entered it in to the database. I performed all the statistical analysis except for multiple time points where I had to seek an expert help of the statistician Dr Francesca Chapel. I analysed all the spectroscopy data but did not set up the algorithms, which was done by Professor Ian Marshall and practically implemented by Karolina Wartolowska. I checked all the spectra manually, entered all the data in to the programme for the analysis and drew around all the spectroscopy regions of interests.

Professor Wardlaw performed all the coding for the infarct swelling and supervised scientists Dr M. Bastin, Dr P. Armitage, Dr C.S.Rivers and Dr Trevor Carpenter who analysed diffusion and perfusion images. Professor Wardlaw and Dr C.S.Rivers drew around all DWI regions of interests.

All of the work contributing to the thesis was undertaken whilst I was in post of a Clinical Research Registrar at the Western General Hospital in Edinburgh. Clinical fellowship was funded by the Stroke Association.

Work from chapters 4 and 6 have been presented as platform and poster presentations at the national and international conferences (The European stroke conference 2004, 2006 and 2007, The World Stroke Congress 2004, British Association of Stroke Physicians meeting 2005, The UK Stroke Forum 2006 and The British Geriatric Society Annual Meeting 2004.

Also, the data from chapters 4 and 5 has been published in peer reviewed journals:

1) *Choline and Creatine are not Reliable Denominators for Calculating Metabolite Ratios in Acute Ischaemic Stroke*; Stroke 2008; 39: 2467-2469;

2) *Changes in NAA and lactate following ischemic stroke: A serial MR spectroscopic imaging study; Neurology 2008; 71:1993-1999;*

3) *Association Between Diffusion and Perfusion Parameters, N-Acetyl Aspartate, and Lactate in Acute Ischaemic Stroke;* Stroke 2009; 40: 767-772;

4) *MR Diffusion and Perfusion Parameters: Relationship to Metabolites in Acute Ischaemic Stroke; JNNP 2010; 81: 185-91.*

This thesis has not been submitted in candidature for any other degree, postgraduate diploma or professional qualification.

Acknowledgements

I would like to thank all of the patients who agreed to participate in this study. It was a demanding study for the patients as most of them attended several times for lengthy MRI scans.

I have been welcomed and received support from the staff at the Division of Clinical Neurosciences at the Western General Hospital in Edinburgh. Professor M Dennis, Dr S. Keir, Professor C.Warlow, Dr C Sudlow and professor Sandercock were all great teachers and helped with any clinical queries I had about the patients. Mrs Vera Soosay designed my database. Mrs Brenda Thomas helped with advice and design of the search strategy for the systematic review.

The radiographers of the SHEFC Brain Imaging Research Centre – Mrs Annette Blane, Mrs Evelyn Cowie, and Miss Lorna Cunningham were most helpful in scanning patients. Dr Anne Rowat provided support in helping to identify suitable patients, performed monitoring of the patients whilst in the scanner and helped with setting up pump and the contrast for perfusion imaging.

I also have to thank my colleagues from NHS Fife department of Geriatric Medicine who have had lots of patience and allowed me the time off from the department for writing.

Special thanks goes to my supervisor, Professor Joanna Wardlaw who will remain constant source of inspiration. I thank her for all the support and encouragement that she provided over all these years.

Dedication: This thesis is dedicated to my parents Vukosava and Cedomir, my husband Zoran and son Sasha for their patience, love and support during all this time.

Glossary of terms

ADC	Apparent diffusion coefficient
CBF	Cerebral blood flow
CBV	Cerebral blood volume
$CMRO_2$	cerebral metabolic rate of oxygen
CNL	Contralateral normal tissue
CPP	Cerebral perfusion pressure
CSI	Chemical shift imaging
CSF	Cerebrospinal fluid
DAL	Definitely abnormal tissue
DTI	Diffusion tensor imaging
DWI	Diffusion weighted imaging
IN	Ipsilateral normal tissue
MRS	Magnetic resonance spectroscopy
MRI	Magnetic resonance imaging
MTT	Mean transit time
OEF	Oxygen extraction fraction
PAL	Possibly abnormal tissue
PET	Positron emission tomography
PWI	Perfusion weighted imaging
ROI	Region of interest

Preface

The magnetic resonance imaging (MRI) made it possible to study brain pathophysiology in humans in vivo, rather then being dependent on laboratory experiments. Initially, our insight in to the development, evolution and the mechanisms of damage in cerebral ischaemia was very much based on animal studies. The development of MRI and spectroscopy (MRS) made it possible to have longitudinal studies of the patients and study disease progression in individuals and groups over time. The development of diffusion weighted imaging (DWI) enabled early detection of the ischaemic lesion which is clearly delineated (Moseley *et al.,* 1995). The ability to have repeated measurements has allowed us to study the natural disease course, but also to observe the effect of treatments. Many MRI sequences have been developed to provide information on morphology, diffusion and perfusion state and the metabolic condition of the ischaemic tissue (Fisher *et al.,* 1995).

The concept of ischaemic penumbra has been developed in the late seventies and eighties (Astrup *et al.,* 1981). The penumbra (from the Latin *paene* "almost, nearly" and *umbra* "shadow") is considered to be hypoperfused tissue where neurons are functionally silent but retain structural integrity and are potentially salvageable if blood flow can be restored quickly. Permanently damaged tissue would not be salvaged by restoration of blood flow. It is hoped that these tissues could be distinguished in patients by using imaging techniques. For example, the mismatch between magnetic resonance (MR) diffusion-weighted (DWI) and perfusion (PWI) imaging has often been regarded as synonymous with penumbra. The more "penumbra" was imaged it became clear that there is a lack of standardisation of the definition of penumbra as well lack of standardisation of the measurements (such as perfusion) that contribute to the penumbra (Bandera *et al.,* 2006; Davis *et al.,* 2008; Kane *et al.,* 2007b; Kidwell *et al.,* 2003a). Proton MR spectroscopy (MRS) has been available for many years but its use in acute stroke was limited by long acquisition times. MRS can now be performed within minutes, making it feasible in the clinical setting (Karaszewski *et al.,* 2006; Stengel *et al.,* 2004).

N-acetyl aspartate (NAA), found in intact neurones, is reduced in acute ischaemia (Labelle *et al.,* 2001;Saunders *et al.,* 1995). The precise function of NAA is not clearly

understood. NAA is present in sufficient quantity in the human brain to provide a clear measurable signal on MRS, and loss of NAA indicates neuronal death (Monsein LH *et al.*, 2008; Demougeot *et al.*, 2004; Tsai and Coyle 1995). The reduction in NAA also correlated closely with histological evidence of neuronal loss in ischaemia models (Sager *et al.*, 2000; Sager *et al.*, 1995). Lactate, produced predominantly by anaerobic metabolism, rises sharply in acute ischemic tissue, and in the acute stage is a marker of ischaemia (Lanfermann *et al.*, 1995; Lemesle *et al.*, 2000; Parsons *et al.*, 2000). Spectroscopy could potentially help to determine the association between diffusion and perfusion levels and salvageable versus non-salvageable tissue.

The aim of this thesis was two fold; *firstly*, to evaluate if proton MRS, by identifying neuronal death (reduced NAA) and ischemia (raised lactate), could help clarify the relationship between DWI and PWI parameters and tissue damage in acute ischemic stroke. If ADC or PWI directly indicate neuronal damage, then ADC and PWI values should correlate closely with NAA; if they mainly indicate ischemia, then ADC and PWI values should correlate closely with lactate rather than NAA; *secondly*, the aim was to examine temporal variation of NAA and lactate within the ischaemic stroke lesion over the period of three months and correlate radiological appearances of the ischaemic lesion with the functional outcome at three months.

Chapter 1 explores the concept of stroke, its incidence, anatomical and pathological basis for stroke and pathophysiological findings as known to date. It also examines different MRI techniques and their use in stroke imaging.
Chapter 2 is a systematic review of the literature of MR spectroscopy studies in stroke patients with particular attention to the studies that compared DWI and PI with spectroscopy.

The recruitment of acutely ill patients into any MR imaging study poses many challenges. This is partly due to limited access to MRI facilities but also these patients are often acutely ill and not tolerant of long MRI scans. For this study, patients were prospectively recruited over the period of 24 months. The recruitment methods, imaging details and types of data analysis are all described in the methods

Chapter 3. Two approaches were used to evaluate the acute ischemic lesion – 'region of interest', drawing around the whole lesion and 'voxel based approach', across the whole slice of the brain therefore including the lesion and surrounding

tissue. The analysis to determine the relationship between spectroscopy, diffusion, and perfusion values is presented in Chapter 4.

Patients were followed up for 3 months and at regular intervals. The longitudinal changes in spectroscopy data are presented in Chapter 5.

The relationship between imaging parameters and functional outcome is presented in Chapter 6.

Finally, the summary of the findings of this study is presented in the conclusion.

In summary, there are number of MR methods available to explore characteristics of the ischaemic stroke lesion in vivo and the techniques are becoming faster and easier to use in a clinical setting. This study uses MR spectroscopy to try and correlate the metabolic changes of the acute ischaemic stroke lesion with diffusion and perfusion parameters at the onset of stroke and also looks at the trends of the metabolites over the period of three months within the lesion.

Chapter 1: Background

1.1 Introduction

Stroke is defined by the World Health Organisation as the clinical syndrome of rapid onset of focal (or global, as in subarachnoid haemorrhage) cerebral deficit, lasting more then 24 hours or leading to death, with no apparent cause other then the vascular one. It is not a new disease, but certainly one that has been ignored by health professionals and officials for decades, partly because little has been known about what exactly happens with the tissue when it infarcts and as a consequence "no cure" has been available. The last two decades have changed considerably our knowledge of stroke disease although attitudes may take longer!

The first record of what we would describe a stroke today dates back to Hippocrates (5th century BC), who used term *'apoplexy'* to describe the sudden cataclysmic event involving paralysis of the body (Clarke 1963).

In the last few decades, stroke has started to receive deserved attention from health professionals and officials and although the incidence of stroke is falling in UK and Scotland (Figure 1), it still remains the third largest cause of death (after coronary heart disease and cancer) and the largest cause of disability.
Stroke incidence varies around the world between 300/100 000 and 500/100 000 for ages between 45 and 84 (Sudlow and Warlow 1997).

There are three pathological types of stroke: Ischaemic, which accounts for around 80% in white population, primary intracerebral haemorrhage (around 15%) and subarachnoid haemorrhage (about 5%) (Warlow CP *et al.*, 2008). In order to distinguish between types of stroke, imaging of the brain is essential. The type of imaging used will depend on the timing of imaging from the onset of symptoms and the availability. Computed tomography (CT) is widely available and reliable within the first week of stroke for differentiating between ischaemic and haemorrhagic event. Magnetic resonance imaging (MRI), except in the first few hours of the haemorrhagic stoke, is the method that is more sensitive to ischaemic stroke and can identify ischaemic stoke early with the very sensitive diffusion

weighted imaging (DWI) sequence but it is not so readily available to a majority of stroke patients.

This chapter will explore what is known to happen when blood vessel occludes, the use of MRI in imaging in ischaemic stroke and value of various sequences in the assessment of the progression of the stroke lesion.

Fig1. Incidence of stroke in Scotland (adapted from ISD Scotland) http://www.scotland.gov.uk/Publications

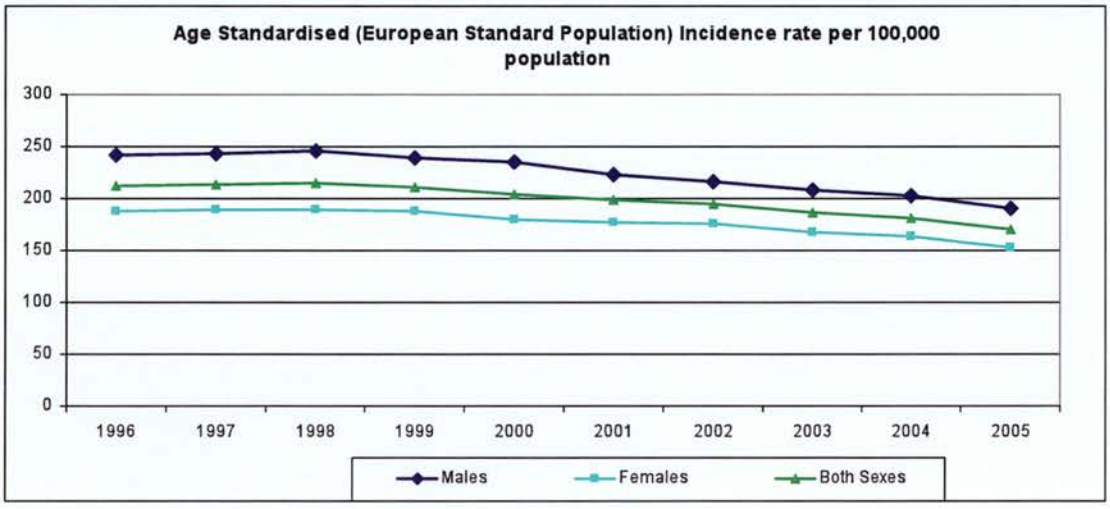

1.2 The anatomical and pathological bases of stroke

1.2.1 The blood supply

The brain receives blood from two sources: the internal carotid arteries and the basilar artery. The internal carotid artery (ICA) is a branch of the common carotid artery after its bifurcation in the neck, which on the right arises from the brahiocephalic trunk and on the left from the aortic arch. Each ICA enters the subarachnoid space by piercing the roof of the cavernous sinus. In the subarachnoid space it gives off ophthalmic, posterior communicating and anterior choroidal arteries before dividing in to two major cerebral arteries, the anterior and middle cerebral arteries. The right and left vertebral arteries, after arising from the subclavian arteries and passing through foramen magnum at the base of the skull

come together at the level of the pons on the ventral surface of the brainstem to form the basilar artery (BA). Vertebral artery prior to forming BA gives of its biggest branch, posterior inferior cerebellar arteriey. From the basilar arise paired anterior inferior cerebellar arteries, superior cerebellar arteries, perforating arteries to the brainstem and it ends by dividing in to the posterior cerebral arteries.

The basilar artery joins the blood supply from the internal carotids in an arterial ring at the base of the brain (in the vicinity of the hypothalamus and cerebral peduncles) called the circle of Willis. The posterior cerebral arteries arise at this confluence, as do two small bridging arteries, the anterior and posterior communicating arteries to complete the circle of Willis. Variations of the circle of Willis are common. Post mortem studies report variations as high as 54.8% (Kapoor *et al.*, 2008). Variations of the anterior and posterior half of the circle of Willis vary between the studies but overall there seems to be predominance of the posterior variations. The frequency of variations will also depend if the studies were conducted on normal brains or in patients with brain disorders. When comparing patients who had infarct with controls, an abnormally small posterior communicating artery was the commonest anomaly observed and was found in greater frequency in the infarct group. The incidence in the control group was 39 % and in the infarct group 59 % (Battacharji *et al.*, 1967;Kapoor et al.,2008).

The main reported variations of the circle of Willis include absence, hypoplasticity, duplication, triplication or persistence of embryonic pattern.

The territories supplied by each artery vary. Therefore, when the stroke lesion is found on neuroimaging, it may not be possible to establish the affected vessel without further imaging of the vasculature.

Figure 2. Blood supply to the brain a) Major cerebral arteries including aortic arch. b) Circle of Willis.

a) *b)*

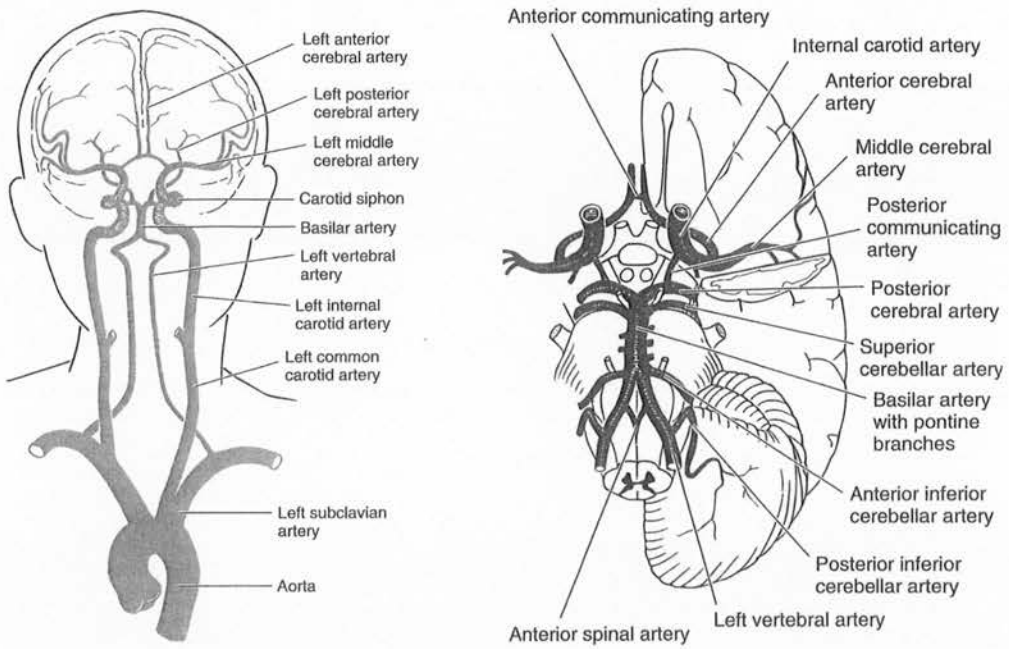

Reproduced from Waxman S.G.: correlative neuroanatomy (Waxman S.G 2000)

The anterior cerebral artery (ACA) passes above the optic chiasm over the medial surface of the cerebral hemisphere and it forms an arch around the genu of the corpus callosum. It supplies anterior frontal lobes and the medial aspect of the cerebral hemispheres. Right and left ACAs are connected by the anterior communicating artery (ACoA), which is an important route of collateral blood supply in case of the occlusion of an internal carotid.

The middle cerebral artery (MCA) supplies the majority of the cerebral cortex (around 70%). It is divided anatomically into several regions: the first part (segment M1) passes along the Sylvian fissure after giving off multiple small penetrating arteries with virtually no collateral circulation (lenticulo-striate arteries) that supply the basal ganglia; the second segment (M2) runs through the insular cortex and then branches further to supply the frontal lobe, parietal temporal lobes and the mid region of the optic radiation (M3-M5) (Hacke W *et al.*, 1989).

The posterior cerebral artery (PCA) winds around the brainstem to supply the splenium of the corpus callosum and the cortex of the occipital and temporal lobes.

It gives off branches to the midbrain and a posterior choroidal artery to the choroid plexus of the lateral ventricle. The central branches called thalamoperforating and thalamogeniculate, supply the thalamus, subthalamic nucleus and optic radiation.

Figure3. Diagram of the vascular territories as depicted in four axial sections. ACA: anterior cerebral artery, MCA: middle cerebral artery, PCA: posterior cerebral artery, LSA: lenticulostriate arteries, PP: posterior perforators, SCA: superior cerebellar artery, PICA: posterior inferior cerebellar artery, BP: basilar perforators.

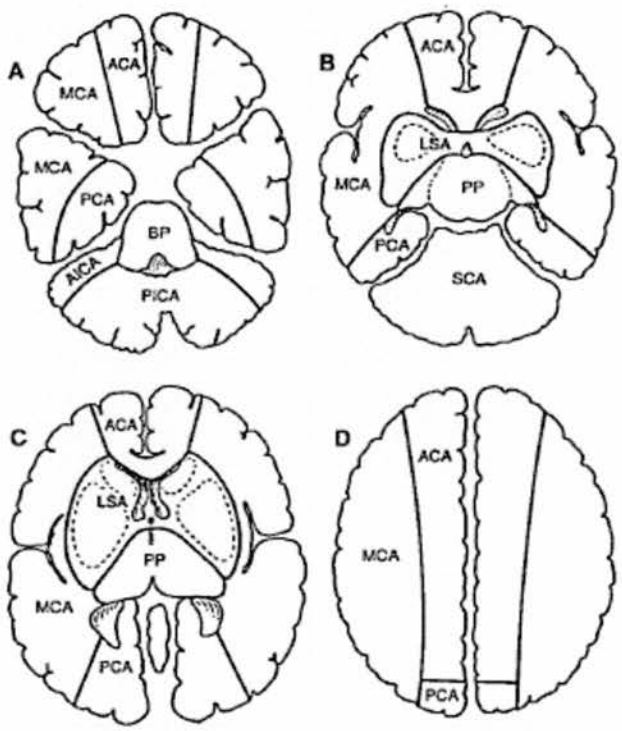

Reproduced from Cinnamon 1995 (Cinnamon et al., 1995)

From all cortical branches, deep penetrating arteries pass through the gray matter and penetrate the white matter to a depth of 3-4 cm, where they supply the core of the hemisphere's white matter. These vessels intercommunicate very little, and thus constitute many independent small systems - terminal arteries. This is in contrast to the surface arteries supplying the cortical gray matter that anastomose to form a continuous network of tiny arteries covering the perimeters or border zones between the core (central) territories of the three major cerebral arteries. In addition, there is a great variability of the size of the arteries and exact zones that they supply, found in vivo and post mortem studies (Hendrikse *et al.*, 2004;van der Zwan A. *et*

al., 1992;van der Zwan A. *et al.*, 1993;van Laar *et al.*, 2006). The biggest contributor to the variability seems to be the circle of Willis. Anatomical variation in the circle of Willis causes flow variations in the territories of ICA and posterior circulation(van Laar et al.,2006).

This very simple overview of the anatomy of the cerebral arterial blood flow shows the complexity of the cerebral circulation in health. In cerebrovascular disease, especially where there is gradual narrowing of the arteries leading to an occlusion, it becomes even more complex with the development of collateral circulation (van Laar *et al.*, 2007). Although imaging can tell us the location and the size of the lesion, it is not always possible to be certain of the vascular territories involved as they are quite variable between individuals.

1.2.2 The pathology of ischaemic stroke

In this section I will discuss ischaemic stroke only, as it is the type studied in this thesis.

About 50% of all ischaemic strokes are caused by the thrombotic or embolic complications of atheroma, a disorder of large and medium sized arteries. 25% are due to intracranial small vessel disease causing lacunar infarction and 20% are due to embolism from the heart. Remaining 5% are due to rarities (Bamford *et al.*, 1991).

The formation, progression, and consequences of atheroma

Atheroma begins as intimal streaks in childhood (Strong 1999), and over many years circulating monocyte derived macrophages adhere to and invade the arterial wall resulting in cytokine production and T-lymphocyte activation. Intra and later extracellular lipids are deposited, particularly in macrophages which are then described as foam cells. Arterial smooth muscle cells migrate in to the lesion and proliferate causing fibrosis and formation of fibrolipid plaque. These plaques spread around and along arterial wall, the arterial wall thickens, the vessel dilates and the lumen narrows and the artery becomes stiffer and tortuous. Atheromatous plaque promotes platelet adhesion, activation and aggregation which initiates blood coagulation and thrombus formation (Fuster *et al.*, 1996; Libby 2009). As a result of

this process the lumen may obstruct or thrombus may embolise (in whole or a part) to obstruct a distal intracranial artery.

Figure 4: The growth, progression, and complications of atheromatous plaques: (a) early deposition of lipid in the artery wall as a fatty streak; (b) further build-up of fibrous and lipid material; (c) necrosis, inflammatory cell infiltrate, calcification and new vessel formation, leading to (d) plaque instability, ulceration and platelet-fibrin thrombus formation on the plaque surface.

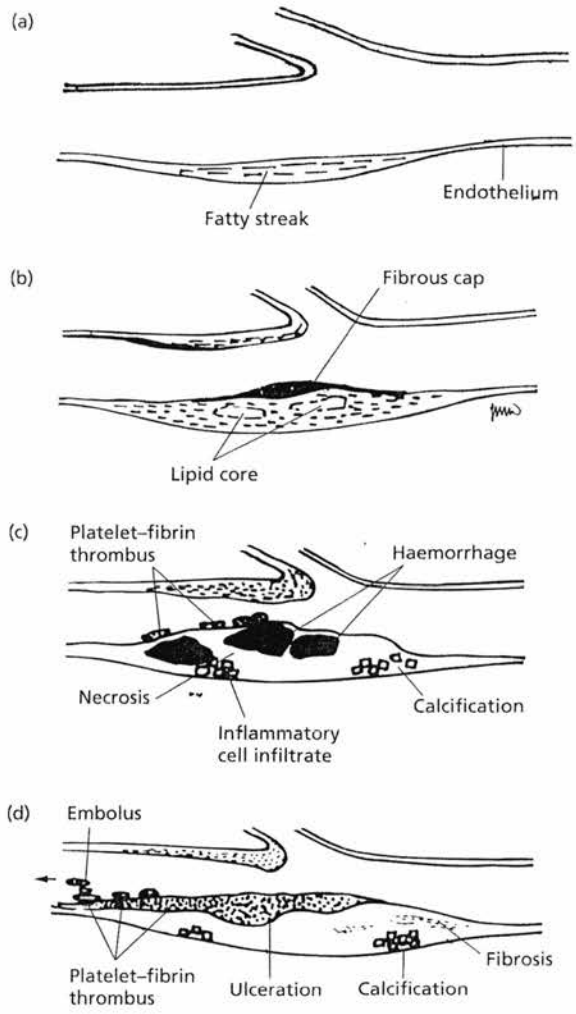

Reproduced from Warlow C 2008 (Warlow C et al., 2008)

Intracranial small vessel disease

This is not the topic of this thesis but it is mentioned here for completeness. Small vessels can be affected by a number of the pathologies such as amyloid angiopathy, vasculitis, atheroma near the origin of the deep perforating arteries but much more common is hyaline arteriosclerosis. This is almost universal in the small vessels of the aged brain but sometime seen in young patients without any of the classical risk factors (Lammie 2000). In addition to hypertension and diabetes mellitus, breakdown of blood brain barrier with incorporation of plasma proteins in to the vessel wall may be an important factor in development of the disease. Smooth muscle cells in the wall are replaced with collagen which reduces distensibility of the vessel but does not necessarily affect the lumen. More acute change is described by the term "fibrinoid vessel wall necrosis", as for example in accelerated hypertension. Unfortunately, there is very little post mortem evidence about the changes in these vessels as these patients usually have smaller strokes and survive. However, it is widely accepted but not uniformly that lacunar infarction has different pathology and is seldom a result of embolisation from the proximal sites. Further research is needed to determine whether abnormal blood–brain barrier might predate development of lacunar disease (Wardlaw *et al.*, 2009; Wardlaw *et al.*, 2008) and the mechanism of development of the lacunar infarction.

Embolism from the heart

Embolism can come directly from the heart or from the venous circulation through the heart to the brain (paradoxical embolism). The size and characteristics of the emboli vary. The most substantial threat is from non-rheumatic and rheumatic atrial fibrillation, infective endocarditis, prosthetic heart valves, recent myocardial infarction, dilated cardyomyopathy, intracardiac tumours and rheumatic mitral stenosis. Altered blood flow in atrial fibrillation (AF) may lead to stasis and formation of a cardiac thrombus. The left atrial appendage is the most common site for thrombus formation in patients with AF. A small thrombus from the left atrium can embolize to the brain and occlude a major intracranial artery thus causing a large stroke.

1.3 The pathophysiological changes in ischemic stroke

Injury from ischemic stroke is the result of a complex series of cellular metabolic events that occur rapidly after the interruption of nutrient blood flow to a region of the brain. The duration, severity, and location of focal cerebral ischemia determine the extent of brain function and thus the severity of stroke. In this section I will talk about the cerebral metabolism in health and mechanisms that lead to cell death.

1.3.1 Cerebral metabolism in health

Energy production and demand

The human brain has high metabolic demand for energy and, unlike other organs uses glucose as its sole substrate for energy metabolism (about 75-100 mg/min, or 125 g/day). It is metabolised entirely via the glycolytic sequence and tricarboxylic acid cycle where glucose is metabolised to pyruvate. During this process, the oxidised form of nicotinamide-adenine dinucleotide (NAD^+) is reduced (NADH). Pyruvate is then oxidised in the mitochondria to carbon dioxide and water and maximum energy yield is 36 moles of ATP. Neurones require a constant supply of ATP to maintain their integrity and to keep the major intracellular cation, potassium ions, within the cell, and the major extracellular cations, sodium and calcium, outside the cell. In the absence of oxygen, the anaerobic pathway takes over which produces 2 moles of ATP and in addition lactic acid which accumulates within and outside cells. The cells become acidified and mitochondria lose their ability to sequester calcium and as a consequence intracellular calcium rises (Kristian and Siesjo 1998; Siesjo *et al.*, 1996). As the brain is unable to store energy, it requires a constant supply of oxygen and glucose to maintain its functional and structural integrity.

Cerebral blood flow

Global cerebral blood flow (CBF), reflecting both gray and white matter per unit of brain in a healthy young adult, is about 50-55 ml/100 g of brain per minute. These values are higher in those younger then 20 years of age and lower in those over 60

years of age (Leenders *et al.*, 1990). The brain is only 2% total body weight and therefore has disproportionately high total CBF for it's weight of 800 ml/min which is 15-20% of total cardiac output. At this level of blood flow, the whole brain oxygen consumption, expressed as cerebral metabolic rate of oxygen ($CMRO_2$), is about 3.3-3.5 ml/100g of brain per minute, or 45 ml of oxygen per minute, which makes it 20% of the total body oxygen consumption at rest. The fraction of oxygen extracted from blood (OEF) is fairly constant and coupled with CBF, cerebral blood volume, $CMRO_2$ and cerebral metabolic rate of glucose (Leenders *et al.*, 1990). In health CBF is a good measure of OEF, but if CBF reduces the OEF increases to maintain $CMRO_2$.

Cerebral autoregulation

Cerebral blood flow is maintained at a constant level despite changes in cerebral perfusion pressure under normal conditions (mean systemic arterial pressure within 60-160 mmHg). This relationship is human autoregulation. The relationship between the CBF and cerebral perfusion pressure (CPP) can be expressed as CBF=CPP/CVR (cerebrovascular resistance). The CPP represents a difference between arterial pressure forcing blood into the cerebral circulation and the venous back pressure. Usually, CVR is negligible and CPP equals arterial pressure. Maintaining flow with changes in pressure is achieved by altering vascular resistance (by dilatation or constriction of intracerebral and pial arterioles). Other influences on CBF are systemic arterial oxygen content, carbon dioxide tension, local pH and the degree of local functional activation of neurones (Paczynski R. *et al.*, 1995). If the capacity to autoregulate is lost, the CBF becomes directly dependent on systemic arterial pressure and even very small reductions in arterial pressure can cause significant reductions in cerebral perfusion (Powers 1993).

1.3.2 The consequences of arterial occlusion

Acute cerebral ischaemia usually begins with occlusion of the artery (occasionally vein), but can also happen as a consequence of a low flow (less common on its own). When there is a sudden occlusion of the artery, blood pressure and cerebral blood flow fall, distally to the site of the occlusion, and an area supplied becomes ischaemic. Occlusion of the artery rarely completely abolishes supply of oxygen and

glucose to the affected area due to existence of collateral channels which partly maintain blood flow in the ischaemic territory and in some cases can produce areas of relatively increased CBF so called "luxury perfusion."

The site of ischaemia is also important to cell survival. Neurones are most sensitive to ischaemia followed by oligodendroglia, astrocytes and endothelial cells. Even among neurons there are different sensitivities and those in hippocampus are thought to be most sensitive with neocortex being least sensitive.

The duration of ischaemia will determine the fate of the tissue. This can be thought of in terms of three main types of the tissue which are: tissue that is destined to die (infarct core), tissue that will survive, and the tissue that may die or survive (penumbra).

Critical thresholds of blood flow

Models of focal cerebral ischaemia have identified critical flow thresholds for certain cell functions. The development of infarction is critically dependent on blood flow (Astrup et al.,1981).

Figure 5. Cerebral blood flow (CBV) thresholds for cerebral dysfunction and death

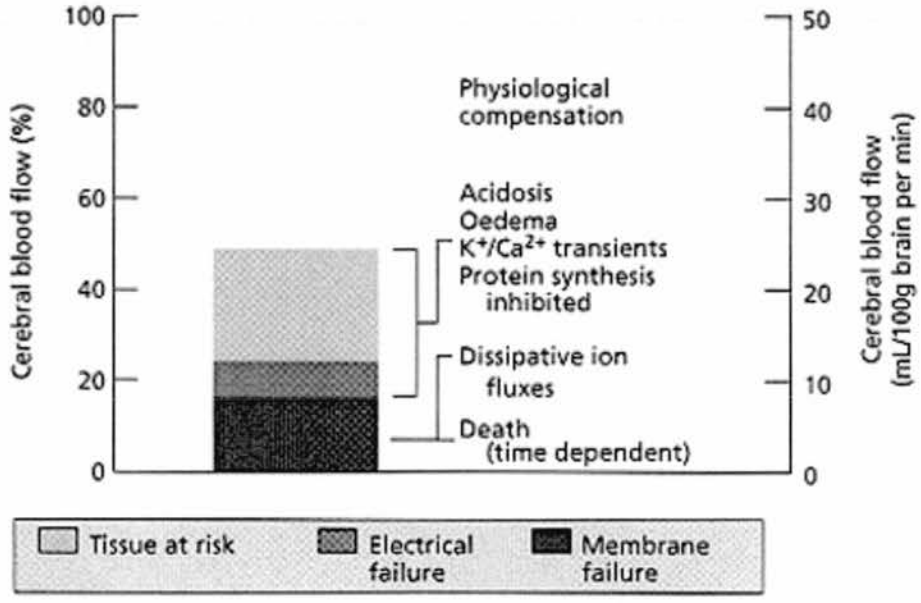

(Reproduced from Warlow C et al. Stroke Practical Management (Warlow C et al.,2008)

Initially, small reductions in CPP and CBF (<50 ml/100g/min) are compensated by regional vasodilatation to maintain CBF. With continued reduction in CPP (<45 ml/100g/min) and dilatation of all vessels to capacity, OEF and glucose extraction are increased to maintain a normal $CMRO_2$ and cerebral metabolic rate of glucose (Powers 1991). Protein synthesis becomes inhibited. This is a state of "misery perfusion" and the tissue is at risk (Baron 1999). The gold standard method of studying this process in vivo is by a positron emission topography (PET) which is the quantitative imaging technique that allows to obtain maps of the main physiological variables involved in tissue ischaemia, perfusion and oxygen conssumption. (Baron1999).

Further ischaemia (<35 ml/100g/min) causes inhibition of mitochondrial metabolism and activates inefficient anaerobic glycolysis with elevation of lactate levels and extra and intracellular acidosis. The energy dependant functions of the cell membrane fail allowing intracellular potassium (K^+) to leak out and allowing extracellular sodium (Na^+) and water to enter cells causing cytotoxic oedema. Calcium (Ca^{++}) also moves in to the cells causing mitochondrial failure and compromises the ability of cell membrane to control ion fluxes (Kristian and Siesjo1998). When CBF reduces to below 20 ml/100g/min, electrical failure begins to occur. Compensatory mechanisms temporarily sacrifice electrophysiological activity to preserve cell viability, and suppression is seen on electroencephalogram with evoked potentials attenuated. At this point, a focal neurological deficit will be present (Fisher M 1999). The OEF is maximal and $CMRO_2$ begins to fall. With further reduction in blood fallow, the electrical activity now fails, evoked potentials are lost, the EEG flattens, and finally becomes isoelectric. With reduction of CBF to 15 ml/100 g/min, membrane failure occurs, leading to cytotoxic oedema, calcium enters the cells leading to failure of mitochondria. The critical threshold for the beginning of irreversible cell damage is a CBF of about 10 ml/100 g/min.

Duration of ischaemia

There are two main factors that determine tissue outcome, the severity of flow reduction and its duration (Heiss and Rosner 1983) (Figure 6). The CBF threshold for membrane failure (infarction) depends on the time elapsed since vessel occlusion. The tissue with CBF 15 ml/100g/min may withstand three hours of

occlusion, but tissue with CBF 10 ml/100g/min may withstand only two hours. The data from PET studies indicate that substantial penumbra is present within six hours of onset (around 90%), but falls to around 50% within nine hours. There is still evidence of intact penumbra at 18 hours in about 30% (Marchal *et al.*, 1996). The data from thrombolytic trials of desmoteplase between 3 to 9 hours in patients with a diffusion perfusion mismatch (Hacke *et al.*, 2005), in addition to data from PET studies (Baron1999;Baron 2001), suggests that the window for a therapeutic intervention may be longer then the currently accepted 4.5 hours (Hacke *et al.*, 2008). However, the data on tissue survival in relation to duration of ischaemia is still limited.

Figure 6. Combined effect of residual cerebral blood flow (CBF) and duration of ischaemia on reversibility on neuronal dysfunction during focal cerebral ischaemia.

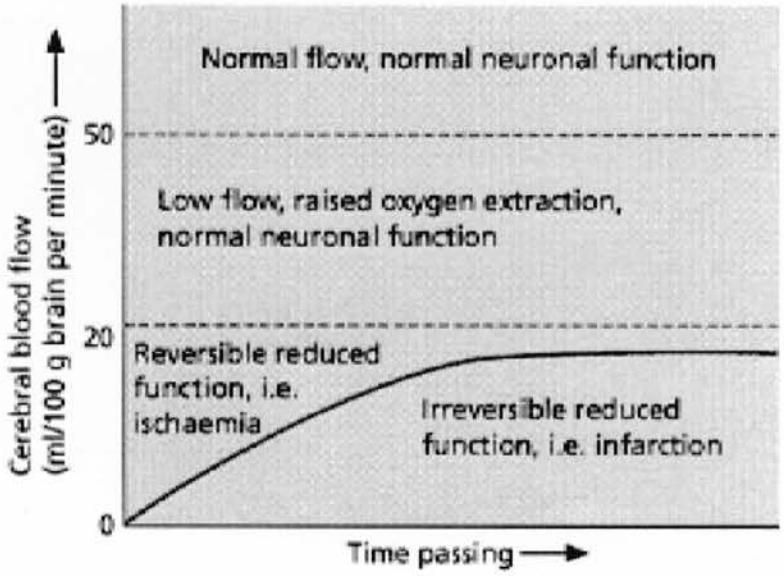

Reproduced from Warlow C et al. Stroke Practical Management (Warlow C et al.,2008)

Penumbra

The ischaemic penumbra can be defined as severely ischaemic, functionally impaired tissue but still surviving. It is at risk of infarction but it can be saved and recover if reperfused before permanent damage occurs. In threshold terms it means that cells falling between suppression of electrical activity and the next threshold when cells start breaking down are in the penumbra (Keith W Muir *et al.*, 2006) . Penumbra has been the target of acute stroke therapy and "Time is brain" is very important concept to remember when treating acute stroke patients. Penumbral tissue needs to be distinguished from the ischemic core (tissue that is already irreversibly injured even if blood flow is re-established) and from tissue experiencing benign oligemia, in which the mild reductions in tissue perfusion do not actually place the tissue at risk Figure 7.

Figure 7. The ischaemic penumbra (Baron 1999). Idealised diagram of the baboon's brain showing the topography of the ischaemic core, the pneumbra, and the oligaemia, following occlusion of the MCA.

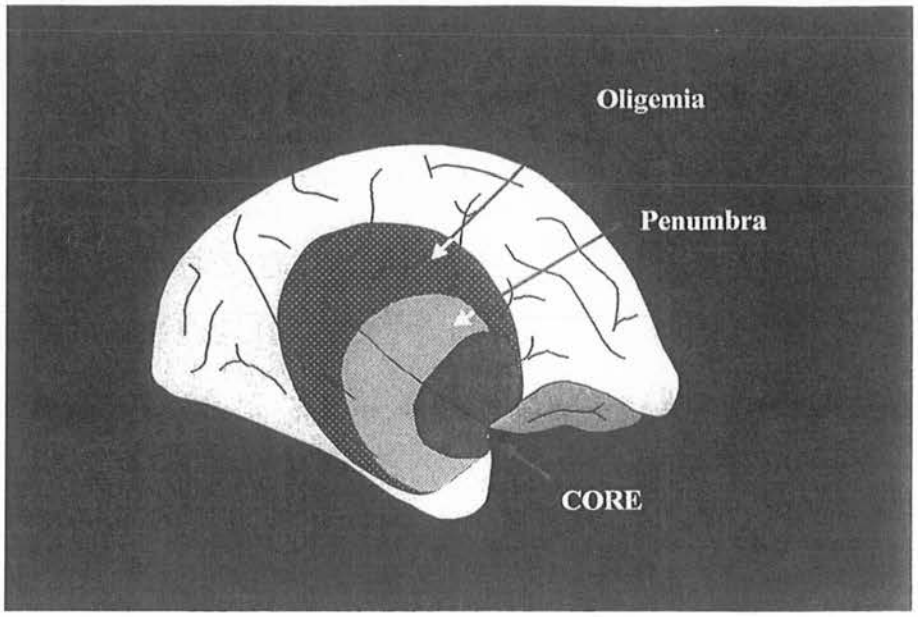

Reproduced from Baron 1999 (Baron1999)

The duration of the penumbra in humans varies, probably substantially from person to person depending on a variety of factors, including location of the vessel occlusion, degree of collateral blood flow, intrinsic susceptibility to ischemia of

hypoperfused tissues (grey versus white matter), and other patient-specific factors. Therapeutic strategies in acute stroke are based on the concept of arresting the transition of the penumbral region into infarction, thereby limiting ultimate infarct size and improving neurological and functional outcome (Fisher 1997). It is thought that direct visualization of the location and extent of the penumbra could greatly improve our ability to determine which patients may benefit from therapy and allow treatment decisions to be based on individualised pathophysiology rather than arbitrary chronological time thresholds.

Although the time varies, it is certain that if no reperfusion occurs, the area that defines the core of the lesion increases with time until it reaches penumbral threshold, at which point the entire penumbra has been recruited Figure8.

Figure 8. Idealised diagram of the baboon's brain showing the time course of infarct growth at the expense of the pneumbra, from the situation immediately following MCA occlusion (top left), to 3 h later (bottom right). The oligaemia is not a risk of infarction.

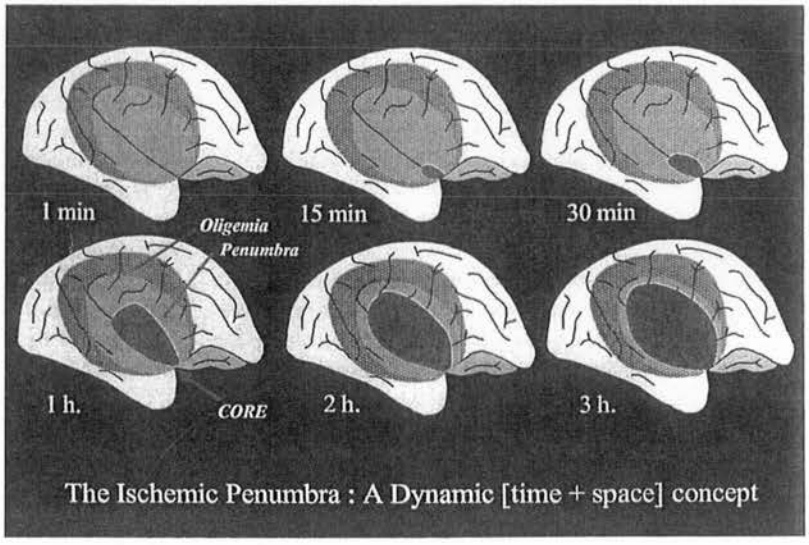

Reproduced from Baron 1999 (Baron1999b)

Imaging of the ischaemic penumbra

The main methods of imaging the ischaemic penumbra in vivo are by positron emission tomography (PET), MRI, CT perfusion and single photon emission tomography (SPECT). PET is able to differentiate between normal, penumbral and infarcted tissue in the acute stages of ischaemic stroke. It is often referred to as a

gold standard as it uses validated thresholds but because of its logistic and practical limitations, its clinical role in acute stroke is limited.

MRI is more widely available and the mismatch between magnetic resonance (MR) diffusion-weighted (DWI) and perfusion (PWI) imaging has often been regarded as synonymous with penumbra (PWI> DWI is associated with subsequent infarct enlargement). This is an oversimplification and it is recognised that mismatch region will also include tissue with benign oligaemia and that some of the DWI infarct core may in fact be salvageable (Kidwell *et al.*, 2003,). This is discussed later in the section on MRI imaging.

There are no studies that used MR spectroscopy in the assessment of the penumbra. CT perfusion is a relatively new technique and not fully validated but it may be able to delineate between infarcted and penumbral tissue. It provides CBF, CBV and MTT and it is not best for visualising posterior fossa. SPECT is cheap and relatively available but provides perfusion only and has limited spatial resolution.

At the present moment all potential penumbral imaging methods have drawbacks for use in the acute setting and/or question about how accurately they can identify tissue at risk.

1.4 Magnetic resonance imaging

1.4.1 Basic principles of MRI

The physics underlying MR imaging is extremely complex and beyond the scope of this thesis. What follows is therefore a summary of basic principles.

Magnetic resonance imaging (MRI) is based on the principles of nuclear magnetic resonance. The term "nuclear" has been dropped from the description of medical MR techniques because of its association with radiation and radioactivity. Hydrogen nuclei (protons) have magnetic properties, called nuclear spin. They behave like tiny rotating magnets, represented by vectors in Figure 9a. The sum of all the tiny magnetic fields of each spin is called net magnetization. Normally, the direction of these vectors is randomly distributed. Thus, the sum of all the spins

gives a null net magnetization. Within a large external magnetic field (called B_0), nuclear spins align with the external field as in Figure 9b. Some of the spins align with the field (parallel) and some align against the field (anti-parallel).

Figure 9 a) In the absence of a strong magnetic field, hydrogen nuclei are randomly aligned b) When the strong magnetic field, B_0, is applied, the hydrogen nuclei align with B_0 and precess about the direction of the magnetic field.

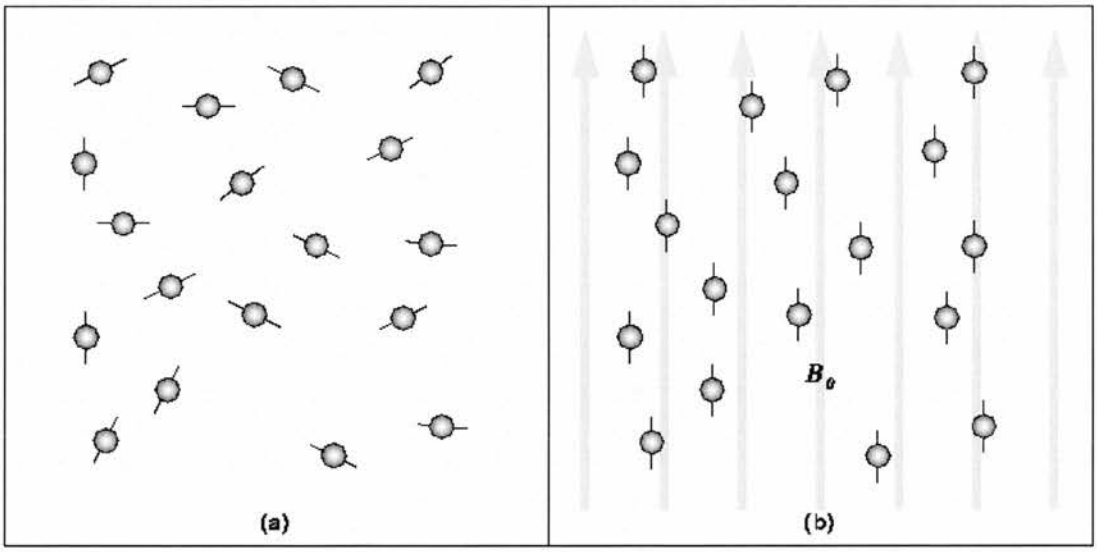

a) b)

(Reproduced from Basic Principles of MRI http://www.cs.sfu with permission from *Blair Mackiewich*)

Protons wobble (or precess) about the axis of the B_0 field so as to describe a cone. This is called precession. Spinning protons are like "spinning tops," spinning about their axis. The resonance frequency, called Larmor frequency (ω_0) or precessional frequency, is proportional to the main magnetic field strength. The magnetic vector of spinning protons can be broken down into two orthogonal components: a longitudinal or Z component, and a transverse component, lying on the XY plane. Precession corresponds to rotation of the transverse component about the longitudinal axis. Within the B_0 magnetic field, there are more spins aligned with the field (parallel - low energy state) than spins aligned against the field (anti-parallel - high energy state). Due to this slight excess of parallel spins, net magnetization (macroscopic magnetization) has a longitudinal component (along

the Z axis) aligned with B_0. As spins do not rotate in phase, the sum of all the microscopic transverse magnetizations tend to zero so that there is no net transverse macroscopic magnetization.

Exchange of energy between two systems at a specific frequency is called resonance. Magnetic resonance corresponds to the energetic interaction between spins and electromagnetic radiofrequency (RF). When a RF pulse is applied, the net magnetization vector tips down during excitation but the microscopic spin magnetization vectors do not. Modifications of the energy state and phase of spins depend on intensity, waveform, and duration of RF pulse.

Figure 10. a) The RF pulse causes the net magnetic moment of the nuclei to tilt away from B_0 b) When the RF pulse stops, the nuclei return to equilibrium such that magnetic moment is again parallel to B_0. During realignment, the nuclei lose energy and a measurable RF signal

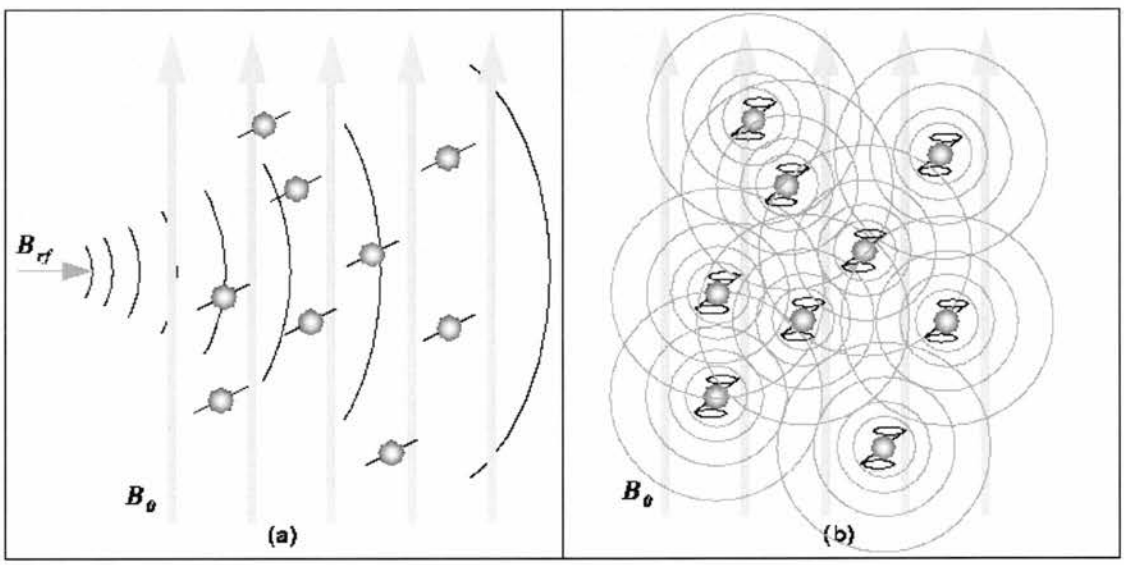

a) b)

(Reproduced from Basic Principles of MRI http://www.cs.sfu with permission from *Blair Mackiewich*)

Once the RF signal is removed, the nuclei realign themselves such that their net magnetic moment is again parallel with B_0. This return to equilibrium is referred to as relaxation. During relaxation, the nuclei lose energy by emitting their own RF signal (see Figure 10 b). This signal is referred to as the free-induction decay (FID) response signal. The FID response signal is measured by a conductive field coil placed around the object being imaged. This measurement is processed or

reconstructed to obtain 3D grey-scale MR images. To produce a 3D image, the FID resonance signal must be encoded for each dimension. The encoding in the axial direction, the direction of B_0, is accomplished by adding a gradient magnetic field to B_0. This gradient causes the Larmor frequency to change linearly in the axial direction. Thus, an axial slice can be selected by choosing the frequency of RF pulse to correspond to the Larmor frequency of that slice. The 2D spatial reconstruction in each axial slice is accomplished using frequency and phase encoding.

The voxel intensity of a given tissue type (i.e. white matter vs grey matter) depends on the proton density of the tissue; the higher the proton density, the stronger the FID response signal. MR image contrast also depends on two other tissue-specific parameters: a) the longitudinal relaxation time, T1, and b) the transverse relaxation time, T2. T1 characterizes the rate at which the longitudinal component of the magnetization vector returns to equilibrium (i.e. realign itself with B_0), while T2 characterizes the rate at which the magnetization vector decays in the transverse plane for a given tissue type. When MR images are acquired, the RF pulse is repeated at a predetermined rate. The period of the RF pulse sequence is the repetition time TR. The FID response signals can be measured at various times within the TR interval. The time between which the RF pulse is applied and the response signal is measured is the echo delay time TE. By adjusting TR and TE the acquired MR image can be made to contrast different tissue types.

In clinical MRI, hydrogen is the most frequently imaged nucleus due to its great abundance in biological tissues. Other nuclei such as ^{13}C, ^{19}F, ^{31}P, ^{23}Na have a net nuclear spin and can potentially also be imaged using MR, albeit with vastly reduced spatial resolution. However, they are much less abundant than hydrogen in biological tissues and require a dedicated RF chain, tuned to their resonance frequency.

1.4.2 Structural MR imaging sequences

A routine MR brain imaging sequence of a stroke patient consists of a combination of a T1 weighted midline sagital view of the brain, a T2 axial image, a fluid attenuated inversion recovery (FLAIR) axial image, a gradient echo (or T2*) axial image and diffusion weighted (DWI) axial image covering the whole brain (DeLaPaz RL and Mohr JP 1998;Wardlaw JM 2008). The exact sequence performed

depends on the preference of the neuroradiologist. The images obtained with these routine sequences provide information about the structure of the brain. T2* gradient echo is sensitive to the presence of blood in acute and chronic haemorrhage (DeLaPaz RL and Mohr JP1998;Patel *et al.,* 1996;Wardlaw JM2008) or in more chronic small petechial minor haemorrhages (Keir 2002).

The FLAIR images are T2-weighted with the CSF signal suppressed. This means the lesions near the brain surface stand out more clearly. It appears to detect ischaemic abnormalities better then T2 weighted imaging (Lansberg *et al.,* 2000;Oppenheim *et al.,* 2000) and shows small cortical and periventricular infarcts well. However, it cannot distinguish between acute and subacute infarcts and may miss posterior fossa lesions. It can also be oversensitive especially for asymptomatic white matter lesions (Wardlaw JM2008;Oppenheim et al.,2000). Diffusion and perfusion imaging will be discussed in more detail as it is a major part of the imaging protocol.

1.4.3 Diffusion weighted imaging

Diffusion weighted imaging (DWI) is the most sensitive way to image acute infarcts. Diffusion-weighted imaging sequences now are incorporated into most MR imaging protocols and are essential component of an acute stroke evaluation (Schaefer *et al.,* 2000).

Basic physics of DWI

Diffusion explores the micromovements of water molecules. It is often thought of as a redistribution of molecules from a region of high concentration to a region of low concentration. However, in MRI, the "random walk model" is more suitable because it describes the effects of diffusion in the absence of any concentration gradient (Figure 11). Because of random thermal motions (Brownian motion), water molecules in a pure sample change position and direction of movement in a random fashion. This process is called *isotropic diffusion*. In biological systems, water diffusion is not truly random because diffusion is restricted by natural barriers such as cell membranes, protein molecules and fibres. When the observation time is very short, most molecules do not have enough time to reach the barriers; therefore, they behave as if they are diffusing freely. If the observation time increases, the restricted

molecule will strike the boundaries in its motion, and therefore its displacement will deviate from its behaviour in a free medium. Diffusion is a three-dimensional process, and the molecular mobility in different directions may be affected by the presence of natural barriers that limit free diffusion. This spatial dependency is called *anisotropic diffusion* (Schaefer et al.,2000;Moseley *et al.*, 1991). For example, water diffuses readily up and down white matter tracts, but diffusion perpendicular to the fibre is restricted by axonal membranes and the myelin sheath (Baird and Warach 1998) Figure 12..

Figure 11. Schematic representation of a diffusion process described as "random walk." Four particles (different colour), all begin at the same origin but follow different chaotic paths.

Diffusion – Random Walk

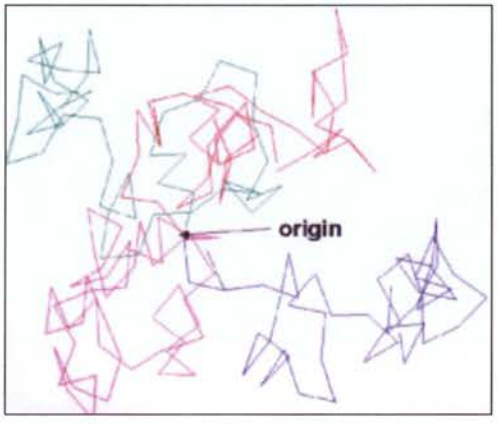

Displacement of 4 particles starting at the same origin

Reproduced from C. Beaulieu(Beaulieu 2002)

Figure 12. Exemples of isotropic diffusion and anisotropic diffusion

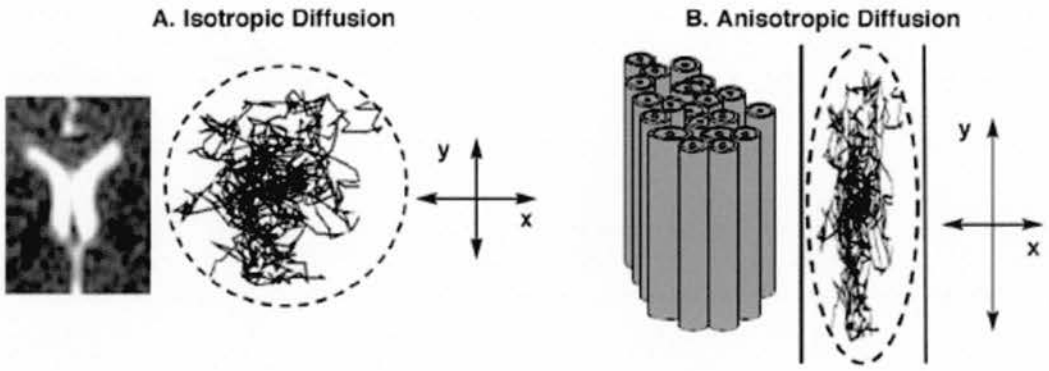

(A) Water molecules in the brain are constantly moving (i.e., in Brownian motion). When motion is unconstrained, as in the large fluid–filled spaces deep in the brain (i.e., the ventricles, as illustrated in the MR image on the left), diffusion is isotropic, which means that motion occurs equally and randomly in all directions. (B) When motion is constrained, as in white–matter tracts (illustrated on the right), diffusion is anisotropic, meaning that motion is oriented more in one direction than another (e.g., along the y *axis rather than along the* x *axis).*

Reproduced from M. Rosenbloom (http://pubs.niaaa.nih.gov/publications)

The principles of DW imaging

The overall principle of diffusion measurement is that the spatial location of each water molecule is tagged such that any net movement of a water molecule during the observed period results in signal loss (darkening of the images). This is achieved by a pair of very strong pulsed magnetic field gradients (diffusion gradients) to each side of a 180° pulse, which are added to a spin-echo sequence (typically T2-weighted). The first of these diffusion gradients (the dephasing gradient) causes the spinning protons to fall out of phase with one another whilst the second diffusion gradient (the rephasing gradient), rephases the protons completely with one another. If there has been no movement of the water molecules between the application of the two diffusion gradients, and a T2-weighted image would result as if the pair of diffusion gradients had not been added. When there is movement of water, the protons are not brought back completely into phase by the second diffusion gradient. The further the water has moved, the more out of phase it will be, and the more signal attenuation (signal loss or image darkening) will occur. Regions of fast diffusion (CSF) appear darker then normal brain tissue because

movement of water results in signal loss (Baird and Warach1998). Normal brain will appear darker then the regions of hyperacute injury which have restricted diffusion. The amount of signal loss in DWI is related to the magnitude of the molecular translation (i.e., net diffusion) and to the strength of the diffusion weighting, given by the b-value. The b value is specific for the particular pulse sequence used to measure diffusion and is a function of the diffusion gradient strength, the duration of the diffusion gradient pulse and the time of the diffusion measurement (the time between the beginning of the two diffusion gradients).The higher the b-factor the greater the diffusion weighting.

The diffusion description needs to account for the spatial dimension (axial, sagittal, or coronal) that the diffusion is measured in. In practice, the so-called trace of the diffusion tensor can be measured by averaging images obtained with diffusion gradients applied in three orthogonal planes (x, y, and z) to give average diffusion coefficient (Ulug *et al.*, 1997;Warach *et al.*, 1995). Average diffusion coefficient is not dependent on the orientation of the subject with respect to the magnetic field gradient axes and provides a good approximation to the mean of the diffusion tensor (Ulug et al.,1997). The earliest DWI studies were limiting due to very slow acquisition time (used spin-echo type sequences) (Warach *et al.*, 1992). With the implementation of echoplanar imaging (EPI) much faster acquisition of DWI images was possible. The effects of bulk motion were minimized and DWI became practical for the acute stroke setting (Warach et al.,1995). The advantages of DWI using EPI are: (1) the acquisition is very rapid (on the order of tens of milliseconds) so that multiple slices from a whole brain can be imaged in a few seconds, (ii) the effect of head motion leading to poor image quality can be reduced to a minimum, and (iii) studies of multiple different diffusion properties are possible. Limitations of EPI of the brain are strong chemical shift artefacts making precise fat suppression techniques obligatory, and strong susceptibility artifacts that cause image distortions, particularly in the posterior fossa and at the margins (inferior frontal and anterior temporal lobes)(Warach et al.,1995).

Apparent diffusion coefficient

The rate of diffusion can be quantified and is expressed as apparent diffusion coefficient (ADC). For the calculation of the ADC, at least two b values are required, (typically b = 0 no diffusion weighting and 1000 s/mm2). The accuracy of the ADC

calculation is directly related to the range and number of b values used for the measurement, and the signal-to-noise ratio of the T2-weighted EPI acquisition. ADC removes T2 effect and is useful mostly in cases of lesion with a T2 hyperintensity appearing as a hyperintensity on DWI (differentiates between T2-shine-through and diffusion restriction).
The abnormality on ADC is the inverse of its appearance on DWI. Therefore, CSF that has unrestricted water movement is bright whilst the lesion with low diffusivity is dark.

Anisotropic diffusion

The ADC in certain regions of the brain appears to depend on the direction of the applied diffusion gradient (Moseley *et al.*, 1990a) implying that ADC is directionally dependent. Beailieu and Allen performed a number of experiments in the 1990s to determine the origin of diffusion anisotropy. By the process of elimination they were able to rule out the effects of susceptibility induced gradients (Beaulieu and Allen 1996), axonal cytoskeleton (Beaulieu and Allen 1994a;Moseley et al.,1990a) and fast axonal transport (Beaulieu and Allen 1994b;Moseley et al.,1990a). They concluded that the main determinant of anisotropy in nervous tissue is the presence of intact cell membranes and that myelination serves to modulate anisotropy (Beaulieu2002).

Diffusion Tensor Imaging (DTI)

Water molecule diffusion is a three-dimensional process. In order to acquire more detailed information about anisotropic diffusion properties of the tissue, simple DWI is not sufficient. While ADC maps reveal the tendency of water molecules to diffuse within a voxel, directional variation is also required to image 3D anisotropic diffusion. By sampling 6 or more diffusion directions and establishing a relationship between the acquired data and applied diffusion gradients in the pulse sequence, the directional variation in the tendency of water molecules to diffuse within a voxel can be imaged.It describes the diffusion along each direction and interactions between the directions providing important information about tissue connectivity. However, complex maths is required to determine the diffusion tensor for each voxel in the brain, and this analysis is beyond the scope of this thesis.

DWI in ischaemia

Acute stroke restricts supply of glucose and oxygen and eventually results in failure of cell membrane pumps and influx of sodium and water into the cell (see Pathophysiology section earlier in this chapter). Water enters the cells from extracellular space where it can diffuse freely, to intracellular space where its movement is restricted (Beauchamp, Jr. *et al.*, 1999). It is generally accepted that high signal on DWI (low ADC) is due to excess intracellular water accumulation, or cytotoxic edema, with an overall decreased rate of water molecular diffusion within the affected tissue (Albers 1998;Beauchamp, Jr. et al.,1999;Fisher et al.,1995) .

Figure 13. Slice from the brainstem of diffusion image and corresponding ADC lesion.

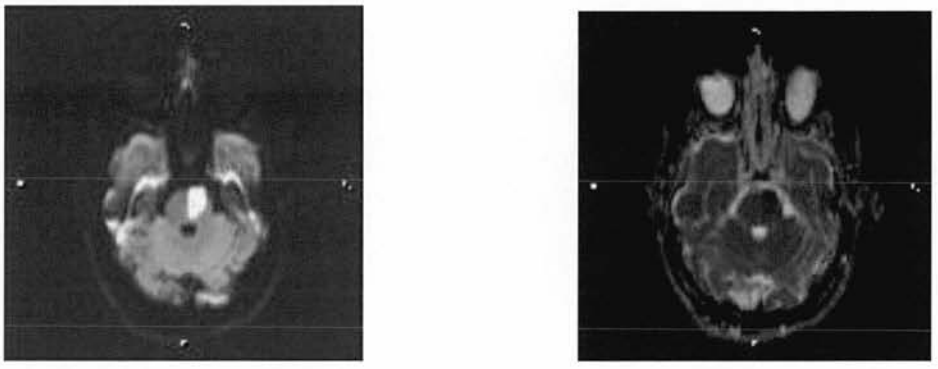

Although there is an "agreement" that decrease in ADC in ischemic stroke reflect early cytotoxic oedema, the exact mechanism is not known. Various other mechanisms have been proposed such as decreased extracellular space (Hasegawa *et al.*, 1996) or restricted intracellular diffusion (Neil *et al.*, 1996).

The time course of ADC/DW lesion

DWI is capable of detecting cerebral ischaemia very early, within minutes in animal models (Moseley *et al.*, 1990b), and within first hour in human ischaemia (Yoneda *et al.*, 1999). In acute stroke studies, ADC values decrease after stroke onset, then normalise before becoming high in the chronic phase. The decrease can be very rapid after stroke, and can reach minimum value within 1.5 hours (Kucinski *et al.*,

2002). A decrease in ADC always precedes the development of infarction but not all low ADC lesions will necessarily go on to infarct. So, the diffusion lesson appears to be heterogeneous and includes reversibly and irreversibly damaged tissue (Guadagno *et al.*, 2004;Kidwell *et al.*, 2000;Kidwell et al.,2003;Rivers and Wardlaw 2005;Rivers *et al.*, 2006b). A DWI lesion can be found in some patients with a transient ischaemic attack (Ay *et al.*, 2002) whilst others with a clinical stroke may never develop a DWI lesion (Ay *et al.*, 1999).

In animal models, the ADC value falls as neuronal *and* glial swelling develops, and then either remains low in persistent occlusion models until dead cells of all types are lysed, or rises in transient ischemia models due primarily to resolution of *glial* swelling (Rivers and Wardlaw2005). Indeed histological comparisons suggest that the ADC is a better marker of glial cell status than of neuronal viability, with the DWI signal ("whiteness") being a better marker of neuronal death than the ADC (Rivers and Wardlaw2005;Rivers et al.,2006b). So far, no consensus has been reached on the threshold of cerebral perfusion that results in a diffusion abnormality (Bandera et al.,2006;Fiehler 2003).

1.4.4 Perfusion weighted imaging (PWI)

Perfusion MRI provides a relative and/or "absolute" measurement of the parameters of cerebral microvascularisation: regional blood volume, mean transit time and regional blood flow. Two types of MR perfusion imaging have found applicability to be used clinical practice and research; 1) susceptibility-based techniques that use either paramagnetic contrast agents such as those containing gadolinium (contrast agent bolus tracking) also called (dynamic susceptibility contrast [DSC] imaging), or endogenous changes in deoxyhemoglobin, which is an intrinsic paramagnetic molecule (blood oxygen level dependent [BOLD]); and 2) arterial spin labelling techniques.

In the ASL method, water proton spins in the extracranial blood are saturated and inverted electromagnetically, and these labelled protons mix with extravascular water in the brain. The imaging before and after spin inversion detects the difference in tissue magnetization, which is proportional to local perfusion. The method has a relatively low signal-to-noise ratio, requiring long imaging times as compensation, but may provide quantifiable data. This is an experimental method with few data regarding its utilization in acute or chronic ischaemia.

DSC imaging relies on the intravenous administration of an MR contrast agent. Gadolinium based contrast is injected fast into arm (usually through a pump) and rapid imaging performed immediately before and 1.5 minutes after the injection to capture the first pass of the contrast agent. This imaging is typically susceptibility based and depends on T2* effects. This may be T2 weighted instead, but the signal is not as strong. The passage of an intravascular MR contrast agent through the brain capillaries causes a transient loss of signal because of the T2* effects of the contrast agent. The concentration difference between intravascular and extravascular contrast agent (for intact blood brain barrier) leads to local magnetic field gradient, which in turn results in a decrease of T2* signal. The signal decrease in brain tissue is dependent on perfused cerebral volume and the signal drop in gray matter exceeds that of white matter which in turns appear more hyperintense compared to gray matter (Figure 14). In ischaemic tissue, only a small amount of contrast agent passess throught the capillaries, the signal intensity during bolus maximum passage is even brighter then normally perfused white matter.

The dynamic contrast-enhanced MR perfusion imaging technique involves tracking of the tissue signal changes caused by susceptibility (T2*) effects to create a hemodynamic time–signal intensity curve. The time course of the (relative) contrast agent concentration is calculated using: the relative concentration of the contrast agent in the region of interest or the voxel ($C_{(t)}$), the signal intensity ($S_{(t)}$), and the mean signal intensity (S_0) before the bolus appears within the region of interest.

Figure 14 Signal-time course in normally perfused gray and white matter: The signal drop of gray matter is larger than that of white matter.

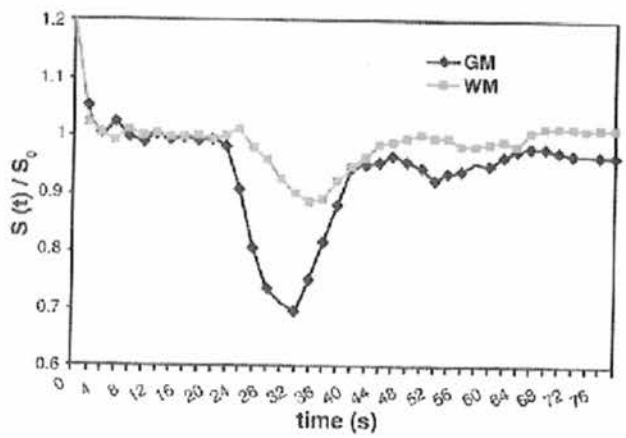

Reproduced from von Kummer R(von Kummer R and Back T 2006)

In the concentration time curve the first pass of the bolus appears after the pre contrast baseline. After the first pass, the concentration does not return to zero, but remains increased. This effect is due to contrast agent molecules remaining within the capillary network and second pass effects. One way to avoid these effects is to fit a gamma-variate function to the measured values of contrast agent concentration (Belliveau *et al.*, 1991).

Semiquantitative parameters

From the concentration time curve several parameters can be calculated. These physiological parameters are used to diagnose and/or monitor pathophysiological processes. These parameters are: cerebral blood volume (CBV) which is defined as an area under concentration/time curve; mean transit time (MTT) defined as first moment of concentration/time curve; the time between contrast agent injection and arrival of the first contrast agent within the region of interest (TTA) also called bolus arrival time (BAT), the time between contrast agent injection and the maximum contrast agent concentration within the region of interest (TTP), maximum concentration value C_{max}; first moment "balancing point" of curve along the time axis (FWHM) "full width half maximum"; and cerebral blood flow (CBF) which is calculated from the knowledge of CBV and MTT as CBV/MTT , Figure 15.

Figure 15. Contrast-time curve showing the different parameters used to estimate perfusion. FWHM first moment "balancing point" of curve along the time axis; Cmax (also known as peak height), TTP (also known as Tmax after deconvolution), and BAT bolus arrival time. AUC indicates area under the curve.

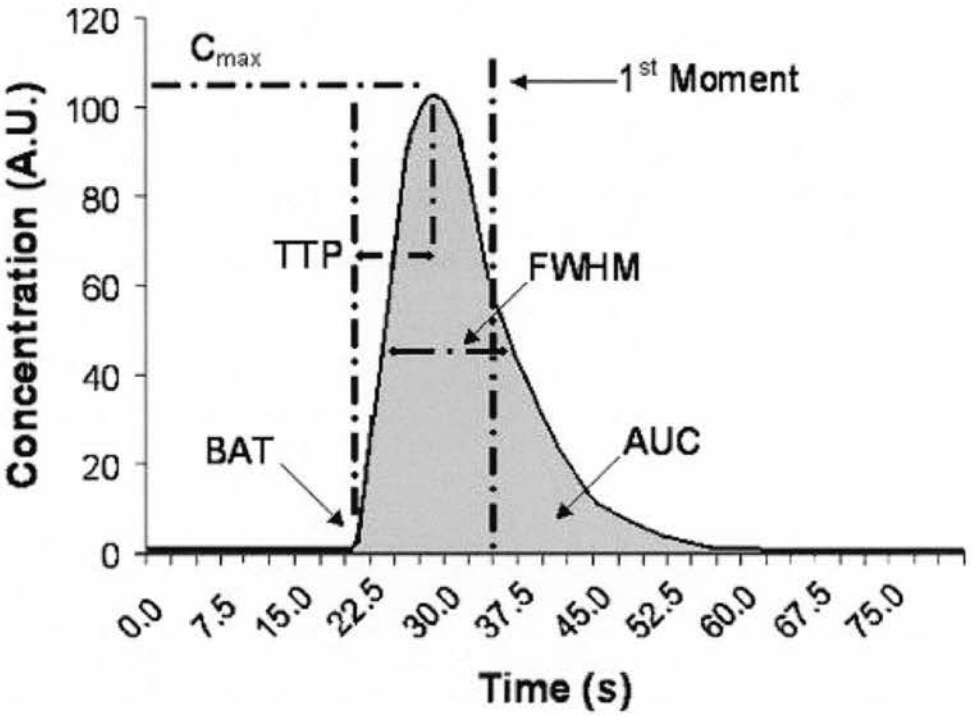

Reproduced from Kane I et al. 2007(Kane et al., 2007a)

Qualitative parameters

In order to obtain quantitative values, the knowledge about the arterial input function (AIF) is required. In DSC imaging with EPI sequences there are usually several slices where major feeding blood vessels can be visualised. The AIF can be measured in both internal carotid arteries (ICA) and middle cerebral arteries (MCA). For practical reasons, the MCA measurements are used most frequently as image data mostly contain these arteries. The voxels that represent the AIF must meet certain criteria; the maximum signal drop is larger, the TTA is shorter and the MTT is lower then the normal brain tissue (Figure 16). With the knowledge of the AIF and the concentration time curve within the tissue, quantitative ("absolute") values of the perfusion parameters can be calculated by deconvolution (Calamante *et al.*, 2002; Ostergaard *et al.*, 1996b; Ostergaard *et al.*, 1996a). Quantitative CBF can be calculated as a height, CBV as the area under the deconvoluted concentration time curve and MTT as a CBV/CBF (Calamante et al.,2002; Ostergaard et al.,1996b;

Ostergaard et al.,1996a). The deconvolution required to produce the quantitative perfusion measurement can be performed in several different ways but the one most frequently used in clinical and research studies is singular value decomposition (SVD)(Ostergaard et al.,1996b; Ostergaard et al.,1996a).

Figure 16. Signal time curves determined in normal tissue and in the feeding arteries (AIF). The signal drop in the arteries is much larger than in tissue.

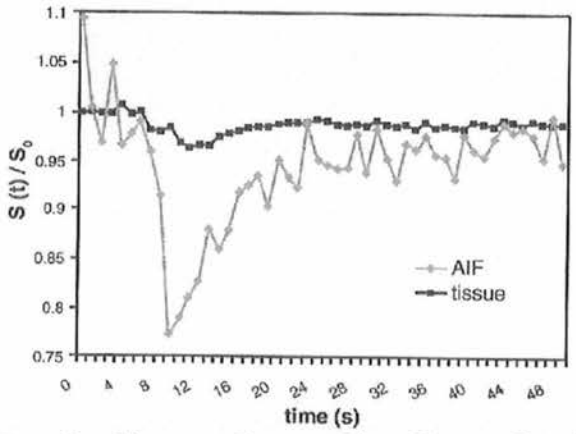

Reproduced from von Kummer R(von Kummer R and Back T2006)

Use of perfusion in diagnosis of ischaemic stroke

Perfusion imaging is used in stroke, both in clinical practice and research. There is a potential for perfusion imaging to identify tissue, not visible by other means, which may go on to infarct without any intervention. Many studies have looked at the changes in perfusion parameters after the acute stroke and the territory that is supplied by the occluded artery can be defined by the changes in MTT, TTP and CBF. Both MTT and TTP are prolonged significantly due to the decline in CBF (Thijs *et al.*, 2002).

The study of 46 patients has compared semi quantitative CBF and MTT and DWI lesion size and final T2 infarct volume at least one month after the stroke who did not receive thrombolysis (Rivers *et al.*, 2006a). The baseline DWI and semi quantitative CBF lesion sizes were not significantly different from final T2 weighted lesion volume, but semi quantitative MTT lesion was significantly larger. The correlation with final T2 weighted volume was strongest for DWI, followed by semi quantitative CBF and weakest for semi quantitative MTT baseline lesion volumes. The results of this study are in agreement with previous studies indicating that MTT

lesions overestimate tissue at risk, and CBF provides a closer estimate of final infarct extent.

Different centres use different ways of analysing perfusion data. Kane at al. assessed ten different perfusion processing methods (Kane *et al.*, 2007a), and showed that different PWI parameters produce very different estimates of abnormal perfusion in the same data from the same patient and therefore, very different estimates of the volume of "tissue at risk." This study showed that relative perfusion parameters performed as well as quantitative ones. Some parameters (mainly representing MTT measures) were correlated with clinical scores, others were correlated with final infarct size, and only arrival time of the contrast (BAT or TTA) was correlated with both. If perfusion is to be used in the selection process of patients that are to be treated then a consensus is required on which perfusion measurement and processing methods should be used.

In addition to problems with use of different processing methods, many studies of perfusion imaging have tried to identify a threshold beyond which the tissue is not salvageable but so far there does not appear to be an MR perfusion threshold that reliably distinguishes between dead and salvageable tissue (Bandera et al.,2006).

Diffusion perfusion mismatch

In the very early stage of ischaemia, the volume of hypoperfused tissue often exceeds the volume of ischaemic core, where tissue injury is irreversible. The core can roughly be delineated by the DWI (Moseley et al.,1990b;Schellinger *et al.*, 2001), and this has led to the concept of the "diffusion – perfusion mismatch." This concept has become synonymous with the "penumbra" (see 1.3.2), reversibly damaged but potentially salvageable tissue if perfusion to the brain is restored. Knowledge of the extent of this salvageable brain would be useful to guide the choice of acute stroke treatment, such as thrombolysis (Hjort *et al.*, 2005). The concept of diffusion perfusion mismatch may be oversimplification of the complex process taking place when blood vessel occludes complicated further by the uncertainties about how to extract perfusion data.

Initial natural history studies supported this simple diffusion perfusion mismatch model by demonstrating that if early reperfusion of the perfusion lesion occurs,

growth of the acute DWI lesion is inhibited (Barber *et al.*, 1998). The duration and extent of the penumbra in humans varies substantially from person to person depending on a variety of factors, including location of the vessel occlusion, degree of collateral blood flow supply, intrinsic susceptibility to ischemia of tissues hypoperfused (eg, gray versus white matter), and other patient-specific factors. Direct visualisation of the tissue at risk would greatly benefit the decision making process which then could be based on the pathophysiological processes rather then arbitrary chronological time windows (Thrombolytic treatment in stroke was until recently licensed up to three hours from onset of symptoms (NINDS 1995), but there is also evidence that it is effective up to 4.5 hours (Hacke et al.,2008) and the licence has been extendeds).

Number of studies found presence of diffusion perfusion mismatch up to 24 hours following stroke (Baird *et al.*, 1997;Beaulieu *et al.*, 1999;Darby *et al.*, 1999;Neumann-Haefelin *et al.*, 1999;Parsons *et al.*, 2001;Schellinger *et al.*, 2000;Sorensen *et al.*, 1999). The volume and presence of mismatch tissue decreases with time, at least 50% of patients have significant tissue at risk after 24 hours from onset of stroke. There have been number of studies of DWI and PWI suggesting that mismatch does predict infarct growth by demonstrating that thrombolysis "rescues" mismatch tissue from infarction (Jansen *et al.*, 1999;Kidwell et al.,2000;Parsons *et al.*, 2002;Schellinger et al.,2000).

However, there are number of challenges to the above described "simple" mismatch concept. The diffusion lesion is not uniform (Guadagno *et al.*, 2004;Nicoli *et al.*, 2003), diffusion lesion (parts of it or whole) is reversible (Chalela *et al.*, 2002;Fiehler *et al.*, 2002;Kidwell et al.,2000;Lutsep *et al.*, 2001;Uno *et al.*, 2000), and perfusion imaging exaggerates the areas of truly ischaemic tissue and includes the area of benign oligaemia (Kidwell et al.,2003a). The model for the salvageable tissue proposed by Kidwell (Kidwell et al.,2003a) is shown in Figure 17

Figure 17. Modified view of MRI-defined ischemic penumbra in which the penumbra equals not only regions of diffusion-perfusion mismatch but also a portion of the diffusion abnormality itself

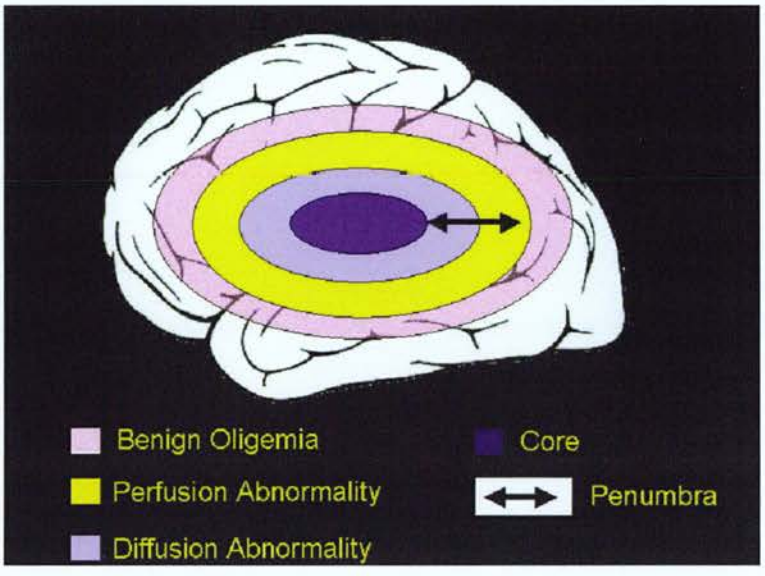

Figure reproduced from Kidwell, C. S. et al.(Kidwell et al.,2003a)

How good is the evidence that mismatch predicts patients with different outcome or who might benefit more from the same treatment as those without mismatch? Systematic review by Kane (Kane et al.,2007b) that looked at mismatch for thrombolysis found that of the methodologically sound studies (total sample size 641 patients), less then half provided the data on outcome. The studies used different mismatch definitions and different perfusion methods. Mismatch (v no mismatch) without thrombolysis was associated with a non-significant twofold increase in the odds of infarct expansion (OR 2.2), which did not change with thrombolysis (OR 2.0). Half of the patients without mismatch also had infarct growth (with or without thrombolysis). No data were available on functional outcome. From these data it cannot be reliably concluded whether thrombolysis changes infarct growth. The mismatch hypothesis was tested in a prospective trial of the echoplanar imaging thrombolysis evaluation trial (EPITHET) which did not confirm lower infarct growth with thrombolysis in mismatch patients but this changed when baseline lesions of less than 5 mL were excluded. More importantly, the functional outcome was the same between the patients that received the thrombolysis and those that did not.

It is possible that mismatch in the future could be used for extending time window for thrombolythic treatment in stroke as there is evidence as discussed earlier that the tissue can survive up to 24 hours. At the same time, there is a need for standardising the mismatch definition before it is more widely used in a clinical practice as well perfusion processing method.

1.4.5 Magnetic Resonance Spectroscopy and Chemical Shift Imaging in stroke

What is MR spectroscopy?

Magnetic resonance spectroscopy (MRS) detects signals from water soluble metabolites and can demonstrate metabolic changes in ischaemic tissue in vivo(Beauchamp, Jr. et al.,1999). MRS can be performed on all nuclei with a spin and depending on the chosen nucleus, different compounds can be detected. The most frequently used nucleus in MRS is hydrogen (proton, ^{1}H) which is abundant in the body. Other nuclei used in MRS are ^{31}P, ^{13}C, ^{15}N, ^{19}F, and ^{23}Na. Of these, ^{31}P has also been used in stroke studies in the evaluation of sources of metabolic energy in the brain, giving insights into the energetic pathways, including, for example ATP and phosphocreatine (PCr). ^{13}C, ^{15}N are at low natural abundance and must be administered as labelled compounds and therefore have not been studied as much. At the strength of the magnetic field used in clinical practice only ^{1}H nuclei shows sufficient sensitivity to be detectable in small volumes within reasonable acquisition time. To be able to acquire signals representing metabolic compounds of interest, the brain water resonance which is the main signal source in ^{1}H-MRS and exceeds the metabolite signal by approximately 10^{4}, has to be suppressed. Special water suppression pulses are added to saturate water signal.

MRS techniques

There are two imaging methods of proton magnetic resonance spectroscopy acquisition: single voxel (SVS) and multivoxel spectroscopy or chemical shift imaging (CSI).

Single voxel spectroscopy

In SVS, the signal is received from a volume limited to a single voxel. This acquisition itself is fairly fast (1 to 3 minutes) and a spectrum is easily obtained, but there are three steps to this method. First, suppression of the water signal; the most commonly used method to suppress the water peak is CHESS (CHEmical Shift Selective). CHESS consists in applying three couples (90° RF pulses + dephasing gradients), one in each spatial direction. The bandwidth of these RF pulses is narrow and centered on the resonance frequency of the water peak in order to saturate the water signal and preserve the signal from the other metabolites. The second step is a selection of the voxel of interest which is done by a succession of three selective radiofrequency pulses (accompanied by gradients) in the three directions in space. These pulses determine three orthogonal planes whose intersection corresponds to the volume studied. Only the signal of this voxel will be recorded, by selecting only the echo resulting from the series of three radiofrequency pulses. Two types of sequence are available; PRESS - Point-RESolved Spectroscopy and STEAM - STimulated Echo Acquisition Mode (Frahm *et al.*, 1989).

In the STEAM the three voxel-selection RF pulses have flip angles of 90°. The stimulated echo is recorded from the cumulated effect of the three pulses, thus corresponding to the signal from the only voxel of interest. The TE of the stimulated echo corresponds to double the time interval between the first two pulses. The delay between the second and third RF pulses is the mix time TM. This technique is particularly adapted to short TE spectral acquisitions.

In the PRESS method, the RF pulses have flip angles of 90° - 180° - 180°. The signal emitted by the voxel of interest is thus a spin echo. The amplitude of this spin echo is two times greater than the stimulated echo obtained by STEAM. The PRESS technique thus offers a better signal-to-noise ratio than STEAM. It can be used with short TE (15 – 20 ms) or long TE (135 – 270 ms)(Figure 18).

Figure 18. Single-voxel pulse sequences: (a) schematic illustration of three orthogonal slice selective pulses. The size and position of the voxel is controlled by the frequency and bandwidth of the slice selective pulses, as well as by the amplitude of the associated slice selective field gradients, (b) STEAM and (c) PRESS. Simplified diagrams are presented which do not show all crusher gradients, gradient lobes and RF pulse shapes.

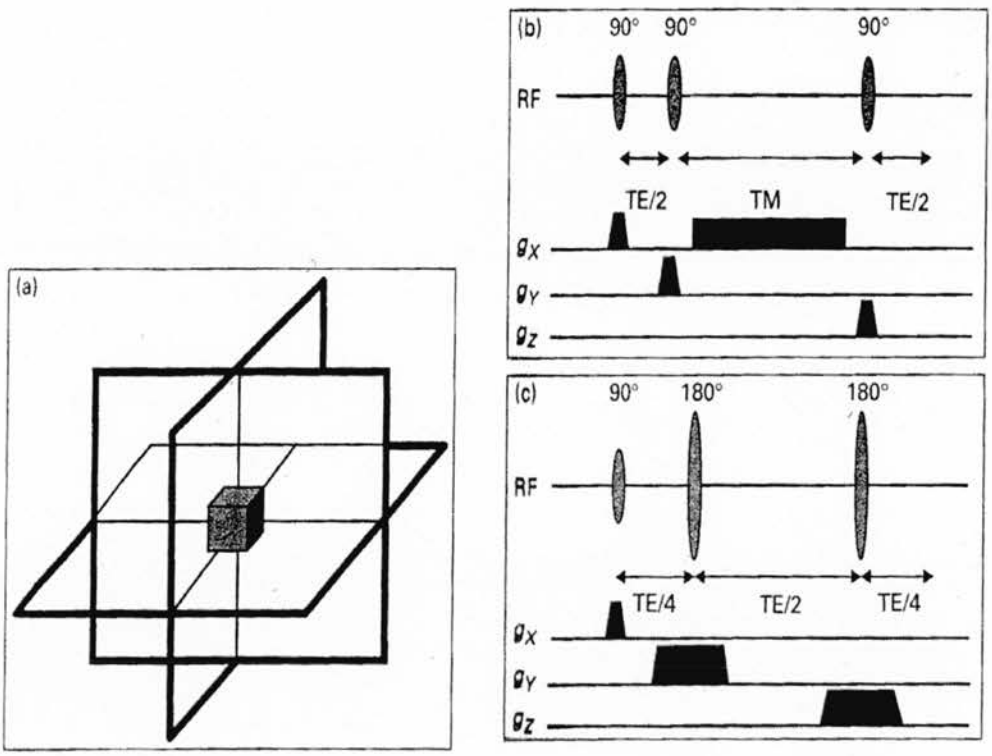

Figure reproduced from P. Barker, Fundamentals of MR spectroscopy in Clinical MR Imaging (Gillard J H et al., 2004)

SVS was frequently used in clinical practice as it is quick to perform, widely available, can be done at short TE and are relatively easy to interpret. However it does have limitations, the most significant one being the lack of ability to determine spatial heterogeneity of spectral patterns and also the fact that only a small number of brain regions can be covered within the constraints of clinical examination. For the example of the single voxel spectra see Figure 19.

Figure 19. Single voxel within a T2 image of the brain slice and examples of spectra from normal and stroke tissue (long TE).

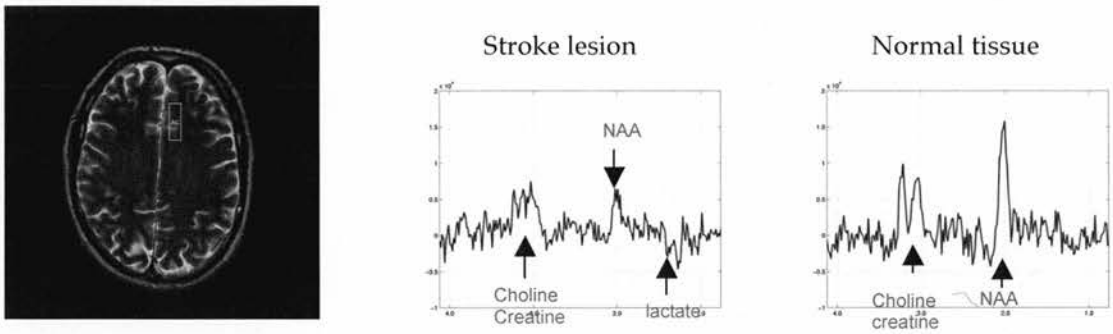

Multivoxel magnetic resonance spectroscopy (MRSI,CSI)

MRSI was developed in an attempt to overcome the problems of SVS. The data is recorded for a group of voxels. The first attempt was by using phase encoding gradient in one direction (Petroff *et al.,* 1992) but this was not enough to show the detail required. The technique was then developed in to two dimensional (2D) by using phase – encoding gradient in two directions (Duyn *et al.,* 1993) and then by using full three-dimensional (3D)encoding (Nelson *et al.,* 1999).

As in single voxel spectroscopy due to small concentration of brain metabolites in comparison to protons in the water, as well as presence of pericranial fat it is essential to perform water and lipid suppression. The most common method of water suppression is to pre-saturate the water signal using frequency selective, 90° pulses – chemical shift selective water suppression (CHESS) pulses (Haase *et al.,* 1985) prior to localization of pulse sequence Figure 20. Good suppression can be achieved by using a combination of more then one pulse and correct flip angle. Lipid signal can be suppressed by using STEAM or PRESS localization to avoid exciting lipid containing regions (see above SVS), but there is also an option of using outer volume suppression (OVS) to pre-saturate lipid signal (Duyn et al.,1993). An inversion pulse can also be used to suppress lipid signal by using the difference in T1 between metabolites and lipids. Using short inversion time will selectively null the lipid signal.

Figure 20. Schematic illustration of pulse sequence for multi- slice MRSI with CHESS water suppression and outer volume saturation bands for lipid suppression (Duyn et al.,1993)(for clarity, not all crusher gradients are illustrated). A slice selective spin-echo sequence is used, with interleaved acquisition (in this example) or four slices within one TR period. (b)The orientation and locations of the eight OVS pulses are schematically illustrated on sagittal and axial views; an octagonal pattern is prescribed in order to saturated as much peri-cranial lipid as possible while signal from grain is un-perturbed. Ideally, sharp profile, high bandwidth pulses (to minimize chemical shift effects) should be used for OVS.

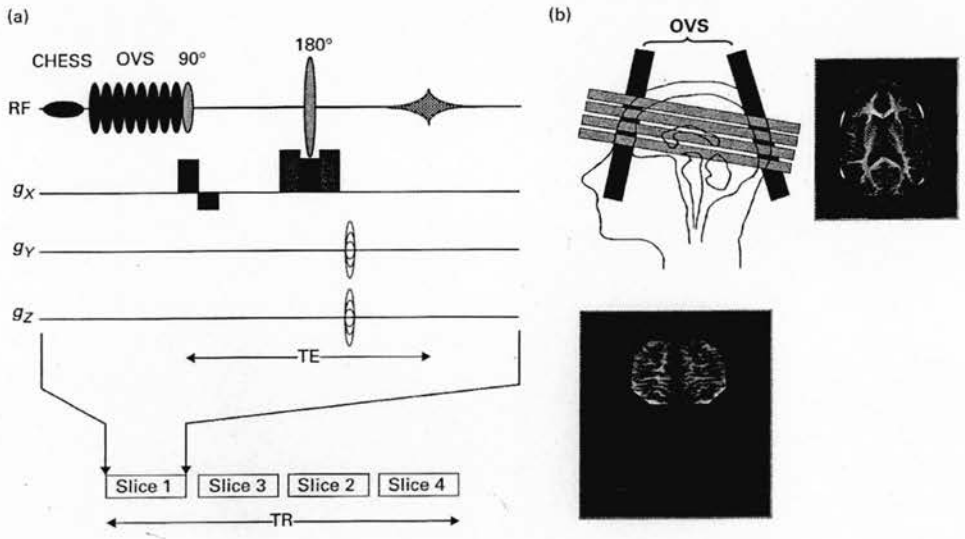

Figure reproduced from P. Barker, Fundamentals of MR spectroscopy in Clinical MR Imaging (Gillard J H et al.,2004)

MRSI is based on a repetition of STEAM or PRESS type sequences to which is added spatial phase encoding. Signal processing uses Fourier transformation and requires data correction. The results appear in the form of parametric images (metabolite maps) or a matrix of the spectra of the region studied.

Figure 21.Brain slice with the CSI grid covering the whole slice. On the right is an example of processed (fitted) spectra with the representative spectra from the normal and stroke tissue.

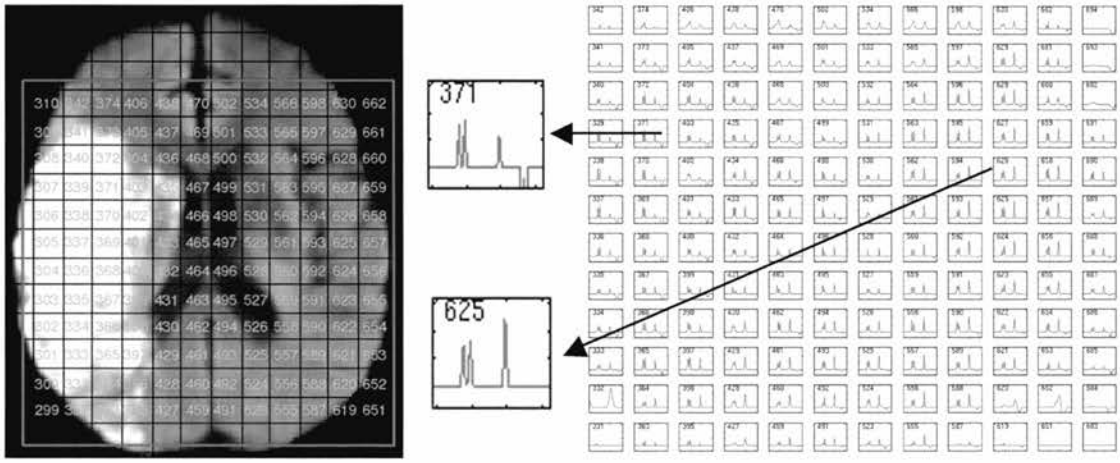

Another essential variable in the acquisition of proton magnetic resonance spectroscopy is the choice of echo time. With short echo times (less than 30 milliseconds), the magnetic resonance spectrum detects larger numbers of metabolites, but it is more likely that peaks will superimpose over each other, causing difficulty in spectroscopic curve interpretation. Macromolecules also cause a complex baseline. Short echo times are indicated for the study of metabolic and diffuse diseases. By using long echo times (more than 135 milliseconds), smaller numbers of metabolites are detected, but with better definition of peaks and better reproducibility. Long echo times are more used in focal brain lesions.

Spectroscopic signal recording does not use a frequency encoding readout gradient, as the frequency is used to constitute the spectrum (rather than the position). Protons in different molecules resonate at slightly different frequencies because the local electron cloud affects the magnetic field experienced by the proton. A Fourier transform is applied to the signal to separate (or resolve) the chemical shifts of different metabolites. Resonant frequencies are expressed in parts per million (ppm) relative to a reference frequency, and the scale reads from right to left. In a proton spectrum at 1.5 T, the metabolites are spread out over a range of approximately 300 Hz (5 ppm).

It takes considerably longer to acquire data for MRSI than the single voxel, but with continuous improvement in the software the acquisition time has reduced significantly (Stengel *et al.*, 2004).

Quality of spectra and technical requirements

In spectroscopy, MR signals correspond to biochemical compounds investigated and these are presented as peaks (also called resonances); MR spectra is with long and short TE is illustrated in Figure 22. Obtaining good quality spectra is not easy and certain technical requirements need to be fulfilled. Shim procedures represent one of the major challenges in clinical MRS, as the separation of resonances requires a field homogeneity exceeding standards known from conventional MRI. A heterogeneous magnetic field leads to resonance frequency dispersion, spreading out the peaks or even causing them to disappear into the background noise. Prior to any MRS acquisition, the magnetic field is homogenized (shimming) in the region of interest. The bigger the region, the harder it is to homogenize the magnetic field throughout. Close to bone, calcifications, hemorrhagic zones or air filled cavities, spectroscopic quality will be poorer due to disruption in the field caused by the differences in magnetic susceptibility compared to soft tissue. The precession frequency of the water must be optimized to adequately suppress the water peak, using selective frequency pulses and dephasing gradients. The other problem with MRS concerns the weak signal-to-noise ratio. This entails multiplying the number of measurements and limits spatial resolution. Spectrum quality is evaluated according to two main criteria: signal-to-noise ratio (height of metabolite peaks in relation to background noise) and spectral resolution (peak width, which determines whether the different metabolites can be separated).
Spectral resolution will depend on the homogeneity of the magnetic field B_0 and on digital resolution, i.e. the precision with which the signal is sampled, determined according to sampling time and the total number of points measured.

Evaluation of metabolite concentration

The accuracy of the metabolite concentration depends on the approach used for data quantification. Generally, the spectrum is evaluated by measuring the area under the metabolite signal peak. This can be done by numerical integration of metabolite

peaks or by using sophisticated tools which perform a nonlinear fit of the entire spectrum. Depending on the tool, it can be done off line (Naressi *et al.*, 2001) or online on the scanner console (Provencher 1993). All methods report signal intensities that are proportional to the metabolite concentrations in the studied volume of interest. Conversion of these hardware specific units to absolute concentrations is not simple and requires a set of correction factors which are dependant on the pulse sequence used, hardware parameters like signal amplification and coil loading, relaxation times (T1, T2) of the metabolites as well as fraction of gray, white matter and CSF in the volume of interest (VOI). Hardware parameters can be corrected for by using either "phantom replacement method" (Michaelis *et al.*, 1993)or scaling relative to the water signal (Barker *et al.*, 1993).
The absolute concentration method is rather cumbersome and not practical for clinical use. The semi quantitative method is much easier to use in the acute setting and the correction for hardware sensitivity can easily be applied.

Also of note is that spectroscopic data are prone to artifacts. If the data are visualised as metabolite maps it is important to be aware of the method used to calculate the maps; are they based on a simple integration of marked metabolite specific regions or on fitting of the spectra. It is also important to be aware of the processing steps involved such as baseline correction or frequency correction before final signal analysis. All these will affect metabolite concentration but cannot be properly evaluated just by looking at the metabolite map. Careful inspection of the entire spectrum is required in order to exclude artifacts, which may have caused apparent concentration change. Lactate metabolite maps are prone to contamination by lipids (from skull base, vault, and orbits) which can be misleadingly interpreted as lactate. If the spectra are carefully analysed, lactate can be distinguished from lipids by its unique doublet signal (two peaks of identical intensity separated by 7.4 Hz) which may be inverted at an ECHO time of 144ms.

The 1H MRS spectrum

The metabolites that can be measured in the brain give rise to different measurable peaks. A change in the resonance intensity of these peaks represents a change in the concentration of the compound.

During the acquisition with long TE the only measurable metabolites are N acetyl aspartate (NAA), creatine (Cr)/phosphocreatin (PCr) and choline (Cho) in normal brain. Lactate is measured during anaerobic metabolism. The acquisition with shorter TE reduces the effect of signal loss due to T2 relaxation and therefore provides spectra with increased signal to noise. In the normal brain, it detects resonances from metabolites with complex MR spectra such as myo-inositol, glutamate, glutamine, and lipids. In addition it also detects succinate, acetate, amino acids acetoacetate, acetone, manitol and ethanol which are not usually detected in the normal brain. The problem with short TE is that in addition to providing more information on metabolites it also includes a broad background signal consisting of low concentration metabolites and macromolecules and lipids with short T2 relaxation times. This complex picture therefore increases the difficulty of accurate peak area estimation.

Figure 22.Proton spectra of the human brain recorded at both (a,b) long (TE 272) and c) short (TE 35ms) TEs, in the long TE spectra from a patient with an acute right middle cerebral artery (MCA) stroke, the normal spectrum (a) from the left hemisphere shows signs from Choline (Cho), Cretine (Cr) and N-acetyl aspartate (NAA). In the short TE spectrum of normal frontal WM (c), in addition to NAA, Crand Cho, signals can be detected from myo-inositol (mI), Glutamate and Glutamine (Glx), and lipids. (a) and (b) are from a multi-slice MR spectroscopic imaging (MRSI) data set(normal voxel size 0.8cm^3), while (c) is recorded from an 8cm^3 single voxel using the Point resolved spectroscopy (PRESS) sequence.

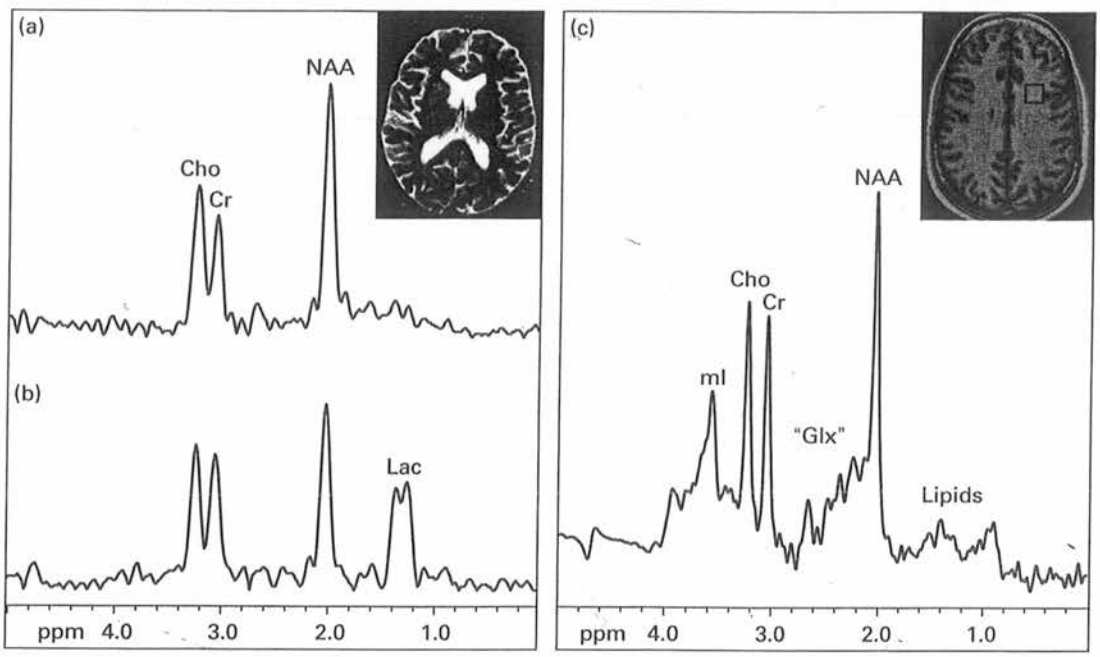

Figure reproduced from P. Barker, Fundamentals of MR spectroscopy in Clinical MR Imaging (Gillard J H et al.,2004)

For the purpose of this thesis I will discuss the metabolites measured in this study at long TE: NAA, Choline, Creatine and lactate.

N acetyl aspartate (NAA)

NAA is found in very high concentrations in the human brain and gives powerful signal when examined with water suppressed proton magnetic resonance spectroscopy (H MRS). The methyl group of NAA resonates at 2.01 ppm producing a large sharp peak. It is second only to glutamate in terms of free amino acid concentrations. The "NAA" signal includes smaller contributions from other acetylated compounds, such as from the neuron-specific dipeptide, N-acetylaspartylglutamate (NAAG)(Caramanos *et al.*, 2005), N- acetylneuraminic acid (Varho *et al.*, 1999), and underlying coupled resonances of glutamate and glutamine. NAA was initially described by Tallan (Tallan et al., 1956;Tallan 1957) but to date, the precise function of NAA is still debated. Various roles have been assigned to NAA in the function of the brain; from being a source of acetyl groups for lipid synthesis, a storage form of acetyl-CoA or aspartate, a breakdown product of NAAG, a regulator of protein synthesis, "molecular water pump" or an osmolyte (Barker 2001). However, NAA is often thought of as a "marker of intact neurons" in the literature on brain imaging in stroke. Immunocytochemical techniques suggest that NAA is mostly localised in the neurons, axons and dendrites of the central nervous system (Simmons et al., 1991). Levels of NAA are reduced or absent in a number of diseases that cause neuronal and or axonal loss such as multiple sclerosis (DeStefano N. et al., 2001), tumour (Goebell et al., 2006) or stroke (Saunders et al., 1995;Wild et al., 2000). NAA's place as a neuronal marker is not completely certain yet. There are reports of NAA being detected in other types of cells such as oligodendrocyte type II astrocyte progenitor cells in rats (Urenjak et al., 1993), but these cells represent only a small proportion of human glial cells (Wolswijk et al., 1991). Also, NAA was identified in mast cells and oligodendroglial preparations (Bhakoo and Pearce 2000) but this work so far has been in vitro and not reproduced in vivo. For now, NAA seems to be the best available marker of neuronal integrity available that can be measured non-invasively.

NAA changes in ischaemic stroke have been discussed in the systematic review (chapter 2) and in the results chapters 4, 5, and 6.

Choline (Cho)

The choline signal resonates at 3.24 ppm and arises from several compounds: glycerophosphocholine, phosphocholine, and a small amount of free choline which is involved in membrane synthesis and degradation. It is often thought of as a marker of membrane damage. In stroke, early studies reported no significant changes in choline concentrations in the ischemic lesion (Fenstermacher and Narayana 1990), but other studies found either an increase (Graham *et al.*, 1992;Sappey-Marinier *et al.*, 1992) or a decrease in choline levels (Duijn *et al.*, 1992;Lanfermann *et al.*, 1995)in stroke lesions. Changes in choline levels have been also reported in other pathological processes such as multiple sclerosis where levels are increased during active disease (Davie *et al.*, 1993)as well as diabetic ketoacidosis (Kreis and Ross 1992), and hepatic encephalopathy where levels are decreased (Kreis *et al.*, 1992).

Creatine

This is a composite signal coming from the two main compounds involved in energy metabolism, creatine and phosphocreatine. Both compounds have signals that resonate at 3.94 ppm (methylene singlet) and 3.03 ppm (methyl singlet). It is impossible to distinguish between the two on MRSI and therefore total creatine/phosphocreatine signal is measured by MRSI. In events such as ischemia, creatine concentration varies with the anaerobic tissue conditions and there is a general decrease in the concentration of creatine in the ischemic lesion (Duijn et al.,1992;Lanfermann et al.,1995). Creatine levels also vary in other brain disorders most of them related to enzyme deficiencies leading to either lack of production or defective transport to the brain (Bizzi *et al.*, 2002). Creatine is present in both neurons and glial cells (Urenjak et al.,1993;Wolswijk et al.,1991).

Lactate

Lactate signal resonates at 1.33 ppm as a doublet. Lactate is not "usually" present in normal human brain. It is produced as a result of anaerobic metabolism, as the end product of glycolysis. When the glycolytic rate exceeds the tissue's capacity to catabolise it or remove it from the blood stream, the concentration of lactate will

rise. Increased lactate has been observed in acute (Gideon *et al.*, 1992;Graham *et al.*, 1993;Muñoz Maniega *et al.*, 2008) and chronic stroke (Muñoz Maniega et al.,2008;Saunders et al.,1995) as well as other conditions such as brain tumours. Small amounts of lactate can be detected in the cerebrospinal fluid (CSF) of normal ageing brain(Sijens *et al.*, 2001). Changes in lactate in acute stroke are further discussed in the systematic review chapter and the results chapters.

Pathophysiological processes visualised by MRSI

Early ischaemic changes can be visualised by using MR diffusion and perfusion imaging but neither of these methods are able to record pathophysiological processes that happen between reduction in blood flow and cell swelling. MRS, however can offer some insight in to pathophysiological events in that critical period following arterial occlusion.

The cascades of events after the arterial occlusion are described earlier in this chapter. Oxygen depletion will induce anaerobic glycolysis, which in turn will cause lactate production, leading to lactate accumulation especially in the presence of hypoperfusion. Lactate accumulation and persisting lack of glucose and oxygen supply will lead to drop in ATP and pH, both of which can be measured by ^{31} P MRS. Drop in ATP will lead to failure of Na^+-K^+ ATPase activity and influx of Na^+ ions which can be monitored by ^{23}Na MRS (Hilal *et al.*, 1983). Influx of Na will lead to development of cytotoxic oedema which can be visualised by DWI. Once neuronal death ensues, monitoring of NAA as a neuronal marker can provide information on viable neurons. There is a considerable overlap between these stages that can be measured by MRSI Figure 23. Whilst it is relatively easy to include HMRS into acute stroke protocol that is not the case for ^{31}P which requires further equipment. ^{23}Na MRS has not been studied in humans.

Figure 23. Pathophysiological stages of ischaemia that can be measured by the MRSI

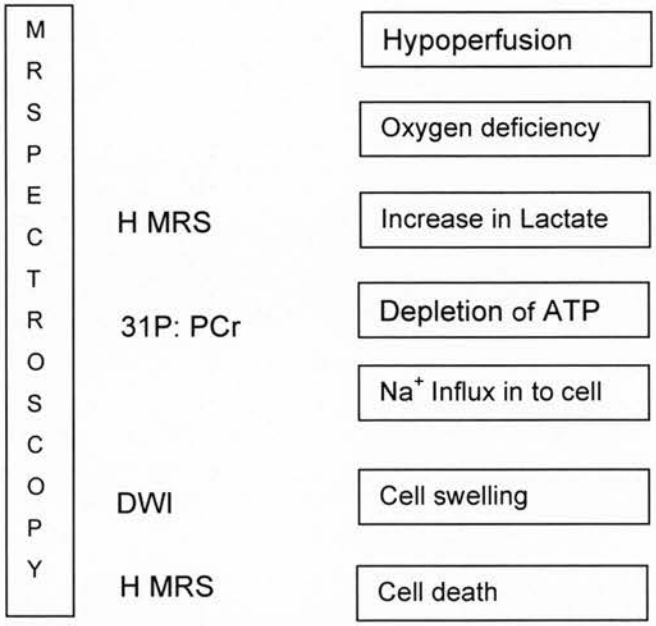

Figure adapted from von Kummer R (von Kummer R and Back T2006)

Application of MRSI in clinical practise

Although H MRSI is relatively fast technique in comparison to ^{31}P spectroscopy, it is still not "fast enough" for a routine use in clinical practice especially in the acutely ill stroke patients. The acquisition time of the MRSI spectra can be as fast as 6 minutes (Stengel et al.,2004), but it still requires significant time for the data processing and would not facilitate immediate decision making in the treatment of acute stroke. Magnetic resonance spectroscopy in stroke is further discussed in the systematic review chapter 2.

Reference List

Albers GW. Diffusion-weighted MRI for evaluation of acute stroke. Neurology 1998; 51(Suppl): S47-S49.

Astrup J, Siesjo BK, Symon L. Thresholds in cerebral ischemia - the ischemic penumbra. Stroke 1981; 12: 723-725.

Ay H, Buonanno FS, Rordorf G, Schaefer PW, Schwamm LH, Wu O et al. Normal diffusion-weighted MRI during stroke-like deficits. Neurology 1999; 52: 1784-1792.

Ay H, Oliveira-Filho J, Buonanno FS, Schaefer PW, Furie KL, Chang YC et al. 'Footprints' of transient ischemic attacks: a diffusion-weighted MRI study. Cerebrovasc Dis 2002; 14: 177-186.

Baird AE, Benfield A, Schlaug G, Siewert B, Lovblad KO, Edelman RR. Enlargement of human cerebral ischemic lesion volumes measured by diffusion-weighted magnetic resonance imaging. Ann Neurol 1997; 41: 581-589.

Baird AE, Warach S. Magnetic resonance imaging of acute stroke. J Cereb Blood Flow Metab 1998; 18: 583-609.

Bamford J, Sandercock P, Dennis M, Burn J, Warlow C. Classification and natural history of clinically identifiable subtypes of cerebral infarction. Lancet 1991; 337: 1521-1526.

Bandera E, Botteri M, Minelli C, Sutton A, Abrams KR, Latronico N. Cerebral blood flow threshold of ischemic penumbra and infarct core in acute ischemic stroke. A systematic review. Stroke 2006; 37: 1334-1339.

Barber PA, Davis SM, Infeld B, Baird AE, Donnan GA, Jolley D et al. Spontaneous reperfusion after ischemic stroke is associated with improved outcome. Stroke 1998; 29: 2522-2528.

Barker PB. N-acetyl aspartate--a neuronal marker? Ann Neurol 2001; 49: 423-424.

Barker PB, Soher BJ, Blackband SJ, Chatham JC, Mathews VP, Bryan RN. Quantitation of proton NMR spectra of the human brain using tissue water as an internal concentration reference. NMR Biomed 1993; 6: 89-94.

Baron JC. Mapping the ischaemic penumbra with PET: implications for acute stroke treatment. Cerebrovasc Dis 1999; 9: 193-201.

Baron JC. Mapping the ischaemic penumbra with PET: a new approach. Brain 2001; 124: 2-4.

Battacharji SK, Hutchinson EC, McCall AJ. The Circle of Willis--the incidence of developmental abnormalities in normal and infarcted brains. Brain 1967; 90: 747-758.

Beauchamp NJ, Jr., Barker PB, Wang PY, vanZijl PC. Imaging of acute cerebral ischemia. Radiology 1999; 212: 307-324.

Beaulieu C. The basis of anisotropic water diffusion in the nervous system - a technical review. NMR Biomed 2002; 15: 435-455.

Beaulieu C, Allen PS. Determinants of anisotropic water diffusion in nerves. Magn Reson Med 1994; 31: 394-400.

Beaulieu C, Allen PS. Water diffusion in the giant axon of the squid: implications for diffusion-weighted MRI of the nervous system. Magn Reson Med 1994; 32: 579-583.

Beaulieu C, Allen PS. An in vitro evaluation of the effects of local magnetic-susceptibility-induced gradients on anisotropic water diffusion in nerve. Magn Reson Med 1996; 36: 39-44.

Beaulieu C, de Crespigny A, Tong DC, Moseley ME, Albers GW, Marks MP. Longitudinal magnetic resonance imaging study of perfusion and diffusion in stroke: evolution of lesion volume and correlation with clinical outcome. Ann Neurol 1999; 46: 568-578.

Belliveau JW, Kennedy DN, Jr., McKinstry RC, Buchbinder BR, Weisskoff RM, Cohen MS et al. Functional mapping of the human visual cortex by magnetic resonance imaging. Science 1991; 254: 716-719.

Bhakoo KK, Pearce D. In vitro expression of N-acetyl aspartate by oligodendrocytes: implications for proton magnetic resonance spectroscopy signal in vivo. J Neurochem 2000; 74: 254-262.

Bizzi A, Bugiani M, Salomons GS, Hunneman DH, Moroni I, Estienne M et al. X-linked creatine deficiency syndrome: a novel mutation in creatine transporter gene SLC6A8. Ann Neurol 2002; 52: 227-231.

Calamante F, Gadian DG, Connelly A. Quantification of perfusion using bolus tracking magnetic resonance imaging in stroke: assumptions, limitations, and potential implications for clinical use. Stroke 2002; 33: 1146-1151.

Caramanos Z, Narayanan S, Arnold DL. 1H-MRS quantification of tNA and tCr in patients with multiple sclerosis: a meta-analytic review. Brain 2005; 128: 2483-2506.

Chalela JA, Ezzeddine MA, Calabrese TM, Latour LL, Baird AE, Luby ML et al. Diffusion and perfusion changes two hours after intravenous rt-PA therapy: A preliminary report. Stroke 2002; 33: 356-357.

Cinnamon J, Viroslav AB, Dorey JH. CT and MRI diagnosis of cerebrovascular disease: going beyond the pixels. Semin Ultrasound CT MR 1995; 16: 212-236.

CLARKE E. APOPLEXY IN THE HIPPOCRATIC WRITINGS. Bull Hist Med 1963; 37:301-14.: 301-314.

Darby DG, Barber PA, Gerraty RP, Desmond PM, Yang Q, Parsons M et al. Pathophysiological topography of acute ischemia by combined diffusion-weighted and perfusion MRI. Stroke 1999; 30: 2043-2052.

Davie CA, Hawkins CP, Barker GJ, Brennan A, Tofts PS, Miller DH et al. Detection of myelin breakdown products by proton magnetic resonance spectroscopy. Lancet 1993; 341: 630-631.

Davis SM, Donnan GA, Parsons MW, Levi C, Butcher KS, Peeters A et al. Effects of alteplase beyond 3 h after stroke in the Echoplanar Imaging Thrombolytic Evaluation Trial (EPITHET): a placebo-controlled randomised trial. Lancet Neurol 2008; 7: 299-309.

DeLaPaz RL, Mohr JP. Magnetic resonance scanning. In: Barnett HJ, Mohr JP, Stein BM, Yatsu FM, editors. Stroke. Pathophysiology, diagnosis, and management. 1998. p. 227-57.

Demougeot C, Marie C, Giroud M, Beley A. N-acetylaspartate: a literature review of animal research on brain ischemia. J Neurochem 2004; 90: 783.

DeStefano N., Narayanan S, Francis GS, Arnaoutelis R, Tartaglia MC, Antel JP et al. Evidence of axonal damage in the early stages of multiple sclerosis and its relevance to disability. Arch Neurol 2001; 58: 65-70.

Duijn JH, Matson GB, Maudsley AA, Hugg JW, Weiner MW. Human brain infarction: proton MR spectroscopy. Radiology 1992; 183: 711-718.

Duyn JH, Gillen J, Sobering G, van Zijl PC, Moonen CT. Multisection proton MR spectroscopic imaging of the brain. Radiology 1993; 188: 277-282.

Fenstermacher MJ, Narayana PA. Serial proton magnetic resonance spectroscopy of ischemic brain injury in humans. Invest Radiol 1990; 25: 1034-1039.

Fiehler J. ADC and metabolites in stroke: even more confusion about diffusion? Stroke 2003; 34: 6-7.

Fiehler J, Foth M, Kucinski T, Knab R, von Bezold M, Weiller C et al. Severe ADC decreases do not predict irreversible tissue damage in humans. Stroke 2002; 33: 79-86.

Fisher M. Current review of Cerebrovascular Disease. Boston: Butterworth Heineman; 1999.

Fisher M. Characterizing the target of acute stroke therapy. Stroke 1997; 28: 866-872.

Fisher M, Sotak CH, Minematsu K, Li L. New magnetic resonance techniques for evaluating cerebrovascular disease. Ann Neurol 1995; 32: 115-122.

Frahm J, Michaelis T, Merboldt KD, Hanicke W, Gyngell ML, Chien D et al. Localized NMR spectroscopy in vivo. Progress and problems. NMR Biomed 1989; 2: 188-195.

Fuster V, Badimon J, Chesebro JH, Fallon JT. Plaque rupture, thrombosis, and therapeutic implications. Haemostasis 1996; 26 Suppl 4:269-84.: 269-284.

Gideon P, Henriksen O, Sperling B, Christiansen P, Olsen TS, Jorgensen HS et al. Early time course of N-acetylaspartate, creatine and phosphocreatine, and compounds containing choline in the brain after acute stroke. A proton magnetic resonance spectroscopy study. Stroke 1992; 23: 1566-1572.

Gillard J H, Waldman A D, Barker PB. Clinical MR Neuroimaging, Diffusion, Perfusion and Spectroscopy. Cambridge: Cambridge University Press; 2004.

Goebell E, Fiehler J, Ding XQ, Paustenbach S, Nietz S, Heese O et al. Disarrangement of fiber tracts and decline of neuronal density correlate in glioma patients--a combined diffusion tensor imaging and 1H-MR spectroscopy study. AJNR Am J Neuroradiol 2006; 27: 1426-1431.

Graham GD, Blamire AM, Howseman AM, Rothman DL, Fayad PB, Brass LM et al. Proton magnetic resonance spectroscopy of cerebral lactate and other metabolites in stroke patients. Stroke 1992; 23: 333-340.

Graham GD, Blamire AM, Rothman DL, Brass LM, Fayad PB, Petroff OA et al. Early temporal variation of cerebral metabolites after human stroke. A proton magnetic resonance spectroscopy study. Stroke 1993; 24: 1891-1896.

Guadagno JV, Warburton EA, Aigbirhio FI, Smielewski P, Fryer TD, Harding S et al. Does the acute diffusion-weighted imaging lesion represent penumbra as well as core? A combined quantitative PET/MRI voxel-based study. J Cereb Blood Flow Metab 2004; 24: 1249-1254.

Haase A, Frahm J, Hanicke W, Matthaei D. 1H NMR chemical shift selective (CHESS) imaging. Phys Med Biol 1985; 30: 341-344.

Hacke W, Hennerici M, Gelmers HJ, Kramer G. Applied anatomy of the cerebral arteries. In: Hacke W, Hennerici M, Gelmers HJ, Kramer G, eds, editors. Cerebral Ischaemia. Berlin: Springer-Verlag; 1989. p. 1-16.

Hacke W, Albers G, Al Rawi Y, Bogousslavsky J, Davalos A, Eliasziw M et al. The Desmoteplase in Acute Ischemic Stroke Trial (DIAS): a Phase II MRI-based 9-hour window acute stroke thrombolysis trial with intravenous desmoteplase. Stroke 2005; 36: 66-73.

Hacke W, Kaste M, Bluhmki E, Brozman M, Davalos A, Guidetti D et al. Thrombolysis with alteplase 3 to 4.5 hours after acute ischemic stroke. N Engl J Med 2008; 359: 1317-1329.

Hasegawa Y, Formato JE, Latour L, Gutierrez JA, Liu K-F, Garcia JH et al. Severe transient hypoglycemia causes reversible change in the apparent diffusion coefficient of water. Stroke 1996; 27: 1648-1656.

Heiss WD, Huber M, Fink GR, Herholz K, Pietrzyk U, Wagner R et al. Progressive derangement of periinfarct viable tissue in ischemic stroke. J Cereb Blood Flow Metab 1992; 12: 193-203.

Heiss WD, Rosner G. Functional recovery of cortical neurons as related to degree and duration of ischemia. Ann Neurol 1983; 14: 294-301.

Hendrikse J, van der GJ, Lu H, van Zijl PC, Golay X. Flow territory mapping of the cerebral arteries with regional perfusion MRI. Stroke 2004; 35: 882-887.

Hilal SK, Maudsley AA, Simon HE, Perman WH, Bonn J, Mawad ME et al. In vivo NMR imaging of tissue sodium in the intact cat before and after acute cerebral stroke. AJNR Am J Neuroradiol 1983; 4: 245-249.

Hjort N, Butcher K, Davis SM, Kidwell CS, Koroshetz WJ, Rother J et al. Magnetic resonance imaging criteria for thrombolysis in acute cerebral infarct. Stroke 2005; 36: 388-397.

Jansen O, Schellinger PD, Fiebach JB, Hacke W, Sartor K. Early recanalisation in acute ischaemic stroke saves tissue at risk defined by MRI. Lancet 1999; 353: 2036-2037.

Kane I, Carpenter T, Chappell F, Rivers C, Armitage P, Sandercock P et al. Comparison of 10 different magnetic resonance perfusion imaging processing methods in acute ischemic stroke. Effect on lesion size, proportion of patients with diffusion/perfusion mismatch, clinical scores, and radiologic outcomes. Stroke 2007; 38: 3158-3164.

Kane I, Sandercock P, Wardlaw J. Magnetic resonance perfusion diffusion mismatch and thrombolysis in acute ischaemic stroke: a systematic review of the evidence to date. J Neurol Neurosurg Psychiatry 2007b; 78: 485-491.

Kapoor K, Singh B, Dewan LI. Variations in the configuration of the circle of Willis. Anat Sci Int 2008; 83: 96-106.

Karaszewski B, Wardlaw JM, Marshall I, Cvoro V, Wartolowska K, Haga K et al. Measurement of brain temperature with magnetic resonance spectroscopy in acute ischaemic stroke. Ann Neurol 2006; 60: 438-446.

Keir SL. The identification of haemorrhagic and ischaemic stroke by neuroimaging: present practice and future needs. Edinburgh University; 2002. p. 135-45.

Keith W Muir, Alastair Buchan, Rudiger von Kummer, Joachim Rother, Jean-Claude Baron. Imging of acute stroke. 2006. p. 755-68.

Kidwell CS, Alger JR, Saver JL. Beyond mismatch: evolving paradigms in imaging the ischemic penumbra with multimodal magnetic resonance imaging. Stroke 2003; 34: 2729-2735.

Kidwell CS, Saver JL, Mattiello J, Starkman S, Vinuela F, Duckwiler G et al. Thrombolytic reversal of acute human cerebral ischemic injury shown by diffusion/perfusion magnetic resonance imaging. Ann Neurol 2000; 47: 462-469.

Kreis R, Ross BD. Cerebral metabolic disturbances in patients with subacute and chronic diabetes mellitus: detection with proton MR spectroscopy. Radiology 1992; 184: 123-130.

Kreis R, Ross BD, Farrow NA, Ackerman Z. Metabolic disorders of the brain in chronic hepatic encephalopathy detected with H-1 MR spectroscopy. Radiology 1992; 182: 19-27.

Kristian T, Siesjo BK. Calcium in ischemic cell death. Stroke 1998; 29: 705-718.

Kucinski T, Vaterlein O, Glauche V, Fiehler J, Klotz.E., Eckert B et al. Correlation of apparent diffusion coefficient and computed tomography density in acute ischemic stroke. Stroke 2002; 33: 1786-1791.

Labelle M, Khiat A, Durocher A, Boulanger Y. Comparison of metabolite levels and water diffusion between cortical and subcortical strokes as monitored by MRI and MRS. Invest Radiol 2001; 36: 155-163.

Lammie GA. Pathology of small vessel stroke. British Medical Bulletin 2000; 56: 296-306.

Lanfermann H, Kugel H, Heindel W, Herholz K, Heiss W-D, Lackner K. Metabolic changes in acute and subacute cerebral infarctions: findings at proton MR spectroscopic imaging. Radiology 1995; 196: 203-210.

Lansberg MG, Norbash AM, Marks MP, Tong DC, Moseley ME, Albers GW. Advantages of adding diffusion-weighted magnetic resonance imaging to conventional magnetic resonance imaging for evaluating acute stroke. Arch Neurol 2000; 57: 1311-1316.

Leenders KL, Perani D, Lammertsma AA, Heather JD, Buckingham P, Healy MJ et al. Cerebral blood flow, blood volume and oxygen utilization. Normal values and effect of age. Brain 1990; 113 (Pt 1): 27-47.

Lemesle M, Walker P, Guy F, D'Athis P, Billiar T, Giroud M et al. Multi-variate analysis predicts clinical outcome 30 days after middle cerebral artery infarction. Acta Neurol Scand 2000; 102: 11-17.

Libby P. Molecular and cellular mechanisms of the thrombotic complications of atherosclerosis. J Lipid Res 2009; 50 Suppl:S352-7. Epub;%2008 Dec 18.: S352-S357.

Lutsep HL, Nesbit GM, Berger RM, Coshow WR. Does reversal of ischemia on diffusion-weighted imaging reflect higher apparent diffusion coefficient values? Journal of Neuroimaging 2001; 11: 313-316.

Marchal G, Beaudouin V, Rioux P, de IS, V, Le Doze F, Viader F et al. Prolonged persistence of substantial volumes of potentially viable brain tissue after stroke: a correlative PET-CT study with voxel-based data analysis. Stroke 1996; 27: 599-606.

Marchal G, Benali K, Iglesias S, Viader F, Derlon JM, Baron JC. Voxel-based mapping of irreversible ischaemic damage with PET in acute stroke. Brain 1999; 122 (Pt 12): 2387-2400.

Michaelis T, Merboldt KD, Bruhn H, Hanicke W, Frahm J. Absolute concentrations of metabolites in the adult human brain in vivo: quantification of localized proton MR spectra. Radiology 1993; 187: 219-227.

Monsein LH, Mathews VP, Barker PB, Pardo CA, Blackband SJ, Whitlow WD et al. Irreversible regional cerebral ischemia: serial MR imaging and proton MR spectroscopy in a non-human primate model. Am J Neuroradiol 2008; 14: 963-970.

Moseley ME, Butts K, Yenari MA, Marks M, de Crespigny A. Clinical aspects of DWI. NMR Biomed 1995; 8: 387-396.

Moseley ME, Cohen Y, Kucharczyk J, Mintorovitch J, Asgari HS, Wendland MF et al. Diffusion-weighted MR imaging of anisotropic water diffusion in cat central nervous system. Radiology 1990a; 176: 439-445.

Moseley ME, Kucharczyk J, Asgari HS, Norman D. Anisotropy in diffusion-weighted MRI. Magn Reson Med 1991; 19: 321-326.

Moseley ME, Kucharczyk J, Mintorovich J, Cohen Y, Kurhanewicz J, Derugin N. Diffusion-weighted MR imaging of acute stroke: correlation with T2-weighted and magnetic susceptibility-enhanced MR imaging in cats. Am J Neuroradiol 1990b; 11: 423-429.

Muñoz Maniega S, Cvoro V, Chappell FM, Armitage PA, Marshall I, Bastin ME et al. Changes in NAA and lactate following ischemic stroke: a serial MR spectroscopic imaging study. Neurology 2008; 71: 1993-1999.

Naressi A, Couturier C, Castang I, de BR, Graveron-Demilly D. Java-based graphical user interface for MRUI, a software package for quantitation of in vivo/medical magnetic resonance spectroscopy signals. Comput Biol Med 2001; 31: 269-286.

Neil JJ, Duong TQ, Ackerman JJ. Evaluation of intracellular diffusion in normal and globally-ischemic rat brain via 133Cs NMR. Magn Reson Med 1996; 35: 329-335.

Nelson SJ, Vigneron DB, Dillon WP. Serial evaluation of patients with brain tumors using volume MRI and 3D 1H MRSI. NMR Biomed 1999; 12: 123-138.

Neumann-Haefelin T, Wittsack HJ, Wenserski F, Siebler M, Seitz RJ, Modder U et al. Diffusion- and perfusion-weighted MRI. The DWI/PWI mismatch region in acute stroke. Stroke 1999; 30: 1591-1597.

Nicoli F, Lefur Y, Denis B, Ranjeva JP, Confort-Gouny S, Cozzone PJ. Metabolic counterpart of decreased apparent diffusion coefficient during hyperacute ischemic stroke: a brain proton magnetic resonance spectroscopic imaging study.[see comment]. Stroke 34(7):e82-7, 2003.

NINDS. Tissue plasminogen activator for acute ischemic stroke. The National Institute of Neurological Disorders and Stroke rt-PA Stroke Study Group. N Engl J Med 1995; 333: 1581-1587.

Oppenheim C, Logak M, Dormont D, ricy S, Mana&#x00EF, R et al. Diagnosis of acute ischaemic stroke with fluid-attenuated inversion recovery and diffusion-weighted sequences. Neuroradiology 2000; 42: 602-607.

Ostergaard L, Sorensen AG, Kwong KK, Weisskoff RM, Gyldensted C, Rosen BR. High resolution measurement of cerebral blood flow using intravascular tracer bolus passages. Part II: Experimental comparison and preliminary results. Magn Reson Med 1996a; 36: 726-736.

Ostergaard L, Weisskoff RM, Chesler D, Gyldensted C, Rosen BR. High resolution measurement of cerebral blood flow using intravascular tracer bolus passages. Part I: mathematical approach and statistical analysis. Magn Reson Med 1996b; 36: 715-725.

Paczynski R., Hsu CY, Diringer MN. Pathophysiology of ischaemic injury. In: Fisher M,editor. Boston: Butterworth-Heinemann; 1995. p. 29-64.

Parsons MW, Barber PA, Chalk J, Darby DG, Rose S, Desmond PM et al. Diffusion- and perfusion-weighted MRI response to thrombolysis in stroke. Ann Neurol 2002; 51: 28-37.

Parsons MW, Li T, Barber PA, Yang Q, Darby DG, Desmond PM et al. Combined 1H MR spectroscopy and diffusion-weighted MRI improves the prediction of stroke outcome. Neurology 2000; 55: 498-505.

Parsons MW, Yang Q, Barber PA, Darby DG, Desmond PM, Gerraty RP et al. Perfusion magnetic resonance imaging maps in hyperacute stroke: relative cerebral blood flow most accurately identifies tissue destined to infarct. Stroke 2001; 32: 1581-1587.

Patel MR, Edelman RR, Warach S. Detection of hyperacute primary intraparenchymal hemorrhage by magnetic resonance imaging. Stroke 1996; 27: 2321-2324.

Petroff OAC, Graham GD, Blamire AM, al Rayess M, Rothman DL, Fayad PB et al. Spectroscopic imaging of stroke in humans: Histopathology correlates of spectral changes. Neurology 1992; 42: 1349-1354.

Powers WJ. Cerebral hemodynamics in ischemic cerebrovascular disease. Ann Neurol 1991; 29: 231-240.

Powers WJ. Acute hypertension after stroke: the scientific basis for treatment decisions. Neurology 1993; 43: 461-467.

Provencher SW. Estimation of metabolite concentrations from localized in vivo proton NMR spectra. Magn Reson Med 1993; 30: 672-679.

Rivers CS, Wardlaw JM. What has diffusion imaging in animals told us about diffusion imaging in patients with ischaemic stroke? Cerebrovasc Dis 2005; 19: 328-336.

Rivers CS, Wardlaw JM, Armitage P, Bastin ME, Carpenter TK, Cvoro V et al. Do acute diffusion- and perfusion- weighted MRI lesions identify final infarct volume in ischemic stroke? Stroke 2006a; 37: 98-104.

Rivers CS, Wardlaw JM, Armitage PA, Bastin M, Carpenter T, Cvoro V et al. Persistent infarct hyperintensity on diffusion-weighted imaging late after stroke indicates heterogeneous, delayed, infarct evolution. Stroke 2006b; 37: 1418-1423.

Sager TN, Hansen AJ, Laursen H. Correlation between N-acetylaspartate levels and histopathologic changes in cortical infarcts of mice after middle cerebral artery occlusion. J Cereb Blood Flow Metab 2000; 20: 780-788.

Sager TN, Laursen H, Hansen AJ. Changes in N-acetyl-aspartate content during focal and global brain ischemia of the rat. J Cereb Blood Flow Metab 1995; 15: 639-646.

Sappey-Marinier D, Calabrese G, Hetherington HP, Fisher SN, Deicken R, Van Dyke C et al. Proton magnetic resonance spectroscopy of human brain: applications to normal white matter, chronic infarction, and MRI white matter signal hyperintensities. Magnetic Resonance in Medicine 1992; 26: 313-327.

Saunders DE, Howe FA, van den BA, McLean MA, Griffiths JR, Brown MM. Continuing ischemic damage after acute middle cerebral artery infarction in humans demonstrated by short-echo proton spectroscopy. Stroke 1995; 26: 1007-1013.

Schaefer PW, Grant PE, Gonzalez RG. Diffusion-weighted MR imaging of the brain. Radiology 2000; 217: 331-345.

Schellinger PD, Fiebach JB, Jansen O, Ringleb PA, Mohr A, Steiner T et al. Stroke magnetic resonance imaging within 6 hours after onset of hyperacute cerebral ischemia. Ann Neurol 2001; 49: 460-469.

Schellinger PD, Jansen O, Fiebach JB, Heiland S, Steiner T, Schwab et al. Monitoring intravenous recombinant tissue plasminogen activator thrombolysis for acute ischemic stroke with diffusion and perfusion MRI. Stroke 2000; 31: 1318-1328.

Siesjo BK, Katsura K, Kristian T. Acidosis-related damage. Adv Neurol 1996; 71: 209-233.

Sijens PE, den HT, de Leeuw FE, de Groot JC, Achten E, Heijboer RJ et al. MR spectroscopy detection of lactate and lipid signals in the brains of healthy elderly people. Eur Radiol 2001; 11: 1495-1501.

Simmons ML, Frondoza CG, Coyle JT. Immunocytochemical localization of N-acetyl-aspartate with monoclonal antibodies. Neuroscience 1991; 45: 37-45.

Sorensen AG, Copen WA, Ostergaard L, Buonanno FS, Gonzalez RG, Rordorf G et al. Hyperacute stroke: simultaneous measurement of relative cerebral blood volume, relative cerebral blood flow, and mean tissue transit time. Radiology 1999; 210: 519-527.

Stengel A, Neumann-Haefelin T, Singer OC, Neumann-Haefelin C, Zanella FE, Lanfermann H et al. Multiple spin-echo spectroscopic imaging for rapid quantitative assessment of N-acetylaspartate and lactate in acute stroke. Magnetic Resonance in Medicine 52(2):228-38, 2004.

Strong JP. Atherosclerosis in the young: risk and prevention. Hosp Pract (Minneap) 1999; 34: 15-16.

Sudlow CLM, Warlow CP. Comparable studies of the incidence of stroke and its pathological types. Results from an international collaboration. Stroke 1997; 28: 491-499.

Tallan HH. Studies on the distribution of N-acetyl-L-aspartic acid in brain. J Biol Chem 1957; 224: 41-45.

Tallan HH, Moore S, Stein WH. N-Acetyl-L-aspartic acid in brain. J Biol Chem 1956; 219: 257-264.

Thijs VN, Adami A, Neumann-Haefelin T, Moseley ME, Albers GW. Clinical and radiological correlates of reduced cerebral blood flow measured using magnetic resonance imaging. Arch Neurol 2002; 59: 233-238.

Tsai G, Coyle JT. N-acetylaspartate in neuropsychiatric disorders. Prog Neurobiol 1995; 46: 540.

Ulug AM, Beauchamp N, Jr., Bryan RN, van, Zijl PC. Absolute quantitation of diffusion constants in human stroke. Stroke 1997; 28: 483-490.

Uno M, Harada M, Okada T, Nagahiro S. Diffusion-weighted and perfusion-weighted magnetic resonance imaging to monitor acute intra-arterial thrombolysis. Journal of Stroke & Cerebrovascular Diseases 2000; 9: 113-120.

Urenjak J, Williams SR, Gadian DG, Noble M. Proton nuclear magnetic resonance spectroscopy unambiguously identifies different neural cell types. J Neurosci 1993; 13: 981-989.

van der Zwan A., Hillen B, Tulleken CA, Dujovny M. A quantitative investigation of the variability of the major cerebral arterial territories. Stroke 1993; 24: 1951-1959.

van der Zwan A., Hillen B, Tulleken CA, Dujovny M, Dragovic L. Variability of the territories of the major cerebral arteries. J Neurosurg 1992; 77: 927-940.

van Laar PJ, Hendrikse J, Golay X, Lu H, van Osch MJ, van der GJ. In vivo flow territory mapping of major brain feeding arteries. Neuroimage 2006; 29: 136-144.

van Laar PJ, Hendrikse J, Klijn CJ, Kappelle LJ, van Osch MJ, van der GJ. Symptomatic carotid artery occlusion: flow territories of major brain-feeding arteries. Radiology 2007; 242: 526-534.

Varho T, Komu M, Sonninen P, Holopainen I, Nyman S, Manner T et al. A new metabolite contributing to N-acetyl signal in 1H MRS of the brain in Salla disease. Neurology 1999; 52: 1668-1672.

von Kummer R, Back T. Magnetic Resonance Imaging in Ischaemic Stroke. Berlin-Heidelberg: Springer; 2006.

W.C.Dickinson. Dependence of the F19 Nuclear Resonance Position on Chemical Compound. 1950. p. 736.

Warach S, Chien D, Li W, Ronthal M, Edelman RR. Fast magnetic resonance diffusion-weighted imaging of acute human stroke. Neurology 1992; 42: 1717-1723.

Warach S, Gaa J, Siewert B, Wielopolski P, Edelman RR. Acute human stroke studied by whole brain echo planar diffusion-weighted magnetic resonance imaging. Ann Neurol 1995; 37: 231-241.

Wardlaw JM. What pathological type of stroke is it,cerebral ischaemia or haemorrhage? In: Warlow C, van Gijn J, Dennis M et al, editors. Stroke. Practical management. Oxford. Blackwell Science; 2008. p. 181.

Wardlaw JM, Doubal F, Armitage P, Chappell F, Carpenter T, Munoz MS et al. Lacunar stroke is associated with diffuse blood-brain barrier dysfunction. Ann Neurol 2009; 65: 194-202.

Wardlaw JM, Farrall A, Armitage PA, Carpenter T, Chappell F, Doubal F et al. Changes in background blood-brain barrier integrity between lacunar and cortical ischemic stroke subtypes. Stroke 2008; 39: 1327-1332.

Warlow C, van Gijn J, Dennis M et al. Stroke Practical Management. Oxford: Blackwell Publishing; 2008.

Waxman S.G. Vascularization. In: Butler J, Lebowitz H, editors. Correlative Neuroanatomy. New York: McGraw/Hill; 2000. p. 168-87.

Wild JM, Wardlaw JM, Marshall I, Warlow CP. N-acetylaspartate distribution in proton spectroscopic images of ischemic stroke: relationship to infarct appearance on T2-weighted magnetic resonance imaging. Stroke 2000; 31: 3008-3014.

Wolswijk G, Munro PM, Riddle PN, Noble M. Origin, growth factor responses, and ultrastructural characteristics of an adult-specific glial progenitor cell. Ann N Y Acad Sci 1991; 633:502-4.: 502-504.

Yoneda Y, Tokui K, Hanihara T, Kitagaki H, Tabuchi M, Mori E. Diffusion-weighted magnetic resonance imaging: Detection of ischemic injury 39 minutes after onset in a stroke patient. Ann Neurol 1999; 45: 794-797.

Chapter 2: Spectroscopy in the last 20 years – literature review

---

In the previous chapter I have described the anatomy and pathophysiological processes relevant to the patients in this study. I have also described all of the imaging sequences used to study this population.

In this chapter, I will discuss the evidence and findings from spectroscopic imaging in human stroke, especially in relation to diffusion and perfusion imaging.

2.1 Background

Recent advances in neuroimaging and development of new techniques, such as diffusion and perfusion imaging, have raised hopes of quickly and accurately identifying tissue at risk in the acute ischaemic stroke. This, in turn, would help identify patients who would benefit the most from the acute stroke treatments. However, no consistent perfusion threshold has so far distinguished dead from salvageable tissue reliably.

Proton magnetic resonance spectroscopy (MRS) is a non-invasive in-vivo method which is used to visualise metabolic abnormalities in the brain. MRS can potentially lead to better understanding of the pathophysiology of the ischaemic stroke, which helps us target potentially dangerous treatments more appropriately, thus reducing the risk of side effects. MRS has evolved from being a very slow method, covering only a limited area of the brain with often poor signal to noise ratio (and therefore not practical to be used in the every day clinical practice), to a much more efficient technique (data can be acquired within six minutes) which covers one or more slices of brain. This increases the chances of performing spectroscopic imaging in acutely ill stroke patients (although not always possible) and has the potential to help us unravel the metabolic changes in acute stroke which might increase detection of dead versus at risk tissue.

2.2 Aim and methods

One of the aims of this review is to determine whether the data published so far is sufficient to establish the role of MRS technique in every day clinical practice. In addition, it examines what information there is on the levels and the distribution of metabolites in the acute stroke and their temporal evolution, as well as the relationship of metabolite levels with blood flow, diffusion imaging (DWI) and final outcome.

2.2.1 Methods

The review was conducted according to the methods used by the Cochrane Database of Systematic Reviews.

Search strategy

An electronic search of all published records of MR Spectroscopy in stroke was preformed using the electronic databases MEDLINE and EMBASE from 1980 to 2009. Reference lists of the relevant articles were also checked manually (see Appendix 1 for the search strategy).

Selection criteria

All prospective and retrospective studies that had well defined population group with ischaemic stroke were included. Other types of stroke were excluded. Only original articles were selected. Case reports and studies that appeared only in abstract form were excluded. All patients had Proton magnetic resonance spectroscopy (HMRS) in addition to any other imaging (data on phosphorus (P), sodium (Na) and carbon (C) spectroscopy was not collected). Only data on humans with stroke were included.

Data extracted:

- Main purpose of the study
- Stroke severity / subtype
- How the diagnosis of stroke was made and by whom
- Time from onset/ diagnosis to scanning was recorded and any follow up that has been arranged. If no arranged follow up, then timing of any follow up was noted and its range
- Outcome data if available
- Relationship of MRS findings to clinical outcome (short or long term)
- Relationship of MRS to other imaging modalities such as DWI/ PI
- Metabolites measured and change in metabolite concentration if followed up
- Image analysis (whether the reader was blinded to clinical data and other imaging modalities).

For each trial, the number of patients was recorded including their age and sex.
Quality score (*based on type of the study, blinding to image analysis and final outcome, systematic follow up, who made the diagnosis, validated spectroscopy technique and description of patient population*) was applied to each paper. (Appendix 2)

The studies selected for the review were subdivided according to the time from onset to the imaging. The times were specified as follows; Acute stroke (within 24 hours of onset), subacute stage (mean time less then one week but included patients within first 24 hours from the onset of symptoms), subacute stage (mean time around one week but did not include the patients within first 24 hours of onset) and the chronic stage (included patients with strokes older then 1 month).
The studies that investigated the time course of metabolites were subdivided in to those that followed the patients up from onset to three months and those that followed them up longer (up to 17 months). In addition studies were also divided in to those that investigated the core of the lesion and the area around it, also studies that compared the metabolites to the blood flow and diffusion imaging and the final outcome. The rationale for this subdivision of the studies in this way was due to significant diversity of the studies and rather loose description of the terms acute and subacute.

2.2.2 Results

The initial search identified 2985 articles using systematic search strategy. After excluding animal studies, reviews, case reports, studies that did not measure metabolites within the stroke lesion and non-English language publications, there were 39 original papers (761 patients) included. Some of the patients were possibly included twice (separate publications by the same author analysing data in a different way) therefore the actual number of unique patients is fewer (Graham *et al.*, 1995).

2.2.3 Studies quality

Only two studies met all the quality criteria (Parsons *et al.*, 2002f;Wardlaw *et al.*, 1998). Another six studies met at least 5/7 criteria (Federico *et al.*, 1996; Federico *et al.*, 1998; Lemesle *et al.*, 2000; Liu *et al.*, 2003; Parsons *et al.*, 2000; Pereira *et al.*, 1999). Only one study was retrospective (Graham et al.,1995). However, due to different study designs, not all the quality criteria were necessarily applicable to all the studies. Design of the studies varied enormously. Initial studies were usually very small or even case reports, mostly concentrating on the feasibility of the technique in the acute setting, but also reporting the findings of MRS. Some of the larger studies looked at the possibility of predicting the outcome by using metabolites, either with or without combining other MR sequences. Several studies used different ways of measuring blood flow and only eight studies, in addition to conventional MR imaging, also used DWI sequence. I have reported all the data available on N Acetyl aspartate (NAA) and lactate and their relation to the acute lesion as shown on T2 or DWI, blood flow and outcome.

2.3 N-Acetyl Aspartate (NAA)

It is widely accepted that NAA is a marker of intact neurons (see Chapter1) as suggested by the balance of evidence. When the tissue NAA content is reduced it is suggestive of neuronal or axonal loss. Therefore, in stroke, NAA can be used as a surrogate marker for neuronal function and integrity and, if temporal measurements available, a degree of stroke progression and severity. All studies

that measured NAA were categorised according to timing and then the time course if available was reviewed.

2.3.1 NAA levels within the stroke lesion

Although quite a few studies investigated "acute" stroke, timing of the scans from the onset of symptoms were widely varied. Only seven studies included patients before 24 hours. Significant number of studies included patients from the onset up to a week in the acute stroke group.

2.3.2 NAA within 24 hours

Seven studies (73 patients in total) measured the metabolites in patients within 24 hours (Felber *et al.*, 1992; Gillard *et al.*, 1996; Labelle *et al.*, 2001; Liu et al.,2003; Nicoli *et al.*, 2003; Parsons et al.,2000; Stengel *et al.*, 2004). The studies had different aims; using metabolites to estimate prognosis (Parsons et al.,2000), to diagnose acute and chronic stroke (Felber et al.,1992), exploratory (Barker *et al.*, 1994; Gillard et al.,1996; Stengel et al.,2004), examining pathophysiological processes in acute stroke (Liu et al.,2003;Labelle et al.,2001) and comparison to other imaging (Nicoli et al.,2003). Half of the studies measured metabolites from a single voxel placed within the lesion and the other half used a CSI technique (Table1). Also, most studies (six of them) used a ratio to express the concentration of NAA with denominators including: choline (2), creatine (1), contralateral normal (2), sum of metabolites in the acute lesion (1) and one used absolute metabolite (Table 1). The prognostic study did not comment on the ratio of NAA to Choline but only looked at its prognostic value and neither did comparative study, but expressed the result as a correlation, therefore no actual metabolite values were reported. Interestingly, two studies that use the ratio to contralateral side report exactly the same reduction in NAA in the stroke lesion with a ratio of 6.3. All studies agreed that NAA was reduced within the lesion as visualised on T2 and DWI, in the first 24 hours measured either by the ratio or absolute values.

Table 1. NAA within the lesion in the first 24 hours from the onset of stroke

Author	*Aim of the study*	*Hours from onset*	*Mean +/-SD*	*Number patients*	*MRS method*	*Results reporting (ratio vs absolute)*	*Result NAA*
Felber et al.,1992	Diagnosis of acute stroke	4-8	5.8	8	Single voxel	Ratio to choline	decreased NAA in all patients. Mean ratio 1.2
Gillard et al.,1996	Exploratory and feasibility	2-24h	12 hours	11	Single voxel	Ratio to contralateral creatine	Mean ratio within the lesion 0.6
Parsons *et al.*, 2000	Prognostic	3-22	11	19	Single voxel	Ratio to choline	1.84
Labelle et al.,2001	Pathophysiology	5.25-24	17.3+/-6	14	Single voxel	Ratio to contralateral NAA	0.63
Liu et al.,2003	Pathophysiology	0-6		25	CSI	Ratio to contralateral normal	0.63
Nicoli et al.,2003	Comparative to diffusion imaging	3.5-7	5	6	CSI	Ratio to sum of metabolites within the lesion	NAA/sum vs ADC r2=o.48 (p<0.0001) (NAA values not given)
Stengel et al.,2004	Exploratory (new faster CSI technique)	0-6 h 6-24h	7.2+/-5.1	10	CSI	Absolute values in mmols	6.7+/- 1.6 (0-6 hours) 4.8 +/- 1.4 mmol/l (6-24hours) Compared to lactate increase, NAA tended to drop at the slower rate. Severe NAA reduction within ADC lesion found only in 2 cases.

2.3.3 NAA within the lesion in the first week from stroke

Fourteen studies measured metabolites in the patients from onset (within hours) up to maximum of 1 week (Federico et al.,1996; Federico et al.,1998; Gideon *et al.*, 1992; Gideon *et al.*, 1994; Graham *et al.*, 1993; Houkin *et al.*, 1993; Lauriero *et al.*, 1996; Lemesle et al.,2000; Pereira et al.,1999; Rumpel *et al.*, 2001; Saunders *et al.*, 1995; Stengel et al.,2004; Wardlaw et al.,1998; Wild *et al.*, 2000). Although some of these studies measured NAA within 24 hours of onset of symptoms, it was not possible to group them in to the category of <24 hours as all the data was analysed together including the patients at later times.

The aims of the studies were different; assessing contribution of metabolites to estimate prognosis (5), measuring the longitudinal changes in metabolites (4), comparative to other imaging parameters (4) and the feasibility of the technique (1). For the method of acquiring spectroscopy data and the way the results were expressed see Table 2. All of the studies show reduction of NAA within the lesion. Two studies did not report actual values but commented on NAA reduction and reported the association with outcome. Twelve studies reported numerical values, eight as a ratio and four as an absolute value. The four studies that used ratio of NAA to contralateral side had the results ranging from 0.42 - 0.51. It is difficult to compare this to the other ratios that were done to a different standard (eg water), choline and/or creatine (see Table 2). The studies that reported absolute values (although they may not be necessarily comparable) range from 2.8-8.9 (for the units see Table 2). These levels of NAA appear lower then the studies that reported the NAA level within 24 hours from the onset of symptoms although the methods used to quantify the NAA may have differed. All studies commented that the reduction in NAA was significant

.

Table 2. NAA from onset to one week

Author	*Aim of the study*	*Days from onset*	*Mean +/-SD*	*No patients*	*MRS method*	*Results reporting*	*Result NAA*
Gideon et al.,1992	Temporal variation & comparative	6 hours - 2.16 days		8	Single voxel	Relative to water	Reduction in NAA from 5-52 hours significantly Mean 1.75
Houkin et al.,1993	Temporal variation	< 48 hours (2 or 3 exams in 48 h)	No exact time	6	Single voxel	Ratio to contralateral NAA	Exact number not given but significant fall 12 h -24h – 48h Est 0.5 - - - - - ~ 0.1
Graham et al. 1993	Temporal variation & prognostic	11hours - 2.5 days	30.6+/- 5.3	8	Single voxel, multiple voxels measured	Ratio to external standard (10 mMol)	Reduction in NAA in all but 2 patients 2.2+/-0,37
Gideon et al.,1994	Prognostic	6hours – 2 days	28h	6	Single voxel	Absolute and ratio to Cho and Cr	Absolute 6.03 Ratio to Cho 1..3 Ratio to Cr 1.46 Reduced within the lesion
Saunders *et al.*, 1995	Temporal variation & defining penumbra	4.8 hours - 1.16 days	0.8 days	10	Single voxel	Absolute values	8.8 +/- 4.3 Significant reduction cw contralateral side(14.7+/- 1.6)
Lauriero F et al. 1996	Comparative and exploratory	1-3 days 7-19 days		10 4	Single voxel	Ratio to contralateral NAA	0.42+/-0.11
Federico F et al. 1996	Prognostic	1-7	2.97	14	Single voxel	Ratio to contralateral NAA	0.43+/-0.17

Table 2 Continued. NAA from onset to one week

Author	*Aim of the study*	*Days from onset*	*Mean +/-SD*	*No patients*	*MRS method*	*Results reporting*	*Result NAA*
Wardlaw et al. 1998	Exploratory & comparative	0-4 days	Not availab le	17	Mix of CSI & single voxel	Ratio to contralateral NAA	Loss of NAA in first 4 days assoc with large infarcts
Federico *et al.*, 1998	Prognostic	7.2 hours - 7 days	3.5+/- 2.1	26	Single voxel	Ratio to contralateral NAA	Significant reduction in NAA, NAAr=0.43+/-0.17
Pereira *et al.*, 1999;	Prognostic	0-3 days	Not availab le	31	Single voxel	Absolute values	8.9+/3.9(independent) 2.8+/-3.5(dependent) 4.2+/- 4.2(dead)=p=0.005
Lemesle M et al. 2000	prognostic	1-5 days	3.7+/- 1.2	77	Mix of single voxel and CSI	Ratio to Cho and contralateral side	5.5+/-3.2
Wild JM et al. 2000	Exploratory and comparative	1-3 days	1.8	11	CSI	Absolute values in institutional units	Core lesion 5.78
Rumpel *et al.*, 2001	Comparison to ADC values	18 hours-3.6 days	1.87 days	15	Single voxel	Ratio to contralateral NAA	NAA ratio mean=0.51
Stengel et al.,2004	Exploratory of the new technique	6 hous - 2 days	7.2+/- 5.1	10	CSI	Absolute	4.8 +/- 1.4 mmol/l Severe NAA reduction in ADC lesion only in 2 cases

2.3.4 NAA within the lesion in the first two weeks from stroke

Five of the studies measured NAA from onset up to 2 weeks, including a total of 89 patients (one patient was scanned at 19 days) (Graham *et al.*, 1992; Graham et al.,1995; Graham *et al.*, 2001; Marshall and Sellar 1994; Mathews *et al.*, 1995). The studies had different aims and the majority were single voxel spectroscopy acuisition (see table 3). The three studies that reported actual values were expressed as a ratio to the contralateral side. The values ranged from 0.21-0.62. The bottom value of the range is smaller then the previous category, but overall the values are quite similar.The other two studies measured NAA value in absolute units, but only one study reported the actual value at 5.5.

Table 3. NAA from onset to two weeks

Author	*Aim of the study*	*Days from onset*	*Mean +/- SD*	*No patient*	*MRS method*	*Results reporting (ratio vs absolute)*	*Result NAA*
Graham G et al. 1992	Follow up	2-19	7.7	16	CSI(10 voxels)	Ratio to contralateral NAA	0.62
Marshall I 1994	Exploratory	<2 weeks		6	Single voxel	Ratio to contralateral NAA	0.21+/-0.22
Mathews *et al.*, 1995	Feasibility	2h-10 days	4 days	14	Single voxel	Absolute values	NAA reduced 5.5+/-3.2
Graham *et al.*, 1995	Correlation with clinical outcome	0-19 days	4.9 days	32	Multi voxel	Ratio to contralateral NAA	0.57; NAA corr with lesion volume, +ve corr with BI
Graham *et al.*, 2001	Temporal evolution and evaluation of short TE	3-10	Not available	21	Single voxel	Absolute units (arbitrary)	NAA values not given but significantly reduced cw contralat

2.3.5 NAA within the lesion from one day to six weeks

Only three studies measured metabolites between one day and 42 days (Demougeot *et al.*, 2002; Fenstermacher and Narayana 1990; Lanfermann *et al.*, 1995). None of the three studies included patients within 24 hours. The studies had a similar aim, mostly exploring the ischaemic lesion with spectroscopy (Table 4). Two studies used CSI method for data acquisition and one of the studies was single voxel. Two studies reported the ratio of NAA either to contralateral side or to choline. However one study did not report numerical value but reduction in NAA within the lesion, as defined on T2 weighted MRI. The values of NAA (ratio to contralateral side) were from 0.2 – 0.73 in the large and small infarcts respectively. The range of these values is similar to the previous category that measured NAA up to two weeks. In the study that used the ratio to Choline it was reported as 1.0.

Table 4. NAA between 1 and 42 days

Author	*Aim of the study*	*Days from onset*	*Mean +/- SD*	*No patient*	*MRS method*	*Results reporting (ratio vs absolute)*	*Result NAA*
Lanferman H et al. 1995	Exploratory	1-35 days	12.1+/-10.1	18	CSI	Ratio to contralateral NAA	small 0.73+/-0.28 large 0.2+/-0.08
Fenstermacher MJ 1990	Follow up study pathophysiology	3-24	11.75	4	Single voxel	Ratio to contralateral NAA	Reduction in NAA within T2 lesion
Demougeot C et al. 2002	exploratory	1-42	7.9+/-9.1	25	CSI	Ratio to contralateral Cho	1.0 +/- 0.3

2.3.6 NAA within the lesion in the chronic stage (mean of one to fifteen months)

Chronic stage for the purpose of grouping the data was defined from one month onward. Only six studies included patients at the chronic stage (Duijn *et al.*, 1992; Felber et al.,1992; Kamada *et al.*, 1997b; Ford *et al.*, 1992; Kamada *et al.*, 1997a; Sappey-Marinier *et al.*, 1992). Some of the studies at the chronic stage are part of evaluation of metabolite change over time, but the actual values of the metabolites in the chronic stage will also be discussed in this section.

Four studies included patients over a year since the onset of stroke (Table 5). They show that NAA is present within the lesion, but reduced compared to the contralateral side. Only one study had patients with a completely absent NAA. All studies reported the result as a ratio but only three used a ratio to the contralateral side. The ranges of values were from 0.23-0.63. It is not possible to analyse the data separately for the studies that included patients >1 year due to different way of the results reporting.

Table 5. NAA in the chronic stage of the infarction

Author	*Aim*	*Days from onset*	*Mean +/- SD*	*MRS method*	*No of patients*	*(ratio vs absolute)*	*Result NAA*
Duijn et al. 1992	exploratory	5-1400 days (only 2 infarcts <200 days)	461.5	Single voxel	10	Ratio to contralateral NAA	Significantly reduced 0.23+/- 0.08
Felber et al. 1992	Diagnostic	8 months-6 years-		Single voxel	8	Ratio to Choline	Reduced signal 1.6-2.3 (1.9 mean)
Ford et al. 1992	Exploratory	37-154 days	81.8	CSI	4	Ratio to creatine	Reduced; 1.4
Sapey-Marinier et al. 1992	exploratory	90-450 days	365+/- 120 days	Single voxel	7	Ratio to creatine and NAA	NAA reduced by 30%
Lauriero F et al. 1996	Comparative and exploratory	90-210 days		Single voxel	14 (21 overall)	Ratio to contralateral NAA	0.43+/-0.11
Kamada et al. 1997a	comparative	180-940 days	293.9 (median)	Single voxel	16	Ratio to choline	Reduced or absent
Kamada et al. 1997 b	Comparative (metabolites vs magneto-ence phalography (MEG))	7-93 days	29.2	Single voxel	11	Ratio to normal NAA from the occipital lobe	Reduced NAA within the lesion 0.63 +/- 0.23

2.3.7 NAA outside the MRI visible lesion

A number of studies had a specific aim to investigate the distribution of metabolites in the core of the lesion, as defined on T2 or DWI, and around it whilst others noted the varied distribution as part of a different aim (see Table 6). All together, seven studies investigated metabolites across the stroke lesion and around it (Gideon et al.,1992; Wild et al.,2000; Gillard et al.,1996; Stengel et al.,2004; Labelle et al.,2001; Demougeot et al.,2002; Kamada et al.,1997b).

The majority of the patients were recruited within 24 hours, two studies having the mean time of 1.8 and 7.9 days and one study with more chronic strokes of a mean of 29.2 days. All together there were 83 patients in the studies. Only two studies used diffusion weighted imaging for visualising the lesion (Labelle et al.,2001; Stengel et al.,2004). Both studies recruited patients within 24 hours but in both studies the NAA levels were similar within and outside the DWI lesion.

Five studies found only minimal reduction in NAA outside the T2 lesion. Only one study by Demougeot (that included patients at the considerably later time point) showed more significant reduction outside the T2 abnormality compared to contralateral normal tissue (but still significantly higher then within the T2 core lesion). The study by Kamada that also included more chronic patients gave no numerical data but commented that NAA outside the lesion was slightly reduced.

Table 6. NAA in symptomatic hemisphere outside visible lesion onT2 or DWI MRI

Author	*Aim of the study*	*Time from onset*	*Mean +/- SD*	*No of pateints*	*MRS method*	*ratio vs absolute*	*Result NAA*
Gideon et al. 1992	Longitudinal and comparative to CBF	6-52h		8	Single voxel	Absolute and ratio	NAA loss more pronounced in central then outer part of **T2 lesion**
Wild et al. 2000	exploratory	1-3 days	1.8days	11	CSI	absolute	Little evidence of neuronal loss beyond **T2 lesion**
Gillard et al. 1996	exploratory	0.08-1 days	0.5 days	11	Single voxel	Ratio to contralateral NAA	Slight reduction of NAA outside **T2**; significantly less then core but not sig to contralateral; core (mean) 0.66; around 0.87
Stengel et al. 2004	Exploratory-new technique	2-24h	7.2+/-5.1	10	CSI	Absolute value	No significant reduction of NAA outside **ADC lesion**
Labelle et al. 2001	Temporal observational, comparing cortical vs lacunar stroke	5.5-24h	17.3+/-6h	7 each group	Single voxel	Ratio to contralateral NAA	No significant decrease in NAA outside **DWI lesion**
Demougeot et al. 2002	exploratory	1-42 days	7.9+/-9.1	25	CSI	Ratio to Cho	Reduction of NAA outside the **T2 lesion** Core 1.0+/-0.3 Outside 1.3+/-0.3 Contralat 1.8+/-0.3
Kamada et al. 1997 b	Comparative	7-93	29.2	Single voxel	11	Ratio to contralateral NAA (internal standards)	Reduced NAA outside **T2 lesion** (not detected in all patients)

2.3.8 Time course of NAA

Out of 37 studies of MRS in stroke, 19 looked at the time course of metabolites, either as primary or secondary aim. Only a few studies had predetermined time follow up points, but frequently did not manage to recruit in all pre set time points. Often, the metabolites reported were from different patients scanned at different time points.

The studies were grouped in to those with short and intermediate follow up (mainly up to a month and 3 months), and long term (up to a year or longer). I have excluded one study from this discussion at the outset, as the data on NAA was not presented in the right format due to different aim of the study (Parsons et al.,2000).

Time course of NAA from onset to three months

Nine studies (114 patients) followed the NAA from onset up to three months (Lanfermann et al.,1995; Gideon et al.,1992; Houkin et al.,1993; Graham et al.,1993; Saunders et al.,1995; Wardlaw et al.,1998; Liu et al.,2003; Labelle et al.,2001; Fenstermacher and Narayana1990). One study only followed the patients up for 10 days (Rumpel et al.,2001).

All of the studies show initial reduction in NAA. There seemed to be at least two temporal patterns. Although the timing of the second scan is varied, it seems that the majority of the reduction in NAA happened after the first 24 to 52 hours, and then a further reduction occurred up to a week. One study that scanned patients frequently in the first week noted reduction in the first two days, but then further reduction on day three and four. A similar pattern is seen in one study that followed the patients up for 10 days only. None of the studies showed recovery of NAA up to a month, and in one study that followed patients up to three months, there was a partial recovery of NAA in 2/7 patients. Extrapolating slightly from the data, it is possible that NAA falls markedly after hyperacute phase, 24-48 hours. It then continues to fall up to a week but at a slower rate.

The second pattern is more varied and shows all three possible variations with increase, decrease and no change in the level of NAA; in one study the initial scan was performed within the first four days, but it is not clear if the subsequent

measurements were taken at 5-10 days or 10-31 days. Finally, one study showed partial recovery of NAA in the period of three weeks to two months (see Table 7).

Table 7. Time course of NAA from onset up to three months.

Author	*Aim of the study*	*Follow up period*	*Patient selection*	*No of patients*	*MRS method*	*ratio vs absolute*	*Result NAA*
Lanfermann et al.,1995	exploratory	1-35 days	Different patient scanned at different time points.	20	CSI	Ratio to contralateral NAA	NAA reduced but no measurable dependence on the time between onset of infarct and signal intensity. NAA reduced in the first week and stayed low.
Gideon et al.,1992	Temporal variation & comparative	<1 day 1 week 2-4 weeks	Patients scanned in the prespecified times	8	Single voxel	Relative to water	Reduction in NAA from 5-52 hours significantly (data from different patients). No further change at 1 and 2-4 weeks. Mean NAA acutely 1.75
Houkin et al.,1993	Temporal variation	< 2 days Every 1-2 w (for 5 w)	Patients scanned in the prespecified times	6	Single voxel	Ratio to contralateral NAA	Followed up in the same 6 patients NAA sig. dropped from first 6h -48 (almost undetectable). NAA remained depressed but present at follow up stage
Graham et al. 1993	Temporal variation & prognostic	<2.5 days 8-17 days	6/8 patients scanned in the prespecified times	8	Single voxel (multiple voxels measured	Ratio to external standard (10 mMol)	NAA declined significantly between 2 time points (29%, p=0.02), but only if measured in the voxel with max lesion lactate. Not across whole lesion.

Table 7 continued. Time course of NAA from onset up to three months.

Author	*Aim of the study*	*Follow up period*	*Patient selection*	*No of patients*	*MRS method*	*ratio vs absolute*	*Result NAA*
Saunders et al. 1995	Temporal variation	<1 day 7-10 days 3 months	Patients scanned in the prespecified times	10 (7 follow up)	Single voxel	Absolute values	NAA fell significantly from day 1 to day 7-10. Partial recovery to 3 months seen in 2/7 patients.
Wardlaw et al. 1998	Exploratory & comparative	0-4 days 5-10 days 10-31 days	Patients scaned in the prespecified times	34 17 9	Mix of CSI & single voxel	Ratio to contralateral NAA	Wide range of NAA between initial and follow up scan, 3 trends: fell in 5, increased in 5 and remained the same in 8. NAA measured on T2.
Liu et al. 2003	Temporal variation & comparative & difference watershed vs teritorial	<6 hours 6h-<2days 3-4 days 7-9 days 10-15 days 30-31 days	Not all patients scanned at all time points including hyperacute	16 territorial 9 water-shed	Single voxel	Ratio to contralateral NAA	NAA in territorial infarcts decreased to half its value in 2 days (from hyperacute decrease). Further reduction to day 3-4.Remained at that level to 30 days with no recovery. In watershed infarct much lower decrease but downward trend up to 30 days.

Table 7 continued. Time course of NAA from onset up to three months.

Author	*Aim of the study*	*Follow up period*	*Patient selection*	*No of patients*	*MRS method*	*ratio vs absolute*	*Result NAA*
Labelle et al.2001	Temporal variation &comparison of cortical and lacunar strokes	< 1day 7 days 30 days	Same patients followed up	14 (7cortical, 7 subcortical)	Single voxel	Ratio to contralateral NAA	In DWI lesion of cortical infarct significant reduction of NAA in <24h by 37% and to 59% by 1 week. No further significant reduction at 1 month. In subcortical strokes, smaller reduction, 21% <24 h, 24% 1 week, 32% 1 month.
Fensterma cher et al 1990	Temporal variation & exploratory	3-24h 20-69days	Patients scanned at different time points	4	Single voxel	Ratio to contralateral NAA	In T2 lesion original reduction of NAA was observed with subsequent partial recovery in 3 patients and one patient having the same level (scanned 2 days apart)
Rumpel *et al.*, 2001	Comparative	18-88hours 4-10 days	Same patients scanned but not all	6/15 followed up	Single voxel	Ratio to contralateral NAA	NAA ratio mean=0.51; 4.5 day FU(4 pt) mean=0.48 9.5 day FU (2pt) NAA ratio mean=0.36

Long term temporal variation of NAA

Ten studies measured metabolites from the acute or subacute stage right through to the chronic stage (from three months to over a year, and in some cases several years) (Federico et al.,1996; Federico et al.,1998; Felber et al.,1992; Ford et al.,1992; Gideon et al.,1994; Graham et al.,1992; Graham et al.,2001; Lauriero et al.,1996; Rutgers *et al.,* 2000; Walker *et al.,* 2004). All 10 studies confirmed the variability of NAA and several possible patterns; levels staying the same as in subacute stage, further declining or in some cases increasing as well as increasing and declining again. Five out of 10 studies concluded that the levels stay the same as in subacute stage; three studies show gradual increase and recovery after three months. Two studies described both trends with some patients continuing to decline and others partially recovering. Only one patient showed temporary increase and then decline in NAA.

Table 8. NAA temporal variation from onset to 17 months

Author	Aim of the study	Follow up period	Patient selection	No of patients	MRS method	ratio vs absolute	Result NAA
Graham et al.,1992	Temporal and spatial variation	2-19days From 20 – 251days	Patients followed up at varied time points	16 total 6 followed up	Single voxel & CSI	Ratio to contralateral NAA	Initial decline in NAA in all subjects. Average NAA up to 3/12 was 0.4 3. Patients studied on multiple occasions showed 2 patterns: decline and partial recovery. 2 had absent NAA. Ratio > 3/12 was 0.48
Felber SR 1992	Assessment of technique in dg of stroke	4-8 h mean 5.8 hours 8months-6years	Only 2 patients followed up from acute to chronic. The others independent	8 chronic 8 acute(2 fu to chronic)	Single voxel	Ratio to choline	NAA depletion was more pronounced if entire MCA was involved Acute infarct; mean ratio 1.2 Chronic infarct: mean ratio 1.9
Gideon et al.,1994	Prognostic	< 2 days 4-10 days 12-16 days 2.5 –7 months 12-17 months	Not all patients scanned at all time points	6	Single voxel	Absolute and ratio to Cho and Cr	Initially reduced NAA levels. Half of the patients showed continuous decline (beyond 12 days in one patient), others shows increase and one slight increase and then slight decline
Lauriero et al.,1996	Comparative to blood flow	1-3 days 7-9 days 3-9 months	Not all patients scanned at all time points	21	Single voxel	Ratio to contralateral NAA	Reduction of NAA in the acute phase; 0.42+/-0.11 No significant difference between the levels of the acute and chronic stages
Walker et al.,2004	Temporal variation	2-365days	No follow up but different patients studied at different time points	71	CSI	NAA transverse relaxation times	Significant reduction starting from aprox day 5 to day 20. NAA also depressed in peripheral voxels. NAA appears to normalise in chronic lesions > 3months

Table 8 continued. NAA temporal variation from onset to 17 months

Author	Aim of the study	Follow up period	Patient selection	No of patients	MRS method	ratio vs absolute	Result NAA
Graham *et al.*, 2001	Temporal evolution& evaluation of short TE	11-241 days	Variable number of patients scanned at different time points	21	Single voxel	Absolute units (arbitrary)	NAA reduced but no results available to say by how much except for the 1st time point; reduced by 56% cw contralateral. No data for NAA on subsequent time points
Federico et al.,1996	prognostic	1-7 days Mean 3.14+/-2.17 28-251 days Mean 111.6+/-75.7	Same patients followed up at a variety of time points	14	Single voxel	Ratio to contralateral NAA	Initial scan NAAr=0.43+/-0.17 Follow up NAAr=0.43 Significant reduction initially but note further reduction at follow up.
Ford et al.1992	Exploratory	4-55 days, mean 16 45-154 mean 82 days	4/8 patients followed up	4/8	Single voxel	Ratio to choline	NAA reduced in acute and chronic stages
Federico *et al.*, 1998	Prognostic	0.3-7 days (3.5+/-2.1) 8-121 days (59.6+/-38.5)	20 patients out of 26 followed up at various time points	26	Single voxel	Ratio to contralateral NAA	NAA significantly reduced in the infracted area cw contralateral. At the second exam significant reduction persisted; 0.45 and 0.4
Rutgers RD et al., 2000	Time course and comparative	101+/-57 292+/-61 496+/-73	50 patients followed up in pre determined time points. 9/50 had transient ischaemia	50	Single voxel	Ratio to Creatine	NAA significantly reduced cw contralateral side in the first 6 months. Slight recovery continues to 18 months.

2.3.9 NAA and lesion size

All the studies that measured lesion size (either DWI or T2) found correlation between reduced levels of NAA and increasing lesion size.

NAA in relation to final outcome and comparison to other imaging will be discussed together with lactate in section 2.4.

.

2.4 Lactate

Lactate is not "usually" present in normal human brain but there is some evidence that small amounts can be detected in the ageing brain (Sijens *et al.,* 2001), and in the cerebrospinal fluid (CSF) of normal subjects.

It is generally accepted that lactate is produced as a result of anaerobic glycolysis. The concentration of lactate rises when the production exceeds the tissue capacity to catabolise it or remove it from the blood stream. Lactate has been demonstrated by HMRS at the various stages of brain ischaemia, early and late. Removal of lactate depends on number of factors such as tissue perfusion, the permeability of the blood brain barrier and the diffusion of the metabolites through the damaged tissue. Various studies recorded lactate at different stages of ischaemia and also looked in to the predictive value of lactate in the stroke.

2.4.1 Lactate within acute stroke lesion within 24 hours of onset

Eight studies, including 95 patients in total, measured lactate within the lesion in the first 24 hours from onset (Felber et al.,1992; Gillard et al.,1996; Labelle et al.,2001; Liu et al.,2003; Nicoli et al.,2003; Parsons et al.,2000; Parsons *et al.,* 2002a; Stengel et al.,2004). For the type of measurement and result reporting see Table 9. All 95 patients had lactate present at this stage.

Table 9. Lactate in the acute stroke lesion

Author	*Aim of the study*	*Hours from onset*	*Mean +/-SD*	*Number patients*	*MRS method*	*Results reporting (ratio vs absolute)*	*Result Lactate*
Felber et al.,1992	diagnostic	4-8	5.8	8	Single voxel	Ratio to choline	0.8
Gillard et al.,1996	exploratory	2-24h	12 hours	11	Single voxel	Ratio to contralateral creatine	2.35
Parsons *et al.*, 2000	prognostic	3-22	11	19	Single voxel	Ratio to choline	No numerical value, increased
Labelle et al.,2001	Pathophysiolo-gy	5.25-24	17.3+/-6	14	Single voxel	Absolute	7.2
Parsons et al.,2002	prognostic	<24 h			Single voxel	Ratio to choline	increased
Liu et al.,2003	Pathophysiolo-gy	0-6		25	CSI	Ratio to contralateral NAA	1.5
Nicoli et al.,2003	comparative	3.5-7	5	6	CSI	Ratio to sum of metabolites within the lesion	No numerical value, increased
Stengel et al.,2004	exploratory	0-6 h 6h-24h	7.2+/-5.1	10	CSI	absolute	3.7+/- 1.8(0-6 hours) 7.4 +/- 2.8 (6-24hours)

2.4.2 Lactate within the lesion in the first week from stroke

Eleven studies with a total of 224 patients measured lactate from onset (within hours) up to maximum of 1 week (Federico et al.,1996; Federico et al.,1998; Gideon et al.,1992; Gideon et al.,1994; Graham et al.,1993; Houkin et al.,1993; Lauriero et al.,1996; Lemesle et al.,2000; Pereira et al.,1999;Rumpel et al.,2001; Saunders et al.,1995; Stengel et al.,2004; Wardlaw et al.,1998; Wild et al.,2000). Although some of these studies mesured lactate within 24 hours of onset of symptoms, as before, it was not possible to group them in to the category of <24 hours hours as all the data was analysed together including the patients at later times.

The aims of the studies were different; assessing contribution of metabolites to estimate prognosis (5), measuring the longitudinal changes in metabolites (4), comparative to other imaging parameters (2). For the method of acquiring spectroscopy data and the way the results were expressed see Table 10.

In most patients lactate was present; but not all and lactate levels varied widely. Five studies did not report the results as a numerical value. The studies that expressed the result as a ratio used different denominators and cannot be compared. Only a couple of studies used absolute values and ranged from 16.6-24.3. Some of the studies looked at the outcome in relation to lactate (to be discussed later). Houkin found lactate increased immediately and the maximum level of lactate was reached in 48 hours. Also, in another study by Federico, seven out of 26 patients did not have lactate present (three of them were scanned on days one and three and the others on days five and seven).

Table 10. Lactate in the first week from stroke

Author	*Aim of the study*	*Days from onset*	*Mean +/- SD*	*No patient*	*MRS method*	*Results reporting*	*Result for lactate*
Gideon et al. 1992	Longitudinal and comparative to CBF	6-52h		8	Single voxel	Absolute and ratio	Present in all lesions. No numerical value
Houkin et al.,1993	Temporal variation	< 48 hours (2or 3 exams in 48 h)	Exact timing not specified	6	Single voxel	Ratio to contralateral NAA	Lactate increased immediately and reached high levels in the first 48 h
Graham et al. 1993	Temporal variation & prognostic	11-60h	30.6+/-5.3	8	Single voxel, multiple voxels measured	Ratio to external standard (10 mMol)	Lactate increased 3.96+/-1
Gideon et al.,1994	Prognostic	6-48h	28h	6	Single voxel	Absolute and ratio to Cho and Cr	Present in all patients Lact 0.63 Lac/Cho 3.15
Saunders *et al.*, 1995	Temporal variation and definition penumbra	0.2-1.16 days	0.8 days	10	Single voxel	Absolute values	19.2+/-0.5 Significant elevation cw contralateral side
Lauriero et al.,1996	Comparative to blood flow	1-3		21	Single voxel	Expressed as absolute value: high, average, low and absent	Present in high concentration
Federico et al.,1996	prognostic	1-7	2.97	14	Single voxel	Ratio to contralateral NAA	Present in all acute cases 0.58 mean

Table 10 continued. Lactate in the first week from stroke

Author	*Aim of the study*	*Days from onset*	*Mean +/- SD*	*No patient*	*MRS method*	*Results reporting*	*Result for lactate*
Wardlaw et al. 1998	Explorator & comparativ	0-4 days	Not available	17	Mix of CSI & single voxel	Ratio to contralateral NAA	if present in first 4 days associated with extensive infarction
Federico *et al.*, 1998	Prognostic	0.3-7 days	3.5+/-2.1	26	Single voxel	Present or absent	7/26 patients did not have lactate present
Pereira *et al.*, 1999;	Prognostic	0-3 days	Not available	31	Single voxel	Absolute values	16.6+/-7.4(independent) 21.4+/9.9(dependent) 24.3+/11(dead) p=0.3
Lemesle et al.,2000	Prognostic	1-5 days	3.7+/-1.2	77	Mix of single voxel and CSI	Ratio to choline	16.8+/-1.3

2.4.3 Lactate within the lesion in the first two weeks from stroke

Five studies measured lactate from onset up to 2 weeks, including a total of 89 patients (one patient was scanned at 19 days) (Graham et al.,1992; Graham et al.,1995; Graham et al.,2001; Marshall and Sellar1994; Mathews et al.,1995). The studies had different aims and the majority were single voxel spectroscopy acquisition (see Table 11).

The lactate was absent in four patients. Two studies reported the result as a ratio to NAA and the values were very similar at 1.26 and 1.3. The absolute values were 7.5 and 12 and also reported only in two studies. These overall seem to be smaller then the values of lactate in the first week from stroke.

Table 11. Lactate in the first two weeks from stroke

Author	*Aim of the study*	*Days from onset*	*Mean +/-SD*	*Number patients*	*MRS method*	*Results reporting (ratio vs absolute)*	*Result Lactate*
Graham et al.,1992	Temporal variation	2-19 days	7.7	12 cortical	CSI (10 voxels)	Ratio to contralateral NAA	1.26 (absent in 2/12)
Marshall and Sellar1994;	Exploratory	<14 days		6	Single voxel	Ratio to contralateral side (WM)	Present in 4/6 patients (not quantified)
Graham *et al.*, 1995	Correlation with clinical outcome	0-19 days	4.9	32	Multi voxel	Ratio to contralateral NAA	1.3 Lactate was strongly associated with acute stroke severity(lesion volume, TSS,SPECT) and BI on dc
Mathews *et al.*, 1995	Feasibility	2h-10 days	4 days	14	Single voxel	Absolute values	Lactate elevated 7.5+/-8.9
Graham *et al.*, 2001	Temporal evolution and evaluation of short TE	3-10 days		21	Single voxel	Absolute units (arbitrary)	12, lactate increased in all stroke lesions

2.4.4 Lactate within the lesion from one day to six weeks

Only three studies measured lactate between one day and 42 days (Demougeot et al.,2002; Fenstermacher and Narayana1990; Lanfermann et al.,1995). None of the three studies included patients within 24 hours. The studies had a similar aim, mostly exploring the ischaemic lesion with spectroscopy (Table 12). Two studies used CSI method for data acquisition and one of the studies was single voxel. Two studies reported the ratio of lactate to contralateral choline. The ratio ranged from 0.54 in a small lesion to 1.31 in the large lesion and up to 1.7 in the second study. One study did not report numerical value but presence of lactate within the lesion as defined on T2 weighted MRI in 50% of the patients.

Table 12. Lactate within the lesion from day 1-42

Author	*Aim of the study*	*Days from onset*	*Mean +/- SD*	*Number patients*	*MRS method*	*Results reporting (ratio vs absolute)*	*Result Lactate*
Lanfermann et al.,1995;	Exploratory	1-35 days	12.1+/-10.1	18	CSI	Ratio to choline	Small 0.54+/-0.21 Large 1.31+/-0.8
Fenstermacher and Narayana1990;	Pathophysiology, longitudinal	3-24	11.75	4	Single voxel	Ratio to contralateral side	Lactate present in 50% patients
Demougeot et al.,2002;	Exploratory	1-42	7.9+/-9.1	25	CSI	Ratio to contralateral choline	1.7+/- 1.6 (range 0.3 – 6.0)

2.4.5 Lactate in the chronic stage

As mentioned with NAA, chronic stage for the purpose of grouping the data was defined from one month onward. Only six studies included patients at the chronic stage (Duijn et al.,1992; Felber et al.,1992; Ford et al.,1992; Kamada et al.,1997b; Kamada et al.,1997a; Sappey-Marinier et al.,1992). The aims of the studies and the type of MRS are presented in Table 13. The studies included a total of 60 patients. Four studies included patients over a year since the onset of stroke. Only four patients did not have lactate present in the chronic stage from only one study.

Table 13. Lactate in the chronic stages of stroke

Author	*Aim*	*Days from onset*	*Mean +/- SD*	*MRS method*	*No of patients*	*(ratio vs absolute)*	*Result Lactate*
Duijn et al. 1992	exploratory	5-1400 days (2 patients at 5 and 10 days. Next 200days)	461.5	Single voxel	10	Ratio to contralateral NAA	All of the subacute infarctions had persistent lactate within infarct and/or ventricles.
Felber et al. 1992	Diagnostic	8 months-6 years-		Single voxel	8	Ratio to Choline	Highest Lac was found in complete infarction of the MCA & Insular infarct.
Ford et al. 1992	Exploratory	4-55 days	16	CSI	8	Ratio to creatine	Lactate increased initially but present in chronic stage
Kamada et al. 1997a	comparative	180-940 days	293.9 (median)	Single voxel	16	Ratio to choline	Lactate present in 12/16 patients and correlates with poor motor recovery
Kamada et al. 1997 b	Comparative (metabolites vs magneto-encephalography MEG)	7-93 days	29.2	Single voxel	11	Ratio to contralateral NAA (internal standards)	Lactate present in the lesion with highly concentrated slow wave activity on MEG
Sappey-Marinier et al. 1992	exploratory	90-450 days	365+/- 120 days	Single voxel	7	Ratio to creatine and NAA	Lactate ratio to NAA 0.38+/-0.09. Lactate present in all patients.

2.4.6 Lactate outside visible lesion on MRI

Five studies measured lactate outside the visible lesion on MRI (as seen on diffusion or T2)(Demougeot et al.,2002; Gillard et al.,1996; Kamada et al.,1997b; Labelle et al.,2001; Stengel et al.,2004) (see Table 14). All of the studies showed higher levels of lactate within the lesion compared to the region just outside of the lesion

Table 14. Lactate outside visible lesion

Author	*Aim of the study*	*Time from onset*	*Mean +/- SD*	*No of patients*	*MRS method*	*ratio vs absolute*	*Result Lactate*
Gillard et al. 1996	exploratory	0.08-1 days	0.5 days	11	Single voxel	Ratio to contralat creatine area of T2 abnormality	lesion =2.35 around=1.96
Stengel et al. 2004	Exploratory-new technique	2-24h	7.2+/-5.1h	10	CSI	Absolute value	Within **ADC lesion** Lactate 18mmol/l, outside 9 mmol/l. Compared to lactate increase, NAA conc decreased at the slower rate
Labelle et al. 2001	Temporal observational, comparing cortical vs lacunar stroke	5.5-24h	17.3+/-6h	7 each group	Single voxel	Absolute $M/H_2O(x10^3)$	**DWI lesion** acute Core 7 Outer 2.1 1 week Core 4, Outer 0.3 3 months 0.2 &0.1
Demougeot et al. 2002	exploratory	1-42	7.9+/-9.1	25	CSI	Ratio to contralateral Cho	**T2 lesion** Within 1.7 +/- 1.6 Outer 0.5+/-0.6
Kamada et al. 1997 b	Comparative	7-93	29.2	Single voxel	11	Ratio to contralateral NAA (intermnal standars)	Possibly slightly lower lactate in the region outside highest conc of magnetoecepha-logrphy (MEG)

2.4.7 Time course of lactate

As with NAA, a number of studies investigated time course of lactate. To facilitate the data interrogation, the studies were split into two groups: those that measured metabolites up to three months and those that took measurements over the longer period.

In the first group there were 12 studies that measured lactate (Fenstermacher and Narayana1990; Gideon et al.,1992; Graham et al.,1993; Houkin et al.,1993; Labelle et al.,2001; Lanfermann et al.,1995; Lauriero et al.,1996; Liu et al.,2003; Parsons *et al.*, 2002a; Saunders et al.,1995;Wardlaw et al.,1998). Further details about these studies can be found in table 10. In total, 167 patients were followed up for temporal variaton of lactate. It is not clear how many patients did not have lactate at follow up measurement (at least 9). Where lactate was present at the initial measurement, levels decreased gradually, but there is no clear indication of the rate of reduction. It appears that at some point between 10 -30, days lactate levels fall to a very low level, but stay detectable at that level thereafter.

Eight studies measured lactate in the period longer then three months (Federico et al.,1996; Federico et al.,1998; Felber et al.,1992; Ford et al.,1992; Gideon et al.,1992; Gideon et al.,1994; Graham et al.,2001; Rutgers et al.,2000). In total, the studies included 123 patients, but one study that scanned patients in the first six months, rather then acutely, contributed 50 patients. 23 of these patients did not have any lactate detected at the follow up. Overall, the trend was of gradual decline and presence of low level lactate at the later stages. There was no indication of any factors that might be associated with persistance of lactate (eg appearance of lesion, age of patient, evidence of ongoing inflamation) although the number of patients was probably too few to give meaningful result.

Table 15. Lactate from onset to 3 months

Author	*Aim of the study*	*Follow up period*	*Patient selection*	*No of patients*	*MRS method*	*ratio vs absolute*	*Result Lactate*
Fenstermacher et al 1990	Temporal variation & exploratory	3-24 20-69	Patients scanned at different time points	4	Single voxel	Ratio to contralateral side	Did not measure lactate peak at follow up.
Gideon et al.,1992	Temporal variation & comparative	<1 day 1 week 2-4 weeks	Patients scanned in the **pre specified** times	8	Single voxel	Relative to water	Lactate present in all acute lesions but not detected 2-4 weeks
Henriksen O et al., 1992		Acute 1 week 2-4 weeks		8			A high lactate level was found in the acute phase. The lactate content decreased to barely detectable levels during the following 3 weeks. The lactate level was still above normal in the subacute phase with hyperemia, suggesting lactate production through aerobic glycolysis. The lactate level in the subacute phase may not reflect the degree of anaerobic glycolysis in hypoxic neuronal tissue.
Houkin et al.,1993	Temporal variation	< 2 days Every 1-2 w (for 5 w)	Patients scanned in the **pre specified** times	6	Single voxel	Ratio to contralateral NAA	Lact increased immediately and reached high levels in the first 48 h; Lact remained high for more then 1 month ; reduced thereafter but still present
Graham et al. 1993	Temporal variation & prognostic	<2.5 days 8-17 days	7/10 patients scanned in the **pre specified** times	10 acutely 7 f/u	Single voxel (multiple voxels	Ratio to external standard (10 mMol)	35% reduction in lactate between 1st and 2nd time point. 1/7 patients did not have measurable lactate on fu.

Table 15 continued. Lactate from onset to 3 months

Author	*Aim of the study*	*Follow up period*	*Patient selection*	*No of patients*	*MRS method*	*ratio vs absolute*	*Result Lactate*
Lanfermann et al.,1995	exploratory	1-35 days	Different patient scanned at different time points.	20 infarcts	CSI	Ratio to choline	Small infarcts 0.54+/- 0.21, large infarcts 1.31+/-0.8 Lactate reduced with time from stroke. Only a few patients scanned at 30 days but lactate present in small amounts.
Saunders et al. 1995	Temporal variation	<1 day 7-10 days 3 months	Patients scanned in the **pre specified** times	10 7 follow up	Single voxel	Absolute values	Concentration of lactate fell in 6/7 patients but overall mean decrease of lactate in the first 7-10 days NS. ?lactate present at 3/12
Lauriero F et al. 1996	Comparative & exploratory	1-3 days 7-19 days		10 4	Single voxel	Expressed as absolute value: high, average, low and absent	Present in all patients in the acute phase. Present in6/14 patients in chronic phase.
Wardlaw et al. 1998	Exploratory & comparative	0-4 days 5-10 days 10-31 days	Patients scaned in the **pre specified** times	50 scans	Mix of CSI & single voxel	Absolute value: present or absent	Lactate in first 4 days associated with larger infarcts and reduced NAA. Lactate was present in some patients up to 30 days post stroke (but not in all)

Table 15 continued. Lactate from onset to 3 months

Author	*Aim of the study*	*Follow up period*	*Patient selection*	*No of patients*	*MRS method*	*ratio vs absolute*	*Result Lactate*
Labelle et al. 2001	Temporal variation &to compare cortical and lacunar strokes	< 1day 7 days 1 month	Same patients being scanned but not all followed up.	14 (7cortical, 7 subcorti-cal)	Single voxel	Relative to contralateral area	In DWI lesion of cortical infarct significant increase in lactate hyperacute<6h 1.44, acute very high 2.21, and then gradually reduced to level of normal NAA or even lower 1.04, 0.84, 0.43 and 0.87
Parsons et al.,2002	prognostic	<24 h 3 days 90 days		30	Single voxel	Ratio to choline	Increased between acute and subacute phase in mismatch group. Higher glucose means higher lactate production and reduced penumbral salvage
Liu et al. 2003	Temporal variation & comparative & watershed vs teritorial	<6 hours 6h-<2days 3-4 days 7-9 days 10-15 days 30-31 days	Not all patients scanned at all time points including hyperacute	16 territorial 9 watershed	Single voxel	Ratio to contralateral normal NAA	NAA in territorial infarcts decreased to half its value in 2 days (from hyperacute decrease). Further reduction to day 3-4.Remained at that level to 30 days with no recovery. In watershed infarct much lower decrease but downward trend up to 30 days.

Table 16. Lactate temporal variation from onset to 17 months

Author	*Aim of the study*	*Follow up period*	*Patient selection*	*No of patients*	*MRS method*	*ratio vs absolute*	*Result Lactate*
Graham et al.,1992	Temporal and spatial variation	2-19 From 20 – 251 days	Patients followed up at varied time points	16 total 6 followed up	CSI (10 voxels in a row)	Ratio to contralateral NAA	Lactate highest in the acute stage. Gradually reduces but still present at 251 days. Ratio <3/12 was 1.42 Ratio >3/12 was 0.74
Ford et al.1992	Exploratory	4-55 days, mean 16 45-154 mean 82 days	4/8 patients followed up	4/8	Single voxel	Ratio to choline	Increase in lactate in all patents ad persisting to later time points
Felber SR 1992	Assessment of technique in dg of stroke	4-8 h mean 5.8 hours 8months-6years	2 patients followed up from acute to chronic. The others just measured at different times	8chronic 8acute(2 fu to chronic)	Single voxel	Ratio to choline	Highest Lac we found in complete infarction of the MCA & Insular infarct. Acute infarct; mean ratio 0.8 (0.2-1.8) Chronic infarct: no Lactate detected
Gideon et al.,1994	Prognostic	< 2 days 4-10 days 12-16 days 2.5 –7 months 12-17 months	Not all patients scanned at all time points	6	Single voxel	Absolute and ratio to Cho and Cr	Lactate present in all patients in acute stage. In 3/8 patients lactate present in chronic stage and in 2 of these lactate reappeared within the lesion

Table 16 continued. Lactate temporal variation from onset to 17 months

Author	*Aim of the study*	*Follow up period*	*Patient selection*	*No of patients*	*MRS method*	*ratio vs absolute*	*Result Lactate*
Federico et al.,1996	prognostic	1-7 days Mean 3.14+/-2.17 28-251 days Mean 111.6+/-75.7	Same patients followed up at a variety of time points	14	Single voxel	Ratio to contralat NAA	Initial 0.58 +/- 0.59, follow up 0.35+/-0.22 Present in all initial scans but absent in 6/14 follow up scans
Federico *et al.*, 1998	Prognostic	0.3-7 days (3.5+/-2.1) 8-121 days (59.6+/-38.5)	20 patients out of 26 followed up at various time points	26	Single voxel	Ratio to contralateral NAA	7/26 patients had lactate absent during the first scan 10/20 had lactate absent during the second scan
Rutgers RD et al., 2000	Time course and comparative	101+/-57 292+/-61 496+/-73	50 patients followed up in pre determined time points. 9/50 had transient ischaemia	50	Single voxel	Ratio to Creatine	Lactate present in the first 6 months and reduces slightly in the following 12 months.
Graham *et al.*, 2001	Temporal evolution & evaluation of short TE	11-241 days	Variable number of patients scanned at different time points	21	Single voxel	Absolute units*	Lactate present initially in all cases, declined with time. 3-5 days – 12 au 6-10 days and 11-30 days – 6 au >30 days – 5 au

*Arbitrary institutional units (au)

3.1 Comparison of metabolites to blood flow imaging

Eleven studies assessed the adequacy of the blood flow in the lesion in some way (Gideon et al.,1992; Gideon et al.,1994; Gillard et al.,1996; Graham et al.,1995; Henriksen *et al.*, 1992; Houkin et al.,1993; Kamada et al.,1997a; Lauriero et al.,1996; Lemesle et al.,2000; Liu et al.,2003; Wardlaw et al.,1998). The methods varied from formal angiography being most invasive, MR angiography (MRA), SPECT and trans cranial Doppler ultrasound (TCD). The reason for measurement were varied, from investigating the aetiology of stroke, finding an occluded vessel to actually looking at the relationship between blood flow and metabolites.

Hoewer 5/11 studies gave no data on the blood flow measurements. In studies that did present the blood flow measurement data, SPECT was the most frequently used imaging method (five studies), followed by MR relative cerebral blood flow (rCBF) (two studies) and MR angiography (two studies) and finally, one study measured the blood flow with TCD and one study performed carotid Dopplers ultrasound.
All three studies that reported SPECT results showed reduction of blood flow in the acute phase (day one), slight increase at day seven, and hyperemia at subacute stage. One study quantified blood flow as 51% day one, 94% day seven and 125% day 14 -28 (Gideon et al.,1992). Only one of the three studies measured the blood flow with SPECT beyond a month. This study showed reduction of blood flow similar to the acute level when measured from 7-17 months from onset.

Lauriero tried to correlate metabolites with blood flow and showed a correlation between rCBF and NAA at < 3 days from onset (Spearman r=0.73), but this was lost in the hyperemic stage. Chronic (up to three months) rCBF reduction also correlated with NAA level. The other two studies did not specifically look at the metabolites and blood flow. In both studies NAA levels fell and lactate was increased in the acute stage whilst rCBF was reduced. In one of the studies, in the hyperemic stage, NAA remained low; in the other, one half continued to reduce whilst the other half had a degree of recovery in NAA level. The lactate was elevated in the acute stage but then either dissapeared in the hyperemic stage or stayed present in a few patients at a reduced level.

Only two other studies reported relationship between rCBF and rCBV and metabolites. Henriksen showed an inverse relationship between lactate and rCBF in

the third week, whilst Liu showed a similar pattern as with SPECT, with reduced rCBV being low at the acute stage, and reaching peak values at the early chronic stage. NAA did not follow the same pattern; after a reduction in the acute stage, there was a complete loss after four days. There were also differences between territorial and watershed infarcts. The above described pattern was followed in territorial infarcts, whilst watershed infarcts had consistently high rCBV, with NAA present at one month and lactate levels generaly lower than in territorial infarcts.

Table 17. Comparison to blood flow imaging

Author	*Timing*	*Number of patients*	*Blood flow imaging*	*Result*
Henriksen O et al. 1992	Acute and followed up to 1 month after stroke	8	MRI perfusion imaging Relative cerebral blood flow (rCBF)	A high lactate level was found in the acute phase. The lactate content decreased to barely detectable levels during the following 3 weeks, while regional blood flow increased during this period. The inverse relationship between lactate level and cerebral blood flow suggests that lactate plays no substantial role in the vasodilatation underlying the hyperaemia that follows reperfusion.
Gideon et al.,1992 (stroke)	Acute <24h Follow up to 1 month	8	SPECT (rCBF)	day 1 reduction to 51%; 7 days 94%; 14-28 days 125% (re-perfusion hyperaemia)
Houkin et al.,1993	Acute <24 hours Follow up to 5 weeks	6	Conventional angiography during the first exam	Angiography performed in for patients acutely but not subsequently repeated. Demonstrated occluded relevant vessel. No comment re relationship with infarct or metabolites.
Gideon et al.,1994	Acute <2 days Follow up to 7 months	6	SPECT (rCBF)	Reduced perfusion in the acute and chronic stage with hyperemia in the subacute stage. In the chronic stage 7-17 months, rCBF was similar to that of acute stage.
Graham *et al.*, 1995 stroke	0-19 days (mean 4.9)	16/32	SPECT(rCBF)	16 patients had SPECT within average 2.8 days of MRS. Lesion NAA **was not** correlated with TSS or SPECT scores but was correlated with lesion volume at a lower level of significance then lactate. Unclear if lactate correlated with blood flow.
Gillard et al.,1996 Ann	Acute <12h	11	Time of flight MRA	The data on MRA not presented

Table 17 continued. Comparison to blood flow imaging

Author	*Timing*	*Number of patients*	*Blood flow imaging*	*Result*
Lauriero et al.,1996 nmc	Acute 1-3 days Followed up to 3 months	21	SPECT (rCBF)	Significant correlation between rCBF and NAA and Cr/PCr in the acute phase (r=0.73and r=0.72). No correlation during luxury perfusion. Significant r in the chronic phase rCBF/NAA r=0.63 and rCBF/Cr-PCR r=0.59. There was an evident reduction in the size of the hypo-perfused area in the chronic phase.
Kamada et al.;1997	Median 294 days	16	SPECT and MR Angiography	Used to diagnose occluded vessel and recanalisation. 6/16 patients recanalised occluded vessels. No correlation data to metabolites presented.
Wardlaw et al. 199	Acute <4 days Follow up to a month	22 at first time point (50 scans)	TCD	Massive infarct swelling 5-10 days post stroke was weakly associated with reduced blood velocity to the infarct (p=0.07) and large infarcts (p=0.08), but not the presence of lactate (on the scans within 4 days of infarct or later) or degree of reduction of NAA (on initial and subsequent scans). (small numbers)
Lemesle et al.,2000	subacute	77	Carotid Doppler's	Only used to diagnose the aetiology of stroke but not to look at the correlation with metabolites.
Liu et al.,2003	Acute <6 hours, followed up to 1 month	25	MRI perfusion rCBF	Territorial infarcts showed progressively increasing pattern of rCBV from hypoperfusion at the acute to hyperperfusion at early chronic stage. Relative NAA level decreased to 0.4 during acute stage and was completely lost at 4 days. Max lactate increase et 48 h and then gradual decline. Watershed infarcts showed persistent post ischaemic hyperperfusion in all stages up to 1 month. The data not statistically correlated with metabolites. NAA follows slightly different pattern.

3.2 Relationship of metabolites to diffusion imaging

Only eight studies measured metabolites within the diffusion weighted (DWI) lesion or apparent diffusion coefficient (ADC) lesion (Labelle et al.,2001; Liu et al.,2003; Nicoli et al.,2003; Parsons et al.,2000; Parsons *et al.*, 2002; Rumpel et al.,2001; Stengel et al.,2004; Walker et al.,2004). Only three studies investigated the correlation between ADC levels and metabolites. Rumpel found close correlation between ADC and creatine and two different patterns of reduction in NAA, but did not correlate NAA or lactate with ADC. Labelle found no correlation between metabolites and ADC, either acutely or in the chronic stage. Finally Nicoli, who investigated the ADC lesion, looked at the ratio of lactate and NAA to the sum of metabolites (sum) and found significant correlation between NAA/sum and lact/sum and ADC. However, the number of patients in this study was tiny (see Table 18).

Table 18. Comparison to diffusion imaging

Author	*Number of patients*	*Result*
Parsons et al.,2000	19	Used DWI and MRS to predicy outcome. Measured DWI lesion volume but no correlation between DWI paremeters and MRS.
Rumpel et al., 2001	15	Lesion to contralateral ADC ratio. There is a close correlation between ADC and Cre level. Choline levels elevated within stroke lesion in white matter otherwise paralel that of Cr. 2 different pattern of reduction in NAA; 1st selective decrease only, NAA<70% but normal Cr; 2nd generalised decrease in all metabolites. Lactate noted in 4/15 cases irrespective of other metabolites.
Labelle et al., 2001	14	Metabolites measured in a voxel within DWI leson and adjacent voxel. No correlation between metabolite ratios and ADC values in the acute phase and NHSS scores in the chronic phase. Also no correlation established in the acute phase.
Parsons et al.,2002	30	Higher acute blood glucose **in patients with DWI/PWI mismatch** was associated with greater acute-subacute lactate production, which, in turn, was independently associated with reduced penumbral salvage.
Walker et al., 2002	77	Significant reduction starting from aprox day 5 to day 20. Centre (NAA T2)226+/-48 vs 393+/-27 (normal); peripheral voxels also depressed 317+/- 28. NAA appears to normalise in chronic lesions > 3months(396+/-41 centre and 381+/-37 periphery)
Liu et al., 2003	25	The CSI grid positioned on DWI image but no correlation between diffusion parameters and metabolites or perfusion parameters investigated
Nicoli et al., 2003	6	lac/sum vs ADC r2=0.47 (p<0.0001); NAA/sum vs ADC r2=o.48 (p<0.0001) ; Lac/NAA vs ADC r2=0.6 (p<0.0001) Region with very low mean ADC values during hyperacute ischaemic stroke contains areas of various tissue damage intensity characterised by SI in realtion to different stages of cellular metabolic injury.
Stengel et al. 2004	10	Metabolites measured within and outside the ADC lesion but no correlation with metabolites given. NAA reduced and lactate increased but the changes much more pronaunced in the acute rather then hyperaccute stage (<6h). Metabolic border extends beyond ADC lesion.

3.3 Relationship of metabolites to the lesion volume

Thirteen studies in total measured lesion volume but only eight commented on their relationship with metabolites in any way (Federico et al.,1996; Graham et al.,1993; Graham et al.,1995; Lemesle et al.,2000; Parsons et al.,2000; Pereira et al.,1999; Wardlaw et al.,1998) (see Table 19). Three of the stuides correlated lactate with a larger infarcts but there was no influence on outcome. Two studies corelated reduction in NAA with larger infarct volume. Three of the stuides did not correlate NAA or lactate with infarct size but discussed reduction in NAA and increase in infarct size as a predicor of poor outcome see Table 19.

A further five studies measured lesion volume but gave no correlation with metabolites (Duijn et al.,1992; Gideon et al.,1992; Lanfermann et al.,1995; Liu et al.,2003; Parsons *et al.,* 2002; Stengel et al.,2004). The study by Parsons had a rather different aim and he looked at the progression of the mismatch area whilst Liu compared volumes of watershed and territorial infarctions and their progression with time

Table 19. Relationship of metabolites to lesion volume

Author	*Number of patients*	*Relationship to lesion volume*
Graham et al. 1993	10	1st exam-lactate positively correlated with lesion volume r=0.75 as was the maximum lesion lactate. Inverse relationship between lesion size & lactate % washout r = -0.7
Graham et al 1995	32	Lactate and NAA both correlated with lesion volume but lactate was more significant.
Lanferman et al 1995		Larger the infarct, bigger the NAA reduction. NAA concentration was reduced to 20% of the contralateral in a very larger infarcts.
Federico et al. 1996	14	Those patients with extensive lesion and low NAA presented worst clinical outcome , whilst those with lesser reduction in NAA had better outcome irrespective of lactate
Wardlaw et al. 1998	50	The presence of lactate was related to large infarcts and reduced NAA.
Pereira et al. 1999	31	Higher lesion volume (>70) irrespective of NAA carried poor prognosis but those with lesion <70 and NAA >7 did well, whilst those with lesion <70 and NAA <7 had poor outcome.
Lemesle et al.,2000	77	Decrease in NAA/choline ratio was correlated with large infarction and subsequently poor outcome. Lactate/cho ratio had no significant influence on outcome.
Parsons *et al.*, 2000	19	At the acute stage lact/cho ratio, NAA/cho ratio and DWI lesion volume were correlated with final infarct size.

3.4 Relationship to the final clinical outcome

Thirteen studies in total looked at the correlation between metabolites and clinical outcome including a total of 322 patients (Federico et al.,1996; Federico et al.,1998; Ford et al.,1992; Gideon et al.,1994; Graham et al.,1993; Graham et al.,1995; Kamada et al.,1997b; Lemesle et al.,2000; Parsons et al.,2000; Parsons *et al.,* 2002; Pendlebury *et al.,* 1999; Pereira et al.,1999; Wardlaw et al.,1998).

Six studies found that better preserved NAA was associated with better functional outcome but no association between lactate and clinical outcome(see Table 20). Three studies found that elevated lactate correlated with functional outcome but not NAA (see Table 20). One study found that both NAA and lactate correlated with outcome. In one of the studies, lactate did not correlate with clinical outcome but did correlate with the lesion volume. Two studies found no correlation between any of the metabolites and clinical outcome (see Table 20).

It is important to note that none of the studies recruited patients within 24 hours of onset. The majority of studies recruited patients within a week of stroke onset (Federico et al.,1996; Federico et al.,1998; Gideon et al.,1994; Graham et al.,1993; Graham et al.,2001; Lemesle et al.,2000; Pereira et al.,1999; Wardlaw et al.,1998), two studies recruited within a month (Graham et al.,1995; Parsons et al.,2000), and two recruited patients over a month since the stroke onset (Ford et al.,1992; Kamada et al.,1997a; Pendlebury et al.,1999).

Table 20. Relationship of metabolites to the final outcome

Author	*Timing Day (d) Month (m)*	*Number of patients*	*Clinical outcome*
Ford et al. 1992	37+/- 154 d	8	Comment on outcome for 4 patients studied; those who had better preserved levels of Choline, Creatine and NAA seem to have better outcome.
Graham et al. 1993	<2.5 d 8-17 d	10	No actual clinical outcome measured. Lactate was positively correlated with lesion volume as was the max lesion lactate.
Gideon et al. 1994	< 2 d 4-10 d 12-16 d 2.5 –7 m 12-17 m	6	No clear correlation found between the Lact and NAA in the acute stage of stroke and clinical outcome. There appears to be connection between the reduction of rCBF & MRSI findings in the chronic stage & to some extent the clinical outcome. Only 6 patients studied.
Graham et al 1995	0-19 d	32	Correlations with outcome. Lactate was strongly associated with acute stroke severity (lesion volume, Toronto stroke scale TSS, SPECT) and eventual clinical outcome (BI on dc). NAA correlation with lesion volume.
Author	*Timing Day (d) Month (m)*	*Number of patients*	*Clinical outcome*
Federico et al. 1996	1-7 d 28-251 d	14	Significant correlation (Spearman) between clinical outcome (evaluated by SSS) and both initial and final NAA levels. Those patients with extensive lesion and low NAA presented worst clinical outcome , whilst those with lesser reduction in NAA had better outcome irrespective of lactate
Kamada et al.1997	180-940 d	11	In chronic infarction (median 294 days) all patients with residual NAA signal had very mild paresis or none. The NAA/Cho ratio correlated well with residual motor function. Lactate/Cho ratio correlated with poor residual function.

Table 20 continued. Relationship of metabolites to the final outcome

Author	*Timing Day (d) Month (m)*	*Number of patients*	*Clinical outcome*
Wardlaw et al. 1998	0-4 d 5-10 d 10-31 d	50	Poor clinical outcome at 6 months (RS 3-6) was significantly related to the clinical stroke syndrome (p=0.03), the extent of the infarct –the more extensive infarct the worse clinical outcome (p=<0.01), but not the degree of reduction of NAA, the amount of swelling, the blood velocity, or the presence of lactate.
Federico *et al.*, 1998	0.3-7 d 8-121 d	26	In the acute phase NAA, Cr and Ch had +ve correlation with the Scandinavian stroke scale (SSS). Sub acutely, only NAA +ve correlated with SSS. Ratio obtained during 1st exam +ve correlation at 6 months SSS. SSS score was significantly lower in patients that had lactate present on the initial scan.
Pereira et al. 1999	0-3 d	31	Association between initial NAA concentration and clinical outcome. Patients independent at 3 months had significantly higher NAA then those with poor outcome (p<0.01). There was no difference between the NAA conc in the dead and dependent groups. Initial severity assessed by Scandinavian stroke scale (SSS) and infarct size correlated with outcome. Patients with NAA level above 7 did better.
Pendelbury ST et al 1999	1-60 m	18	Chronic infarction between 1 and 60 months. NAA measured in the posterior limb of the internal capsulae shows strong correlation with motor deficit.
Lemesle et al.,2000	1-5 d	77	Good clinical outcome at day 30 depends on good initial clinical score (ORGOGOZO score) at day 1, small volume infarction, a small decrease of NAA/Cho and fm gender
Parsons *et al.*, 2000	3-22 d	19	Acutely lact/Ch ratio had greater correlation with outcome measures (Canadian neurological scale; CNS, Barthel index; BI, Rankin scale; RS) Subacute stage NAA/cho and lactate /choline had similar correlation with outcome. Acute lactate/cho ratio was independent of acute DWI lesion volume.
Parsons et al. 2002	<24 hours 3 d 90 d	30	Higher acute blood glucose **in patients with DWI/PWI mismatch** was associated with greater acute-subacute lactate production, which, in turn, was independently associated with reduced penumbral salvage.

4.1 Discussion and conclusions

"If you wish to converse with me, define your terms." *Voltaire*

4.1.1 Methodological aspects of the studies included in the literature overview

Almost all studies are small and use different definitions, different spectroscopy methods (acquisition and analysis) and different timing of scans, making it difficult to draw firm conclusions. Future studies need to be very clear in their definitions, analysis methods and bias by avoiding use of choline or creatine as denominators because they change in acute stroke(Munoz *et al.*, 2008).

An important source of variability between the studies was the time from onset to scanning and lack of structured follow up, even in the studes that set out to investigate temporal variation of the metabolites. There are several reasons for it. Firstly, one has to take in to consideration technical difficulties of performing an MRI on acutely ill stroke patients. Stroke is a heterogenous disorder and very severe stroke patients, especially ones with aphasia, are unlikely to tolerate prolonged time in the scanner (or even a short time). Doing spectroscopy tended to add on at least 10-15 minutes on to the routine protocol, even with single voxel spectroscopy. It is only in recent years that sequences have become faster, as well as processing; Stengel reported completing a CSI examination in six minutes (Stengel et al.,2004). In addition, it is very difficult to perform physiological monitoring in the scanner and sometimes it is necessary to do so in such acutely ill patients. Significant number of patients desaturate in the MR scanner (Rowat *et al.*, 2002). If no history from the patient is available (or collateral history), occasionally Xray of the orbits is necessary for safe scanning. MRI scanners are often not available out of hours, and therefore significantly reduce the number of patients scanned.

All these factors play a role in the ability to scan patients, especially in the hyperacute and acute stage. Therefore, it is not supprising that only seven studies out of 39 included patients within 24 hours of onset (n=73).

Timing of the follow up of the patients also varied. Again, this is multifactorial. One of the reasons is heterogeneity of the stroke and not all patients will be well at the given time for a follow up. Also, MR scanning is not an easy procedure to tolerate and many patients cannot tolerate repeated exams (Melendez and McCrank 1993). Several studies reported results as part of temporal variation, having scanned different patients at different time points. Although this provides some data on temporal variation, it does not take in to account the individual variation between patients.

Data collection and results reporting

All studies used validated MRS techniques in terms of data collection and analysis of the spectra (but not of the derived metabolites). However, MRS has significantly developed since the mid- to late 1980s, when the first studies were performed. Originally it was a single voxel technique, but with time it developed into a multivoxel MRS, covering a whole slice of the brain and providing a metabolic map that can be superimposed in the structural image. Most studies used single voxel data collection; some of them were multivoxel, whilst some used a combination of the two.

An important cause of variability between the studies comes with the way the metabolite results were reported. The 39 studies presented above used the following approaches to present the data: the ratio to choline, the ratio to creatine, the ratio to an internal standard, the ratio to water, the ratio to the contralateral side, the ratio to the sum of all metabolites in the lesion and various absolute values either expressed as mmoles or arbitrary units validated by an internal standard. One has to be careful when interpreting such data; especially those presented as ratios to choline and creatine. The choline and creatine levels change in the acute stroke and therefore the potential ambiguity could be introduced into the ratios by the variation of these metabolites. This ambiguity should be carefully considered when interpreting the results (Munoz et al.,2008).

In addition, one of the important weaknesses of all spectroscopy studies is a partial volume effect. When imaging a focal lesions or particular brain areas, they often have an irregular shape that does not neatly fit in to a rectangle or a square. The partial volume effect happens either due to contributions from surrounding tissue

or because only a part of the region of interest is covered. Most studies have commented on the possible ways they dealt with the problem but it could not be completely eliminated. The majority of studies commented that they excluded the voxels contaminated by the cerebrospinal fluid (CSF).

4.1.2 The metabolite levels in the acute stroke and temporal variations

All spectroscopy studies of human stroke agree on one point; that there is a decrease in NAA level within the stroke lesion. There is no definite agreement on the timing and the rate of decrease, but that is likely to be multifactorial and dependent on other factors such as blood flow, size of the lesion and clinical severity. In general, the NAA decline seems to occur rapidly in the first 48 hours and then continues to decline at the slower rate thereafter.

The size of the lesion in all studies (where measured) correlated with the metabolites (Graham et al.,1993;Graham et al.,1995;Lemesle et al.,2000;Wardlaw et al.,1998). However, this is not a uniform agreement, as Lemesle et al. found NAA to be associated with lesion size and outcome, but two other studies found high lactate but not NAA to be associated with a large lesion and one study found both lactate and NAA to have a correlation with the lesion size.

It is interesting to point out the differences in the distribution of the NAA across the lesion, where the lesion and surrounding area were studied with DWI and T2 imaging. In the studies that used DWI, there is no significant decrease in NAA levels between the core and outside of the lesion, whilst in T2 lesion there is a slight decrease in the levels of NAA within the lesion centre compared to outside of the lesion. Studies that used DWI had slightly shorter time from onset to imaging (<24h), whilst ones that used T2 scanned patients up to 3 days (Table 5). This may indicate that NAA levels may be preserved up to 24 hours in the lesion as well as the surrounding area but, as times moves on and the lesion is visible on the T2, the levels change. We do know from previous studies of DWI , SPECT and MRS that DWI lesion is heterogeneous at the acute stage (Guadagno *et al.*, 2004;Guadagno *et al.*, 2005;Nicoli et al.,2003). Lactate was highest in the centre and present in lower levels, immediately outside the lesion as delineated on both DWI and T2.

Unfortunately, only a couple of studies that measured blood flow investigated the correlation with metabolites. The blood flow measurements follow the pattern of reduced blood flow in the acute stage with a gradual increase to normal levels and then hyperaemia in the subacute stage. One study repeated measurements at the chronic stage and showed them to be similar to the acute stage. Lauriero et al. found a positive correlation between NAA and rCBF in the acute and chronic stage, but not in the hyperaemic phase (Table 12). None of the studies examined lactate in relation to rCBF.

Temporal variation of metabolites

At least half of the studies investigated temporal variation of the metabolites. All the difficulties with the timing of the follow up studies were discussed earlier. Also, the number of patients that were followed up was rather small. The largest study that looked at the temporal variation of metabolites did not follow up the same patients but scanned different patients at different times from onset.

From the studies included in the review, a NAA level continue to fall further after the acute stage; most rapidly up to three days and then continues to fall at a slower rate up to one to two weeks. A similar pattern has been demonstrated in an animal ischemia model with an initial rapid decrease of NAA following induction of ischemia, then a further slower decline or persistent absence (Higuchi *et al.*, 1996;Monsein *et al.*, 1993) . These changes in NAA correlated closely with histological evidence of neuronal death (Sager *et al.*, 1995;Sager *et al.*, 2000). In addition to neuronal loss, a few other explanations of reduced levels of NAA were offered. The accumulation of oedema in the ischaemic lesion could "dilute" the NAA and account for some of the apparent reduction in NAA (Bruhn *et al.*, 1989;Dzialowski *et al.*, 2004). It was also suggested that NAA is degraded by an enzyme in the first few days after injury (Bruhn et al.,1989). At the subacute stage of injury, there is some uncertainty about whether any residual NAA detected spectroscopically represents a few still viable neurons, neuronal debris, infiltrating microglia, or possibly migrating neural stem cells (Demougeot *et al.*, 2004). NAA seems to be at it's nadir in the period of one to two weeks from the onset of symptoms. From the data presented, there is very little recovery of NAA up to a month. After a month the time course of NAA is more variable. The levels may stay the same as in a subacute stage, decline further or in some cases increase, but very

rarely reach normal level again. However, these data are derived from very few patients.

The time course of a lesion lactate is different from that of NAA. The level is highest initially and it seems to stay high for up to two weeks. At some point between two to four weeks, its level drops significantly. In some patients it disappears completely, whilst in others it remains present even after a year. The lactate in the acute stage represents anaerobic metabolism (Monsein et al.,1993), which may not be the case with lactate at the chronic stage. There are several plausible explanations for persistent lactate: It is possible that there is still some ongoing ischaemia even at the chronic stage of infarction. In addition, changes in phosphorus metabolites and alkalosis can cause increased lactate production. Alkalosis has been measured especially in the hyperaemic stage of the infarction (Syrota *et al.*, 1985). It is possible that relatively increased cerebral blood flow, associated with a decrease of oxygen extraction fraction and lower tissue pCO2, causes intracellular alkalosis which selectively stimulates glycolysis (Sappey-Marinier et al.,1992). Lactate can also be produced by phagocytic glial cells, macrophages or leucocytes in the infarct, as these cells are known to have a high rate of anaerobic glycolysis (Kely JP 1985).

4.1.3 DWI and MRS in acute stroke

Of the small number of studies that used DWI in combination with MRS, only two tried to correlate metabolites with diffusion and perfusion parameters. One study found no correlation whilst the other found correlation between the ADC and NAA and lactate, expressed as a ratio to the sum of lesion metabolites, but this ratio is difficult to interpret as none of these metabolites are stable in the acute stroke.

4.1.4 Correlation of metabolites with outcome

Thirteen studies investigated the correlation between the metabolites and clinical outcome. The results were varied. Half of the studies found that NAA correlated with outcome, and three studies found that lactate correlated with outcome. Only in one study, both NAA and lactate correlated with outcome. Finally, two studies showed no correlation with metabolites. There are important variations in the baseline characteristics between the studies that may have influenced long term

outcome. Also, timing of the recruitment of the patients differed between the studies and the baseline severity of the stroke of the included patients would also have a major impact on the outcome but has not always been specified.

No studies of MRS in the acute stage and follow up have been big enough to be able to establish the role of metabolites with certainty in the diagnosis or prognosis of stroke patients. There is also no clear correlation of metabolites with blood flow or diffusion imaging.

Larger, carefully designed studies with pre-specified follow up would be necessary to establish the role of MRS in clinical use and to clarify the pattern of metabolite change in and around the lesion over time.

Barker PB, Gillard JH, van Zijl PC, Soher BJ, Hanley DF, Agildere AM *et al.* Acute stroke: evaluation with serial proton MR spectroscopic imaging. Radiology 1994; 192: 723-732.

Bruhn H, Frahm J, Gyngell ML, Merboldt KD, Hanicke W, Sauter R. Cerebral metabolism in man after acute stroke: new observations using localized proton NMR spectroscopy. Magnetic Resonance in Medicine 1989; 9: 126-131.

Demougeot C, Marie C, Giroud M, Beley A. N-acetylaspartate: a literature review of animal research on brain ischemia. J Neurochem 2004; 90: 783.

Demougeot C, Walker P, Beley A, Marie C, Rouaud O, Giroud M *et al.* Spectroscopic data following stroke reveal tissue abnormality beyond the region of T2-weighted hyperintensity. Journal of the Neurological Sciences 2002; 73-78.

Duijn JH, Matson GB, Maudsley AA, Hugg JW, Weiner MW. Human brain infarction: proton MR spectroscopy. Radiology 1992; 183: 711-718.

Dzialowski I, Weber J, Doerfler A, Forsting M, von Kummer R. Brain tissue water uptake after middle cerebral artery occlusion assessed with CT. J Neuroimaging 2004; 14: 42-48.

Federico F, Simone IL, Conte C, Lucivero V, Giannini P, Liguori M *et al.* Prognostic significance of metabolic changes detected by proton magnetic resonance spectroscopy in ischaemic stroke. Journal of Neurology 1996; 243: 241-247.

Federico F, Simone IL, Lucivero V, Giannini P, Laddomada G, Mezzapesa DM *et al.* Prognostic value of proton magnetic resonance spectroscopy in ischemic stroke. Archives of Neurology 1998; 55: 489-494.

Felber SR, Aichner FT, Sauter R, Gerstenbrand F. Combined magnetic resonance imaging and proton magnetic resonance spectroscopy of patients with acute stroke. Stroke 1992; 23: 1106-1110.

Fenstermacher MJ, Narayana PA. Serial proton magnetic resonance spectroscopy of ischemic brain injury in humans. Investigative Radiology 1990; 25: 1034-1039.

Ford CC, Griffey RH, Matwiyoff NA, Rosenberg GA. Multivoxel 1H-MRS of stroke. Neurology 1992; 42: 1408-1412.

Gideon P, Henriksen O, Sperling B, Christiansen P, Olsen TS, Jorgensen HS *et al.* Early time course of N-acetylaspartate, creatine and phosphocreatine, and compounds containing choline in the brain after acute stroke. A proton magnetic resonance spectroscopy study. Stroke 1992; 23: 1566-1572.

Gideon P, Sperling B, Arlien-Soborg P, Olsen TS, Henriksen O. Long-term follow-up of cerebral infarction patients with proton magnetic resonance spectroscopy. Stroke 1994; 25: 967-973.

Gillard JH, Barker PB, van Zijl PC, Bryan RN, Oppenheimer SM. Proton MR spectroscopy in acute middle cerebral artery stroke. Ajnr: American Journal of Neuroradiology 1996; 17: 873-886.

Graham GD, Blamire AM, Howseman AM, Rothman DL, Fayad PB, Brass LM *et al.* Proton magnetic resonance spectroscopy of cerebral lactate and other metabolites in stroke patients. Stroke 1992; 23: 333-340.

Graham GD, Blamire AM, Rothman DL, Brass LM, Fayad PB, Petroff OA *et al.* Early temporal variation of cerebral metabolites after human stroke. A proton magnetic resonance spectroscopy study. Stroke 1993; 24: 1891-1896.

Graham GD, Hwang JH, Rothman DL, Prichard JW. Spectroscopic assessment of alterations in macromolecule and small-molecule metabolites in human brain after stroke. Stroke 32(12):2797-802, 2001.

Graham GD, Kalvach P, Blamire AM, Brass LM, Fayad PB, Prichard JW. Clinical correlates of proton magnetic resonance spectroscopy findings after acute cerebral infarction. Stroke 1995; 26: 225-229.

Guadagno JV, Warburton EA, Aigbirhio FI, Smielewski P, Fryer TD, Harding S *et al.* Does the acute diffusion-weighted imaging lesion represent penumbra as well as core? A combined quantitative PET/MRI voxel-based study. J Cereb Blood Flow Metab 2004; 24: 1249-1254.

Guadagno JV, Warburton EA, Jones PS, Fryer TD, Day DJ, Gillard JH *et al.* The diffusion-weighted lesion in acute stroke: heterogeneous patterns of flow/metabolism uncoupling as assessed by quantitative positron emission tomography. Cerebrovasc Dis 2005; 19: 239-246.

Henriksen O, Gideon P, Sperling B, Olsen TS, Jorgensen HS, rlien-Soborg P. Cerebral lactate production and blood flow in acute stroke. J Magn Reson Imaging 1992; 2: 511-517.

Higuchi T, Fernandez EJ, Maudsley AA, Shimizu H, Weiner MW, Weinstein PR. Mapping of lactate and N-acetyl-L-aspartate predicts infarction during acute focal ischemia: in vivo 1H magnetic resonance spectroscopy in rats. Neurosurgery 1996; 38: 121-129.

Houkin K, Kamada K, Kamiyama H, Iwasaki Y, Abe H, Kashiwaba T. Longitudinal changes in proton magnetic resonance spectroscopy in cerebral infarction. Stroke 1993; 24: 1316-1321.

Kamada K, Houkin K, Iwasaki Y, Abe H, Kashiwaba T. Metabolic and neurological patterns in chronic cerebral infarction: a single-voxel 1H-MR spectroscopy study. Neuroradiology 1997a; 39: 560-565.

Kamada K, Saguer M, Moller M, Wicklow K, Katenhauser M, Kober H *et al.* Functional and metabolic analysis of cerebral ischemia using magnetoencephalography and proton magnetic resonance spectroscopy. [see comments]. Ann Neurol 1997b; 42: 554-563.

Kely JP. Reactions of neurons to injury. In: Kandel ER, Schwartz J, editors. Principals of neural science. Elsevier; 1985. p. 187-95.

Labelle M, Khiat A, Durocher A, Boulanger Y. Comparison of metabolite levels and water diffusion between cortical and subcortical strokes as monitored by MRI and MRS. Investigative Radiology 2001; 36: 155-163.

Lanfermann H, Kugel H, Heindel W, Herholz K, Heiss WD, Lackner K. Metabolic changes in acute and subacute cerebral infarctions: findings at proton MR spectroscopic imaging. Radiology 1995; 196: 203-210.

Lauriero F, Federico F, Rubini G, Conte C, Simone I, Inchingolo V *et al.* 99Tcm-HMPAO SPET and 1H-MRS (proton magnetic resonance spectroscopy) in patients with ischaemic cerebral infarction. Nuclear Medicine Communications 1996; 17: 140-146.

Lemesle M, Walker P, Guy F, D'Athis P, Billiar T, Giroud M *et al.* Multi-variate analysis predicts clinical outcome 30 days after middle cerebral artery infarction. Acta Neurologica Scandinavica 2000; 102: 11-17.

Liu YJ, Chen CY, Chung HW, Huang IJ, Lee CS, Chin SC *et al.* Neuronal damage after ischemic injury in the middle cerebral arterial territory: deep watershed versus territorial infarction at MR perfusion and spectroscopic imaging. Radiology 229(2):366-74, 2003.

Marshall I, Sellar RJ. 1H spectroscopy in stroke. Magnetic Resonance Materials in Physics, Biology, & Medicine 1994; 2: 351-352.

Mathews VP, Barker PB, Blackband SJ, Chatham JC, Bryan RN. Cerebral metabolites in patients with acute and subacute strokes: concentrations determined by quantitative proton MR spectroscopy. AJR 1995; American Journal of Roentgenology. 165: 633-638.

Melendez JC, McCrank E. Anxiety-related reactions associated with magnetic resonance imaging examinations. JAMA 1993; 270: 745-747.

Monsein LH, Mathews VP, Barker PB, Pardo CA, Blackband SJ, Whitlow WD *et al.* Irreversible regional cerebral ischemia: serial MR imaging and proton MR spectroscopy in a nonhuman primate model. AJNR Am J Neuroradiol 1993; 14: 963-970.

Munoz MS, Cvoro V, Armitage PA, Marshall I, Bastin ME, Wardlaw JM. Choline and creatine are not reliable denominators for calculating metabolite ratios in acute ischemic stroke. Stroke 2008; 39: 2467-2469.

Nicoli F, Lefur Y, Denis B, Ranjeva JP, Confort-Gouny S, Cozzone PJ. Metabolic counterpart of decreased apparent diffusion coefficient during hyperacute ischemic stroke: a brain proton magnetic resonance spectroscopic imaging study.[see comment]. Stroke 34(7):e82-7, 2003.

Parsons MW, Barber PA, Desmond PM, Baird TA, Darby DG, Byrnes G *et al.* Acute hyperglycemia adversely affects stroke outcome: a magnetic resonance imaging and spectroscopy study. Ann Neurol 2002a; 52: 20-28.

Parsons MW, Li T, Barber PA, Yang Q, Darby DG, Desmond PM *et al.* Combined (1)H MR spectroscopy and diffusion-weighted MRI improves the prediction of stroke outcome. Neurology 2000; 55: 498-505.

Pendlebury ST, Blamire AM, Lee MA, Styles P, Matthews PM. Axonal injury in the internal capsule correlates with motor impairment after stroke. Stroke 1999; 30: 956-962.

Pereira AC, Saunders DE, Doyle VL, Bland JM, Howe FA, Griffiths JR *et al.* Measurement of initial N-acetyl aspartate concentration by magnetic resonance spectroscopy and initial infarct volume by MRI predicts outcome in patients with middle cerebral artery territory infarction. Stroke 1999; 30: 1577-1582.

Rowat AM, Hand PJ, Janneke H, Wardlaw JM. Hypoxia in the acute phase of stroke during MR Brain imaging. Stroke 2002; 33: 383 (No P119).

Rumpel H, Khoo JB, Chang HM, Lim WE, Chen C, Wong MC *et al.* Correlation of the apparent diffusion coefficient and the creatine level in early ischemic stroke: a comparison of different patterns by magnetic resonance. Journal of Magnetic Resonance Imaging 2001; 13: 335-343.

Rutgers DR, Klijn CJ, Kappelle LJ, van der GJ. Cerebral metabolic changes in patients with a symptomatic occlusion of the internal carotid artery: a longitudinal 1H magnetic resonance spectroscopy study. Journal of Magnetic Resonance Imaging 2000; 11: 279-286.

Sager TN, Hansen AJ, Laursen H. Correlation between N-acetylaspartate levels and histopathologic changes in cortical infarcts of mice after middle cerebral artery occlusion. J Cereb Blood Flow Metab 2000; 20: 780-788.

Sager TN, Laursen H, Hansen AJ. Changes in N-acetyl-aspartate content during focal and global brain ischemia of the rat. J Cereb Blood Flow Metab 1995; 15: 639-646.

Sappey-Marinier D, Calabrese G, Hetherington HP, Fisher SN, Deicken R, Van Dyke C *et al.* Proton magnetic resonance spectroscopy of human brain: applications to normal white matter, chronic infarction, and MRI white matter signal hyperintensities. Magnetic Resonance in Medicine 1992; 26: 313-327.

Saunders DE, Howe FA, van den BA, McLean MA, Griffiths JR, Brown MM. Continuing ischemic damage after acute middle cerebral artery infarction in humans demonstrated by short-echo proton spectroscopy. Stroke 1995; 26: 1007-1013.

Sijens PE, den HT, de Leeuw FE, de Groot JC, Achten E, Heijboer RJ *et al.* MR spectroscopy detection of lactate and lipid signals in the brains of healthy elderly people. Eur Radiol 2001; 11: 1495-1501.

Stengel A, Neumann-Haefelin T, Singer OC, Neumann-Haefelin C, Zanella FE, Lanfermann H *et al.* Multiple spin-echo spectroscopic imaging for rapid quantitative assessment of N-acetylaspartate and lactate in acute stroke. Magnetic Resonance in Medicine 52(2):228-38, 2004.

Syrota A, Samson Y, Boullais C, Wajnberg P, Loc'h C, Crouzel C *et al.* Tomographic mapping of brain intracellular pH and extracellular water space in stroke patients. J Cereb Blood Flow Metab 1985; 5: 358-368.

Walker PM, Ben Salem D, Lalande A, Giroud M, Brunotte F. Time course of NAA T2 and ADC(w) in ischaemic stroke patients: 1H MRS imaging and diffusion-weighted MRI. Journal of the Neurological Sciences 220(1-2):23-8, 2004.

Wardlaw JM, Marshall I, Wild J, Dennis MS, Cannon J, Lewis SC. Studies of acute ischemic stroke with proton magnetic resonance spectroscopy: relation between time from onset, neurological deficit, metabolite abnormalities in the infarct, blood flow, and clinical outcome. Stroke 1998; 29: 1618-1624.

Wild JM, Wardlaw JM, Marshall I, Warlow CP. N-acetylaspartate distribution in proton spectroscopic images of ischemic stroke: relationship to infarct appearance on T2-weighted magnetic resonance imaging. Stroke 2000; 31: 3008-3014.

Chapter 3: Methods of patient recruitment, image acquisition and image processing

Introduction

Previous chapter, the systematic review of MRI spectroscopy, clearly demonstrated difficulties with drawing conclusions from the studies that were generally small and used different definitions, methods and analysis.

The aim of this study was to evaluate if proton MRS, by identifying neuronal death (reduced NAA) and ischemia (raised lactate), could help clarify the relationship between DWI and PWI parameters and tissue damage in acute ischemic stroke. If ADC or PWI directly indicate neuronal damage, then ADC and PWI values should correlate closely with NAA. If they mainly indicate ischemia, then ADC and PWI values should correlate closely with lactate rather than NAA. Second aim was to examine temporal variation of NAA and lactate within the ischaemic stroke lesion over the period of three months and correlate radiological appearances of the ischaemic lesion with the functional outcome at three months. This was going to be achieved by following patients up in a structured way and at fixed time points up to three months following initial stroke.

In this chapter I will describe the study design, patient recruitment, clinical assessment, data collection, and entry used to gather data for the project. I will also describe imaging methods, image analysis, data analysis, and clinical follow up. Statistical tests used will be described in the individual results chapters dealing with the analysis. The study recruitment and patients' assessment method are both reported in this chapter whilst demographic data is presented with the results.

3.1. Study design

This study was a prospective observational study in which I recruited patients within 24 hours of an acute ischaemic stroke and performed imaging and clinical follow-up for 3 months. I recruited patients with acute stroke who presented and

could have all initial assessments within 24 hours of the onset of symptoms. The patients were assessed at 5 time points:

1) 0-24 hours – 1st assessment consisted of full clinical and functional assessment, magnetic resonance scan (MRI) and carotid Doppler.

2) 5-7 days - MRI

3) 10-14 days - MRI

4) 30 days - MRI

5) 90 days - MRI and functional assessment (modified Rankin scale, Barthel Index, extended Nottingham ADL scale).

The study was granted ethical approval by the Lothian Research and Ethics Committee (LREC 2002/4/30). In addition to patient consent we were granted relative consent, witnessed consent and waiver consent. (For samples of the patient information leaflet and consent forms see Appendix 3 and 4). All patients who were enrolled (or their relatives) signed an informed consent form. Only one patient was enrolled by waiver consent.

3.2 Patient recruitment

3.2.1 Source of patients

I assessed over 300 patients in 24 months that presented at the Western General Hospital in Edinburgh with symptoms of acute focal neurological deficit. Most patients were directly seen at the point of entry to the hospital, acute receiving unit (ARU), but some of them were assessed on a different medical or stroke ward, if admitted and moved overnight. I carried an "acute stroke bleep" and was therefore contactable between 9.00-17.00 hours which made it relatively easy to assess all the referrals.

3.2.2 Inclusion criteria

Inclusion criteria were:

- cortical stroke (Total anterior circulation stroke – TACS or partial anterior circulation stroke – PACS, Oxfordshire Community Stroke Project (OCSP) classification (Bamford et al., 1991)

- symptoms onset less then 24 hours / or able to be scanned within 24 hours of onset of symptoms. Patient woken up from sleep were also included, but time "last known to be well" was noted.
- no contraindication to MRI

In the majority of the assessed patients that were thought to have cortical stroke but were excluded, the main reasons were: late presentation, not able to be scanned within 24 hours of the onset, or too-ill and unstable to be taken to the MR scanner.

3.2.3 Initial clinical assessment

All patients entered in to the study had detailed clinical assessment which included presenting history, past medical history and risk factors for stroke, full general clinical examination including blood pressure, temperature, and blood glucose. They also had complete neurological examination, including National Institute for Health Stroke Scale (NIHSS) score, to assess the degree of initial neurological impairment. (*http://www.strokecenter.org/trials/scales/*). If there was more than a 30 minutes delay between assessment and scanning, NIHSS was repeated and the assessment closest to scanning used in the analysis. Ideally, patients were assessed as they came in to the hospital but also if they were admitted through the night and could have MRI within 24 hours of the onset of symptoms. Out of the 51 patient with ischaemic stroke, 17 were scanned within 6 hours, 15 between 6-12 hours, and 19 between 12-24 hours.

3.2.4 Follow up of the patients

All patients who entered the study agreed originally to the follow up scans. However, the follow up varied depending on the clinical condition of the patient and their experience and tolerance of MRI scanning. 21/50 patients had all 5 scans. Two patients had 1st and final scan as they found MRI unpleasant and would not have tolerated it so closely together. Three patients found MRI claustrophobic and refused further scanning whilst two patients refused to have further MRI beyond the first one with no further explanation and were discharged from hospital within a week of stroke, so had very mild stroke. Ten patients died at various time points during the study (4 patients died after the 1st scan, 2 after the 2nd scan, 2 after the 3rd

and 2 after the 4th scan). Patients attended follow up initially from the same hospital but for subsequent scans (especially beyond two weeks), the patient usually attended either from home or the nearby rehabilitation unit at the Victoria Hospital Edinburgh. Full details of the number of scans per patient at each time point are in Table 1.

At 3 months, at the same time as the MRI, each patient had NIHSS as well as functional assessment including 6 point modified Rankin scale, Barthel Index and Extended Nottingham ADL scale (see appendix 5 for examples of the scales). For the patients who had their final scan at three months, the assessment was performed during their final attendance, soon after or before the MRI scan. For the small number of patients who refused the scan, the final functional outcome scales were completed over the phone with a help of the relative if required. It would have been impossible to be blinded for the patient details, structural, and DWI imaging during their final functional assessment as I assessed all the patients initially, performed all TCDs, kept all the notes, and was present during the scanning of all of the patients. However, both the spectroscopy and perfusion data were processed afterward using identification numbers rather then names so the analysis was performed blinded to patient clinical details.

Table 2. Number of patients scanned at each time point

1st time point	2nd time point	3rd time point	4th time point	5th time point
51	37	32	26	23

3.2.5 The patient data

The data acquired was recorded on an acute assessment data form, and NIHSS was recorded on the forms downloaded form the Stroke Centre website (*http://www.strokecenter.org/trials/scales/*) (see Appendix 6). This data was then entered in to a "Foxpro" database designed for the study by the departmental computer programmer V S. The foxpro database was used for the ease of data entry and handling. The database allows export in to Excel spreadsheets for further analysis.

3.3 Imaging

3.3.1 Magnetic resonance Imaging

All MR imaging was performed on a GE 1.5 T Signa LX (General Electric, Milwaukee, WI, USA) scanner situated in the SFC Brain Imaging Research Centre at the Western General Hospital (Figure 1). After the consent was signed, all patients (or their relatives), completed the standard MRI safety questionnaire. In some instances, dysphasic patients required a skull X ray, especially if there was a history of previous injury to the eyes with metal. If required, patients could be given oxygen during the scanning and peripheral oxygen concentration was monitored throughout with pulse oximetry. Each patient required an intravenous cannula for administration of contrast for perfusion imaging. Once positioned in the scanner, coordinates of the exact position of the patient's head were recorded for positioning for the follow up scans. Those coordinates were used to achieve the same patient position during all subsequent imaging. The minimum time required to acquire all the sequences was 35 minutes. The length of the scan depended on the patient degree of cooperation, and dysphasic patients often required someone present in the scanner with them for reassurance.

Figure 1. Research MRI at the SHEFC Western General Hospital Edinburgh

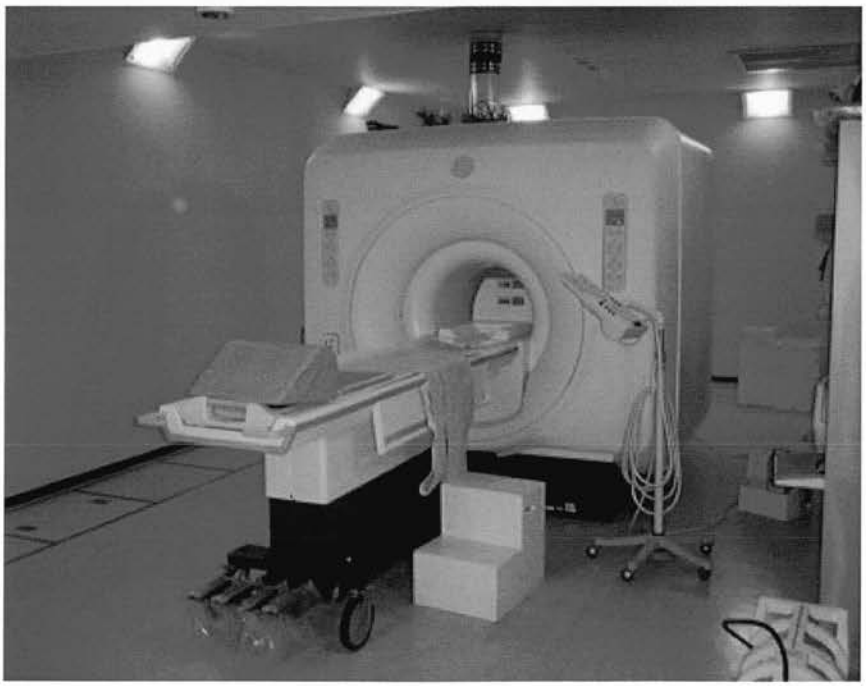

3.3.2 MR imaging sequences

The imaging included axial T2-weighted fast spin echo (T2W), axial diffusion tensor imaging (DTI) based on spin-echo echo-planar imaging (EPI), axial dynamic susceptibility contrast PWI using gradient-echo EPI, and single slice point resolved spectroscopy (PRESS) proton MRS chemical shift imaging (CSI).

The imaging parameters for DTI were: field-of-view (FOV) 240 × 240 mm, 15 axial slices of thickness 5 mm, slice gap 1 mm, acquisition matrix 128 × 128, echo time (TE) 97.4 ms and repetition time (TR) 10 s. Diffusion sensitising gradients with scalar b-values of 1000 s/mm2 were applied in six non-collinear directions. The imaging slices were positioned so as to access the whole brain.

Cerebral brain perfusion was measured from the dynamic signal change following a bolus injection of a gadolinium-based contrast agent (10 mL of 1mmol/mL Gadovist or 20 mL of 0.5 mmol/mL Omniscan) over a period of 85 seconds. We used an automated pump connected to the scanner for injecting the contrast (see Figure 1). We collected thirty-four volumes of 15 axial slices using the same FOV, acquisition matrix and slice locations as the DTI data, but with a TE of 30 ms and TR of 2.5 s.

Spectroscopy was performed with a chemical shift imaging technique in which a large volume of interest is divided in to individual grid square (Fig2). The acquisition volume of interest (VOI) was centred on the diffusion weighted image (DWI) that showed the maximum extent of the acute stroke lesion. The MRS acquisition parameters were: FOV 320 mm, slice thickness 10 mm, acquisition matrix 24×24, TE 145 ms and TR 1000 ms. Automatic shimming and water suppression were applied. For each phase encoding, 512 complex data points were acquired with a sampling interval of 1 ms. The VOI typically covered the ischaemic area and some ipsilateral and contralateral normal brain. A screen capture image was take to show the slice and VOI position for subsequent scanning. Sequential imaging was set up with axial slices chosen carefully to be in the same position for each scanning episode by reference to the "scout" images and the image of the slice with the spectroscopy grid positioned on it.

3.3.3 Mapping of the MRS data to the DWI image

The MRS CSI slice was 10 mm thick and the DWI and PWI slices were only 5 mm thick. During scanning, the CSI slice was positioned so that the DWI/PWI slice showing the maximum acute stroke lesion extent run through the centre of the CSI slab with <2.5 mm overlap of the DWI/PWI slice on either side of the CSI slice. The grid voxel coding was performed on the DWI slice (5mm) that ran through the centre of the MRS slice, i.e. so that 2.5mm of the 10mm thick MRS slice overlapped on either side of the DWI/PWI slice, and the coded slice captured the most reliable (central) MRS information. Because the spectroscopy slice covered the entire thickness of the DWI and PWI slice that showed the maximum lesion extent, plus 2.5mm on either side, thereby capturing representative spectroscopic information across a large proportion of the stroke lesion, we tested ways of including the DWI/PWI slices on either side of the central DWI/PWI slice in the analysis. However, we found this to introduce more error due to lack of complete overlap of the additional DWI/PWI slices with the CSI slice and increased risk of partial volume averaging. During protocol development, we also tested the alternative placement of the CSI slab with one edge starting with the top edge of a DWI/PWI slice so that the CSI slab then covered one DWI/PWI slice, plus a slice gap, plus 4mm of the next DWI/PWI slice but this resulted in more problems due to difficulty in averaging the DWI tissue classification of two adjacent slices except in the very largest lesions. We have tried various other ways of matching the CSI to the DWI/PWI by varying slice thickness and gaps but the constraints of slice number and need for brain coverage mean that there really is no better way of dealing with this problem. The thickness of the CSI slab is limited by signal to noise – too thin a slab results in very poor signal to noise. The MRS slab provided much more information than the single voxel MRS used in most previous studies. Acquisition of multiple adjacent spectroscopy slices would be too time-consuming to be feasible in acute stroke.

3.3.4 Image processing

DTI and PWI processing. The images were transferred to a Sun Ultra Sparc Station 10 (SUN Microsystems, Mountain View, CA, USA) and converted to Analyze format (Mayo Foundation, Rochester, MN, USA). Subsequent processing was performed in

MATLAB (The MathWorks, Natick, MA, USA). Using FLIRT (*www.fmrib.ox.ac.uk/fsl*), a three-dimensional computational image alignment program, bulk patient motion and eddy current induced artefacts were removed from the DTI data by registering the component EPI volumes to the T2-weighted volumes acquired as a part of the DTI protocol. Maps of DTI were obtained from the six DW images acquired for each slice, while ADC maps were calculated from the diffusion tensor fitted voxel-by-voxel to the DTI data. Cerebral blood volume (CBV, calculated as area under concentration/time curve), mean transit time (MTT, calculated as first moment of concentration/time curve) and cerebral blood flow (CBF, calculated as CBV/MTT) images were calculated from gamma-variate functions with arterial input function but without deconvolution (Carpenter *et al.*, 2006). The gamma variate functions were fitted on a voxel-by-voxel basis to PWI concentration-time curves obtained from the dynamic signal change following injection of the contrast agent. PWI data were also corregistered to T2/DWI. The DWI, PWI and CSI data were all registered to the B_0T2 image from the baseline DWI acquisition; all subsequent scans for each patient were also registered to the baseline B_0T2 image.

MRS processing. Spectroscopic data were interpolated to a 32×32 matrix, and 10 mm^3 voxels, followed by zero-order phase correction using the residual water signal (effectively bringing water to a chemical shift of 4.70 ppm) and removal of the residual water signal using the Hanckel-Lanczos singular value decomposition (HLSVD) method(van den Boogaart A 1994). Following Fourier transformation, the resulting spectra were modelled by five Gaussian peaks (corresponding to choline, creatine, NAA containing compounds and lactate) using the AMARES algorithm (Vanhamme L 1997) within the MRUI package (van den Boogaart A 1996). Spectra were automatically discarded if fitted line widths were less than 1 Hz or greater than 10 Hz, if the metabolite peaks were more than 0.1 ppm offset from their expected position, if the voxels lay on the edges of the PRESS excitation region, if the spectra were of poor quality, fell outside brain parenchyma or were >25% CSF. In addition to automated exclusion of the spectra, I visually inspected all spectra including raw data and fitted spectra. Spectra were discarded if judged to be of poor quality eg. having a badly elevated baseline or containing spurious peaks. This also meant that for some patients there were only a few voxels contributing to some of the tissue types. Metabolite peak areas (reported in "institutional" units) were corrected for any drift in scanner performance by reference to monthly spectroscopy phantom quality assurance data.

3.4 Spectroscopy data analysis

I approached the data analysis from two different aspects: a) using a voxel based grid analysis and b) using a region of interest analysis (ROI). The ROI analysis captures large area of "core" and "normal" tissue but does not allow the analysis of the complex stroke lesion in great detail for all the parameters of diffusion, perfusion, and spectroscopy and their associations. It also theoretically can map to subsequent scans more accurately. The grid classification method and analysis will be discussed first followed by the region of interest (ROI).

3.4.1 Diffusion grid classification

Classification of the visual appearance of each voxel in the diffusion weighted image (DWI) was used so as to relate the degree of tissue damage in the diffusion lesion to the blood flow changes on the perfusion lesion and the metabolite values derived from spectroscopy on a detailed voxel by voxel basis. It also allowed the tissue changes on the initial scan to be mapped to changes on subsequent scans to chart lesion evolution in relation to blood flow and metabolite changes.

Diffusion grid classification is based on the visual inspection of the diffusion lesion that corresponds to the brain slice with the MRS position (ie. the slice that showed most extensive stroke lesion on DWI). A program developed in MATLAB® (The MathWorks, Natick, MA, USA) to perform this sub-regional voxel-based classification. The voxels were classified according to appearance on the diffusion image by applying a grid with voxels of dimension 4.7×4.7 mm over the entire DWI slice corresponding to the MRS slice position (Figure 2). This small voxel grid was applied to the DWI image because smaller voxels on the DWI image allowed more precise and reproducible classification of individual voxels than did larger voxels (equivalent in size to the CSI grid) in pilot testing. The DWI images were all windowed on the same standard signal intensity to optimize signal contrast between normal and abnormal tissue. A neuroradiologist, blind to all other data, classified each voxel as: 'definitely abnormal' (DAL), 'possibly abnormal' (PAL), or normal 'ipsilateral' (IN) or 'contralateral'(CN) according to the DWI appearance. The classification also distinguished between the cerebrospinal fluid (CSF), midline, and voxels that fall outside the brain but still `within the CSI box'.

The operational voxel classification(Karaszewski *et al.*, 2006) was used to avoid introducing bias that might occur by using ADC or PWI thresholds that so far have not been shown to discriminate between viable and non-viable tissue(Bandera *et al.*, 2006;Fiehler 2003); DWI signal intensity (not ADC) was the parameter which correlated most closely with cell death or viability in experimental models in comparison with histology(Rivers and Wardlaw 2005), and because the DWI appearance is immediately visible and rapidly assessed in the acute stroke situation (all other parameters including ADC values require some image processing).

The diffusion grid 'Definitely abnormal' (DAL) voxels contained clearly hyperintense (bright white) tissue; 'possibly abnormal' (PAL) voxels contained tissue which appeared subtly hyperintense relative to normal tissue (i.e. in between background normal tissue and hyperintense 'definitely' abnormal tissue); 'normal' (N) voxels contained normal-appearing tissue (Figure2). Voxels falling outside brain parenchyma were excluded. For the longitudinal analysis of choline and creatine (Chapter 5) we combined DAL and PAL tissue in to the one category labelled abnormal (Figure 3). Mismatch was defined as voxels which fell within MTT-abnormal, DWI-normal tissue. The DWI map overlaid on the CSI grid and MTT map were visually inspected and the voxels that fell in the mismatch tissue identified. The data was then extracted from the relevant voxels using specifically designed programme "Brainer" (Figure4).

The inter-rater reliability of classifying voxels was tested by two observers independently and blindly classifying voxels on 20 scans. The classification based on DWI compared with the ADC or PWI values (Rivers C.S. 2006) is the most reproducible. The limits of agreement of the DWI signal values were less than +/- 10% where as variation in ADC and PWI values were much larger (Rivers C.S.2006). This is in accordance with the experimental literature and probably occurs because the variation in DWI signal is less, with narrower standard deviations than is the case with either ADC or PWI values.

The DWI voxel (4.7 x4.7 mm) classification was interpolated to the MRS voxel grid (size 10x10 mm). The MRS voxels were weighted by the proportion of each DWI-coded tissue present in each DWI voxel. The DWI voxels interpolated very well to the MRS voxels as the majority contained tissue of only one classification. In order to calculate the best proportional representation I used the formula where half of the 'possibly abnormal' tissue was added to 'definitely abnormal' tissue voxel (DWI

classification). This meant that all CSI voxels had >75% of the one tissue type. Majority of voxels however did not change the original classification with this formula but it did improve the proportional representation in those few CSI voxels that had mixed tissue within it.

3.4.2 Follow up scans

The same tissue classification was used to extract metabolite concentrations from the follow-up scans and the subsequent time points were mapped on to the original coding of the DWI image. We used the interscan registration matrices to ensure that the spectroscopy voxels from the later time points spatially matched those on the initial scan. We also assessed changes in infarct extent and swelling using a previously validated visual rating scale that codes infarct extent according to typical patterns of involvement in each of the main vascular territories and swelling according to a validated ordinal 7-point scale (Wardlaw and Sellar 1994). The scale ranges from 0 (no swelling) to 6 (indicates shift of the midline away from the side of the infarction with effacement of basal cisterns, thus differentiating between volume increase due to increase in lesion extent and that due simply to swelling.

Figure 2. A) Diffusion grid, CSI grid, CSI colour map (lactate) and corresponding MTT image.

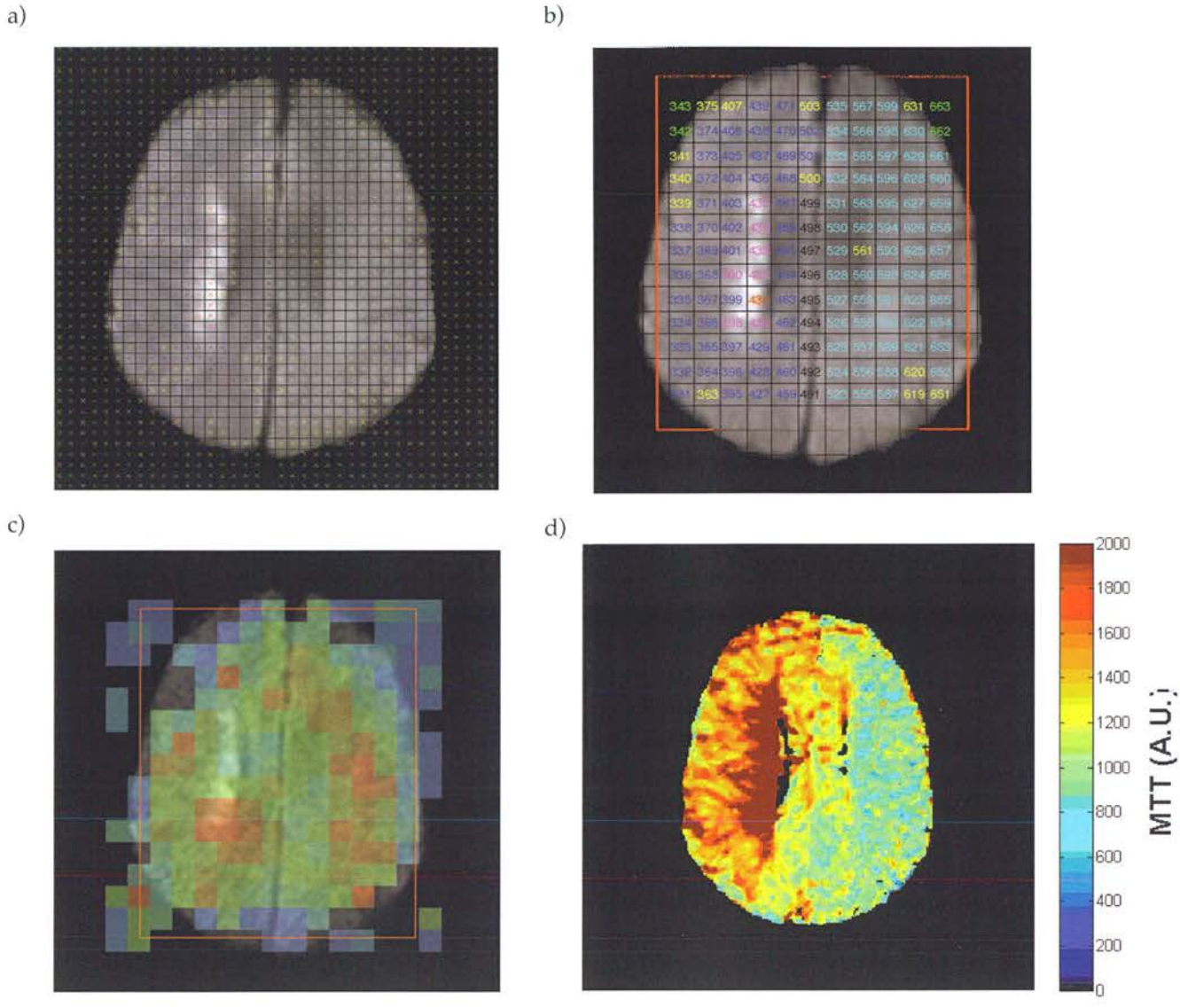

a) Classification voxel grid (4.7x4.7mm) overlaid on DWI image.
x ipsilateral normal (IN) x contralateral normal (CNL)
x cerebrospinal fluid (CSF) x midline
x definitely abnormal (DAL) x outside
x possibly abnormal (PAL)

b) Fine diffusion grid was transposed over the larger CSI grid. Tissue was classified according to the maximum percentage of tissue present.
c) Colour CSI map
d) Perfusion map (visually inspected and compared against the diffusion image). Mismatch region was identified and the data extracted form the area

2 B) MRS grid with the representative processed spectra (right)

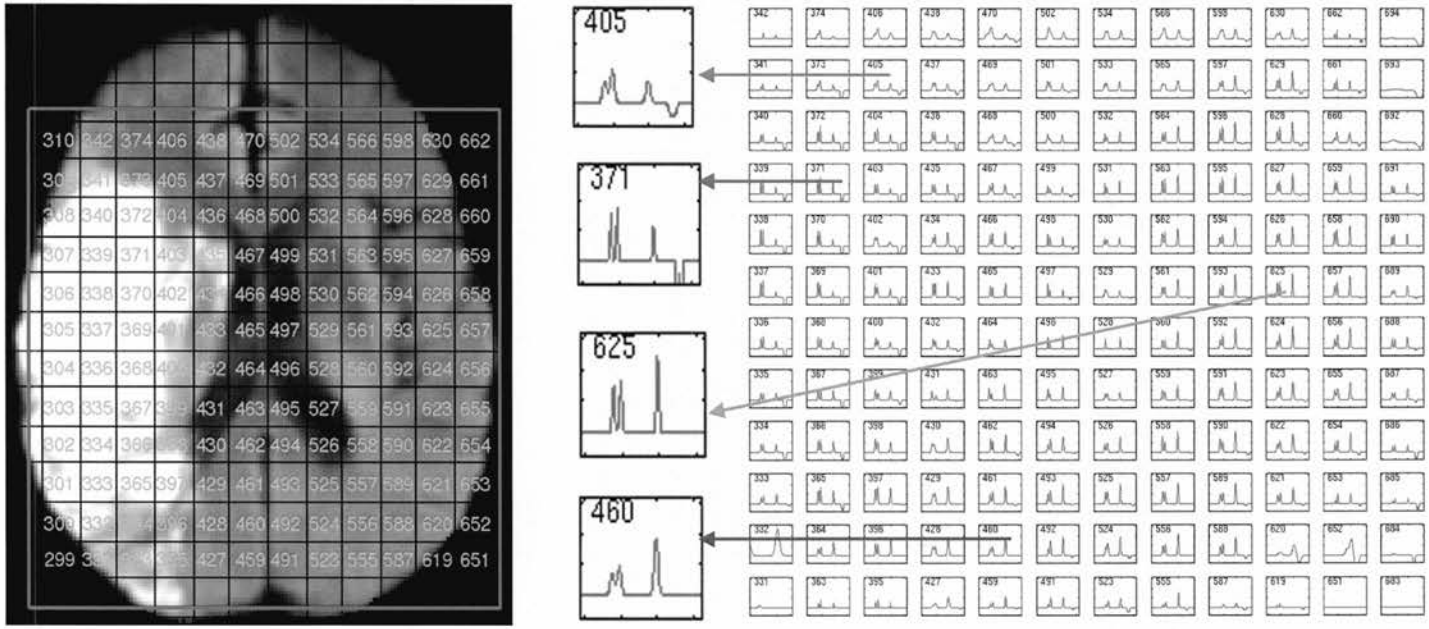

Legend: The representative voxels from the MRS showing spectra from different tissue type using coloured arrow: PAL tissue (cerise), DAL (red), CNL (turquoise) and IN (blue)

*Figure 3. **A**, Classification grid overlaid on the averaged diffusion-weighted image; the classification in each voxel is indicated by a color cross: Yellow, normal; blue, abnormal; gray, cerebrospinal fluid or background.*
***B**, MR spectroscopic image of choline levels of the same subject; each 10×10×10 mm3 voxel is color-coded according to concentration of choline measured. Color bar shows choline concentration in institutional units.*

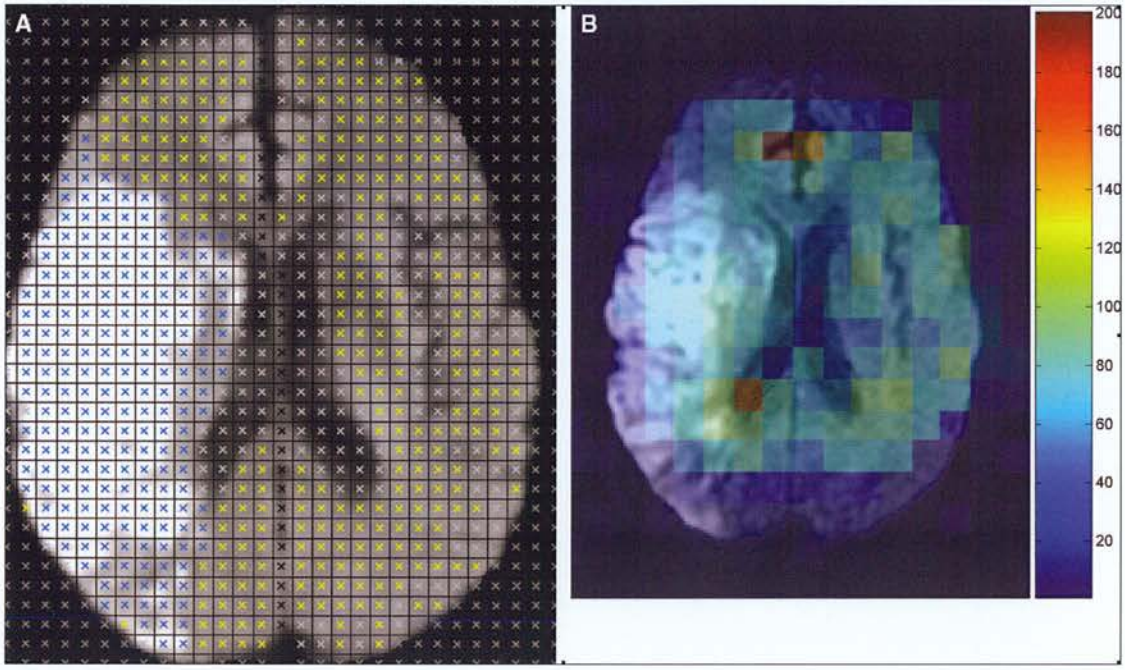

3.4.3 Grid analysis of the first time point

Metabolites (in absolute "institutional units"), perfusion (CBF, CBV and MTT, expressed as "index units" normalised to the contralateral normal hemisphere) and diffusion (ADC) values (expressed as absolute values) were extracted from each voxel type in to spreadsheets.

However, to compare different tissue types we required median values of the metabolites, diffusion and perfusion parameters of all DWI tissue types for each patient. This was made possible by developing a program, whereby entering tissue type classification from the MRS slice in to the matching template, mean and median values for each tissue type were calculated. (Figure 4) This was less labour intensive but meant that all the data was entered manually and a second quality check was performed to exclude any voxels that were at the edge of the lesion or contaminated by the CSF.

Figure 4. The appearance of the screen of the program for the data entry by tissue type and calculation of mean and median values. Tissue types were colour coded as seen on the picture and if the voxels fell in the diffusion /perfusion mismatch area they were further marked by a cross.

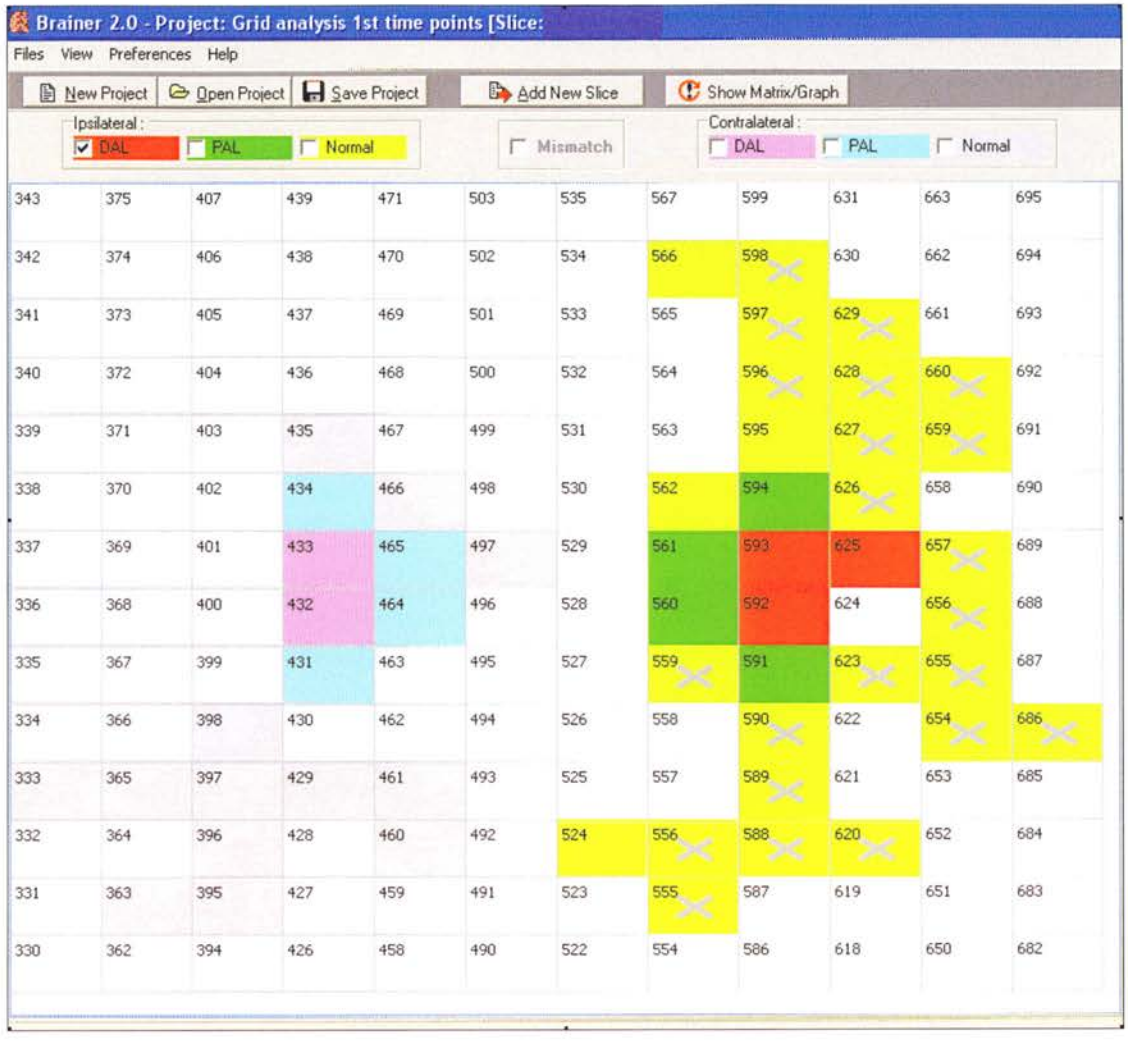

3.4.4 Regions of interest (ROI)

In addition to the voxel grid analysis, we also used regions of interest (ROI) analysis to analyse the diffusion lesion, perfusion and metabolite values in the acute stroke. We outlined the acute ischaemic lesion on the DWI scan, on images with standard contrast settings, using Analyse™ software, blinded to all other imaging and clinical data. Images were outlined by an experienced trained rater. The DWI image (not the ADC map) was used for the reasons already outlined above. A mirror image ROI was placed in the contralateral hemisphere. The ROI was superimposed on the ADC, CBF, MTT, and CSI maps and I extracted corresponding lesion and contralateral normal DWI, PWI values (Figure 5). The DWI ROI covered the whole of the abnormality, whereas CSI was from the 10-mm slab. Care was taken not to include CSI voxels lying at the edge of, but mostly outside the ROI, in the ROI thereby minimizing partial volume effects. Relative metabolites, perfusion and diffusion values were obtained by dividing the stroke ROI values by those from the contralateral mirror image region.

Figure 5.

Region of interest (ROI) outlined on the DWI and superimposed on the same slice perfusion maps and spectroscopic imaging where each coloured square represents a grid box.

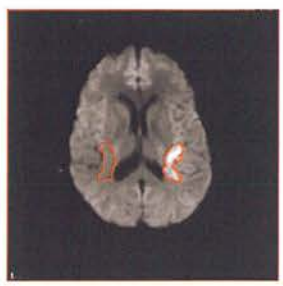

ROI outlined on DTI image

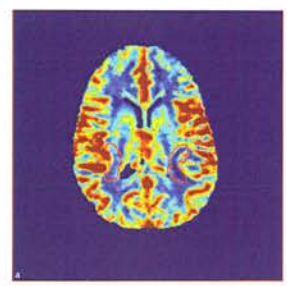

ROI superimposed on CBF map

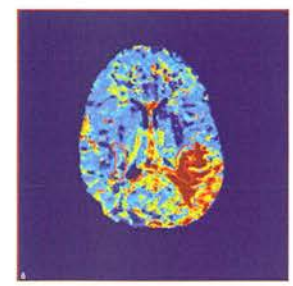

ROI superimposed on MTT map

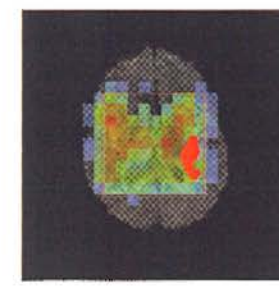

ROI superimposed on CSI image

3.4.5 The metabolites – the rationale for using absolute versus relative values

The metabolites can be presented in different ways as seen in the systematic review of the literature, Chapter 2. The majority of the studies in that chapter presented metabolites in the form of a ratio to either choline, creatine, contralateral normal or an external standard.

In this study, we have elected to use absolute values of the metabolites in institutional units as we had regular phantom checks to account for the drift in the scanner and we have applied an appropriate scaling factor to all the metabolite data. In order to be able to compare the data to some of the other studies we also calculated relative values of the metabolites as a ratio to the contralateral side and in one analysis as a ratio to the sum of the metabolites within the region of interest. As this study involved multiple tome points we have used the opportunity to look at the longitudinal change of choline and creatine and therefore their reliability as a denominator for expressing the metabolite ratio (Chapter 5).

Bamford J, Sandercock P, Dennis M, Burn J, Warlow C. Classification and natural history of clinically identifiable subtypes of cerebral infarction. Lancet 1991; 337: 1521-1526.

Bandera E, Botteri M, Minelli C, Sutton A, Abrams KR, Latronico N. Cerebral blood flow threshold of ischemic penumbra and infarct core in acute ischemic stroke. A systematic review. Stroke 2006; 37: 1334-1339.

Carpenter TK, Armitage PA, Bastin ME, Wardlaw JM. DSC perfusion MRI-Quantification and reduction of systematic errors arising in areas of reduced cerebral blood flow. Magn Reson Med 2006; 55: 1342-1349.

Fiehler J. ADC and metabolites in stroke: even more confusion about diffusion? Stroke 2003; 34: 6-7.

Karaszewski B, Wardlaw JM, Marshall I, Cvoro V, Wartolowska K, Haga K *et al.* Measurement of brain temperature with magnetic resonance spectroscopy in acute ischaemic stroke. Ann Neurol 2006; 60: 438-446.

Rivers C.S. Diffusion and perfusion magnetic resonance imaging in human ischaemic stroke-analysis strategies and measurement isues in the assessment of lesion evolution. University of Edinburgh; 2006.

Rivers CS, Wardlaw JM. What has diffusion imaging in animals told us about diffusion imaging in patients with ischaemic stroke? Cerebrovasc Dis 2005; 19: 328-336.

van den Boogaart A, De Beer R, Van Hecke A, Van Huffel P, Graveron-Demilly S, van Ormondt D. MRUI: a graphical user interface for accurate routine MRS data analysis. Proceedings of the ESMRMB 13th Annual Meeting. Prague 1996; 318.

van den Boogaart A, van Ormondt D, Pijnappel WWF, De Beer R, Ala-Corpela M. Removal of the water resonance from 1H magnetic resonance spectra. In: McWhirter JG, ed. Mathematics in Signal Processing III. Oxford 1994. p. 175-95.

Vanhamme L, van de BA, Van HS Improved method for accurate and efficient quantification of MRS data with use of prior-knowledge. J Magn Reson; 1997. p. 35-43.

Wardlaw JM, Sellar RJ. A simple practical classification of cerebral infarcts on CT and its interobserver reliability. Am J Neuroradiol 1994; 15: 1933-1939.

Chapter 4: Distribution of metabolic changes in the brain within 24 hours of acute ischaemic stroke and their relation to diffusion and perfusion parameters

4.1 Introduction

Ischaemic stroke lesions are known to be heterogeneous especially in the early stages of development of the ischaemia whether imaged by DWI, MRS or SPECT (Guadagno *et al.*, 2005; Guadagno *et al.*, 2006; Nicoli *et al.*, 2003). At this stage it is important to know what proportion of the tissue is salvageable if we are to deliver treatment to the right group of patients and minimise the risk of potentially dangerous side effects.

This chapter will examine brain metabolites within the first 24 hours of the onset of stroke and their relationship with diffusion and perfusion parameters, by using region of interest (ROI) analysis and the CSI grid analysis to determine whether diffusion or perfusion imaging differentiate penumbra from dead tissue .

4.1.1 The ischaemic penumbra and diffusion/perfusion mismatch

In acute ischemic stroke, the ischemic penumbra is considered to be hypoperfused tissue where neurons are functionally silent but retain structural integrity and are potentially salvageable if blood flow can be restored quickly. The mismatch between magnetic resonance (MR) diffusion-weighted (DWI) and perfusion imaging (PWI) may be one way of identifying penumbra, but this approach requires standardisation (Fiehler 2003; Kane *et al.*, 2007b; Sobesky *et al.*, 2005). No consistent perfusion threshold has so far distinguished dead from salvageable tissue reliably (Bandera *et al.*, 2006a; Heiss *et al.*, 2004; Kane *et al.*, 2007a; Sobesky *et al.*, 2004). Several apparent diffusion coefficient (ADC) thresholds have been reported for salvageable/non-salvageable tissue (Fiehler *et al.*, 2002; Loh *et al.*, 2005; Na *et al.*, 2004), but there is considerable overlap between tissue that had already infarcted, tissue that was ischemic but viable, and normal but subsequently infracted (Guadagno et al.,2005; Kidwell *et al.*, 2000).

These studies all use the final infarct as shown on T2 or FLAIR imaging at several days to months after the stroke to determine early tissue viability thresholds. However many changes occurring in between the acute and late phases could influence the final tissue fate and may have added to the variability of acute DWI and PW threshold values.

4.1.2 The role of MRS in understanding metabolic changes in the penumbra

An alternative method of determining early tissue viability would be to use MRS. This detects N-acetyl aspartate (NAA) which, although its precise function is not clearly understood, is almost exclusively found in intact functioning neurons in adults, is present in sufficient quantity to provide a clear measurable signal on MRS, and loss of NAA indicates neuronal death (Demougeot *et al.*, 2004; Monsein *et al.*, 1993; Tsai and Coyle 1995). Thus, NAA is reduced in infarcted tissue in patients (Labelle *et al.*, 2001; Saunders *et al.*, 1995). In a permanent middle cerebral artery occlusion model, by six hours NAA had fallen to 50% of control with 30% of neurons appearing viable histologically; by 24 hours, NAA had fallen to 20% of control with few neurons appearing viable (Sager *et al.*, 1995; Sager *et al.*, 2000). MRS also detects rapid rises in lactate due to anerobic metabolism in acute ischemic tissue (Lemesle *et al.*, 2000; Parsons *et al.*, 2000).

4.1.3 The relationship to diffusion and perfusion parameters

If ADC or PWI directly indicate neuronal damage, then ADC and PWI values should correlate closely with NAA; if they mainly indicate ischemia, then ADC and PWI values should correlate closely with lactate rather than NAA. However, the metabolic counterpart of abnormal DWI and PWI is relatively undefined. As discussed in Chapter 2, there are few studies of MRS and DWI or PWI in acute ischaemic stroke to date (Labelle et al.,2001; Liu *et al.*, 2003; Nicoli et al.,2003; Parsons et al.,2000; Parsons *et al.*, 2002; Rumpel *et al.*, 2001; Stengel *et al.*, 2004; Walker *et al.*, 2004). These studies are small and had a combined total of 190 patients with average study size around 20 patients. While indicating that NAA fell and lactate rose in DWI-abnormal areas, these studies did not examine associations

between metabolites, DWI and PWI parameters in detail across the whole stroke lesion. Many were unable to profile metabolite, diffusion and/or perfusion values because they used single voxel spectroscopy (Labelle et al.,2001; Parsons et al.,2000; Parsons et al.,2002; Rumpel et al.,2001). Many only sampled MRS and diffusion not perfusion (Labelle et al.,2001; Parsons et al.,2000; Parsons et al.,2002; Rumpel et al.,2001; Stengel et al.,2004; Walker et al.,2004). Only one small study compared NAA with both DWI and PWI simultaneously in the DWI-visible lesion, but found very heterogeneous ADC values (Nicoli et al.,2003) (see Chapter 2 for further details).

As DWI and PWI values change immediately with the onset of ischemia, whereas neuronal death occurs after a period of ischemia, one explanation for the variability in reported DWI and PWI thresholds of viability, and in the range of NAA values for a given apparent diffusion coefficient (ADC) value in previous studies, could be that DWI and PWI values mainly indicate the presence of ischemia but are only indirect markers of neuronal loss. Clarification of the association between the DWI (or PWI) abnormality and the amount of neuronal injury at the time of imaging could improve the interpretation of DWI and PWI.

Here, I describe using proton MR spectroscopic imaging to map NAA, lactate, DWI and PWI values across the acute ischaemic lesion and normal brain.

4.1.4 Region of interest (ROI) analysis versus voxel based

We examined the metabolites across the lesion in two different ways; ROI analysis and voxel based analysis, as discussed in methods Chapter 3; The ROI analysis provides a summary estimate of the average change in a parameter within the lesion and in some circumstances has shown better correlation with final infarct size and infarct growth then voxel-based analysis (Na et al.,2004). Voxel based analysis allows more detailed analysis of the lesion by anatomical subregion. In this study the lesion was divided according to DWI appearance.

4.2 Methods for the ROI and grid analysis

Detailed description of methods can be found in Chapter 3.

4.2.1 Statistical analysis

All statistical tests were performed in SPSS 14.0 for Windows (SPSS Inc, Chicago, Ill, USA)for both ROI and grid analysis. The imaging data were not normally distributed (Kolmogorov-Smirnov test, $p>0.01$), so we used non-parametric Wilcoxon Signed Rank Sum Test to compare the metabolite concentrations, ADC and PWI parameters between different voxel classes and ROIs from the ipsilateral and contralateral side. We compared metabolites, DWI and PWI parameters within each voxel class and ROI using the Spearman Rank Correlation coefficient (ρ), and setting significance at the 0.05 level (2-tailed). We examined the relationship between imaging parameters, stroke severity (NIHSS score) and time from stroke to imaging on a per patient basis. We examined the subgroup of patients imaged within six hours of stroke.

We tested for independent associations between metabolites and diffusion/perfusion parameters using general linear modelling in the ROI analysis. In the grid analysis we combined 'definitely' and 'possibly abnormal' tissue to create an 'abnormal' category and performed general linear regression to test for independent associations between metabolites, diffusion and perfusion parameters in the DWI normal versus abnormal appearing tissue. Bonferoni correction was applied by considering $p<0.01$ as significant for multiple comparisons.

In the ROIs, we used lesion metabolite and ADC values in the primary analyses, but repeated the comparison using the lesion/contralateral region ratio as a secondary outcome (for comparison with previous studies). We also calculated lesion [NAA]/[NAA+choline+creatine] ratio for comparison with a previous study (Nicoli et al.,2003).

4.3 Results

4.3.1 Patient characteristics

43 patients in total were used between the two types of analysis. One patient was not included in the ROI analysis which had 42 patients with traceable regions of interest. The age, time from onset and OCSP classification are given in the Table 1. 14 (32%) patients were scanned within six hours, 14 (32%) between six and 12 hours, and 15 (36%) patients between 12 and 24 hours after stroke. 22/43 patients (51%) had DWI/PWI mismatch on MTT. No patients received thrombolysis or investigational treatment and none had carotid stenosis of more than 50%.

Table 1. Age, time from onset, severity and OCSP classification

Age (range+/- SD)	Time from onset to scan (mean) hours	OCSP classification		NIHSS
		TACS	PACS	
76 +/- 11 (37-95)	8+/-6.6 (1.5-24)	19 (44%)	24 (56%)	9+/-7.8 (1-29)

The demographic detail of all individual patients including their risk factors for ischaemic stroke is listed in Table 2.

Table 2. Demographic characteristics of the 43 patients included in the grid and ROI analysis

Sex of the patients	23 male
Side of the lesion	23 left hemisphere
Smoking history	32 non smokers (13 ex smoker)
Cognitive impairment	3 / 43
Ischaemic heart disease	21 / 43
Hypertension	27 / 43
Diabetes mellitus	1 / 43
Peripheral vascular disease	2 / 43
Atrial fibrillation	12 / 43

4.3.2 Region of interest analysis

Metabolites in the DWI lesion

NAA and choline levels were significantly lower in the diffusion lesion than in contralateral normal brain (ipsilateral versus contralateral: NAA 96.0 versus 122.4, *P*=0.0001; choline 63.6 versus 70.1, *P*=0.015 Wilcoxon Rank Sum; Figure 1). Lactate was detected in all but one diffusion lesion (lactate ipsi versus contralateral: 12.5 versus 42.5, *P*=0.0001) (see Table 3, Figure1). Some lactate was detected in 10 patients in the contralateral region; in all cases this was less than in the diffusion lesion and all patients had large diffusion lesions and generalized cerebral atrophy. Creatine did not differ significantly between the lesion and contralateral normal brain.

Table 3. Median metabolite concentrations in the diffusion lesion and mirror image contralateral brain: absolute values in institutional units corrected for the scanner drift.

Metabolites	Ischaemic lesion (ROI) Median (range +/- SD)	Contralateral brain Median (range +/- SD)	Significance of difference (Wilcoxon Rank Sum test)
NAA	96.0 (37 -178, +/-33)	122.4 (44 -175, +/-32)	p=0.0001*
Lactate	42 (0 – 93, +/-26)	12.5 (0 – 59, +/-12)	p=0.0001*
Choline	63.6 (28 – 118, +/-21)	70.1 (24-119, +/-23)	p=0.015*
Creatine	70.0 (26 – 98, +/-19)	71.5 (21-107, +/-19)	p=0.2

.

Figure 1. Box plots of absolute median values of the metabolites in the acute ischemic lesion ROI on diffusion imaging (ipsilateral) and in contralateral normal brain.

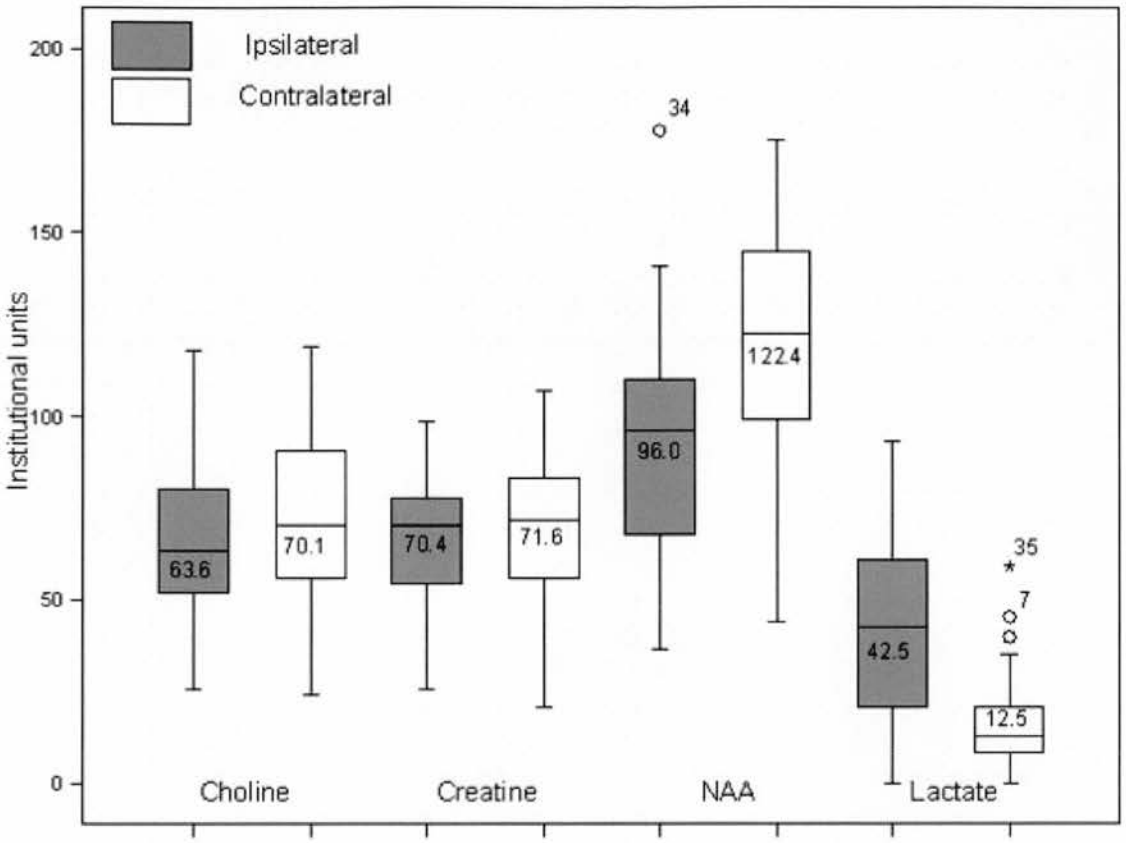

Legend: Box indicates interquartile range; middle bar, median with numeric value; whiskers represent maximum and minimum values; circles above represent outliers

Relationship between metabolites, DWI and PWI parameters

The diffusion and perfusion values in the ROI of the lesion are given in the Table 4. There was no correlation between lesion NAA and ADC ($\rho = 0.15$, p=0.34), MTT ($\rho = 0.16$, p=0.31) or CBF ($\rho = -0.11$, p=0.48)(Table 5). Higher lesion lactate was associated with lower lesion ADC (Spearman $\rho = -0.32$, P=0.039) and prolonged MTT (Spearman $\rho = 0.31$ P=0.04). There were no associations between choline or creatine and DWI or PWI values. These results did not change when we repeated these analyses using metabolite and ADC ratios (Table 5) (ie, relative values) instead of absolute values. Restricting the analyses to those patients imaged within 6 hours did not show any correlation between NAA and ADC, MTT, and CBF (Table 6). Lactate correlated strongly with MTT (Spearman ρ=0.74, P=0.003) and CBF (Spearman $\rho = -0.78$, P=0.001) but not ADC (Spearman $\rho = -0.495$, P=0.07). There was an association

between [lesion NAA]/[lesion NAA+choline+creatine](Nicoli et al.,2003) and reduced ADC (Spearman ρ=0.434, *P*=0.005), but this composite ratio is difficult to interpret given that neither NAA nor choline are constant in acute stroke.

Table 4. The relative values of perfusion and diffusion parameters in the ROI

ADC and perfusion	Median (range +/- SD) Relative to contralateral
CBF	0.7 (0.5-1.5, +/-0.3)
MTT	1.3 (0.3 – 3.4, +/-0.3)
ADC	0.8 (05 – 1.0, +/-0.5)

ADC, absolute apparent diffusion coefficient; MTT, mean transit time; CBF, cerebral blood flow.

Table 5 Spearman's Rank Correlation Coefficient (ρ) Between Metabolites and Diffusion and Perfusion Parameters.

	NAA (absolute)	NAA (relative)	Lactate
ADC	ρ = 0.15, p=0.34	ρ = 0.17, p=0.29	ρ = -0.32, p=0.039
CBF	ρ = -0.11, p=0.48	ρ = -0.01, p=0.93	ρ = -0.10, p=0.52
MTT	ρ = 0.16, p=0.31	ρ = 0.005, p=0.97	ρ = 0.31, p=0.043

Table 6 Spearman's Rank Correlation Coefficient (ρ) Between Metabolites and Diffusion and Perfusion Parameters for the patients scanned within 6 hours of onset.

	NAA (absolute)	Lactate
ADC	ρ = 0.28, p=0.36	ρ = -0.40, p=0.15
CBF	ρ = 0.12, p=0.70	ρ = -0.78, p=0.001
MTT	ρ =-0.13, p=0.64	ρ = 0.75, p=0.002

Metabolites, stroke severity, lesion volume, time from stroke

There was no association between any of the metabolites and the initial NIHSS score. Larger DWI lesion volume was associated with reduced NAA (Spearman's ρ = -0.42, p=0.006) and increased lactate (Spearman's ρ = 0.49, p=0.001) but not with choline or creatine. Longer times to scanning were associated with lower NAA (Spearman's ρ = -0.33, p=0.03) and larger lesion volumes (Spearman's ρ = 0.35, p=0.023) but not with lactate, choline, creatine or ADC (Figure2).

Linear regression analysis

We tested for independent associations between NAA, lactate and diffusion/perfusion parameters, time to scan and stroke severity using linear regression (Table 7). MTT (p=0.02) and DWI lesion volume (p=0.005) were significant predictors in the lactate model and time from onset to scan (p=0.034) in the NAA model.

Table 7. Linear regression analysis with lactate and NAA as constants and DWI, PWI parameters, lesion volume, time to scan (hours), and stroke severity as variables in the model

	Coefficients of the regression line			Coefficients of the regression line		
Model	B	Std. Error	Sig.	B	Std. Error	Sig.
(Constant)	-1.514	37.162	0.968	91.377	49.283	0.072
CBF	16.725	16.908	0.329	2.160	22.423	0.924
MTT	24.988	10.354	0.021	12.793	13.731	0.351
Volume	2.636	0.889	0.005	-2.176	1.179	0.073
ADC	-4.776	28.967	0.870	10.329	38.415	0.790
Onset-scan (hrs)	-0.153	0.607	0.802	-1.772	0.805	0.034
NIHSS	-0.696	0.550	0.214	-0.134	0.729	0.854
	Dependent variable: lesion lactate			Dependent variable: lesion NAA		

ADC indicates absolute apparent diffusion coefficient; MTT, mean transit time; CBF, cerebral blood flow; NIHSS, National Institutes of Health Stroke Scale Score.

Figure 2. Spearman Rank Correlation Coefficient (ROI analysis)

2A)

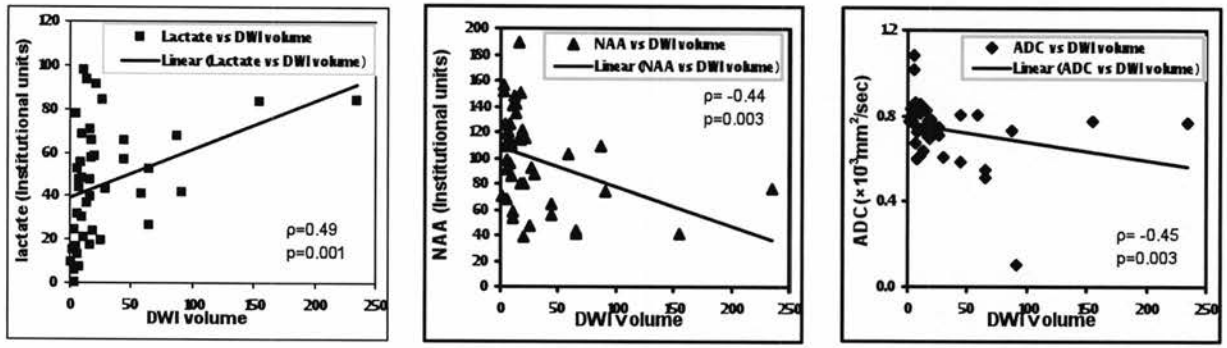

2B)

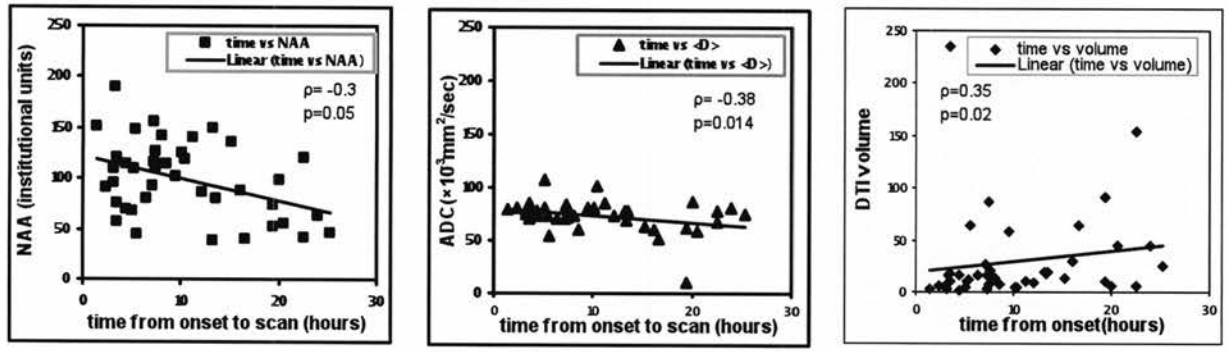

2A) DWI volume versus lactate, NAA, ADC; 2B) time from onset versus NAA, ADC and diffusion volume. Lactate and NAA expressed as absolute values in institutional units.

Summary of the results from the ROI analysis

We found no direct association between NAA as an index of neuronal loss and ADC, CBF, or MTT in the acute diffusion lesion, on either absolute or relative measures. However we did find associations between elevated lactate, reduced ADC, and prolonged MTT, which all indicate the presence of ischemia. The results did not change when the analysis was restricted to patients imaged within 6 hours of stroke. The larger diffusion lesions were associated with lower NAA and higher lactate values which is consistent with findings of previous studies showing that large lesions on T2 weighted imaging had lower NAA and higher lactate than small lesions (Lanfermann *et al.*, 1995; Lemesle et al.,2000; Parsons et al.,2002; Pereira *et al.*, 1999; Wardlaw *et al.*, 1998).

These results also confirm the observations made in previous small MRS studies: there was no correlation between NAA and ADC (Labelle et al.,2001) because the range of NAA values for a given ADC value was very wide (Nicoli et al.,2003). Therefore ADC and perfusion values are useful markers of the presence of ischemia. The lack of correlation with neuronal damage would explain the absence of agreement between previous studies on reported thresholds for salvageable/non salvageable tissue. The heterogeneity of ADC and PWI values (Bandera *et al.*, 2006; Guadagno et al.,2005) within and around the acute stroke lesion, together with recovery of DWI-abnormal tissue in some cases (Davis and Donnan 2005; Kidwell et al.,2000), means that it is unlikely that any single DWI or PWI parameters will reliably indicate the amount of permanent tissue damage.

Further discussion of the results, strength, and weaknesses of the study will be presented together with the results of the grid analysis at the end of this chapter.

4.3.2 Results – MRS grid analysis

Association between metabolites and with tissue appearance on DWI

NAA was lowest in the DWI 'definitely abnormal' voxels (Table 8), and lower in 'definitely' than in 'possibly abnormal' voxels. (97.9 vs 113.3, p=0.01), It was also lower in 'possibly abnormal' than in 'mismatch' and 'normal' voxels (Table 9; Figure 3). There was no difference in NAA between mismatch (DWI/MTT) and normal tissue. That is, NAA was reduced only in tissue that appeared in any way abnormal on DWI; the more abnormal the tissue appeared, the lower the NAA, and therefore the greater the neuronal loss.

Lactate was highest in 'definitely abnormal' voxels (Table 8), and successively lower in 'possibly abnormal', 'mismatch', 'ipsilateral' and 'contralateral normal' tissue (all comparisons $p<0.01$).

There was no difference in ADC between 'definitely' and 'possibly abnormal' voxels, but ADC was reduced in any DWI abnormal ('definitely' or 'possibly') compared with 'mismatch' and 'normal' voxels (Table 8; Figure 3).

There was no difference in CBF or MTT values between 'definitely' and 'possibly abnormal' voxels. CBF was reduced and MTT prolonged in any DWI abnormal ('definitely' or 'possibly') compared to 'mismatch' and 'ipsilateral normal' voxels, and MTT was prolonged in ipsilateral compared to 'contralateral normal' voxels. When the analysis was restricted to the 15 patients imaged within six hours of stroke, the significant associations all became non-significant, probably due to the small number of patients.

Table 8 Median values by tissue type for metabolites, ADC and PWI parameters.

Tissue type	Median ADC, PWI and metabolite values					
	ADC	CBF	CBV	MTT	NAA	LACT
DAL	804.3	0.7	0.9	1.1	97.9	89.8
PAL	857.9	0.8	0.9	1.2	113.3	52.0
INL	1098.5	0.9	1.1	1.1	124.6	21.2
MM	1050.8	1.0	1.6	1.8	124.9	30.7
CNL	1126.6	1.0	1.0	1.0	131.9	16.4

Legend: Tissue Type: DAL-'definitely abnormal', PAL- 'possibly abnormal', INL-'ipsilateral normal', MM-'mismatch', CNL- 'contralateral normal'. CBF, CBV and MTT expressed as Index Units (normalised to the contralateral normal hemisphere), ADC $\times 10^{-6}$ mm^2/sec, and NAA and lactate as absolute values in institutional units

Table 9. Significance of differences between metabolites, DWI and PWI parameters between different voxels classified according to the DWI appearance.

Tissue voxel type	Wilcoxon signed rank sum test comparing tissue types (p values)					
	ADC	CBF	CBV	MTT	NAA	LACT
DAL vs PAL	0.758	0.68	0.636	0.85	**0.01**	**0.001**
PAL vs INL	**0.001**	**0.003**	0.06	**0.006**	**0.007**	**0.0001**
INL vs CNL	0.57	0.32	0.05	**0.0001**	**0.01**	**0.006**
MM vs DAL	0.136	0.435	0.86	0.177	**0.004**	**0.002**
MM vs PAL	0.088	0.095	0.263	0.291	**0.039**	**0.011**
MM vs CNL	0.178	**0.005**	0.158	**0.0001**	0.178	**0.003**

Wilcoxon signed rank test. (* **bold** – statistically significant vaue)

Legend: Tissue Type: DAL-'definitely abnormal', PAL- 'possibly abnormal', INL-'ipsilateral normal', MM-'mismatch', CNL- 'contralateral normal'. CBF,CBV and MTT expressed as Index Units (normalised to the contralateral normal hemisphere), ADC $\times 10^{-6}$ mm^2/sec, and NAA and lactate as absolute values in institutional units

Figure 3: Box plots of median absolute metabolite (in institutional units), ADC and PWI values in the ischemic lesion by voxel classification.

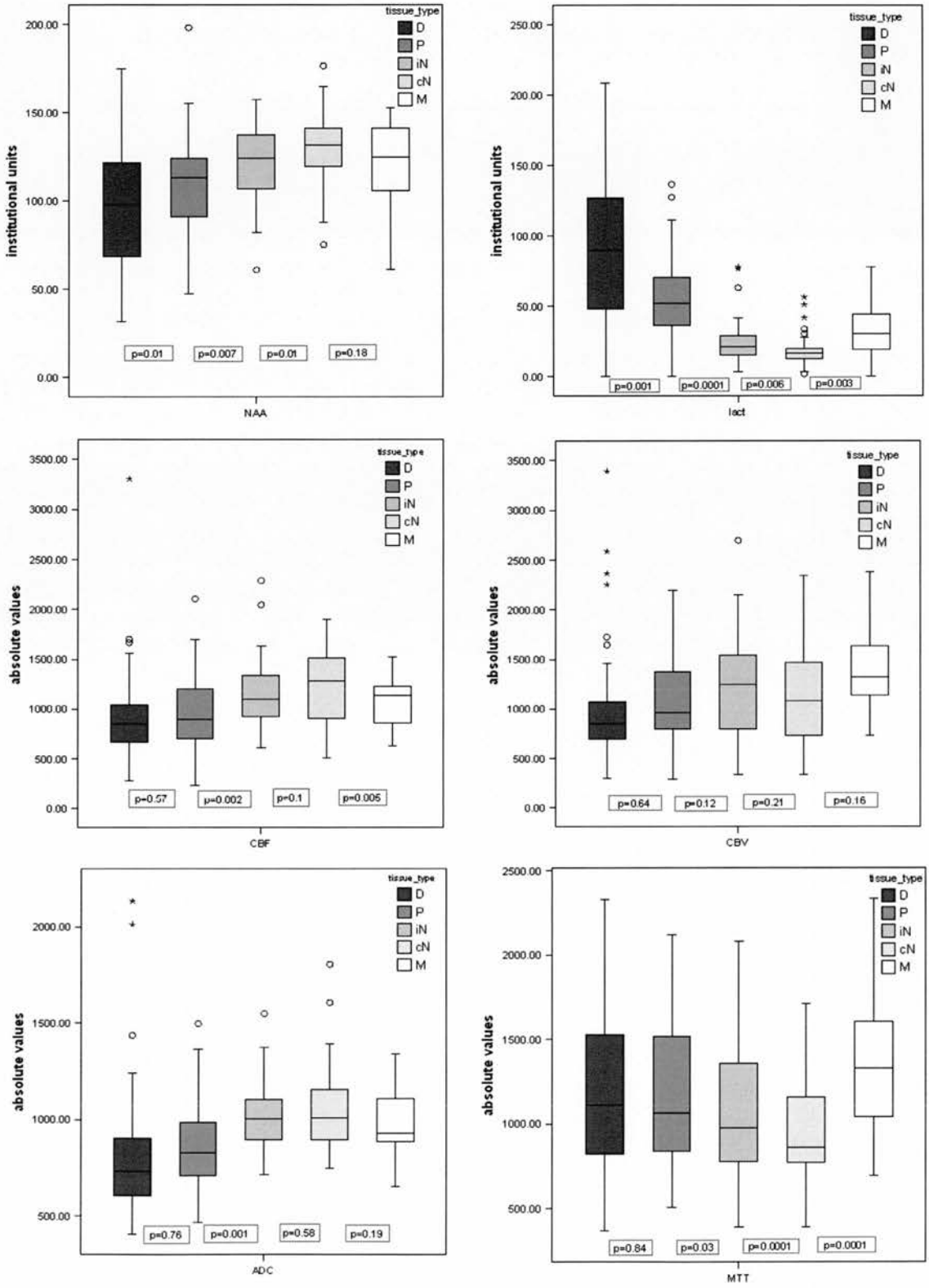

Figure 3 legend: The box represents the interquartile range; the middle bar represents the median; whiskers represent maximum and minimum values; circles above represent outliers. D, 'definitely' abnormal; P, 'possibly' abnormal; iN, ipsilateral normal; cN,contralateral normal; M, mismatch voxels

Associations with time to imaging and stroke severity

NAA was lower in patients scanned at later times after stroke in 'definitely' and 'possibly abnormal' voxels (ρ= -0.4, p=0.03 and ρ = -0.44, p=0.04 in 'definitely' and 'possibly abnormal' tissue respectively) (Table 10). Lactate, ADC and MTT were not associated with time to scanning in any voxel type. Higher CBF and CBV values were associated with increasing time from onset to scanning only in possibly abnormal tissue (ρ =0.52, p=0.0001, ρ =0.4, p=0.008 respectively) (Table 10). When restricted to the 15 patients imaged within six hours, the significant associations became non-significant, probably due to the small sample size. There was no association between NAA or lactate and stroke severity (NIHSS) in any of the voxel types. More severe stroke was associated only with lower ADC and CBF in 'possibly' abnormal voxels (ρ = -0.5, p=0.003, ρ = -0.32, p=0.04 for ADC and CBF respectively) and with prolonged MTT in 'ipsilateral normal' voxels (ρ =0.6, p=0.001) (Table 10). When restricted to the 15 patients imaged within six hours, the association between NAA, lactate and stroke severity remained non-significant; ADC and CBF in 'possibly abnormal' tissue lost the significant association with NIHSS; and the association between CBF, CBV, MTT and NIHSS in 'ipsilateral normal' tissue became significant. These results should be interpreted with caution due to the small number of patients in this subgroup analysis.

Table 10. Correlation (Spearman ρ) between metabolites, ADC and PWI values with time from onset to scan and NIHSS.

	Spearman (ρ) correlation of metabolites, DWI and PWI with time from onset and NIHSS					
	ADC	CBF	CBV	MTT	NAA	LACT
Time from onset						
DAL	ρ = 0.2 p=0.1	ρ = 0.2 p=0.3	ρ = 0.13 p=0.4	ρ = 0.9 p=0.6	**ρ =-0.4 p=0.03**	ρ = 0.1 p=0.4
PAL	ρ = 0.01 p=0.9	**ρ = 0.52 p=0.0001**	**ρ = 0.4 p=0.008**	ρ = -0.1 p=0.6	**ρ =- 0.44 p=0.04**	ρ = 0.04 p=0.8
INL	ρ = 0.09 p=0.5	ρ = 0.08 p=0.6	ρ = -0.06 p=0.7	ρ = 0.02 p=0.9	ρ = -0.2 p=0.3	ρ = 0.08 p=0.6
NIHSS						
DAL	ρ = 0.2 p=0.2	ρ = -0.2 p=0.2	ρ = -0.15 p=0.4	ρ = 0.12 p=0.5	ρ = -0.08 p=0.6	ρ = 0.01 p=0.9
PAL	**ρ =- 0.5 p=0.003**	**ρ = - 0.32 p=0.04**	ρ = 0.18 p=0.25	ρ = 0.2 p=0.21	ρ = -0.2 p=0.2	ρ = 0.2 p=0.1
INL	ρ = 0.1 p=0.3	ρ = 0.13 p=0.4	ρ = 0.07 p=0.63	**ρ = 0.6 p=0.001**	ρ = 0.08 p=0.6	ρ = 0.2 p=0.1

bold- statistically significant correlation.
Legend: Tissue Type: DAL-'definitely abnormal', PAL- 'possibly abnormal', INL-'ipsilateral normal', CNL- 'contralateral normal', NIHSS-National Institute of Health Stroke Scale.

Associations between metabolites and diffusion and perfusion parameters

Univariate analyses showed no association between NAA and ADC or PWI parameters in DWI 'definitely' (NAA vs. ADC, ρ = -0.16, p=0.4; and vs. MTT ρ =0.33, p=0.054) or 'possibly' (NAA vs. ADC, ρ = -0.24, p=0.1; and vs. MTT ρ =0.172, p=0.28) abnormal voxels. Elevated lactate was associated with reduced ADC and prolonged MTT in 'definitely' (lactate vs. ADC, ρ = -0.41, p=0.02; and vs. MTT ρ =0.42, p=0.02) and 'possibly' (lactate vs ADC ρ =-0.32, p=0.04 and vs. MTT ρ =0.37, p=0.02) abnormal voxels. We repeated the analysis in the 15 patients imaged within six hours. The association between NAA, ADC and PI parameters remained negative and the associations between elevated lactate and reduced ADC/prolonged MTT were also unchanged. Multivariate modelling confirmed the association between reduced NAA and increasing time to scanning in the whole patient group (Coefficient B -2.4, p=0.001), and between high lactate and reduced ADC (Coefficient B -0.07, p=0.001), but not between any other variables (Table 11). Restricting the analysis to the 15 patients imaged within six hours did not change these results.

Table 11. Multivariate analysis: Models with NAA and lactate as dependent variable to test for independent association with diffusion and perfusion variables in voxel based analysis.

	Unstandardized Coefficients			Unstandardized Coefficients		
Model	B	Std. Error	Significance	B	Std. Error	Significance
(Constant)	107.351	31.958	0.002	102.387	35.427	0.006
NIHSS	-1.733	0.644	0.11	0.084	0.714	0.907
Onset_MRI	-2.363	0.665	0.001	0.576	0.737	0.439
MTT	0.055	0.025	0.38	0.008	0.028	0.784
ADC	-0.004	0.018	0.820	-0.074	0.020	0.001
CBF	0.029	0.023	0.212	-0.020	-0.026	0.262
CBV	-0.046	0.024	0.063	0.030	0.026	0.262
	Dependent variable: NAA			Dependent variable: lactate		

4.4 Discussion

Summary of the results and main conclusions

This study demonstrates several important points concerning characterisation of tissue damage with imaging in acute ischemic stroke. Firstly, the ADC, PWI and lactate values are sensitive to the presence of ischemia (significant differences between DWI abnormal, mismatch and normal tissue) but the absence of any correlation with NAA indicates that they are less specific for cumulative permanent neuronal damage. A similar conclusion was drawn from the ROI analysis. Secondly, the elevated lactate but normal NAA in 'mismatch' tissue is consistent with the hypothesis that mismatch tissue is ischemic but still viable. Thirdly, the NAA temporal profile was different to that of ADC, PWI and lactate values – NAA declined with time after stroke, consistent with experimental models (Sager et al.,2000), whereas ADC, PWI and lactate values showed no clear temporal profile. Fourthly, the acute ischemic lesion appearance on DWI (the "whiteness"), but not the ADC value, corresponded with the degree of neuronal damage, consistent with experimental data where DWI signal intensity but not ADC level was associated with histologically-determined neuronal damage (Rivers and Wardlaw 2005). Thus in the acute ischemic lesion, the lack of association between NAA and ADC, MTT and lactate, may explain the lack of any consistent ADC or PWI threshold identified to date to distinguish salvageable from non-salvageable tissue(Bandera et al.,2006; Fiehler2003). The findings of the ROI analysis are in agreement with the grid analysis.

The strengths of the study

These include the large sample size (for a complex stroke imaging study), careful patient assessment, careful image registration and detailed voxel-based analysis. The use of DWI appearance in the image analysis means that the results are independent of any threshold values and also directly translatable to clinical practice, fast and immediate to apply – the brighter the DWI signal, the greater the neuronal damage, and presumably the less likely that the tissue will be salvageable (but this would require further testing). We could have used an ADC or PWI threshold to delineate the acute stroke lesion, but no consistent threshold has yet been found that reliably identifies salvageable/non-salvageable tissue (Bandera et al.,2006). Both ROI analysis and voxel-based analysis (although much more detailed than region-of-interest

approaches), may suffer from partial volume effects at lesion edges particularly for CSI. I was very careful to exclude poorly fitted or noise contaminated spectra and all CSF-contaminated voxels. I included patients imaged up to 24 hours after stroke (in pre-specified time windows) so as to be able to examine the temporal profile and because there is evidence of substantial amounts of ischemic but viable tissue (50% of lesion) up to at least 24 hours after stroke (Markus *et al.*, 2004). Whether or not this apparently viable tissue is salvageable with revascularisation therapies beyond six hours is currently uncertain and the subject of ongoing trials. When we restricted analysis to just those patients imaged within six hours of stroke, the results in general did not change although many of the significant associations lost their significance, most likely due to the small sample size (applies to both analyses). We did not use metabolite ratios because their use is questionable as there is no reliable denominator that does not change in acute ischaemic stroke: both choline and creatine are altered by the ischaemic process (discussed in Chapter 5) (Munoz et al., 2008). Some variations in alternative metabolite ratio denominators may be interesting, for example the lactate/NAA ratio which is a sensitive metabolic index of acute ischaemia which was used to demonstrate the wide metabolic heterogeneity inside the abnormal area delineated by ADC map (Nicoli et al.,2003). Indeed, the increasing lactate level combined with the simultaneous decreasing NAA level may enhance the diagnostic value of this metabolic ratio and avoid potential problems due to increased water content from cellular oedema (Nicoli et al.,2003). It is difficult to perform absolute MRS quantification of brain metabolites due to variations in water content arising from brain pathology. The additional sequences (absolute T1 quantification) required to overcome this would make the scan times intolerable for acutely ill patients and as the tissue water increase in the first 24 hours of stroke is less than 6% it would seem reasonable to use standardised individual metabolite values (Dzialowski *et al.*, 2004).

The limitations of the study

Lack of out-of-hours scanner availability hampered recruitment (although there is no evidence that patients admitted during the night are different to those seen during the day). Not all patients were able to complete the scanning protocol, particularly those with severe stroke, so some patients that started imaging did not contribute to the analysis and patients with very severe stroke may be underrepresented in this study. We used a single thick spectroscopic imaging slab centred on the DWI slice that showed the acute stroke lesion at its most extensive; the spectroscopy slice

covered the entire thickness of the DWI and PWI slice that showed the maximum lesion extent, plus 2.5mm on either side, thereby capturing representative spectroscopic information across a large proportion of the stroke lesion. This has been discussed in some detail in the methods chapter 3. The correlations of metabolites with time after stroke should be interpreted cautiously because these data come from different patients imaged at different times after stroke, not the same patients imaged serially. However, it would have been unethical and impractical to image patients every few hours soon after admission with stroke. The time of onset may have been estimated as earlier than it actually was in those who awoke from sleep with stroke (I used the time last known to be normal to the best of my ability), as there is some evidence that the stroke most often occurs shortly before awaking rather than just after falling asleep, but I aimed to be conservative. The multivariate analysis does adjust for some confounding factors, but not all and multiple comparisons should therefore be cautiously interpreted. Thus, associations between time and ADC, NAA, or PWI values may still be confounded by stroke severity or other factors, and these data should be regarded as exploratory. Larger studies with more patients imaged sequentially early after stroke would be required to be certain of overcoming these confounders reliably, although would be practically difficult and may suffer from other sources of bias. The data on patients imaged within six hours should also be interpreted cautiously as the sample size (15 patients) is small. One previous study of six patients found a strong correlation between lesion ADC and NAA and lactate (Nicoli et al.,2003) using a region of interest rather than voxel based approach. The region of interest analysis in the same patient population, found an association between the ratio [lesion NAA]/[lesion NAA+choline+creatine] and reduced ADC (Spearman ρ= 0.434, p=0.005) but it is important to note that this composite ratio is difficult to interpret given that neither NAA nor choline are constant in acute stroke.

Therefore we did not repeat the analysis with that ratio using the grid-based analysis. Also in agreement with Nicoli et al, in both the grid analysis and the ROI analysis, we have shown an association between rising lactate and falling ADC. Nicoli et al (Nicoli et al.,2003) also commented on the pronounced heterogeneity of ADC within the lesion which we have also found. The association of elevated lactate with both falling ADC and prolonged MTT in the present study means that we would most likely have found a similar association to that of Nicoli (Nicoli et al.,2003) for the ratio of lactate/NAA with ADC and MTT. Another study (14 patients) found no correlation between ADC and NAA in the first 24 hours (Labelle et al.,2001). The lack of association between ADC and NAA could be explained by

different rates of change. ADC falls immediately after stroke (Kucinski et al., 2002) before rising, at different rates in different patients, to supra normal values, whilst NAA represents cumulative neuronal death and levels decline more gradually (Sager et al.,1995; Sager et al.,2000; Saunders et al.,1995).

The presence of lactate in normal appearing tissue on T2-weighted imaging has been reported previously in 11 patients between 2-24 hours after stroke. However, as T2-weighted imaging is less sensitive to ischemic change than DWI, it is possible that some of the normal appearing tissue on T2-weighted imaging was actually ischemic (Gillard *et al.,* 1996). Another study found lactate outside the diffusion (ADC) lesion (Stengel et al.,2004). In both studies the lactate could have been in mismatch tissue. Some lactate in DWI normal tissue ipsilateral to the stroke could be accounted for by partial volume effects from adjacent mismatch voxels but we also found lactate in contralateral normal brain. This could be an artefact of fitting lipids, or contamination from lactate entering CSF from ischemic brain in patients with significant cerebral atrophy. However, the most likely reason is that lactate can be found in healthy brain tissue in older people or that MRS may be a better indicator of future pathology (and/or asymptomatic present pathology) than MRI (Sijens *et al.,* 2001).

What do the present findings mean?

NAA is found exclusively in functioning neurons (Demougeot et al.,2004; Tsai and Coyle1995). Several ischemia models demonstrated an initial rapid decrease of NAA following induction of ischemia, then a further slower decline (Monsein et al.,1993), that correlated closely with histological evidence of neuronal death (Sager et al.,1995; Sager et al.,2000). The NAA had fallen to 50% of normal by 6 hours and to 20% of normal by 24 hours, corresponding with similar proportions of non-viable neurons identified histologically (Sager et al.,2000). Although accumulation of oedema fluid in the ischaemic lesion could "dilute" the NAA and account for some of the apparent reduction in NAA, generally within the first 24 hours the increase in water content is around 6% as judged by experimental and patient data (Dzialowski et al.,2004), which would not be enough to account for the magnitude of metabolite changes that we have detected. Thus it is reasonable to regard NAA reduction as specific for neuronal loss in acute ischemia. In contrast, at subacute times, there is some uncertainty about whether any residual NAA detected spectroscopically represents a few still viable neurons, neuronal debris, infiltrating microglia, or possibly migrating neural stem cells (Demougeot et al.,2004). This pattern of early NAA loss has been

confirmed in patients (Gideon *et al.*, 1994; Saunders et al.,1995). In contrast, in animal models, the ADC value falls as neuronal and glial swelling develops, and then either remains low in persistent occlusion models until dead cells of all types are lysed, or rises in transient ischemia models due primarily to resolution of glial swelling (Rivers and Wardlaw 2005). Indeed histological comparisons suggest that the ADC is a better marker of glial cell status than of neuronal viability, with the DWI signal ("whiteness") being a better marker of neuronal death than the ADC (Rivers and Wardlaw 2005), which is why we used the DWI lesion brightness to classify the voxels and placed the ROI around the DWI- visible lesion. The lack of specificity of ADC values for neuronal death is also suggested by the wide range of values found in definite infarcts (Hand *et al.*, 2006). From any one "snapshot" in time, it is not possible to say whether the ADC is falling, at the nadir, or rising. Tissue with very low ADC values may recover in patients (Fiehler et al.,2002) and animal models (Rivers and Wardlaw 2005) providing further evidence that no single ADC threshold is likely to discriminate salvageable from unsalvageable tissue. PWI values are also heterogeneous in stroke lesions (Wu *et al.*, 2006) with no clear threshold for salvageable tissue (Bandera et al.,2006). Therefore it would be difficult for a single "snapshot" of ADC or PWI values to indicate, directly, neuronal loss or tissue salvageability and may explain the lack of any clear ADC or PWI threshold for reliably differentiation of permanently damaged from viable ischemic tissue.

MRS is still not suitable for routine assessment of acute stroke patients though is useful in research. From a clinical perspective, only NIHSS (not metabolites or PWI/DWI parameters) predicted 3-month outcome. This exploratory work suggests that more information is needed to determine whether, and how, imaging metrics of tissue damage can be used to assess tissue salvageability and guide patient management before treatment decisions can be based reliably on imaging indicators of tissue viability.

Reference List

Bandera E, Botteri M, Minelli C, Sutton A, Abrams KR, Latronico N. Cerebral blood flow threshold of ischemic penumbra and infarct core in acute ischemic stroke - A systematic review. Stroke 2006; 37: 1334-1339.

Davis SM, Donnan GA. Using mismatch on MRI to select thrombolytic responders: an attractive hypothesis awaiting confirmation. Stroke 2005; 36: 1106-1107.

Demougeot C, Marie C, Giroud M, Beley A. N-acetylaspartate: a literature review of animal research on brain ischemia. J Neurochem 2004; 90: 783.

Dzialowski I, Weber J, Doerfler A, Forsting M, von Kummer R. Brain tissue water uptake after middle cerebral artery occlusion assessed with CT. J Neuroimaging 2004; 14: 42-48.

Fiehler J. ADC and metabolites in stroke: even more confusion about diffusion? Stroke 2003; 34: 6-7.

Fiehler J, Foth M, Kucinski T, Knab R, von Bezold M, Weiller C *et al.* Severe ADC decreases do not predict irreversible tissue damage in humans. Stroke 2002; 33: 79-86.

Gideon P, Sperling B, Arlien-Soborg P, Olsen TS, Henriksen O. Long-term follow-up of cerebral infarction patients with proton magnetic resonance spectroscopy. Stroke 1994; 25: 967-973.

Gillard JH, Barker PB, van Zijl PC, Bryan RN, Oppenheimer SM. Proton MR spectroscopy in acute middle cerebral artery stroke. Ajnr: American Journal of Neuroradiology 1996; 17: 873-886.

Guadagno JV, Warburton EA, Jones PS, Day DJ, Aigbirhio FI, Fryer TD *et al.* How affected is oxygen metabolism in DWI lesions? A combined acute stroke PET-MR study. Neurology 2006; 67: 824-829.

Guadagno JV, Warburton EA, Jones PS, Fryer TD, Day DJ, Gillard JH *et al.* The diffusion-weighted lesion in acute stroke: heterogeneous patterns of flow/metabolism uncoupling as assessed by quantitative positron emission tomography. Cerebrovasc Dis 2005; 19: 239-246.

Hand PJ, Wardlaw JM, Rivers CS, Armitage PA, Bastin ME, Lindley RI *et al.* MR diffusion-weighted imaging and outcome prediction after ischemic stroke. Neurology 2006; 66: 1159-1163.

Heiss WD, Sobesky J, Hesselmann V. Identifying thresholds for penumbra and irreversible tissue damage. Stroke 2004; 35: 2671-2674.

Kane I, Carpenter T, Chappell F, Rivers C, Armitage P, Sandercock P *et al.* Comparison of 10 different magnetic resonance perfusion imaging processing methods in acute ischemic stroke. Effect on lesion size, proportion of patients with diffusion/perfusion mismatch, clinical scores, and radiologic outcomes. Stroke 2007a; 38: 3158-3164.

Kane I, Sandercock P, Wardlaw J. Magnetic resonance perfusion diffusion mismatch and thrombolysis in acute ischaemic stroke: a systematic review of the evidence to date. J Neurol Neurosurg Psychiatry 2007b; 78: 485-491.

Kidwell CS, Saver JL, Mattiello J, Starkman S, Vinuela F, Duckwiler G *et al.* Thrombolytic reversal of acute human cerebral ischemic injury shown by diffusion/perfusion magnetic resonance imaging. Ann Neurol 2000; 47: 462-469.

Kucinski T, Vaterlein O, Glauche V, Fiehler J, Klotz E, Eckert B *et al.* Correlation of apparent diffusion coefficient and computed tomography density in acute ischemic stroke. Stroke 2002; 33: 1786-1791.

Labelle M, Khiat A, Durocher A, Boulanger Y. Comparison of metabolite levels and water diffusion between cortical and subcortical strokes as monitored by MRI and MRS. Investigative Radiology 2001; 36: 155-163.

Lanfermann H, Kugel H, Heindel W, Herholz K, Heiss WD, Lackner K. Metabolic changes in acute and subacute cerebral infarctions: findings at proton MR spectroscopic imaging. Radiology 1995; 196: 203-210.

Lemesle M, Walker P, Guy F, D'Athis P, Billiar T, Giroud M *et al.* Multi-variate analysis predicts clinical outcome 30 days after middle cerebral artery infarction. Acta Neurologica Scandinavica 2000; 102: 11-17.

Liu YJ, Chen CY, Chung HW, Huang IJ, Lee CS, Chin SC *et al.* Neuronal damage after ischemic injury in the middle cerebral arterial territory: deep watershed versus territorial infarction at MR perfusion and spectroscopic imaging. Radiology 229(2):366-74, 2003.

Loh PS, Butcher KS, Parsons MW, MacGregor L, Desmond PM, Tress BM *et al.* Apparent diffusion coefficient thresholds do not predict the response to acute stroke thrombolysis. Stroke 2005; 36: 2626-2631.

Markus R, Reutens DC, Kazui S, Read SJ, Wright PM, Pearce DC *et al.* Spontaneous salvage of penumbral tissue improves clinical outcomes as late as 12-48 hr after stroke onset. Stroke 2004; 35: 295.

Monsein LH, Mathews VP, Barker PB, Pardo CA, Blackband SJ, Whitlow WD *et al.* Irreversible regional cerebral ischemia: serial MR imaging and proton MR spectroscopy in a nonhuman primate model. AJNR Am J Neuroradiol 1993; 14: 963-970.

Munoz MS, Cvoro V, Armitage PA, Marshall I, Bastin ME, Wardlaw JM. Choline and creatine are not reliable denominators for calculating metabolite ratios in acute ischemic stroke. Stroke 2008; 39: 2467-2469.

Na DG, Thijs VN, Albers GW, Moseley ME, Marks MP. Diffusion-weighted MR imaging in acute ischemia: value of apparent diffusion coefficient and signal intensity thresholds in predicting tissue at risk and final infarct size. AJNR Am J Neuroradiol 2004; 25: 1331-1336.

Nicoli F, Lefur Y, Denis B, Ranjeva JP, Confort-Gouny S, Cozzone PJ. Metabolic counterpart of decreased apparent diffusion coefficient during hyperacute ischemic stroke: a brain proton magnetic resonance spectroscopic imaging study.[see comment]. Stroke 34(7):e82-7, 2003.

Parsons MW, Barber PA, Desmond PM, Baird TA, Darby DG, Byrnes G *et al.* Acute hyperglycemia adversely affects stroke outcome: a magnetic resonance imaging and spectroscopy study. Ann Neurol 2002; 52: 20-28.

Parsons MW, Li T, Barber PA, Yang Q, Darby DG, Desmond PM *et al.* Combined (1)H MR spectroscopy and diffusion-weighted MRI improves the prediction of stroke outcome. Neurology 2000; 55: 498-505.

Pereira AC, Saunders DE, Doyle VL, Bland JM, Howe FA, Griffiths JR *et al.* Measurement of initial N-acetyl aspartate concentration by magnetic resonance spectroscopy and initial infarct volume by MRI predicts outcome in patients with middle cerebral artery territory infarction. Stroke 1999; 30: 1577-1582.

Rivers CS, Wardlaw JM. What has diffusion imaging in animals told us about diffusion imaging in patients with ischaemic stroke? Cerebrovasc Dis 2005; 19: 328-336.

Rumpel H, Khoo JB, Chang HM, Lim WE, Chen C, Wong MC *et al.* Correlation of the apparent diffusion coefficient and the creatine level in early ischemic stroke: a comparison of different patterns by magnetic resonance. Journal of Magnetic Resonance Imaging 2001; 13: 335-343.

Sager TN, Hansen AJ, Laursen H. Correlation between N-acetylaspartate levels and histopathologic changes in cortical infarcts of mice after middle cerebral artery occlusion. J Cereb Blood Flow Metab 2000; 20: 780-788.

Sager TN, Laursen H, Hansen AJ. Changes in N-acetyl-aspartate content during focal and global brain ischemia of the rat. J Cereb Blood Flow Metab 1995; 15: 639-646.

Saunders DE, Howe FA, van den BA, McLean MA, Griffiths JR, Brown MM. Continuing ischemic damage after acute middle cerebral artery infarction in humans demonstrated by short-echo proton spectroscopy. Stroke 1995; 26: 1007-1013.

Sijens PE, den HT, de Leeuw FE, de Groot JC, Achten E, Heijboer RJ *et al.* MR spectroscopy detection of lactate and lipid signals in the brains of healthy elderly people. Eur Radiol 2001; 11: 1495-1501.

Sobesky J, Zaro WO, Lehnhardt FG, Hesselmann V, Neveling M, Jacobs A *et al.* Does the mismatch match the penumbra? Magnetic resonance imaging and positron emission tomography in early ischemic stroke. Stroke 2005; 36: 980-985.

Sobesky J, Zaro WO, Lehnhardt FG, Hesselmann V, Thiel A, Dohmen C *et al.* Which time-to-peak threshold best identifies penumbral flow? A comparison of perfusion-weighted magnetic resonance imaging and positron emission tomography in acute ischemic stroke. Stroke 2004; 35: 2843-2847.

Stengel A, Neumann-Haefelin T, Singer OC, Neumann-Haefelin C, Zanella FE, Lanfermann H *et al.* Multiple spin-echo spectroscopic imaging for rapid quantitative assessment of N-acetylaspartate and lactate in acute stroke. Magnetic Resonance in Medicine 52(2):228-38, 2004.

Tsai G, Coyle JT. N-acetylaspartate in neuropsychiatric disorders. Prog Neurobiol 1995; 46: 540.

Walker PM, Ben Salem D, Lalande A, Giroud M, Brunotte F. Time course of NAA T2 and ADC(w) in ischaemic stroke patients: 1H MRS imaging and diffusion-weighted MRI. Journal of the Neurological Sciences 220(1-2):23-8, 2004.

Wardlaw JM, Marshall I, Wild J, Dennis MS, Cannon J, Lewis SC. Studies of acute ischemic stroke with proton magnetic resonance spectroscopy: relation between time from onset, neurological deficit, metabolite abnormalities in the infarct, blood flow, and clinical outcome. Stroke 1998; 29: 1618-1624.

Wu O, Christensen S, Hjort N, Dijkhuizen RM, Kucinski T, Fiehler J *et al.* Characterizing physiological heterogeneity of infarction risk in acute human ischaemic stroke using MRI. Brain 2006; 129: 2384-2393.

Chapter 5: Longitudinal changes over three months of NAA, lactate, choline, and creatine

Previous chapters dealt with distribution of the metabolites during the first 24 hours of onset of stroke and their relationship with diffusion and perfusion parameters. In this chapter I will report changes in metabolites over three months period at five fixed time points (see Chapter 3, Methods). I have looked at the longitudinal profile of NAA and lactate as well as choline and creatine. The data will be reported in two sections in this chapter.

5.1 Introduction

5.1.1 The changes in NAA and lactate over three months

Much research in ischemic stroke has been devoted to limiting tissue damage by identifying ischemic tissue that could be salvaged before death, and establishing the duration of ongoing tissue injury. Most work has focused on diffusion and perfusion MRI, but proton MR spectroscopy (MRS) is also a valuable tool for identifying metabolic changes occurring during brain ischaemia. NAA appears almost exclusively in normal neurons and has been used to detect neuronal damage in various neurological disorders including stroke (Saunders 2000). This has been extensively discussed in the Introduction. Experimental data confirm the close relationship between NAA detected spectroscopically and the proportion of normal neurons (Rigotti *et al.*, 2007). Lactate appears in ischemic brain and in the acute stage indicates a change from oxidative metabolism to anaerobic glycolysis (Graham *et al.*, 1992; Saunders *et al.*, 1995). Although much of the total tissue damage probably occurs in the first few hours after stroke, the longest duration of survival of ischemic but viable tissue, and the period over which further damage might accumulate from secondary factors, is unknown. There is evidence that damage may continue subacutely (Rivers *et al.*, 2004), offering possible targets for delayed therapeutic interventions if the causes can be identified. Therefore, determining the prolonged time course of changes in NAA and lactate after stroke could identify the period of cumulative tissue damage.

Previous studies of NAA and lactate after stroke, as discussed in chapter 2, unanimously confirm an acute decrease in NAA in the centre of ischemic lesions consistent with neuronal loss, and high concentrations of lactate. However, these studies provided little reliable data on the duration or pattern of metabolite changes as they were generally small, imaged different patients at different times (confounding temporal variation with between-patient differences (Ford *et al.*, 1992; Lanfermann *et al.*, 1995; Walker *et al.*, 2004), used ratios to other metabolites (assuming that these do not change after stroke (Lemesle *et al.*, 2000; Parsons *et al.*, 2000); or only provided data from a single voxel in the lesion (Federico *et al.*, 1998; Gideon *et al.*, 1994; Kamada *et al.*, 1997; Saunders et al.,1995) rather than simultaneous data across normal and abnormal brain. The findings for the duration of detection of lactate were particularly inconsistent, from rapid reduction to undetectable levels (Gideon et al.,1994; Saunders et al.,1995), to persistence weeks or months after stroke (Graham et al.,1992; Sappey-Marinier *et al.*, 1992).

To examine the time course of tissue damage following ischemia, NAA and lactate were measured with proton MRSI, across ischemic and normal brain, in a large group of patients at five fixed time points. I extracted metabolite data from voxels classified according to the appearance of the initial DWI to avoid using thresholds for the reasons extensively discussed in the previous chapters (3 and 4).

5.1.2 Evolution of choline and creatine over three months

Previous studies of ischemic stroke used choline and creatine to calculate ratios of NAA or lactate to compare affected and healthy tissue in individuals or between different subjects (Ford et al.,1992; Kim *et al.*, 2001; Parsons et al.,2000). This is based on the assumption that the concentrations of choline or creatine do not change significantly during ischemia (Fenstermacher and Narayana 1990). Many subsequent studies have used choline or creatine as denominators to measure the ratio of NAA or lactate, assuming that neither choline nor creatine change in ischaemia. I have used data obtained in my research to establish whether choline and creatine could be used as reliable denominators for other brain metabolites in ischemic stroke by investigating how their levels varied within the ischemic lesion over time.

5.2 Methods

Patient recruitment and imaging techniques have been described in chapter 3.

5.2.1 Data analysis

We used the "grid method" of classifying tissue into normal and abnormal areas on the basis of the lesion appearance on the DWI sequence as described in Chapter 3. For each patient, median values of NAA and lactate concentration for each tissue class were calculated. Data from all patients were normally distributed (Kolmogorov- Smirnov tests) and were combined to obtain mean NAA and lactate concentrations for each tissue class at the five time points. The differences in the NAA and lactate concentration time profiles of different tissue classes: definitely (DAB) and possibly abnormal (PAB), ipsi-(INL) and contralateral normal (CNL) voxels in individual patients were assessed using linear mixed model analysis (Brown and Prescott 2006) performed in SAS 9.1 (SAS Institute Inc., Cary, NC). This analysis shares similarities with ordinary linear regression, but allows for missing data and therefore includes data from all patients, independently of the number of time points available. In simple linear regression, if an observation has missing data for any of the explanatory variables, the entire observation cannot be used in the analysis. Another potential drawback of simple linear regression is that it cannot allow for certain structures within the data, for example those that occur when repeated measurements are taken from the same patient, such as is the case here.

The current analysis aimed to predict NAA or lactate using four brain tissue types: DAB, PAB, INL and CNL. In a simple linear regression, if a patient had been missing data on any one of these tissue types, the data from the other tissue types would have been discarded. For example, a patient with a missing PAB would be dropped entirely from the analysis. However, in a linear mixed model, the data from the other tissue types are still used to estimate of the relationship of those tissue types with NAA or lactate, the patient with the missing PAB measurement would still contribute to the estimates for CNL, INL, and DAB.

This also avoids bias due to including only patients who were well enough to complete the five time points. With this method the effect of tissue type and time

after stroke on NAA and lactate concentration could be tested, and also whether the change over time varied between tissue types, while allowing for the differences in NAA and lactate between patients. Lactate values were log-transformed to better fit the linear mixed model.

The levels of choline and creatine were measured in the abnormal tissue (part of grid analysis (see chapter 3), longitudinally at 5 fixed time points up to 3 months after onset. For this analysis more simplified classification was used categorising tissue as normal and abnormal (for details, see chapter 3). Average values of choline and creatine concentrations were calculated for each tissue type in each patient at each time point (Figure2). A general linear model repeated measures regression analysis was used to compare changes over time in the concentrations of choline and creatine in normal and abnormal tissue. General linear model analyses were performed in SPSS 14.

5.3 Results

5.3.1 Patient characteristics

For this analysis, all 51 patients were included, of mean (±SD) age 75 ±15 years (range 37–95), and mean NIHSS 11 ±8 (range 1–29) (for full demographic detail see Table 1). Of these 51, 21 had a total anterior circulation stroke syndrome and 30 had a partial anterior circulation stroke syndrome. Seventeen patients were first imaged within 6 hours after stroke (33%), 15 at 6–12 hours (30%), and 19 at 12–24 hours (37%), giving mean (+/-SD) scanning times of 11 ± 7 hours for the first, and 5 ±1, 12 ±2, 31 ±2, and 95 ±6 days for each of the subsequent scans. Follow-up scanning was not possible in all cases; some patients died or were too ill, while others declined further scanning. From the 51 initial patients, 26 (51%) were scanned up to 1 month and 23 (45%) at 3 months. For a full number of scans at each time point please see Table 1 Chapter 3.

Table 1. Demographic characteristic of the study population (total 51 patients)

Sex of the patients	31 male
Side of the lesion	29 left hemisphere
Smoking history	40 non smokers (13 ex smoker)
Ischaemic heart disease	25 / 51
Hypertension	31 / 51
Diabetes mellitus	2 / 51
Peripheral vascular disease	3 / 51
Atrial fibrillation	15 /51

5.3.2 Results -Temporal evolution of NAA and lactate

In definitely and possibly abnormal and ipsilateral normal voxels, NAA concentration fell over the first two weeks with some increase thereafter, but still remained lower than baseline at three months (Figure 1A). The nadir appeared at about 12 days. For individual tissue classes, both the plot of mean NAA and the linear mixed model showed that NAA concentration was significantly reduced at all time points for definitely and possibly abnormal voxels versus normal brain ($p < 0.01$) (Table 2). Assessment of infarct extent and swelling was possible in 34 patients who had follow up scans, of which 47% presented with swelling in the admission scan. Swelling increased by one or more points in most of these patients at five days (for methods see chapter 3); however, in most (94%) cases the increase was of two points or less in the seven-point swelling scale. Therefore, the changes in swelling were small and cannot explain the altered NAA signal of definitely and possibly abnormal voxels. NAA was not significantly reduced in ipsilateral normal voxels when considering all time points, but its temporal evolution was different from that of contralateral normal voxels, with ipsilateral normal being reduced at two weeks and at three months ($p=0.01$ in both cases), possibly due to infarct growth into tissue which was normal initially. The NAA concentration time curve for possibly abnormal voxels differed from that of definitely abnormal, with possibly abnormal being higher ($p= 0.02$). NAA did not change significantly in contralateral normal voxels at any time.

Lactate levels were initially elevated in both definitely and possibly abnormal voxels, falling sharply thereafter (Figure 1B). Although lactate appeared to normalize at two weeks, some lactate was still present at one and three months in both definitely and possibly abnormal voxels (Figure 1B). The linear mixed model showed elevated lactate in definitely and possibly abnormal and ipsilateral normal voxels, with $p < 0.01$ for both definitely and possibly abnormal and $p = 0.02$ for ipsilateral normal voxels (Table 2). There were no differences between definitely and possibly abnormal voxels ($p= 0.35$). Some lactate was detected at low levels in contralateral normal tissue at all time points, but these did not change over time.

Table 2. Results from the linear mixed model analysis of the time-concentration curves of N-acetylaspartate (NAA) and lactate in each tissue class

Tissue	Difference estimate	t Value	p	95%CI Lower	95%CI Upper
NAA					
DAB vs CNL	-38.2	-5.0	<0.01	-53.4	-23.0
PAB vs CNL	-22.5	-3.0	<0.01	-37.4	-7.6
INL vs CNL	-11.0	-1.5	0.13	-25.4	4.4
PAB vs DAB	15.4	2.4	0.02	2.6	28.2
Log (lactate)					
DAB vs CNL	1.7	11.6	<0.01	1.4	1.9
PAB vs CNL	1.3	9.6	<0.01	1.1	1.6
INL vs CNL	0.3	2.5	0.02	0.1	0.6
PAB vs DAB	-0.1	-0.9	0.35	-0.3	0.1

NAA and lactate are in institutional units. DAB = definitely abnormal; CNL = contralateral normal; PAB = probably abnormal; INL = ipsilateral normal

Figure 1. Temporal evolution of mean N-acetylaspartate (NAA) (A) and lactate (B) concentrations for all patients in standardized institutional units as a function of time foreach tissue class. The error bars indicate standard errors.

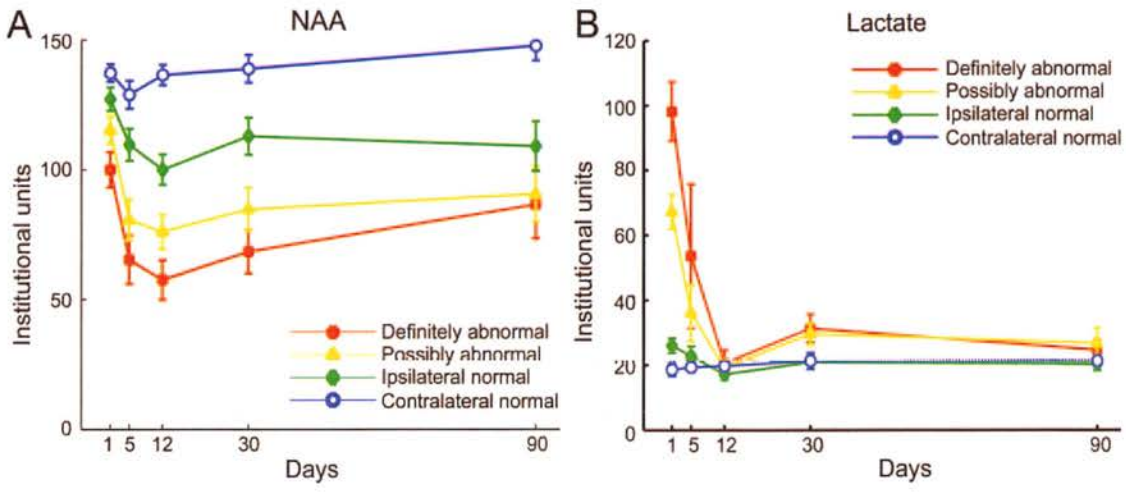

5.3.3 Results – Choline and creatine

Data from 51 patients was used for this analysis (see patients characteristics in the above section); Figure 2 shows the change with time of mean choline (2A) and creatine (2B) concentrations in abnormal and normal tissue regions for all patients at all time points. The general linear model regression analysis did not show any overall difference in the temporal evolution of choline concentration between abnormal and normal tissue over the three months of study, possibly due to sigmoid shape of the recovery curve of abnormal voxels values after two weeks (Table 3; Figure 2A). A further analysis including only data from the first three scans showed that the concentration of choline in abnormal tissue was in fact significantly lower than normal over the first two weeks after stroke (general linear model regression P=0.034). The general linear model regression analysis showed that creatine concentration was significantly reduced in abnormal tissue after the first scan up to 3 months after stroke (P=0.011)(Table 3)

Figure 2. Temporal evolution of mean (A) choline and (B) creatine concentrations in institutional units. The error bars indicate SD. Note: graphs include data from all patients imaged at each time point.

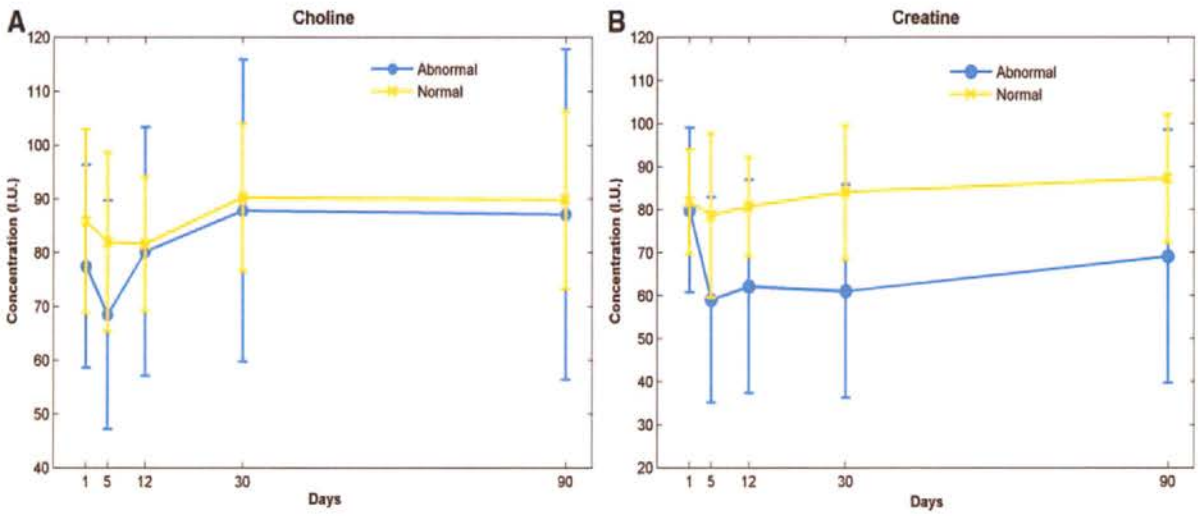

*Table 3. Summary of Tests of Between-Subject Effects for General Linear Model Repeated Measurements Analysis of Choline and Creatine Time Evolution**

Test	Source	Type III Sum of Squares	df	F	p
Choline over 3 months	Intercept	10 901 109.4	1	994.8	<0.001
	Tissue type	1026.4	1	0.937	0.341
	Error	30 682.1	28		
Choline over 2 weeks	Intercept	1 041 281.7	1	1900.5	<0.001
	Tissue type	2586.3	1	4.720	0.034
	Error	29 038.6	53		
Creatine over 3 months	Intercept	971 633.0	1	732.8	<0.001
	Tissue type	9704.2	1	7.319	0.011
	Error	41 103.6	31		

5.4 Discussion

This analysis of longitudinal data of NAA and lactate in acute ischemic stroke provides robust data on the time course of neuronal loss and tissue damage. This data shows that permanent neuronal loss (NAA reduction) is accumulated over the first 12 days. This confirms NAA reductions found in smaller studies (Federico et al.,1998; Ford et al.,1992; Gideon et al.,1994; Graham et al.,1992; Lanfermann et al.,1995; Parsons et al.,2000; Saunders et al.,1995; Wardlaw *et al.,* 1998) but, by including all patients, provides much more reliable time-course data. The very slight rebound in NAA values for definitely, possibly abnormal, and ipsilateral normal voxels at 12 days suggests that the neuronal damage was, on average, maximal at this time. As neurons are not considered to regenerate (Monsein *et al.,* 1993), this minor rebound could be caused by resolving tissue oedema within the lesion and partial volume averaging with normal brain at the edge of the lesion as any mass effect receded. Neuronal damage is considered to occur within the first few hours of stroke. The further decreases in NAA up to 12 days could be caused by increased tissue oedema or changes in metabolite relaxation times (Walker et al.,2004). However, a previous study (Saunders et al.,1995), which corrected for changes in water concentration within the infarct and relaxation times, observed similar NAA changes. Furthermore, in this analysis of longitudinal data an oedema rating scale suggested that increase in oedema at 5 days was minimal in most patients; since infarct mass effect from oedema is maximal at 5–7 days and declines

thereafter (Wardlaw *et al.*, 1993), usually being substantially resolved by 10–14 days, dilution effects of oedema cannot wholly account for the subacute NAA changes. Therefore, the progressive fall in NAA to 12 days cannot only be attributed to changes in metabolite relaxation times or tissue swelling, and it is best accounted for by accumulating neuronal damage.

This interpretation is supported by the return of lactate to normal levels at this time. Hence, the evolution observed for both metabolites suggests that permanent damage continues to accumulate until about 12 days. The initial reduction of NAA concentration in ipsilateral normal tissue could be accounted for by partial volume effects in voxels coded normal but just at the edge of the stroke lesion, thus possibly including some abnormal tissue. The later fall in NAA in ipsilateral normal at subacute times is probably due to infarct growth with "recruitment" of normal voxels into the stroke lesion since in 14% of subjects the lesion grew beyond the initial ischemic area according to the rating scale (Wardlaw and Sellar 1994). The lactate in ipsilateral normal tissue may be due to ischemia beyond the edges of the DWI-visible lesion, e.g., within areas of reduced perfusion, or to partial volume averaging at the edge of the lesion. Lactate rose at 1 and 3 months in both definitely and possibly abnormal voxels. This recurrent lactate elevation after 2 weeks has been noted previously (Federico et al.,1998; Ford et al.,1992; Gideon et al.,1994; Graham et al.,1992; Sappey-Marinier et al.,1992) and attributed to tissue infiltration by inflammatory cells with a high rate of anaerobic glycolysis, such as macrophages. Histologically, these begin to appear three days after infarction and disappear gradually over several months (Petroff *et al.*, 1992). However, as in previous studies, lactate was still detected in the ischemic lesion in some patients beyond the time that most phagocytosis of necrotic cells would be expected to be completed (Federico et al.,1998; Gideon et al.,1994; Graham et al.,1992) suggesting that the processes involved in resolution of tissue damage may continue for much longer than current knowledge suggests.

The lactate in contralateral normal tissue was not anticipated as lactate is generally associated with the presence of pathology. However, lactate appears to be intrinsic to healthy aging, as has been detected in 10% of apparently normal men aged 60 and 25% aged 90 (Sijens *et al.*, 2001)(Chapter 4). The average age in our patients (75+/-15) could therefore explain the low lactate concentration found in contralateral apparently normal tissue.

It is interesting that although reduced, NAA was still clearly detectable in even the most abnormal appearing tissue on DWI where the most damage would be expected, suggesting that in some patients a substantial proportion of neurons were still viable in the core of the stroke lesion even at 12 days. NAA concentration mirrored the "brightness" of the lesion on DWI as NAA was lower in definitely (the whitest) than in possibly abnormal voxels. This suggests that the diffusion lesion appearance reflects the severity of the underlying neuronal damage. The substantial reductions in NAA secondary to ischemia seen in this and other stroke studies are a reasonably reliable indicator of loss of viable neurons. Although animal models have suggested that low levels of NAA (<20%) could be attributable to NAA trapped in cell debris (Sager *et al.*, 2000), evidence to date indicates that the majority of NAA signal is lost at the point of neuronal death (Monsein et al.,1993). Minor reductions in NAA which later recovered (thereby suggesting that the neuronal damage was only transient) have been observed in animal models of HIV infection (Greco *et al.*, 2004) and multiple sclerosis (MS) plaques (Tsai and Coyle 1995), in both cases probably attributable to tissue fluid changes secondary to inflammation. NAA reduction in MS plaques may also be permanent (Tsai and Coyle1995) and correlated with gliosis, consistent with it being a marker of permanent neuronal loss. One small study with monkeys infected with simian immunodeficiency virus suggested that minor (7.7%) reductions in NAA might be attributable to non-permanent neuronal damage (Lentz *et al.*, 2005), but longer studies would be needed to determine what proportion, if any, of NAA reduction could be accepted as transient and what proportion permanent neuronal loss.

Early studies reported no significant changes in choline concentrations in the ischemic lesion (Fenstermacher and Narayana 1990), which prompted the use of choline as a denominator to assess changes in other metabolites in stroke (Parsons et al.,2000). However, other studies found either an increase (Graham et al.,1992; Sappey-Marinier et al.,1992) or a decrease in choline levels (Duijn *et al.*, 1992; Lanfermann et al.,1995) in stroke lesions. Discrepancies might be related to individual variability, the small sample sizes of 10 patients or less in some studies (Duijn et al.,1992; Sappey-Marinier et al.,1992), or to the use of different patients scanned at different time points rather than the same patients scanned at similar times (Lanfermann et al.,1995). The current study is the largest to date following the same group of patients with stroke longitudinally using proton MR spectroscopic imaging at fixed time points to reduce this variability. The choline levels were significantly reduced in stroke compared with healthy tissue during the first two

weeks. Thus, using choline measured within the lesion as a denominator for metabolic ratios would overestimate other metabolites' concentrations. This would introduce ambiguity to the conclusions drawn from MR spectroscopic studies of acute stroke using these ratios, because reported values would be subjected to changes in two metabolites instead of one. For example, it was previously reported that the ratio of lactate/choline in acute stroke is a better predictor of clinical outcome than the ratio NAA/choline (Parsons et al.,2000). This could result from the decrease of choline in the lesion, which makes the NAA/choline ratio less sensitive to reductions in NAA, whereas it enhances the increase of lactate in lactate/choline ratios. Creatine has been used less often than choline to calculate metabolite ratios in stroke. In events such as ischemia, creatine cannot be used as an internal reference because its concentration varies with the anaerobic tissue conditions and, as in the current study, other authors have consistently found a general decrease in the concentration of creatine in the ischemic lesion (Duijn et al.,1992; Lanfermann et al.,1995). Although metabolite ratios are still used because of the simplicity of their calculation, methods for quantifying individual metabolites are now well established. In vivo measurement of metabolite concentrations can be achieved, for example, by calibrating the measured spectral resonance area with the known concentration of a reference solution and using the appropriate corrections for volume normalization, coil loading, and differential T2 attenuation (Michaelis *et al.*, 1993). Future MR spectroscopic studies of ischemic stroke should be aware of temporal changes in choline and creatine within the lesion, particularly choline. If ratios of other metabolites to choline or creatine are to be used during the analysis, the potential ambiguity introduced into the ratios by the variation of these metabolites should be carefully considered.

The strengths of the study

As discussed in Chapter 4 with the first time point analysis, this study has a large sample size for a complex imaging study. The spectroscopy data were acquired using multi-voxel rather than single voxel technique. The patients were scanned at five standard time points, whereas previous studies of ischemic stroke used data from different patients at different times or the same patients but at variable times. All patient data was included and not just those scanned at all times, by using a mixed modelling approach. Extreme care was taken to match the position of voxels on all scans and as discussed earlier I was very careful to exclude all CSF

contaminated voxels as well as ones at the edge of the lesion. The concentrations were expressed as standardized metabolite values (discussed in methods chapter), in the individually examined tissues determined according to the DWI appearance (the implication of using thresholds is discussed in the previous chapter). Previous studies were unable to provide information on metabolite changes in abnormal and normal tissue simultaneously and frequently reported changes in NAA and lactate as ratios to choline or creatine, assuming that these do not change. The changes in the choline and creatine levels are discussed below.

The weaknesses of the study

I was unable to image all patients at all times, since some died, were too unwell, or refused further scanning. Also, regional tissue distortion on follow-up scans due to changes in mass effect of the infarct could not be adjusted for. Finally, partial volume averaging will be present since spectroscopy voxels were 1 cm^3, so some inclusion of two tissue classes in some voxels is inevitable, particularly at the edge of the lesion. However, I did account for partial volume averaging by adjusting the metabolite concentration by the proportion of DWI classified tissue in each voxel (Chapter 3).

Brown H, Prescott R. Applied Mixed Models in Medicine. Chichester: Wiley; 2006.

Duijn JH, Matson GB, Maudsley AA, Hugg JW, Weiner MW. Human brain infarction: proton MR spectroscopy. Radiology 1992; 183: 711-718.

Federico F, Simone IL, Lucivero V, Giannini P, Laddomada G, Mezzapesa DM *et al.* Prognostic value of proton magnetic resonance spectroscopy in ischemic stroke. Archives of Neurology 1998; 55: 489-494.

Fenstermacher MJ, Narayana PA. Serial proton magnetic resonance spectroscopy of ischemic brain injury in humans. Investigative Radiology 1990; 25: 1034-1039.

Ford CC, Griffey RH, Matwiyoff NA, Rosenberg GA. Multivoxel 1H-MRS of stroke. Neurology 1992; 42: 1408-1412.

Gideon P, Sperling B, Arlien-Soborg P, Olsen TS, Henriksen O. Long-term follow-up of cerebral infarction patients with proton magnetic resonance spectroscopy. Stroke 1994; 25: 967-973.

Graham GD, Blamire AM, Howseman AM, Rothman DL, Fayad PB, Brass LM *et al.* Proton magnetic resonance spectroscopy of cerebral lactate and other metabolites in stroke patients. Stroke 1992; 23: 333-340.

Greco JB, Westmoreland SV, Ratai EM, Lentz MR, Sakaie K, He J *et al.* In vivo 1H MRS of brain injury and repair during acute SIV infection in the macaque model of neuroAIDS. Magn Reson Med 2004; 51: 1108-1114.

Kamada K, Houkin K, Iwasaki Y, Abe H, Kashiwaba T. Metabolic and neurological patterns in chronic cerebral infarction: a single-voxel 1H-MR spectroscopy study. Neuroradiology 1997; 39: 560-565.

Kim GE, Lee JH, Cho YP, Kim ST. Metabolic changes in the ischemic penumbra after carotid endarterectomy in stroke patients by localized in vivo proton magnetic resonance spectroscopy (1H-MRS). Cardiovasc Surg 2001; 9: 345-355.

Lanfermann H, Kugel H, Heindel W, Herholz K, Heiss WD, Lackner K. Metabolic changes in acute and subacute cerebral infarctions: findings at proton MR spectroscopic imaging. Radiology 1995; 196: 203-210.

Lemesle M, Walker P, Guy F, D'Athis P, Billiar T, Giroud M *et al.* Multi-variate analysis predicts clinical outcome 30 days after middle cerebral artery infarction. Acta Neurologica Scandinavica 2000; 102: 11-17.

Lentz MR, Kim JP, Westmoreland SV, Greco JB, Fuller RA, Ratai EM *et al.* Quantitative neuropathologic correlates of changes in ratio of N-acetylaspartate to creatine in macaque brain. Radiology 2005; 235: 461-468.

Michaelis T, Merboldt KD, Bruhn H, Hanicke W, Frahm J. Absolute concentrations of metabolites in the adult human brain in vivo: quantification of localized proton MR spectra. Radiology 1993; 187: 219-227.

Monsein LH, Mathews VP, Barker PB, Pardo CA, Blackband SJ, Whitlow WD *et al.* Irreversible regional cerebral ischemia: serial MR imaging and proton MR spectroscopy in a nonhuman primate model. AJNR Am J Neuroradiol 1993; 14: 963-970.

Parsons MW, Li T, Barber PA, Yang Q, Darby DG, Desmond PM *et al.* Combined (1)H MR spectroscopy and diffusion-weighted MRI improves the prediction of stroke outcome. Neurology 2000; 55: 498-505.

Petroff OA, Graham GD, Blamire AM, al Rayess M, Rothman DL, Fayad PB *et al.* Spectroscopic imaging of stroke in humans: histopathology correlates of spectral changes. Neurology 1992; 42: 1349-1354.

Rigotti DJ, Inglese M, Gonen O. Whole-brain N-acetylaspartate as a surrogate marker of neuronal damage in diffuse neurologic disorders. AJNR Am J Neuroradiol 2007; 28: 1843-1849.

Rivers CS, Wardlaw JM, Armitage PA, Bastin ME, Carpenter TK, Cvoro V *et al.* Persistent infarct hyperintensity on diffusion-weighted imaging late after stroke indicates heterogeneous, delayed, infarct evolution. Stroke 2004; 37: 1418-1423.

Sager TN, Hansen AJ, Laursen H. Correlation between N-acetylaspartate levels and histopathologic changes in cortical infarcts of mice after middle cerebral artery occlusion. J Cereb Blood Flow Metab 2000; 20: 780-788.

Sappey-Marinier D, Calabrese G, Hetherington HP, Fisher SN, Deicken R, Van Dyke C *et al.* Proton magnetic resonance spectroscopy of human brain: applications to normal white matter, chronic infarction, and MRI white matter signal hyperintensities. Magnetic Resonance in Medicine 1992; 26: 313-327.

Saunders DE. MR spectroscopy in stroke. [Review] [35 refs]. British Medical Bulletin 2000; 56: 334-345.

Saunders DE, Howe FA, van den BA, McLean MA, Griffiths JR, Brown MM. Continuing ischemic damage after acute middle cerebral artery infarction in humans demonstrated by short-echo proton spectroscopy. Stroke 1995; 26: 1007-1013.

Sijens PE, den HT, de Leeuw FE, de Groot JC, Achten E, Heijboer RJ *et al.* MR spectroscopy detection of lactate and lipid signals in the brains of healthy elderly people. Eur Radiol 2001; 11: 1495-1501.

Tsai G, Coyle JT. N-acetylaspartate in neuropsychiatric disorders. Prog Neurobiol 1995; 46: 540.

Walker PM, Ben Salem D, Lalande A, Giroud M, Brunotte F. Time course of NAA T2 and ADC(w) in ischaemic stroke patients: 1H MRS imaging and diffusion-weighted MRI. Journal of the Neurological Sciences 220(1-2):23-8, 2004.

Wardlaw JM, Dennis MS, Lindley RI, Warlow CP, Sandercock PAG, Sellar R. Does early reperfusion of a cerebral infarct influence cerebral infarct swelling in the acute stage or the final clinical outcome? Cerebrovasc Dis 1993; 3: 86-93.

Wardlaw JM, Marshall I, Wild J, Dennis MS, Cannon J, Lewis SC. Studies of acute ischemic stroke with proton magnetic resonance spectroscopy: relation between time from onset, neurological deficit, metabolite abnormalities in the infarct, blood flow, and clinical outcome. Stroke 1998; 29: 1618-1624.

Wardlaw JM, Sellar RJ. A simple practical classification of cerebral infarcts on CT and its interobserver reliability. Am J Neuroradiol 1994; 15: 1933-1939.

Chapter 6: Relationship of metabolites, diffusion and perfusion parameters with outcome

In the previous two chapters, I explored correlations between diffusion and perfusion parameters and metabolites at various time points from stroke onset and how it helps us in assessing viable brain tissue. In this chapter I will explore the correlation of metabolites, diffusion and perfusion parameters with clinical outcome as measured by the modified Rankin scale (Chapter 3).

6.1 Introduction

Predicting a patient's outcome more accurately when they first present, and using that information to guide the treatment would be of great clinical benefit. The factors that influence the outcome are numerous. Severity of stroke on presentation is well known to predict outcome; the more severe the stroke at onset, the worse the clinical outcome (Derex *et al.*, 2004 ;Wardlaw *et al.*, 1998). However, some of the patients with severe stroke still make a good recovery, and identifying them early would help to improve selection of patients for potentially dangerous treatments.
In recent years, numerous studies have looked at perfusion (PWI) and diffusion imaging (DWI) in acute stroke, and diffusion perfusion mismatch as a way of identifying early on, which patients would potentially benefit from treatment. The diffusion perfusion concept has been discussed in the introduction (Chapter 1.2.4). Numerous studies investigated diffusion perfusion mismatch, but only a few reported the functional outcome of the patients (Kane *et al.*, 2007b). The randomised trial which measured mismatch in thrombolysed and non thrombolysed patients did not show attenuation of infarct growth, but more importantly did not show a better clinical outcome in the thrombolysis group, than in the placebo group (Davis *et al.*, 2008).

In the literature review on spectroscopy in stroke (Chapter 2) I found thirteen studies that investigated the relationship of metabolites to the stroke outcome. None of the studies measured metabolites within 24 hours. There was no consensus among the studies, although, half of the studies found that NAA correlated with

outcome, and only a quarter found that lactate correlated with the outcome. Two studies found that neither of the metabolites correlated with the outcome.

In the analysis of the patients from this study, I investigated the correlation between the initial level of metabolites and diffusion and perfusion parameters, first in the region of interest (ROI) and then using CSI grid analysis. I also investigated diffusion perfusion mismatch lesion, and the correlation of the parameters within the mismatch with an outcome.

6.2 Methods

Detailed description of methods can be found in Chapter 3.

6.2.1 Statistical analysis

All statistical tests were performed in SPSS 14.0 for Windows (SPSS Inc, Chicago, Ill, USA) for both ROI, grid, and mismatch analysis. The imaging data were not normally distributed (Kolmogorov-Smirnov test, $p>0.01$), so the Spearman Rank Correlation coefficient (ρ) was used to examine the correlation between the severity (NIHSS), metabolites, diffusion and perfusion parameters and the outcome measure, setting significance at the 0.05 level (2-tailed). I used linear regression analysis in both the ROI and grid analysis to find out if either the metabolites or DWI and PWI parameters would fit the model predicting the outcome, as measured by modified Rankin scale. I limited the model to a maximum of 5 variables to minimise false positive results.

6.3 Results

6.3.1 Patient characteristics

The age range of the 43 patients that were used for this analysis was (median +/- SD and range) 76 +/- 11 (37-95). All patients were scanned within 24 hours 8+/-6.6 (1.5-24) of which, 14 (32%) patients were scanned within six hours, 14 (32%) between six

and 12 hours, and 15 (36%) patients between 12 and 24 hours after stroke. 22/43 patients (51%) had a DWI/PWI mismatch on the MTT perfusion parameter. None of the patients received thrombolysis or investigational treatment, and none had carotid stenosis of more than 50%. These were mostly moderately severe strokes with NIHSS of 9+/-7.8 (1-29), and according to OCSP classification 19 (44%) were TACS and 24 (56%) PACS. In the "perfusion diffusion mismatch" group 15/22 (68%) patients were TACS whilst in "no mismatch group" 4/21 (19%) were TACS.

6.3.2 Region of interest (ROI) analysis and outcome

Metabolites, stroke severity, lesion volume, time from stroke, and 3 month functional outcome

There was no association between any of the metabolites and the NIHSS score. Larger DWI lesion volume was associated with reduced NAA (Spearman's ρ= -0.42, p=0.006) and increased lactate (Spearman's ρ= 0.49, p=0.001) but not with choline or creatine. Longer times to scanning were associated with lower NAA (Spearman's ρ= -0.33, p=0.03) and larger lesion volumes (Spearman's ρ= 0.35, p=0.023) but not with lactate, choline, creatine or ADC. There was no correlation between the metabolites, ADC, MTT or CBF and three month Rankin score. However, the clinical parameter of NIHSS (measured at baseline) was associated with the three month Rankin score (Spearman's ρ= 0.665, p=0.0001), in keeping with the known strong association between stroke severity and functional outcome.

Linear regression analysis

I used linear regression analysis (Tables 1 and 2) to test whether metabolites, or diffusion and perfusion parameters predict functional outcome. In the model with metabolite values and the volume as variables (Table1), both volume of the lesion (p= 0.027), and lactate (p= 0.029) were statistically significant. In the model with lesion volume, and diffusion and perfusion parameters (Table 2), no parameters reached statistical significance.

Table 1. Linear regression analysis with metabolites and lesion volume as independent variables, and modified Rankin score at 3 months as dependent variable, ROI analysis.

Coefficients(a)

Model		Unstandardized Coefficients		Standardized Coefficients		
		B	Std. Error	Beta	t	Sig.
1	(Constant)	3.183	1.356		2.347	.025
	Volume	1.88E-005	.000	.398	2.305	.027
	Choline	.015	.021	.153	.731	.470
	Creatine	.008	.026	.077	.328	.745
	NAA	-.009	.015	-.151	-.639	.527
	Lactate	-.031	.014	-.372	-2.272	.029

a Dependent Variable: modrank

Table 2. Linear regression analysis with diffusion perfusion parameters and lesion volume as independent variables, and modified Rankin score at 3 months as dependent variable, ROI analysis.

Coefficients(a)

Model		Unstandardized Coefficients		Standardized Coefficients		
		B	Std. Error	Beta	t	Sig.
1	(Constant)	8.848	3.170		2.792	.008
	CBFi	-2.592	1.377	-.353	-1.882	.068
	MTTi	-.844	.887	-.179	-.952	.347
	volume	7.49E-006	.000	.159	.985	.331
	ADC	-3.498	2.818	-.205	-1.241	.222

a Dependent Variable: modrank

6.3.3 Grid analysis and outcome

Correlations of metabolites, diffusion and perfusion parameters from the abnormal tissue, and NIHSS with outcome

None of the metabolites correlated with the outcome as measured by the Rankin scale. MTT correlated significantly with the Rankin scale (Spearman ρ= 0.6, $p<0.0001$), but not CBF, CBV, or ADC. NIHSS was also significantly correlated with the outcome (ρ= 0.7, $p<0.0001$) (Table 3). Both, the MTT and NIHSS were significantly correlated with the outcome when measured in "definitely abnormal" and "possibly abnormal" tissue.

Correlations of metabolites, diffusion and perfusion parameters from the mismatch tissue, and NIHSS with outcome

The PWI parameters from the mismatch tissue (for the definitions of tissue types see Chapter 3) did not correlate with the outcome, but ADC (Spearman ρ= 0.4, p=0.046) was significantly correlated with mRS but not negatively as expected. NAA also correlated with the outcome (Spearman ρ= -0.4, p=0.04), whilst NIHSS was strongly correlated (Spearman ρ= 0.6, p=0.0006) (Table 3).

Table 3. Correlation (Spearman ρ) between metabolites, ADC and PWI values, and NIHSS with outcome (modified Rankin scale) in the grid analysis.

	Abnormal tissue		Mismatch tissue	
	Spearman ρ			
ADC	ρ =0.219	p=0.158	**ρ =0.429**	**p=0.046**
CBF	ρ =-0.274	p=0.075	ρ =-0.172	p=0.445
CBV	ρ =0.295	p= 0.055	ρ =0.319	p=0.148
MTT	**ρ =0.596**	**p= 0.0001**	ρ =0.411	p=0.058
Choline	ρ =0.110	p= 0.482	ρ =-0.076	p=0.738
Creatine	ρ =-0.113	p = 0.470	ρ =0.-280	p=0.207
NAA	ρ =-0.108	p = 0.489	**ρ =-0.442**	**p=0.039**
Lactate	ρ =0.023	p= 0.885	ρ =-0.192	p=0.393
NIHSS	**ρ =0.709**	**p= 0.0001**	**ρ =0.569**	**p=0.006**

Linear regression analysis

In the linear regression analysis model with the DWI, PWI parameters (abnormal tissue) and NIHSS as independent variables, and modified Rankin at three months as a dependent variable, it was only NIHSS that reached statistical significance (p=0.0001)(Table 4). In the model with the metabolites as independent variables (abnormal tissue), none of them reached statistical significance (Table 5).

Table 4. Linear regression analysis DWI, PWI parameters from the abnormal tissue, and NIHSS as independent variables, and modified Rankin score at 3 months as dependent variable, the grid analysis.

Coefficients(a)

Model		Unstandardized Coefficients		Standardized Coefficients	t	Sig.
		B	Std. Error	Beta		
1	(Constant)	1.400	1.765		.793	.433
	ADC	.000	.001	.013	.116	.908
	CBFI	-.001	.001	-.306	-1.180	.246
	CBVI	.001	.001	.343	1.030	.310
	MTTI	.000	.001	-.038	-.121	.904
	nihss	.162	.036	.607	4.537	.000

a Dependent Variable: modrank

Table 5. Linear regression analysis with metabolites from the abnormal tissue as independent variables and modified Rankin score at 3 months as a dependent variable, the grid analysis.

Coefficients(a)

Model		Unstandardized Coefficients		Standardized Coefficients	t	Sig.
		B	Std. Error	Beta		
1	(Constant)	3.542	1.768		2.003	.052
	Cho	.035	.021	.303	1.651	.107
	Cr	-.017	.019	-.168	-.918	.365
	NAA	-.014	.014	-.204	-1.001	.323
	Lact	-.003	.011	-.053	-.316	.753

a Dependent Variable: modrank

6.4 Discussion

The results of this analysis show that MTT and NIHSS are correlated with outcome as measured by the modified Rankin scale (mRS). The metabolites had no correlation with the outcome, except for the correlation of NAA from mismatch tissue and mRS. MTT from the abnormal looking tissue on DWI is correlated with the mRS, but is less significant when taken from the diffusion perfusion mismatch area (Spearman $\rho = 0.4$, $p=0.058$), with the trend in the right direction. This confirms the observation from previous studies that MTT in the acute stage is correlated with functional outcome (Beaulieu *et al.*, 1999; Kane *et al.*, 2007a; Parsons *et al.*, 2002). The MTT lesion area tends to be large and overestimates the lesion size in comparison with other perfusion parameters such as CBF (Parsons et al.,2002; Rivers *et al.*, 2006; Sorensen *et al.*, 1999). Therefore, MTT values from the mismatch region would also include a considerable proportion of the oligaemic, but not "at risk" tissue.

NIHSS was strongly correlated with the outcome, whether measured in patients with mismatch or just with the abnormal looking tissue. This is consistent with previous studies where the initial clinical severity was an independent predictor of the outcome (Derex et al.,2004; Lemesle *et al.*, 2000; Pereira *et al.*, 1999; Rother *et al.*, 2002; Wardlaw et al.,1998). ADC from the mismatch tissue positively correlated with the mRS which is not an expected correlation. When analysed across the whole lesion (chapter 4), ADC did not significantly differ between mismatch and normal tissue. The stroke cohort in this study was elderly and age may be an independent factor in conversion of ischaemic tissue in to infarction (Ay *et al.*, 2005). In addition older patients may have higher number of white matter lesions and increased ADC values (Bugalho et al 2007, Shenkin et al 2005), all of which may contribute toward the correlation between ADC and the outcome. However, this has not been specifically looked at in our or any other studies, and the numbers in this mismatch analysis (23 patients) are rather small and therefore the result should be interpreted with caution.

The metabolites in the diffusion lesion did not show any correlation with the outcome, either independently or as a part of the linear model. This is in agreement with 2 previous studies that measured metabolites in the stroke lesion within the first four days from stroke onset (Gideon *et al.*, 1994; Wardlaw et al.,1998). Studies which found NAA to be a good predictor of the outcome recruited patients either

subacutely (within the first week of stroke), or more chronic, from one to several months (Federico *et al.*, 1996; Federico *et al.*, 1998; Ford *et al.*, 1992; Lemesle et al.,2000; Pendlebury *et al.*, 1999; Pereira et al.,1999). Studies which found lactate to be predictive of outcome also did not recruit patients within 24 hours, but up to 22 days (Graham *et al.*, 1995; Parsons *et al.*, 2000).

Reduction in NAA and persistence of increased lactate beyond 24 hours may be better predictors of outcome than when measured acutely. In the acute stage (within 24 hours) NAA levels have possibly not fallen far enough, as it takes around 10 – 15 days for NAA to reach a nadir (also demonstrated in this data, see previous chapter)(Saunders *et al.*, 1995). Lactate, although a marker of acute ischaemia does not seem to predict tissue fate at this acute stage. NAA, when measured in mismatch tissue, only just reached statistical significance. This would have to be confirmed in the larger sample as this is based only on the data from the 23 patients who had mismatch present.

The strength and weaknesses of the study have been discussed extensively in chapters 4 and 5.

Ay H, Koroshetz WJ, Vangel M, Benner T, Melinosky C, Zhu M *et al.* Conversion of ischemic brain tissue into infarction increases with age. Stroke 2005; 36: 2632-2636.

Beaulieu C, de Crespigny A, Tong DC, Moseley ME, Albers GW, Marks MP. Longitudinal magnetic resonance imaging study of perfusion and diffusion in stroke: evolution of lesion volume and correlation with clinical outcome. Ann Neurol 1999; 46: 568-578.

Bugalho P, Viana-Baptista M, Jordao C, Secca MF, Ferro JM. Age-related white matter lesions are associated with reduction of the apparent diffusion coefficient in the cerebellum. Eur J Neurol 2007; 14: 1063-1066.

Davis SM, Donnan GA, Parsons MW, Levi C, Butcher KS, Peeters A *et al.* Effects of alteplase beyond 3 h after stroke in the Echoplanar Imaging Thrombolytic Evaluation Trial (EPITHET): a placebo-controlled randomised trial. Lancet Neurol 2008; 7: 299-309.

Derex L, Nighoghossian N, Hermier M, Adeleine P, Berthezene Y, Philippeau F *et al.* Influence of pretreatment MRI parameters on clinical outcome, recanalization and infarct size in 49 stroke patients treated by intravenous tissue plasminogen activator. J Neurol Sci 2004; 225: 3-9.

Federico F, Simone IL, Conte C, Lucivero V, Giannini P, Liguori M *et al.* Prognostic significance of metabolic changes detected by proton magnetic resonance spectroscopy in ischaemic stroke. Journal of Neurology 1996; 243: 241-247.

Federico F, Simone IL, Lucivero V, Giannini P, Laddomada G, Mezzapesa DM *et al.* Prognostic value of proton magnetic resonance spectroscopy in ischemic stroke. Archives of Neurology 1998; 55: 489-494.

Ford CC, Griffey RH, Matwiyoff NA, Rosenberg GA. Multivoxel 1H-MRS of stroke. Neurology 1992; 42: 1408-1412.

Gideon P, Sperling B, Arlien-Soborg P, Olsen TS, Henriksen O. Long-term follow-up of cerebral infarction patients with proton magnetic resonance spectroscopy. Stroke 1994; 25: 967-973.

Graham GD, Kalvach P, Blamire AM, Brass LM, Fayad PB, Prichard JW. Clinical correlates of proton magnetic resonance spectroscopy findings after acute cerebral infarction. Stroke 1995; 26: 225-229.

Kane I, Carpenter T, Chappell F, Rivers C, Armitage P, Sandercock P *et al.* Comparison of 10 different magnetic resonance perfusion imaging processing methods in acute ischemic stroke: effect on lesion size, proportion of patients with diffusion/perfusion mismatch, clinical scores, and radiologic outcomes. Stroke 2007a; 38: 3158-3164.

Kane I, Sandercock P, Wardlaw J. Magnetic resonance perfusion diffusion mismatch and thrombolysis in acute ischaemic stroke: a systematic review of the evidence to date. J Neurol Neurosurg Psychiatry 2007b; 78: 485-491.

Lemesle M, Walker P, Guy F, D'Athis P, Billiar T, Giroud M *et al.* Multi-variate analysis predicts clinical outcome 30 days after middle cerebral artery infarction. Acta Neurologica Scandinavica 2000; 102: 11-17.

Parsons MW, Barber PA, Chalk J, Darby DG, Rose S, Desmond PM *et al.* Diffusion- and perfusion-weighted MRI response to thrombolysis in stroke. Ann Neurol 2002; 51: 28-37.

Parsons MW, Li T, Barber PA, Yang Q, Darby DG, Desmond PM *et al.* Combined (1)H MR spectroscopy and diffusion-weighted MRI improves the prediction of stroke outcome. Neurology 2000; 55: 498-505.

Pendlebury ST, Blamire AM, Lee MA, Styles P, Matthews PM. Axonal injury in the internal capsule correlates with motor impairment after stroke. Stroke 1999; 30: 956-962.

Pereira AC, Saunders DE, Doyle VL, Bland JM, Howe FA, Griffiths JR *et al.* Measurement of initial N-acetyl aspartate concentration by magnetic resonance spectroscopy and initial infarct volume by MRI predicts outcome in patients with middle cerebral artery territory infarction. Stroke 1999; 30: 1577-1582.

Rivers CS, Wardlaw JM, Armitage PA, Bastin ME, Carpenter TK, Cvoro V *et al.* Do acute diffusion- and perfusion-weighted MRI lesions identify final infarct volume in ischemic stroke? Stroke 2006; 37: 98-104.

Rother J, Schellinger PD, Gass A, Siebler M, Villringer A, Fiebach JB *et al.* Effect of intravenous thrombolysis on MRI parameters and functional outcome in acute stroke <6 hours. Stroke 2002; 33: 2438-2445.

Saunders DE, Howe FA, van den BA, McLean MA, Griffiths JR, Brown MM. Continuing ischemic damage after acute middle cerebral artery infarction in humans demonstrated by short-echo proton spectroscopy. Stroke 1995; 26: 1007-1013.

Shenkin SD, Bastin ME, Macgillivray TJ, Deary IJ, Starr JM, Rivers CS *et al.* Cognitive correlates of cerebral white matter lesions and water diffusion tensor parameters in community-dwelling older people. Cerebrovasc Dis 2005; 20: 310-318.

Sorensen AG, Copen WA, Ostergaard L, Buonanno FS, Gonzalez RG, Rordorf G *et al.* Hyperacute stroke: simultaneous measurement of relative cerebral blood volume, relative cerebral blood flow, and mean tissue transit time. Radiology 1999; 210: 519-527.

Wardlaw JM, Marshall I, Wild J, Dennis MS, Cannon J, Lewis SC. Studies of acute ischemic stroke with proton magnetic resonance spectroscopy: relation between time from onset, neurological deficit, metabolite abnormalities in the infarct, blood flow, and clinical outcome. Stroke 1998; 29: 1618-1624.

Conclusion

Implications for clinical practice

Magnetic resonance imaging is increasingly used in every day practice in the assessment of stroke but spectroscopy remains largely a research tool. Despite the improvement in the acquisition time, the processing of the data is still very lengthy and one that could not be used in every day clinical practice. The development of new software that would allow processing of the data immediately, preferably on the MRI console, could change how MR spectroscopy (MRS) is utilised in the future.

However, MRS is a unique tool for assessing metabolites in vivo, and in this study we confirmed that N Acetyl aspartate (NAA) represents cumulative permanent neuronal damage whilst lactate is a marker of presence of ischaemia together with perfusion (PWI) and diffusion (DWI) parameters.

What does this mean for acute stroke diagnosis? By correlating DWI with NAA and lactate across the ischaemic lesion (the tissue that looks definitely abnormal, possibly abnormal, and surrounding normal tissue) we could show that the acute ischaemic lesion appearance on DWI (the "whiteness"), but not the ADC value, corresponds with the degree of neuronal damage. This is an important finding, as visual inspection of the lesion is the fastest way of assessment (in comparison to measuring thresholds) and potentially could be very important as speed is crucial when assessing eligibility for the acute stroke treatment.

On the other hand, for the patients that do not present early enough to be considered for acute stroke treatment, there is evidence from the metabolite measurement that NAA levels reduce gradually, reaching its lowest point around 12 days. Studies of diffusion and perfusion imaging and with PET imaging have also found existence of potentially salvageable tissue up to 48 hours following stroke. Furthermore, studies with serial diffusion and perfusion imaging have shown that features of tissue damage, consistent with microvascular blockage and tissue swelling, continue to be present in some patients for weeks after the stroke. No treatments, including neuroprotective agents, are available at present at this late

stage in stroke but these imaging studies show that there is a potentially salvageable tissue beyond conventional time limit of four and half hours, and that other processes may continue to increase tissue damage for days to weeks after stroke that could be amenable to treatment, once the underlying mechanisms are better understood. The focus on the hyperacute phase has deflected attention away from these later stages which might offer additional opportunities to limit the ultimate tissue damage and so improve the chances of recovery.

Previous studies have frequently used choline and creatine as denominators to express the concentration of NAA or lactate. The ratios are still used for simplicity of their calculation, but methods for quantifying individual metabolites are now well established. We showed that choline is significantly reduced in the first two weeks after stroke onset and creatine levels remained significantly low during whole of the three months of the study period. When the ratio of NAA or lactate to choline and/or creatine is used to express the metabolite concentration, the potential large ambiguity introduced in to the metabolite quantification should be carefully considered when interpreting the results. Ratios should be avoided wherever possible.

Implications for research

I would hope that there is a place for MRS to be used in the future clinical research, especially when trying to establish the metabolic state of the infarcted tissue and correlates of the metabolites with other imaging parameters that would help predict the fate of the tissue and, potentially, the clinical outcome. Sequences are now faster and image processing (though not to the refined degree used in this thesis) is available on scanner consoles, making spectroscopy a more accessible tool.

I would encourage studies with larger sample sizes, that include patients without as well as with mismatch, that aim to collect data in such a way that they could be combined into large individual patient data meta analyses in future. It would be important that studies use carefully co registered multisequence image data so as to ensure that the tissue being studied is geographically the same, and to avoid using thresholds to define tissue based on imaging parameters like ADC or perfusion values because they are too variable and probably don't work!!! Also spectroscopy could be valuable tool to study the effects of thrombolysis on changes in metabolite

levels especially whether NAA might actually recover and with the advancement of the spectroscopy techniques in future studies could try to include more slices through the lesion which would give better metabolic reflection of what is going on within the lesion. Also, the elderly population represents the majority of the stroke population but is underrepresented in the studies, especially the very elderly. Metabolites during normal ageing processes have not been studied to any detail. It would be important to know if lactate in the normal ageing brain is a feature of the pathological or physiological processes as it is one of the important variables when analysing spectroscopy data.

Appendices

Appendix 1a: Medline search strategy

MEDLINE spectroscopy
1. Cerebrovascular disorders/
2. exp Brain ischemia/
3. Carotid artery diseases/ or Carotid artery thrombosis/
4. stroke/
5. exp brain infarction/
6. Cerebral arterial diseases/ or Intracranial arterial diseases/
7. exp "Intracranial embolism and thrombosis"/
8. (stroke$ or apoplex$ or cerebral vasc$ or cerebrovasc$ or cva or transient isch?emic attack$ or tia$).tw.
9. (brain or cerebr$ or cerebell$ or vertebrobasil$ or hemispher$ or intracran$ or intracerebral or infratentorial or supratentorial or middle cerebr$ or mca$ or anterior circulation).tw.
10. (isch?emi$ or infarct$ or thrombo$ or emboli$ or occlus$ or hypoxi$).tw.
11. 9 and 10
12. 1 or 2 or 3 or 4 or 5 or 6 or 7 or 8 or 11
13. spectrum analysis/ or exp magnetic resonance spectroscopy/
14. (magnetic resonance adj5 spectroscopy).tw.
15. (mrs or h mrs or h-mrs or mr spectroscopy).tw.
16. ((chemical shift adj10 imaging) or csi).tw.
17. (n-acetylaspartate or NAA or aspartic acid).tw.
18. aspartic acid/
19. 13 or 14 or 15 or 16 or 17 or 18
20. 12 and 19
21. limit 20 to humans

Appendix 1b: Embase search strategy

EMBASE spectroscopy

1. cerebrovascular disease/
2. cerebrovascular accident/
3. stroke/
4. exp carotid artery disease/
5. brain infarction/ or brain stem infarction/ or cerebellum infarction/
6. brain ischemia/ or transient ischemic attack/
7. exp occlusive cerebrovascular disease/
8. (stroke$ or apoplex$ or cerebral vasc$ or cerebrovasc$ or cva or transient isch?emic attack$ or tia$).tw.
9. (brain or cerebr$ or cerebell$ or vertebrobasil$ or hemispher$ or intracran$ or intracerebral or infratentorial or supratentorial or middle cerebr$ or mca$ or anterior circulation).tw.
10. (isch?emi$ or infarct$ or thrombo$ or emboli$ or occlus$ or hypoxi$).tw.
11. 9 and 10
12. 1 or 2 or 3 or 4 or 5 or 6 or 7 or 8 or 11
13. spectroscopy/ or nuclear magnetic resonance spectroscopy/
14. (magnetic resonance adj5 spectroscopy).tw.
15. (mrs or h mrs or h-mrs or mr spectroscopy).tw.
16. proton nuclear magnetic resonance/
17. ((chemical shift adj10 imag$) or csi).tw.
18. n acetylaspartic acid/ or aspartic acid/
19. (n-acetylaspartate or NAA or aspartic acid).tw.
20. or/13-19
21. 12 and 20
22. limit 21 to human

Appendix 2
MR Spectroscopy and Stroke:
A Systematic Review
Data collection forms

Reviewer's Initials:
Date Reviewed:
Paper ID No:
Title:
First Author:
Year of Publication:
Main purpose of the study: (To predict outcome, development new technique, comparative)
QUALITY RATING:
1 Prospective □
2 Blinded to image analysis □
3 Blinded to final outcome □
4 Systematic follow-up □
5 Stroke physician/neurologist initial assessment □
6 Validated spectroscopy technique □
7 Well described patient population (severity, time , outcome) □
STUDY DESIGN:
Prospective/ Retrospective
SUBJECTS:
Total No of Subjects:
No actually included in the analysis:
Reason for the exclusion from the analysis:
Age Range:
Mean + SD of Age:
% Male/ Female:
Subject Inclusion Criteria:
Exclusion Criteria:
Did patient receive any acute experimental treatment?:
Time window (from stroke onset to scanning):

Time range
Mean time+
Median time
Who made the diagnosis: (stroke physician, neurologist, duty medical doctor, A&E doctor, GP or not stated)
Indication of stroke severity/subtype:
Were any outcome data collected and what time after the stroke: (was there a systematic follow-up of the studied patients? If not, when was the follow up? (range)
IMAGING:
MRS Methods:
Scanner Field Strength:
Manufacturer and Model:
Data Acquisition & Processing Method:
Metabolites Measured (+/- quantified):
Choline NAA
Creatine Lactate
Others:
If not quantified, method of data reporting (ratio to Cr, etc):
Data interpretation:
Was a reader blinded to clinical details?
Was a reader blinded to other imaging?
Was a reader blinded to clinical outcome?
Comparison to DWI/PI or any other imaging:
Overall conclusion of the study:
Additional comments on paper quality or result:

Appendix 3

THE MAGNETIC RESONANCE IMAGING AND ULTRASOUND IN ACUTE STROKE

Sample letter to patient's general practitioner about the study

Dear Dr.....,
Re:.....(patient's name, dob, address)

Your patient, Mr X, has agreed to participate in the study of imaging in acute stroke, "Magnetic Resonance Imaging and Ultrasound in Acute Stroke". Mr X had a MRI scan and Carotid Doppler scan which has been used as part of his management and the results will be enclosed in his discharge summary. Mr X will be invited for further scan at one and three months after his initial stroke.
If you require any further information please do not hesitate to contact us.

Yours sincerely

Dr Vera Cvoro
Clinical Research Fellow

Tel 0131 537 1000 bleep 5699

Dr Joanna Wardlaw
Professor of Neuroradiology and
Honorary Consultant Neuroradiologist
Tel 0131 537 2943

MAGNETIC RESONANCE IMAGING AND ULTRASOUND STUDIES IN ACUTE STROKE

PATIENT'S CONSENT FORM

T

he Magnetic Resonance and Ultrasound Imaging Studies in Acute Stroke has been explained to me and I have read the information leaflet about it. I have had time to consider the study and have had all my questions about it answered. ☐

I understand that I am free to withdraw at any time from any part of the study, without giving a reason, and without it adversely affecting my future medical care. ☐

I agree to take part in the above study. ☐

Signed:.....(patient's signature)

Name:.....(patient's name)

Date:.....

Signed: .....(signature of the investigator)

Name: .....(name of the investigator)

Date: .....

MAGNETIC RESONANCE IMAGING AND ULTRASOUND STUDIES IN ACUTE STROKE

RELATIVE'S ASSENT FORM

On behalf of my relative,.....(patient's name),
the Magnetic Resonance Imaging and Ultrasound Studies in Acute Stroke
has been explained to me and I have read the information leaflet about it.
I have had time to consider the study and have had all my questions
about it answered. ☐

I understand that my relative is free to withdraw at any time from any part of the study, without giving a reason, and without it adversely affecting their future medical care. ☐

I give my assent for their participation in the study and magnetic resonance scans of the head and ultrasound examinations of the blood vessels to be carried out. ☐

Signed:.....(relative's signature)

Name:.....(relative's name)

Date:.....

Signed: .....(signature of the investigator)

Name: .....(name of the investigator)

Date: .....

Appendix 4

PATIENT INFORMATION

THE MAGNETIC RESONANCE IMAGING AND ULTRASOUND IN ACUTE STROKE

You have been admitted to the Western General Hospital because you may have had a stroke. We would like you to consider being a part of a study on Magnetic Resonance Imaging (MRI) and Ultrasound scanning of the arteries in patients who have had a stroke. It will provide valuable information about what exactly is happening in the brain when people have a stroke and therefore help us give the right kind of treatment.

You will first be seen by the doctor who will ask you questions about the symptoms that brought you to hospital, then you will have full examination.

As soon as possible after the examination we will organise for you to have an MRI. This scan uses magnetism but will not cause any harm to you. Many other hospitals around the world use the magnetic scan routinely. We do ask you to lie still for around 30 minutes. The machine is slightly noisy so you will have earplugs to protect your ears. You will be able to communicate with us during the scanning. If you feel uncomfortable or claustrophobic, the scan can be stopped at any time. If you know you are
claustrophobic, please tell us and we will not do the MR scan.

This scan is important because it gives us much more detailed pictures of the brain, including what sort of damage may have happened to cause your stroke. We think that in the future, this more detailed information will help us decide what sort of treatment is best for patients like you. In order to record blood flow in your brain you will need a small injection into a vein in your arm through the needle, which usually gets put in, while you are in the admission unit. You will not require a CT (computed tomography) scan of your brain which is a routine treatment in this hospital and gives less information.

You will also have an ultrasound scan of the blood vessels to your head. This does not involve any injections. We simply place a small amount of jelly on your neck and just in front of your ears and look for the blood flow with the small camera. It lasts around 5 to 10 minutes.

In order to monitor what happens to your stroke over the next few weeks, we would like to repeat the magnetic and ultrasound scans in about five days, two weeks, one and three months after your stroke. At three months time you would also have a full examination by the doctor to assess how well have you recovered from the stroke.

You may decide to withdraw from the study at any time. This will make no difference to the care you receive from the stroke team in the hospital and outpatients. If you

decide to take part in this study you will be asked to sign a consent form. Even when you sign a consent form you are still free to withdraw from the study at any time without having to give a reason and without affecting your future care.

Your GP will receive information about your involvement in the study and the results of your scans.

Any information that you give us as well as the results of the scans will be treated as confidential and will only be available to the doctors looking after you and research staff involved in this project.

This study has been funded by the Stroke Association and has been approved by the Lothian Research and Ethics Committee.

If you would like to obtain further information about the study from somebody who is not directly involved you
could speak to Dr Zeman who can be contacted through the Western General switchboard No 0131 537 1000.

If you have any questions about the study even after you leave the hospital, please feel free to contact Dr Cvoro at the Western General Hospital (switchboard no 0131 537 1000, bleep 5699).

Appendix 5: assessment scales

MODIFIED RANKIN SCALE (MRS)

Patient name: _____

Date: _____

Score Description

0	No symptoms at all
1	No significant disability despite symptoms; able to carry out all usual duties and activities
2	Slight disability; unable to carry out all previous activities, but able to look after own affairs without assistance
3	Moderate disability; requiring some help, but able to walk without assistance
4	Moderately severe disability; unable to walk without assistance and unable to attend to own bodily needs without assistance
5	Severe disability; bedridden, incontinent, and requiring constant nursing care and attention
6	Dead

TOTAL (0–6): _____

THE BARTHEL INDEX

Name of the patient: use label if available
Date:

FEEDING
0 = unable
5 = needs help cutting, spreading butter, etc., or requires modified diet
10 = independent _____

BATHING
0 = dependent
5 = independent (or in shower) _____

GROOMING
0 = needs to help with personal care
5 = independent face/hair/teeth/shaving (implements provided) _____

DRESSING
0 = dependent
5 = needs help but can do about half unaided
10 = independent (including buttons, zips, laces, etc.) _____

BOWELS
0 = incontinent (or needs to be given enemas)
5 = occasional accident
10 = continent _____

BLADDER
0 = incontinent, or catheterized and unable to manage alone
5 = occasional accident
10 = continent _____

TOILET USE
0 = dependent
5 = needs some help, but can do something alone
10 = independent (on and off, dressing, wiping) _____

TRANSFERS (BED TO CHAIR AND BACK)
0 = unable, no sitting balance
5 = major help (one or two people, physical), can sit
10 = minor help (verbal or physical)
15 = independent _____

MOBILITY (ON LEVEL SURFACES)
0 = immobile or < 50 yards
5 = wheelchair independent, including corners, > 50 yards
10 = walks with help of one person (verbal or physical) > 50 yards
15 = independent (but may use any aid; for example, stick) > 50 yards _____

STAIRS
0 = unable
5 = needs help (verbal, physical, carrying aid)
10 = independent _____

TOTAL (0–100): _____

NOTTINGHAM EXTENDED ACTIVITIES OF DAILY LIVING (EADL) INDEX

PATIENT'S NAME:

HOSPITAL NUMER:

0 = Not at all
1 = With help
2 = Alone with difficulty
3 = Alone easily

DO YOU.....

	Comments	*Date*			
MOBILITY					
- walk around outside?					
- climb stairs?					
- get in and out of the car?					
- walk over uneven ground?					
- cross roads?					
- travel on public transport?					
TOTAL					
IN THE KITCHEN					
- manage to feed yourself?					
- make yourself a hot drink?					
- take hot drinks from one room to another?					
- do the washing up?					
- make yourself a hot snack?					
TOTAL					
DOMESTIC TASKS					
- manage your own money when out?					
- wash small items of clothing?					
- do your own shopping?					
- do a full clothes wash?					
TOTAL					
LEISURE ACTIVITIES					
- read newspapers and books?					
- use the telephone?					
- write letters?					
- go out socially?					
- manage your own garden?					
- drive a car?					
TOTAL					
GRAND TOTAL					

NIH Stroke Scale *Please circle the most appropriate response for each section*

1a Level of *Consciousness* **(LOC)**	0	Alert – *keenly responsive*
	1	Drowsy – *arousable by minor stimulation to obey, answer, or respond*
	2	Stuporous – *requires repeated stimulation to attend, or is obtunded and requires strong or painful stimulation to make movements (not stereotyped)*
	3	Comatose – *responds only with reflex motor or autonomic effects or totally unresponsive, flaccid*
1b LOC Questions	0	Answers both correctly
	1	Answers one correctly
	2	Incorrect
		Patient is asked to state the month & his/her age
1c LOC Commands	0	Obeys both correctly
	1	Obeys one correctly
	2	Incorrect
		Patient is asked to open & close eyes, grip & release normal hand
2. Best Gaze	0	Normal
	1	Partial gaze palsy – *gaze is abnormal in one or both eyes, no forced deviation/total gaze paresis*
	2	Forced deviation – *or total gaze paresis not overcome by oculocephalic maneouvre*
3. Visual Fields	0	No visual loss
	1	Partial hemianopia
	2	Complete hemianopia
	3	Bilateral Hemianopia – *including cortical blindness*
4. Facial Palsy	0	Normal
	1	Minor - *flattened nasolabial fold, asymmetry on smiling*
	2	Partial – *total or near total paralysis of lower face*
	3	Complete - *absent facial movement in upper and lower face on one or both sides*
5. Best Motor RIGHT ARM	0	No drift – *holds limb at 90 degrees for full 10 seconds*
	1	Drift - *drifts down but does not hit bed*
	2	Some effort against gravity
	3	No effort against gravity
	4	No movement
	x	Untestable
6. Best Motor LEFT ARM	0	No drift – *holds limb at 90 degrees for full 10 seconds*
	1	Drift - *drifts down but does not hit bed*
	2	Some effort against gravity
	3	No effort against gravity
	4	No movement
	x	Untestable
7. Best Motor RIGHT LEG	0	No drift – *holds limb at 45 degrees for full 5 seconds*
	1	Drift - *drifts down but does not hit bed*
	2	Some effort against gravity
	3	No effort against gravity
	4	No movement
	x	Untestable
8. Best Motor LEFT LEG	0	No drift – *holds limb at 45 degrees for full 5 seconds*
	1	Drift - *drifts down but does not hit bed*
	2	Some effort against gravity
	3	No effort against gravity
	4	No movement
	x	Untestable
9. Limb Ataxia	0	Absent
	1	Present in 1 limb
	2	Present in 2 or more limbs
10. Sensory	0	Normal
	1	Partial loss – *patient feels pinprick is less sharp or is dull on affected side*
	2	Dense loss - *patient is unaware of being touched on face, arm, leg*
11. Best Language	0	No dysphasia
	1	Mild – moderate dysphasia *obvious loss of fluency or comprehension, without significant limitation on ideas expressed or form of expression. Makes conversation about provided material difficult or impossible, e.g. examiner can identify picture or naming card from patient's response.*
	2	Severe dysphasia - *all communication is through fragmentary expression; great need for inference, questioning, and guessing by the listener who carries burden of communication. Examiner cannot identify materials provided from patient response*
	3	Mute *no usable speech or auditory comprehension.*
12. Dysarthria	0	Normal articulation
	1	Mild – moderate dysarthria - *patient slurs some words, can be understood with some difficulty.*
	2	Unintelligible or worse - *speech is so slurred as to be unintelligible (absence of or out of proportion to dysphasia) or is mute/anarthric*
	x	Untestable
13. Neglect	0	No neglect
	1	Partial neglect - *Visual, tactile, auditory, spatial, or personal inattention or extinction to bilateral simultaneous stimulation in one of the sensory modalities*
	2	Complete neglect - *Profound hemi-inattention or hemi-inattention to more than one modality. Does not recognise own hand or orients to only one side of space*

Notes for completion of NIHSS:

Administer stroke scale items in the order listed. Record performance in each category after each subscale exam. Do not go back and change scores. Follow directions provided for each exam technique. Scores should reflect what the patient does, not what the clinician thinks the patient can do. The clinician should record answers while administering the exam and work quickly. Except where indicated, the patient should not be coached (i.e., repeated requests to patient to make a special effort).

1a. Level of Consciousness: The investigator must choose a response, even if a full evaluation is prevented by such obstacles as an endotracheal tube, language barrier, orotracheal trauma/bandages. A 3 is scored only if the patient makes no movement (other than reflexive posturing) in response to noxious stimulation.

1b. LOC Questions: The patient is asked the month and his/her age. The answer must be correct - there is no partial credit for being close. Aphasic and stuporous patients who do not comprehend the questions will score 2. Patients unable to speak because of endotracheal intubation, orotracheal trauma, severe dysarthria from any cause, language barrier or any other problem not secondary to aphasia are given a 1. It is important that only the initial answer be graded and that the examiner not "help" the patient with verbal or non-verbal cues.

1c. LOC Commands: The patient is asked to open and close the eyes and then to grip and release the non-paretic hand. Substitute another one step command if the hands cannot be used. Credit is given if an unequivocal attempt is made but not completed due to weakness. If the patient does not respond to command, the task should be demonstrated to them (pantomime) and score the result (i.e., follows none, one or two commands). Patients with trauma, amputation, or other physical impediments should be given suitable one-step commands. Only the first attempt is scored.

2. Best Gaze: Only horizontal eye movements will be tested. Voluntary or reflexive (oculocephalic) eye movements will be scored but caloric testing is not done. If the patient has a conjugate deviation of the eyes that can be overcome by voluntary or reflexive activity, the score will be 1. If a patient has an isolated peripheral nerve paresis (CN III, IV or VI) score a 1. Gaze is testable in all aphasic patients. Patients with ocular trauma, bandages, pre-existing blindness or other disorder of visual acuity or fields should be tested with reflexive movements and a choice made by the investigator. Establishing eye contact and then moving about the patient from side to side will occasionally clarify the presence of a partial gaze palsy.

3. Visual: Visual fields (upper and lower quadrants) are tested by confrontation, using finger counting or visual threat as appropriate. Patient must be encouraged, but if they look at the side of the moving fingers appropriately, this can be scored as normal. If there is unilateral blindness or enucleation, visual fields in the remaining eye are scored. Score 1 only if a clear-cut asymmetry, including quadrantanopia is found. If patient is blind from any cause score 3. Double simultaneous stimulation is performed at this point. If there is extinction patient receives a 1 and the results are used to answer question 11

4. Facial Palsy: Ask, or use pantomime to encourage the patient to show teeth or raise eyebrows and close eyes. Score symmetry of grimace in response to noxious stimuli in the poorly responsive or non-comprehending patient. If facial trauma/bandages, orotracheal tube, tape or other physical barrier obscures the face, these should be removed to the extent possible.

5–8. Motor Arm and Leg: The limb is placed in the appropriate position: extend the arms (palms down) 90 degrees (if sitting) or 45 degrees (if supine) and the leg 30 degrees (always tested supine). Drift is scored if the arm falls before 10 seconds or the leg before 5 seconds. The aphasic patient is encouraged using urgency in the voice and pantomime but not noxious stimulation. Each limb is tested in turn, beginning with the non-paretic arm. Only in the case of amputation or joint fusion at the shoulder or hip may the score be "x" and the examiner must clearly write the explanation for scoring as an "x."

9. Limb Ataxia: This item is aimed at finding evidence of a unilateral cerebellar lesion. Test with eyes open. In case of visual defect, insure testing is done in intact visual field. The finger-nose-finger and heel-shin tests are performed on both sides, and ataxia is scored only if present out of proportion to weakness. Ataxia is absent in the patient who cannot understand or is paralyzed. Only in the case of amputation or joint fusion may the item be scored "9", and the examiner must clearly write the explanation for not scoring. In case of blindness test by touching nose from extended arm position.

10. Sensory: Sensation or grimace to pin prick when tested, or withdrawal from noxious stimulus in the obtunded or aphasic patient. Only sensory loss attributed to stroke is scored as abnormal and the examiner should test as many body areas [arms (not hands), legs, trunk, face] as needed to accurately check for hemisensory loss. A score of 2, "severe or total," should only be given when a severe or total loss of sensation can be clearly demonstrated. Stuporous and aphasic patients will therefore probably score 1 or 0. The patient with brain stem stroke who has bilateral loss of sensation is scored 2. If the patient does not respond and is quadriplegic score 2. Patients in coma (item 1a=3) are arbitrarily given a 2 on this item.

11. Best Language: A great deal of information about comprehension will be obtained during the preceding sections of the examination. The patient is asked to describe what is happening in the attached picture, to name the items on the attached naming sheet, and to read from the attached list of sentences. Comprehension is judged from responses here as well as to all of the commands in the preceding general neurological exam. If visual loss interferes with the tests, ask the patient to identify objects placed in the hand, repeat, and produce speech. The intubated patient should be asked to write. The patient in coma (question 1a=3) will arbitrarily score 3 on this item. The examiner must choose a score in the patient with stupor or limited cooperation but a score of 3 should be used only if the patient is mute and follows no one step commands.

12. Dysarthria: If patient is thought to be normal an adequate sample of speech must be obtained by asking patient to read or repeat words from the attached list. If the patient has severe aphasia, the clarity of articulation of spontaneous speech can be rated. Only if the patient is intubated or has other physical barrier to producing speech, may the item be scored "9", and the examiner must clearly write an explanation for not scoring. Do not tell the patient why he/she is being tested.

13. Extinction and Inattention (formerly Neglect): Sufficient information to identify neglect may be obtained during the prior testing. If the patient has a severe visual loss preventing visual double simultaneous stimulation, and the cutaneous stimuli are normal, the score is normal. If the patient has aphasia but does appear to attend to both sides, the score is normal. The presence of visual spatial neglect or anosagnosia may also be taken as evidence of abnormality. Since the abnormality is scored only if present, the item is never untestab